

# **Modelling future global change impacts on African ecosystems and their carbon dynamics and associated uncertainties and challenges**

Dissertation  
zur Erlangung des Doktorgrades  
der Naturwissenschaften

vorgelegt beim Fachbereich 11 Geowissenschaften / Geographie  
der Johann Wolfgang Goethe - Universität  
in Frankfurt am Main

von  
Carola Martens  
aus Köln.

Frankfurt am Main (2023)  
(D 30)



Vom Fachbereich Geowissenschaften / Geographie der  
Johann Wolfgang Goethe-Universität als Dissertation angenommen.

**Dekan:**

Prof. Dr. Joachim Curtius  
Johann Wolfgang Goethe-Universität  
Institut für Atmosphäre und Umwelt  
Altenhöferallee 1  
D-60438 Frankfurt am Main

**Gutachter:**

Prof. Dr. Thomas Hickler  
Institut für Physische Geographie  
Johann Wolfgang Goethe-Universität  
Altenhöferallee 1  
60438 Frankfurt am Main

apl. Prof. Dr. Simon Scheiter  
Senckenberg Biodiversität und Klima Forschungszentrum  
Senckenberganlage 25  
D-60325 Frankfurt am Main

Datum der Disputation: 27.11.2023



## *Summary*

Today's climate is changing at rates unprecedented in recent human history and it is unequivocal that anthropogenic greenhouse gas emissions such as CO<sub>2</sub> largely drive this change. Terrestrial ecosystems are an important sink of atmospheric CO<sub>2</sub> and savannas and other semi-arid ecosystems, which cover large parts of Africa, drive trends and variability of global, terrestrial carbon dynamics. Yet, uncertainties in modelling dryland vegetation and carbon cycle dynamics remain and our ability to simulate future climate change effects on dryland ecosystems lags behind more mesic systems. Southern Africa's Nama Karoo dwarf shrubland is an example for a semi-arid ecosystem where large uncertainties on ecosystem processes, carbon dynamics and climate change impacts persist.

In African ecosystems, climate-change driven changes have already been observed with regionally varying effects. For example, woody encroachment into savannas as well as expansion of savannas have been described. African ecosystems provide the habitat for a unique biodiversity and the livelihoods and ecosystem services for approximately 1.4 billion people. The population in Africa is projected to grow and potentially double until the end of the 21<sup>st</sup> century. This population growth and the associated changes in land use and land cover are challenges for the conservation of Africa's biodiversity. Understanding the dynamics of ecosystems and their carbon cycles as well as potential climate change impacts in Africa and uncertainties associated with vegetation projections is critical for the planning of climate change adaptation measures. These prospects motivated the research in this thesis with a focus on future climate change impacts on African ecosystems and carbon dynamics and where they may co-occur with the global change drivers population and land use for African protected areas until the end of the 21<sup>st</sup> century. An additional focus lay on uncertainties associated with future projections for African ecosystems and challenges associated with modelling the Nama Karoo as an example for a semi-arid niche ecosystem and its carbon cycle.

Dynamic vegetation models (DVMs) are a widely used tool deployed to improve our understanding of ecosystem processes, attribute ongoing ecosystem changes to different drivers and

mechanisms, and project future ecosystem changes. They simulate ecophysiological processes, such as photosynthesis and plant growth, vegetation dynamics and structure, geographical distribution of plant biomes, and biogeochemical cycles (e.g. water and carbon), in particular in response to climate change. DVMs are therefore the main tool applied in this thesis. For future projections, we used the adaptive dynamic global vegetation model (aDGVM), which was originally developed particularly for African ecosystems and is well tested. We simulated potential natural vegetation until the end of the 21<sup>st</sup> century. For simulations of the Nama Karoo dwarf shrubland, I applied the adaptive dynamic global vegetation model 2 (aDGVM2) which includes a shrub sub-module. The aDGVM2 is based on the aDGVM but implements a more flexible, plant-trait based approach.

In Chapter 2, the focus lay on the impact of climate change on African ecosystems and carbon stocks until the end of the 21<sup>st</sup> century. We forced the aDGVM with regionally downscaled climate scenarios at 0.5° resolution based on an ensemble of climate data from six general circulation models (GCMs) for two representative greenhouse gas concentration pathways (RCPs): RCP4.5, a medium emissions and mitigation scenario and RCP8.5, a high emissions, low mitigation scenario. We also assessed the effects of elevated atmospheric CO<sub>2</sub> on vegetation change and its plant-physiological drivers. In the so-called CO<sub>2</sub> fertilisation effect, increases in atmospheric CO<sub>2</sub> concentration stimulate photosynthesis, which potentially drives increases in vegetation biomass. We investigated uncertainties associated with the choice of climate model that produced climate input data, chosen climate change scenario, and the CO<sub>2</sub> effect. The analysis was focused on biome changes and changes in the water use efficiency of simulated vegetation.

For carbon in aboveground biomass in Africa, the aDGVM projected an increase until the end of the century for both climate scenarios (18-43% for RCP4.5 and 37-61% for RCP8.5). This was associated with woody encroachment into grasslands and increased woody cover in savannas. In simulations where we omitted the direct effects of CO<sub>2</sub> on plants, woody encroachment was muted. In these simulations without CO<sub>2</sub> effects, carbon in aboveground vegetation changed between (-8)-11% for RCP4.5 and (-22)-(-6)% for RCP8.5. Overall, simulated changes in biomes

lacked consistent large-scale geographical patterns of change across scenarios. In Ethiopia and the Sahara/Sahel transition zone, the biome changes forecast by the aDGVM were consistent across GCMs and RCPs. Projected change in aboveground biomass was driven primarily by CO<sub>2</sub> increases and showed that assumptions concerning CO<sub>2</sub> effects caused the strongest variability in future projections. Direct effects from elevated CO<sub>2</sub> were associated with substantial increases in water use efficiency, primarily driven by photosynthesis enhancement. This increase may relieve soil moisture limitations to plant productivity. At the ecosystem level, interactions between fire and woody plant demography further promoted woody encroachment. Even medium-impact scenarios (RCP4.5), irrespective of simulated CO<sub>2</sub> effects on plants, suggested considerable ecosystem change.

We concluded that substantial future biome changes due to climate and CO<sub>2</sub> changes are likely across Africa. The simulations with and without direct effects of CO<sub>2</sub> concentration give an idea of the range of the potential impact of CO<sub>2</sub> fertilisation and future climate change on ecosystems. It is, however, unlikely that CO<sub>2</sub> effects on plants will be negligible in systems such as savannas, where feedbacks between CO<sub>2</sub> effects and fire disturbance affect the competitive balance between trees and grasses. To reduce uncertainties associated with CO<sub>2</sub> effects on ecosystems, focused research and improved model representation of these CO<sub>2</sub> effects will be necessary. In further aDGVM development, the inclusion of nutrient cycles into vegetation dynamics is key to account for nutrient limitation of the CO<sub>2</sub> fertilisation effect. Because of the large uncertainties in future projections, climate change adaptation policies and strategies must be highly flexible.

The simulated vegetation in Chapter 2 represents potential natural vegetation. Simulations of potential natural vegetation are particularly suitable to investigate protected areas with their, in ideal circumstances, anthropogenically undisturbed ecosystems and potential climate change impacts on conservation efforts. However, protected areas do not exist isolated from their environments and societal developments. Africa's protected areas appear increasingly threatened by climate change, substantial human population growth, and land-use change and are at the same time the last stronghold of the continent's unique biodiversity. Conservation planning

is challenged by uncertainty about how strongly and where these drivers will interact over the next few decades. In Chapter 3, we therefore combined the vegetation projections from Chapter 2 inside African protected areas with projections for human population densities and land use in their surroundings. We thus investigated the intersection of climate change impacts and socioeconomic factors for African protected areas until the end of the 21<sup>st</sup> century. For climate change impact simulations, we used only the simulations that included CO<sub>2</sub> effects from Chapter 2, because some effects of atmospheric CO<sub>2</sub> on ecosystems are likely. We analysed protected areas for two future scenarios that are combinations of shared socioeconomic pathways (SSPs) and RCPs. The SSP2–RCP4.5 is the “middle-of-the-road” scenario in which global inequalities in development and income growth continue with some regional improvements and medium climatic changes. In SSP5–RCP8.5, rapid economic and social development is driven by fossil fuel exploitation and associated strong climate change and technological development (“fossil-fueled development”).

Under both scenarios, most protected areas were adversely affected by at least one of the drivers by the end of the 21<sup>st</sup> century, but the co-occurrence of drivers was largely region and scenario specific. The vegetation projections suggested considerable climate-driven tree cover increases and habitat loss in the majority of protected areas in today’s grasslands and savannas. For protected areas in West Africa, the analysis revealed climate-driven vegetation changes combined with hotspots of high future population and land-use pressure. Except for many protected areas in North Africa, protected areas across Africa were generally projected to experience increasing pressure from at least one of the investigated global change pressures under both SSP–RCP scenarios. Future decreases in population and land-use pressures were rare for protected areas outside of North Africa. At the continental scale, SSP5–RCP8.5 led to higher climate-driven changes in tree cover and higher land-use pressure, whereas SSP2–RCP4.5 was characterised by higher future population pressure. Both SSP–RCP scenarios implied increasing challenges for conserving Africa’s biodiversity in protected areas.

Despite the large variation between scenarios and regions, it can be concluded that climate-change impacts on vegetation will likely be exacerbated by socioeconomic pressures for most

protected areas and regions in Africa. This combination of pressures challenges conservation targets of protecting 30% of land areas under the Convention on Biological Diversity. Our findings underline the importance of developing and implementing region-specific conservation responses. Strong mitigation of future climate change and equitable development scenarios could reduce impacts on ecosystems and sustain the effectiveness of conservation in Africa.

The continental scale vegetation simulations and analyses in Chapters 2 and 3 indicate broad patterns of vegetation change under climate change. The resolution of these simulations make them unsuitable for local analyses. In addition, smaller scale ecosystems such as the Nama Karoo dwarf shrubland in southern Africa, an ecosystem which is not found on the grassland-savanna-forest spectrum, are not represented well by plant types implemented in many DVMs. At the same time, the contribution of the Nama Karoo to the variability of the global carbon sink is not clear. Likewise, potential climate change impacts on the Nama Karoo carbon dynamics and the balance of its dwarf shrubs and grasses are uncertain. In Chapter 4, I demonstrated the challenges of simulating the plants and the carbon cycle of the Nama Karoo with the aDGVM2 and its shrub module. I evaluated the simulated carbon fluxes from photosynthesis, respiration and decomposition against recent carbon flux measurements from an eddy covariance flux tower and compared simulated and observed vegetation structure. With reparametrisation of soil water access, soil depth, and photosynthesis modules in aDGVM2, I tested which model setups improve simulation results.

In all simulation setups, simulated carbon fluxes and biomass for the Nama Karoo were vastly overestimated. None of the implemented reparametrisations of the model was able to represent dwarf shrub morphology and carbon fluxes and their intra- and interannual dynamics. Compared to an aDGVM2 base version, the different simulation setups improved the agreement for individual flux components or for biomass. Simulations with limited soil water access led to the extinction of shrubs. In simulations without limitations of soil water access where shrubs established, they grew too tall with heights of 1.5-3.2 m. These heights are common for savanna shrubs, but not for Nama Karoo dwarf shrubs which had an average height of  $\sim 0.25$  m at the research site. The simulations also showed challenges in simulating below-ground water and

carbon processes in semi-arid ecosystems. Simulated soil moisture did not drop to observed levels and heterotrophic respiration was overestimated. In semi-arid ecosystems such as the Nama Karoo, water availability limits plant growth and drives carbon release from decomposition processes. An appropriate model representation of soil moisture dynamics is key for plant growth and simulated carbon balance.

These differences between aDGVM2 simulations and measurements highlighted that dwarf shrub ecology is not represented by the existing shrub-module in aDGVM2. Coping mechanisms of dwarf shrubs in semi-arid regions for dry stress are not reflected well in the aDGVM2 implementation of shrubs and woody vegetation. Further field research on the ecophysiology and processes driving the dynamics of Nama Karoo vegetation and soil water is required to parameterise the aDGVM2 for the Nama Karoo. If this reparametrisation does not lead to an adequate representation, an implementation of dwarf shrubs as a distinct plant functional type may be necessary. Once Nama Karoo vegetation dynamics are improved, including herbivory in aDGVM2 simulations would be an important next step to reflect widespread livestock farming with sheep in the Nama Karoo. Given that these challenges are overcome, DVMs can be a powerful tool for much needed research on climate-change impacts on the ecology but also regional livelihoods in the Nama Karoo.

In this thesis, I showed opportunities but also limitations and uncertainties of simulations and climate change projections with the DVMs aDGVM and aDGVM2 for African ecosystems and their carbon balance as well as the combination of DVM projections with global change projections for African protected areas. The analyses indicated that climate change under medium to high emission scenarios will likely result in large scale ecosystem and carbon balance changes in Africa. The presented uncertainties in the representation of the CO<sub>2</sub> fertilisation effect, of semi-arid soil moisture dynamics, of carbon fluxes, and of vegetation types in more niche ecosystems such as the Nama Karoo highlight the importance of further field research and DVM development. For the medium emission scenario, uncertainties in the CO<sub>2</sub> fertilisation effect resulted in a smaller range of potential future ecosystem states compared to the high emission scenario. This entails that adaptation strategies and measures likely need to be less complex

or extensive, when climate change is minimised. For African protected areas, climate change challenges may be exacerbated by socioeconomic factors to a regionally varying extent. This analysis pointed towards the importance of not only taking climate action but also ensuring equitable, sustainable development to facilitate successful ecosystem conservation.

Overall, this thesis contributed to research on possible climate change impacts on African ecosystems and conservation, the complex links with other global change factors, and research gaps in the representation of African ecosystems in DVMs. Avenues of future research could include the application of DVMs in attribution research by analysing the likelihood of anthropogenic climate change as driver of observed vegetation change. If research finds that anthropogenic climate forcing can likely be attributed as driver of recent vegetation changes, this could be powerful information for the communication on the impacts of climate change and awareness raising. In addition, simulations with DVMs could support the planning of nature-based solutions in terrestrial ecosystems to investigate their potential and to ensure resilient responses to climate change and prevent biodiversity loss.



## Zusammenfassung

Das aktuelle Erdklima wandelt sich in einem Tempo, das beispiellos ist für die jüngste Vergangenheit der Menscheitsgeschichte. Es ist erwiesen, dass insbesondere anthropogene Treibhausgasemissionen von beispielsweise CO<sub>2</sub> diese Veränderungen antreiben. Terrestrische Ökosysteme sind gleichzeitig ein wichtiger Speicher für CO<sub>2</sub> aus der Atmosphäre. Savannen und andere semiaride Ökosysteme, die einen großen Teil von Afrika bedecken, bestimmen Trends und Variabilität der globalen, terrestrischen Kohlenstoffdynamik. Es bestehen jedoch weiterhin Unsicherheiten in der Modellierung von Dynamiken der Vegetation und des Kohlenstoffkreislaufs in Trockengebieten. Unsere Fähigkeiten, Auswirkungen von zukünftigen Klimaveränderungen auf Ökosysteme in Trockengebieten zu modellieren, bleiben hinter denen für gemäßigtere Ökosysteme zurück. Die Zwergsstrauchlandschaft der Nama-Karoo im südlichen Afrika ist ein Beispiel für ein semiarides Ökosystem, für das große Unsicherheiten zu Ökosystemprozessen, Kohlenstoffdynamiken und Auswirkungen des Klimawandels bestehen.

Auswirkungen des Klimawandels wurden für afrikanische Ökosysteme bereits mit regional unterschiedlichen Effekten beschrieben. So wurden für Savannen beispielsweise einerseits Verbuschung und andererseits Gebietsausdehnung beobachtet. Afrikanische Ökosysteme bieten Lebensräume für eine einzigartige Biodiversität und stellen die Lebensgrundlagen und Ökosystemdienstleistungen für etwa 1,4 Milliarden Menschen bereit. Für die Bevölkerung Afrikas wird bis zum Ende des 21. Jahrhunderts ein Wachstum mit einer möglichen Verdopplung prognostiziert. Dieses Bevölkerungswachstum und die damit einhergehenden Veränderungen von Landnutzung und Landbedeckung stellen eine Herausforderung für den Schutz der afrikanischen Biodiversität dar. Für die Planung von Maßnahmen zur Anpassung an den Klimawandel ist ein Verständnis für Dynamiken von Ökosystemen und ihren Kohlenstoffkreisläufen sowie für mögliche Auswirkungen des Klimawandels in Afrika und Unsicherheiten im Zusammenhang mit Vegetationsprojektionen entscheidend. Dieser Hintergrund diente als Motivation für diese Forschungsarbeit mit dem Fokus auf zukünftige Auswirkungen des Klimawandels auf afrikanische Ökosysteme und Kohlenstoffdynamiken bis zum Ende des 21. Jahrhunderts und wo diese für afrikanische Schutzgebiete zusammen mit den weiteren Faktoren des globalen

Wandels Bevölkerung und Landnutzung auftreten könnten. Darüber hinaus lag ein weiterer Fokus dieser Arbeit auf Unsicherheiten bei Zukunftsprojektionen für afrikanische Ökosysteme und Herausforderungen im Zusammenhang mit der Modellierung der Nama-Karoo, als Beispiel für ein semiarides Nischenökosystem, und ihres Kohlenstoffkreislaufs.

Dynamische Vegetationsmodelle (DVMs) sind ein weit verbreitetes Instrument in der Untersuchung von Ökosystemprozessen, der Identifizierung von Antriebsfaktoren und Mechanismen hinter aktuellen Veränderungen in Ökosystemen und für Zukunftsprojektionen von Ökosystemveränderungen. Mit DVMs können ökophysiologische Prozesse wie Photosynthese und Pflanzenwachstum, Vegetationsdynamiken und -strukturen, geographische Verbreitungen von Pflanzenbiomen sowie biogeochemischen Kreisläufen (z.B. Wasser und Kohlenstoff) insbesondere im Zusammenhang mit dem Klimawandel, untersucht werden. DVMs sind daher das Hauptwerkzeug in dieser Arbeit. Für Zukunftsprojektionen haben wir das adaptive dynamic global vegetation model (aDGVM), welches ursprünglich insbesondere für afrikanische Ökosysteme entwickelt wurde und sich bewährt hat, verwendet. Mit dem aDGVM haben wir die potentielle, natürliche Vegetation bis zum Ende des 21. Jahrhunderts simuliert. In Simulationen für die Zwergstrauchlandschaft der Nama-Karoo habe ich das adaptive dynamic global vegetation model 2 (aDGVM2), für das ein Modul für Strauchpflanzen existiert, angewendet. Das aDGVM2 wurde basierend auf dem aDGVM entwickelt, verfügt aber über einen flexibleren Ansatz basierend auf variablen Pflanzenmerkmalen.

In Kapitel 2 lag der Fokus auf den Auswirkungen des Klimawandels auf afrikanische Ökosysteme und Kohlenstoffspeicher bis zum Ende des 21. Jahrhunderts. Dafür haben wir aDGVM-Simulationen mit regional herunterskalierten Klimadaten aus einem Ensemble von sechs globalen Zirkulationsmodellen (general circulation models, GCMs) für zwei repräsentativer Konzentrationspfade (representative concentration pathways, RCPs) mit einer Auflösung von  $0.5^\circ$  als Eingabedaten durchgeführt: RCP4.5, ein Klimawandelszenario mit mittleren Emissionen und mittlerer Eindämmung und RCP8.5, ein Szenario mit hohen Emissionen und niedriger

Minderung des Klimawandels. Darüber hinaus haben wir den Einfluss von erhöhten CO<sub>2</sub>-Konzentrationen in der Atmosphäre auf Vegetationsveränderungen und pflanzenphysiologische Antriebskräfte untersucht. Im sogenannten CO<sub>2</sub>-Düngeeffekt regen erhöhte CO<sub>2</sub>-Konzentrationen die Photosynthese an, was möglicherweise in einer Zunahme von Pflanzenbiomasse resultiert. Wir haben Unsicherheiten im Zusammenhang mit der Wahl des den Klimaeingabedaten zugrundeliegenden Klimamodells, dem gewählten Klimawandelszenario und dem CO<sub>2</sub>-Düngeeffekt untersucht. Die Analyse war dabei auf Biomveränderungen und Veränderungen der Wassernutzungseffizienz der simulierten Vegetation fokussiert.

Für Kohlenstoff, der in oberirdischer Biomasse gespeichert ist, hat das aDGVM eine Zunahme von 18-43% unter RCP4.5 und von 37-61% unter RCP8.5 bis Ende des Jahrhunderts projiziert. Damit einher ging eine Verbuschung von Grasländern und Savannen. In Simulationen, in denen der direkte Einfluss von CO<sub>2</sub> auf Pflanzen ausgeschaltet war, fand kaum Verbuschung statt. In diesen Simulationen ohne CO<sub>2</sub>-Effekt änderte sich der Kohlenstoff in der oberirdischen Biomasse zwischen (-8)-11% unter RCP4.5 und (-22)-(-6)% unter RCP8.5. Insgesamt ergaben sich über die verschiedenen Szenarien hinweg keine großräumig übereinstimmenden geographische Muster der Vegetationsveränderung. Für Äthiopien und die Sahara/Sahel-Übergangszone stimmten die Projektionen über GCMs und RCPs hinweg jedoch überein. Die simulierten Veränderungen der oberirdischen Biomasse wurden in erster Linie durch den Anstieg von CO<sub>2</sub> angetrieben und Annahmen zum CO<sub>2</sub>-Effekt verursachten die größte Variabilität in den Zukunftsprojektionen. Erhöhte CO<sub>2</sub>-Konzentrationen bewirkten ebenfalls eine Erhöhung der Wassernutzungseffizienz, insbesondere aufgrund einer Erhöhung der Photosynthese. Die größere Wassernutzungseffizienz stellt möglicherweise eine Entlastung bei Einschränkungen der Pflanzenproduktivität durch limitierte Bodenwasserressourcen dar. Auf der Ebene der Ökosysteme beförderten Interaktionen zwischen Feuer und Demographieprozessen der hölzernen Vegetation die Verbuschung zusätzlich. Insgesamt wiesen auch die Simulationen mit mittleren Auswirkungen des Klimawandels (RCP4.5) auf beträchtliche Ökosystemveränderungen, unabhängig vom CO<sub>2</sub>-Effekt auf Pflanzen, hin.

Basierend auf diesen Ergebnissen schlossen wir, dass in Afrika in der Zukunft erhebliche Biomveränderungen durch den Klimawandel und erhöhte CO<sub>2</sub>-Konzentrationen wahrscheinlich sind. Von den Simulationen mit und ohne direkte CO<sub>2</sub>-Effekte können wir für Ökosysteme eine Spanne potenzieller Einflüsse des CO<sub>2</sub>-Düngeeffekts im Zusammenspiel mit zukünftigem Klimawandel ableiten. Es ist jedoch unwahrscheinlich, dass CO<sub>2</sub>-Effekte auf Pflanzen in Savannenökosystemen vernachlässigbar sind, da in diesen Ökosystemen Rückkoppelungseffekte zwischen CO<sub>2</sub>-Effekt und Feuerdynamiken das Gleichgewicht zwischen Bäumen und Gräsern verschieben. Um die Unsicherheiten im Zusammenhang mit den CO<sub>2</sub>-Effekten auf Ökosysteme abzubauen, ist eine verbesserte Implementierung in Modellen und gezielte Forschung zu den CO<sub>2</sub>-Effekten notwendig. Der Einbau von Nährstoffkreisläufen ist wichtig für die Weiterentwicklung des aDGVM, um eine Einschränkung der CO<sub>2</sub>-Effekte durch Nährstofflimitierungen abbilden zu können. Aufgrund der großen Unsicherheiten der Zukunftsprojektionen ist es unerlässlich, dass Strategien und Maßnahmen zur Anpassung an den Klimawandel höchstflexibel sind.

Die simulierte Vegetation in Kapitel 2 stellt potenzielle, natürliche Vegetation dar. Simulationen der potenziellen, natürlichen Vegetation eignen sich besonders gut für die Untersuchung von Schutzgebieten mit ihren, im Idealfall vom Menschen ungestörten, Ökosystemen und möglichen Auswirkungen des Klimawandels auf die Schutzgebiete. Schutzgebiete existieren jedoch nicht isoliert von ihrer räumlichen Umwelt und gesellschaftlichen Entwicklungen. Afrikas Schutzgebiete stehen zunehmend durch Faktoren des globalen Wandels, wie beispielsweise Klimawandel, Bevölkerungswachstum und Veränderungen in der Landnutzung, unter Druck und sind gleichzeitig die letzte Hochburg der einzigartigen biologischen Vielfalt des Kontinents. Planungen für den Naturschutz werden dadurch erschwert, dass unklar ist, wie stark und wo diese Einflussfaktoren in den nächsten Jahrzehnten zusammenwirken werden. Deshalb haben wir in Kapitel 3 die Vegetationsprojektionen aus Kapitel 2 für afrikanische Schutzgebiete mit Projektionen für Bevölkerungsdichte und Landnutzung in der Umgebung der Schutzgebiete kombiniert. So konnten wir die Überschneidung von Auswirkungen des Klimawandels

mit sozioökonomischen Faktoren für afrikanische Schutzgebiete bis zum Ende des 21. Jahrhunderts analysieren. Für diese Analyse wurden von den Vegetationssimulationen zu Klimawandelszenarien aus Kapitel 2 nur Simulationen mit CO<sub>2</sub>-Effekten verwendet, da ein gewisser Einfluss des atmosphärischen CO<sub>2</sub> auf die Ökosysteme wahrscheinlich ist. Zwei Zukunftsszenarien, die eine Kombination aus gemeinsam genutzten sozioökonomischen Pfaden (shared socioeconomic pathways, SSPs) und RCPs sind, wurden untersucht. SSP2-RCP4.5 ist das "Mitte des Weges"-Szenario mit mittleren klimatischen Veränderungen und einer Fortsetzung der generellen Entwicklung und globaler Ungleichheiten beim Einkommenswachstum mit einigen regionalen Verbesserungen. Im Szenario SSP5-RCP8.5 basiert eine rasche wirtschaftliche und soziale Entwicklung auf technologischen Entwicklungen und der Nutzung fossiler Brennstoffe, womit ein starker Klimawandel einhergeht ("Fossil befeuerte Entwicklung").

Bei beiden Szenarien wurde für die meisten Schutzgebiete für mindestens einen der drei Einflussfaktoren eine ungünstige Entwicklung bis zum Ende des 21. Jahrhunderts projiziert. Das gemeinsame Auftreten der Faktoren bei Schutzgebieten war von Region zu Region und Szenario zu Szenario unterschiedlich. Die Vegetationsprojektionen wiesen auf eine erhebliche klimabedingte Zunahme der Baumsdeckung und einen Lebensraumverlust in den meisten Schutzgebieten in den heutigen Grasländern und Savannen hin. Für Schutzgebiete in Westafrika ergab die Analyse klimabedingte Vegetationsveränderungen in Kombination mit Hotspots mit hohem zukünftigen Bevölkerungs- und Landnutzungsdruck. Mit Ausnahme vieler Schutzgebiete in Nordafrika wurde für Schutzgebiete in ganz Afrika in beiden SSP-RCP-Szenarien im Allgemeinen eine zunehmende Belastung durch mindestens einen der drei untersuchten Faktoren des globalen Wandels prognostiziert. Zukünftige Abnahmen des Bevölkerungs- und Landnutzungsdrucks waren für Schutzgebiete außerhalb Nordafrikas selten. Auf kontinentaler Ebene führte SSP5-RCP8.5 zu stärkeren klimabedingten Veränderungen der Baumsdeckung und höherem Landnutzungsdruck, während SSP2-RCP4.5 mit einem höheren, zukünftigen Bevölkerungsdruck einherging. Beide SSP-RCP-Szenarien bedeuten zunehmende Herausforderungen für den Erhalt der afrikanischen Biodiversität in Schutzgebieten.

Trotz Unterschieden zwischen den Regionen und Szenarien lassen die Ergebnisse darauf schließen, dass die Auswirkungen des Klimawandels auf die Vegetation in den meisten Schutzgebieten und Regionen Afrikas wahrscheinlich durch sozioökonomischen Wandel noch verschärft werden. Diese Belastungen stellen eine Herausforderung für die Schutzziele des Übereinkommens über die biologische Vielfalt (Convention on Biological Diversity), wonach 30% der Landflächen geschützt werden sollen, dar. Unsere Ergebnisse zeigen, dass es notwendig ist Schutzmaßnahmen regional angepasst zu entwickeln und umzusetzen. Eine starke Eindämmung des zukünftigen Klimawandels zusammen mit gerechten, gesellschaftlichen Entwicklungsszenarien könnten dazu beitragen, die Auswirkungen auf Ökosysteme zu verringern und die Wirksamkeit des Naturschutzes in Afrika zu erhalten.

Die Vegetationssimulationen und -analysen auf kontinentaler Ebene in den Kapiteln 2 und 3 zeigen großräumige Muster für Vegetationsveränderungen unter dem Klimawandel auf. Aufgrund der geringen räumliche Auflösung dieser Simulationen sind sie für lokale Analysen jedoch ungeeignet. Darüber hinaus werden kleinräumigere Ökosysteme wie das Zwergstrauchland der Nama-Karoo im südlichen Afrika, welches nicht auf dem Grasland-Savanne-Wald-Spektrum liegt, durch die in vielen DVMs implementierten Pflanzentypen nicht gut repräsentiert. Gleichzeitig ist der Beitrag der Nama-Karoo zur Variabilität der globalen Kohlenstoffsenke unklar. Mögliche Auswirkungen des Klimawandels auf die Kohlenstoffdynamik der Nama-Karoo und das Gleichgewicht ihrer Zwergstrauch- und Grasvegetation sind ebenso ungewiss. In Kapitel 4 habe ich daher die Herausforderungen bei der Simulation der Pflanzen und des Kohlenstoffkreislaufs der Nama-Karoo mit dem aDGVM2 und seinem Strauchmodul herausgearbeitet. Mithilfe von aktuellen Kohlenstoffflussmessungen eines Eddy-Kovarianz-Turms konnten lokal simulierte Kohlenstoffflüsse, wie Photosynthese, Respiration und biotischer Abbau, eingeordnet werden. Die simulierte Vegetation habe ich darüber hinaus mit der Struktur beobachteter Vegetation verglichen. Für diese Analyse habe ich Module der Bodenwasserverfügbarkeit, Bodentiefe und Photosynthese in aDGVM2 reparametrisiert und getestet, mit welchen Modellkonfigurationen die Simulationsergebnisse verbessert werden.

In allen getesteten Konfigurationen des aDGVM2 wurden in den Simulationen sowohl die Kohlenstoffflüsse als auch die Biomasse für den Standort in der Nama-Karoo deutlich überschätzt. Mit keiner der implementierten Modellkonfigurationen konnten die Morphologie der Zwergsträucher und die Kohlenstoffflüsse sowie deren intra- und interannuelle Dynamik reproduziert werden. Im Vergleich zu einer aDGVM2-Basisversion verbesserten die verschiedenen Konfigurationen die Übereinstimmung für einzelne Komponenten der Kohlenstoffdynamik oder für die Biomasse. Bei Simulationen mit eingeschränkter Bodenwasserverfügbarkeit überlebte die Strauchvegetation nicht. In Simulationen ohne die Einschränkung der Bodenwasser Verfügbarkeit überlebten Sträucher, wurden aber mit Wuchshöhen von 1,5-3,2 m zu groß. Diese Wuchshöhen sind für Savannensträucher üblich, nicht aber für Nama-Karoo-Zwergsträucher mit einer Durchschnittshöhe von ~0,25 m am Untersuchungsstandort. In den Simulationen zeigte sich auch, dass die Simulation von Wasser- und Kohlenstoffprozessen im Boden von semiariden Ökosystemen eine Herausforderung darstellt. Die simulierte Bodenfeuchte senkte sich nicht auf den gemessenen Bereich ab und die heterotrophe Respiration wurde überschätzt. In semiariden Ökosystemen wie der Nama-Karoo begrenzt die Wasserverfügbarkeit einerseits das Pflanzenwachstum und bestimmt andererseits Abbauprozesse, bei denen Kohlenstoff frei gesetzt wird. Eine adequate Umsetzung der Bodenfeuchtedynamik im Modell ist entscheidend für die Simulation von Pflanzenwachstum und der Kohlenstoffdynamik.

Diese Unterschiede zwischen den aDGVM2-Simulationen und den Messungen verdeutlichen, dass die Ökologie von Zwergsträuchern durch das bestehende Strauch-Modul im aDGVM2 nicht abgebildet wird. Die Bewältigungsstrategien von Zwergsträuchern in semiariden Gebieten bei Trockenstress werden in der aktuellen aDGVM2-Implementierung von Sträuchern und holzigen Pflanzen nicht angemessen umgesetzt. Weitere Feldforschung zur Ökophysiologie und zu den Prozessen, die die Dynamik der Vegetation und der Bodenfeuchte in der Nama-Karoo bestimmen, ist notwendig, um das aDGVM2 für die Nama-Karoo zu parametrisieren. Falls eine solche Reparametrisierung nicht zu einer angemessenen Modellierung der Zwergsträucher führt, ist gegebenenfalls eine Implementierung von Zwergsträuchern als eigener funktionaler Pflanzentyp im aDGVM2 erforderlich. Wenn die Vegetationsdynamiken der

Nama-Karoo zufriedenstellend umgesetzt sind, ist die Einbindung von Herbivorie in aDGVM2-Simulationen ein wichtiger nächster Schritt, um so die in der Nama-Karoo weit verbreitete Bewirtschaftung mit Schafen zu berücksichtigen. Wenn diese Herausforderungen bewältigt werden, können DVMs ein mächtiges Instrument für die dringend benötigte Forschung zu den Auswirkungen des Klimawandels auf die Ökologie, aber auch auf die regionalen Lebensgrundlagen in der Nama-Karoo sein.

In dieser Arbeit habe ich Möglichkeiten, aber auch Grenzen und Unsicherheiten, von Simulationen und Klimawandelprojektionen mit den DVMs aDGVM und aDGVM2 für afrikanische Ökosysteme und deren Kohlenstoffbilanz sowie von der Kombination von DVM-Projektionen mit Projektionen zum globalen Wandel für afrikanische Schutzgebiete aufgezeigt. Die Analysen haben gezeigt, dass der Klimawandel unter mittleren bis hohen Emissionsszenarien wahrscheinlich zu großflächigen Veränderungen der Ökosysteme und der Kohlenstoffbilanz in Afrika führen wird. Die gezeigten Unsicherheiten bei der Implementierung des CO<sub>2</sub>-Düngeeffekts, der Dynamik von Bodenfeuchte in semiariden Gebieten, der Kohlenstoffflüsse und der Vegetationstypen in eher nischenartigen Ökosystemen wie der Nama-Karoo unterstreichen die Bedeutung weiterer Feldforschung und der Entwicklung von DVMs. Unsicherheiten beim CO<sub>2</sub>-Düngeeffekt führten für das mittlere Emissionsszenario zu einer kleineren Spanne potenzieller, zukünftiger Ökosystemzustände als beim Szenario mit hohen Emissionen. Dies bedeutet, dass Strategien und Maßnahmen zur Anpassung an den Klimawandel wahrscheinlich weniger komplex oder umfangreich sein müssen, wenn der Klimawandel minimiert wird. Für afrikanische Schutzgebiete könnten die Herausforderungen des Klimawandels durch sozioökonomische Faktoren in regional unterschiedlichem Ausmaß verschärft werden. Diese Analyse deutet darauf hin, dass für den erfolgreichen Schutz von Ökosystemen nicht nur Klimaschutzmaßnahmen entscheidend sind, sondern auch die Gewährleistung einer gerechten, nachhaltigen Entwicklung.

Insgesamt leistete diese Arbeit einen Forschungsbeitrag zu möglichen Auswirkungen des Klimawandels auf afrikanische Ökosysteme und deren Erhaltung, zu komplexen Zusammenhängen mit anderen Faktoren des globalen Wandels und zu Forschungslücken bei der Darstellung

afrikanischer Ökosysteme in DVMs. Zukünftige Forschungsansätze könnten die Anwendung von DVMs in der Attributionsforschung umfassen. Dabei könnte die Wahrscheinlichkeit des anthropogenen Klimawandels als Ursache von heute beobachteten Vegetationsveränderungen analysiert werden. Wenn dabei der anthropogene Klimawandel als wahrscheinliche Ursache für heutige Vegetationsveränderungen identifiziert werden sollte, könnten dies hilfreiche Informationen in der Kommunikation über die Auswirkungen des Klimawandels und der Sensibilisierung dafür sein. Darüber hinaus könnten Simulationen mit DVMs die Planung naturbasierter Lösungen (nature-based solutions) in terrestrischen Ökosystemen unterstützen. So könnte untersucht werden, inwiefern bei bestimmten naturbasierten Lösungen eine robuste Reaktion auf den Klimawandel zu erwarten ist oder der Verlust von Biodiversität verhindert werden kann.



# Contents

<b>Summary</b>	<b>v</b>
<b>Zusammenfassung</b>	<b>xiii</b>
<b>List of Figures</b>	<b>xxix</b>
<b>List of Tables</b>	<b>xliii</b>
<b>1 Introduction</b>	<b>1</b>
1.1 Background . . . . .	5
1.1.1 CO <sub>2</sub> fertilisation and ecosystem-fire dynamics in African savannas . . . . .	5
1.1.2 Dynamic vegetation models . . . . .	9
1.1.3 Scenarios for future climate change and societal developments . . . . .	12
1.2 Scope and overview of this thesis . . . . .	14
<b>2 Large uncertainties in future biome changes in Africa call for flexible climate adaptation strategies</b>	<b>17</b>
2.1 Abstract . . . . .	18
2.2 Introduction . . . . .	19
2.3 Materials and methods . . . . .	21
2.3.1 The aDGVM . . . . .	21
2.3.2 Regional climate model simulations . . . . .	23
2.3.3 Simulation design . . . . .	24
2.3.4 Analysis of simulation results . . . . .	24

2.4	Results . . . . .	27
2.4.1	Current aboveground biomass and future projections . . . . .	27
2.4.2	Future projections of WUE and underlying plant physiological processes	31
2.4.3	Projected biome changes and population dynamics . . . . .	33
2.4.4	Uncertainty of biome projections . . . . .	37
2.5	Discussion . . . . .	39
2.5.1	Plant-physiological effects of eCO <sub>2</sub> and drivers of woody encroachment .	39
2.5.2	Climate change impacts on biome patterns . . . . .	42
2.5.3	Uncertainties of vegetation projections . . . . .	44
2.5.4	Socio-economic development and flexible adaptation . . . . .	46
2.6	Acknowledgements . . . . .	47
2.7	Data Sharing and Accessibility . . . . .	48
<b>3</b>	<b>Combined impacts of future climate-driven vegetation changes and socioeconomic pressures on protected areas in Africa</b>	<b>49</b>
3.1	Abstract . . . . .	50
3.2	Introduction . . . . .	51
3.3	Methods . . . . .	53
3.3.1	Scenarios . . . . .	53
3.3.2	aDGVM and simulation design . . . . .	54
3.3.3	Data sets and data processing . . . . .	55
3.3.4	Data analysis . . . . .	57
3.4	Results . . . . .	59
3.4.1	Climate-driven vegetation changes . . . . .	59
3.4.2	Future socioeconomic pressures . . . . .	61
3.4.3	Co-occurrence of climate-driven vegetation changes and future socioeconomic pressures . . . . .	61
3.5	Discussion . . . . .	66
3.5.1	Climate change impacts on PAs . . . . .	69

3.5.2	Socioeconomic change impacts on PAs . . . . .	70
3.5.3	Combined socioeconomic and climate change impacts on PAs . . . . .	71
3.5.4	Study limitations . . . . .	72
3.5.5	Implications for conservation and management . . . . .	73
3.6	Acknowledgments . . . . .	75
3.7	Supporting Information . . . . .	75
<b>4</b>	<b>Towards carbon accounting in southern Africa's Nama Karoo ecosystem</b>	<b>77</b>
4.1	Abstract . . . . .	78
4.2	Introduction . . . . .	79
4.3	Ecosystem characteristics of the Nama Karoo . . . . .	82
4.3.1	General ecosystem characteristics . . . . .	82
4.3.2	Site description . . . . .	82
4.4	Carbon balance and previous steps towards carbon accounting for the Nama Karoo	85
4.4.1	Ecosystem carbon balance and its components . . . . .	85
4.4.2	Eddy covariance flux towers in Middelburg . . . . .	86
4.4.3	Previous modelling approaches . . . . .	86
4.5	Dynamic vegetation modelling experiment for Nama Karoo vegetation . . . . .	87
4.5.1	Methods . . . . .	87
4.5.1.1	Eddy covariance flux measurements for model evaluation . . . . .	87
4.5.1.2	aDGVM2 . . . . .	88
4.5.1.3	Yasso soil model . . . . .	90
4.5.1.4	Input data . . . . .	92
4.5.1.5	Sensitivity analysis . . . . .	94
4.5.2	Nama Karoo simulation results . . . . .	98
4.5.2.1	Carbon fluxes . . . . .	98
4.5.2.2	Biomass and vegetation structure . . . . .	101
4.5.2.3	Soil moisture and soil temperature . . . . .	103
4.5.3	Discussion . . . . .	105

4.5.3.1	Limitations of the eddy covariance flux tower data and field measurements . . . . .	105
4.5.3.2	Challenges in simulating the Nama Karoo with the aDGVM2 and knowledge gaps . . . . .	106
4.5.4	Requirements for the representation of dwarf shrubs in aDGVM2 . . . . .	110
4.6	Further considerations and future research opportunities . . . . .	115
<b>5</b>	<b>Synthesis</b>	<b>119</b>
5.1	Overview . . . . .	120
5.1.1	How does climate change affect African ecosystems and carbon stocks until the end of the 21 <sup>st</sup> century? . . . . .	121
5.1.2	Where may climate change impacts and the global change drivers human population density and land use co-occur and exert pressure on African protected areas until the end of the 21 <sup>st</sup> century? . . . . .	122
5.1.3	Which uncertainties do these future projections entail? Can the simulations be used to make detailed projections for individual ecosystems and their carbon dynamics or for individual protected areas? . . . . .	124
5.1.4	How well do we understand and reproduce carbon cycle dynamics in semi-arid niche ecosystems such as the Nama Karoo? . . . . .	127
5.2	Vision for future research with DVMs and aDGVM2 in particular . . . . .	130
5.2.1	Future avenues of model development to improve ecosystem representation in DVMs . . . . .	130
5.2.2	Attribution of anthropogenic climate change to observed vegetation change based on ensemble studies . . . . .	131
5.2.3	Dynamic vegetation models and model coupling to support the planning of nature-based solutions . . . . .	134
5.3	Conclusion . . . . .	137
<b>A</b>	<b>Supporting Information for “Large uncertainties in future biome changes in Africa call for flexible climate adaptation strategies”</b>	<b>139</b>

<b>B Supporting Information for “Combined impacts of future climate-driven vegetation changes and socioeconomic pressures on protected areas in Africa”</b>	<b>159</b>
<b>C Supporting Information for “Towards carbon accounting in southern Africa’s Nama Karoo ecosystem”</b>	<b>185</b>
C.1 Measurement campaign in October 2016 in Middelburg, Eastern Cape, South Africa . . . . .	185
<b>Bibliography</b>	<b>187</b>



## List of Figures

- 2.2 Mean total aboveground carbon and WUE in Africa in 2000–2099 under RCP4.5 and RCP8.5 with eCO<sub>2</sub> and fCO<sub>2</sub> simulated by the aDGVM. Thick lines are the mean over all six ensemble members per scenario. Shaded areas are the mean ± standard deviation (SD) of the six ensemble members per scenario. In (a), aboveground carbon for tropical Africa (64.5 Pg C, Baccini *et al.*, 2012), sub-Saharan Africa (Avitabile *et al.* 2016, and 48.3 Pg C, Saatchi *et al.*, 2011) and Africa (55.7 Pg C, Liu *et al.*, 2015) are depicted for comparison. See Appendix A Figure S3 for aboveground carbon time series of all individual ensemble members. Water use efficiency (WUE, b) is defined as the ratio of net primary production and transpiration. See Table S3 for more details on the variability of aboveground carbon and WUE in 2080–2099. aDGVM, adaptive Dynamic Global Vegetation Model; eCO<sub>2</sub>, elevated CO<sub>2</sub>; fCO<sub>2</sub>, CO<sub>2</sub> fixed at 400 ppm; RCP, representative concentration pathway . . . . . 29
- 2.3 Change in WUE (a) and stomatal conductance  $g_s$  (b) under eCO<sub>2</sub> and fCO<sub>2</sub>, and change in NPP versus change in MAP (continental scale, c) between 2000–2019 and 2080–2099 simulated by the aDGVM. Changes are represented by the ratio between values for 2000–2019 and 2080–2099 for each simulated grid cell. Values greater than 1 indicate an increase, values less than 1 indicate a decrease. Black lines in (a) are linear regressions for the respective RCP scenarios with the continental-scale mean of the scenario shown as a black point. Red lines represent the 1:1 lines. Each point represents a grid cell and is shape- and colour-coded according to its assigned biome type in 2000–2019. Lines in (c) are continental-scale regression lines for the four RCP-CO<sub>2</sub> scenario combinations. Appendix A Figure S5 for data points used to derive the MAP-NPP change regression lines for each scenario. Note that x- and y-axes do not have the same scale. aDGVM, adaptive Dynamic Global Vegetation Model; eCO<sub>2</sub>, elevated CO<sub>2</sub>; fCO<sub>2</sub>, CO<sub>2</sub> fixed at 400 ppm; MAP, mean annual precipitation; NPP, net primary production; RCP, representative concentration pathway; WUE, water use efficiency . . . 32

- 2.4 Consensus biome type under RCP8.5-elevated [CO<sub>2</sub>] (eCO<sub>2</sub>) in 2000–2019 (a), biome changes until 2080–2099 (b) and transitions and fractional cover of biomes (c) simulated by aDGVM. The consensus biome type is the biome simulated by at least three ensemble members of the scenario. Grid cells with an agreement of less than three ensemble members do not have a higher probability than an outcome by chance and are marked as ‘No consensus’. The biomes shown in (b) are the biomes that were simulated for 2080–2099 for grid cells where biome transitions were simulated for the consensus biome. Numbers in each coloured circle (c) represent the percentage of area covered by each biome at the respective time step in the consensus map. Arrows show biome changes with regard to the previous time step. Arrow thickness is proportional to the change in total area. In panel (c), only changes that affected more than 0.5% of the African land surface are shown. See Appendix A Figure S6 for RCP4.5-eCO<sub>2</sub>. aDGVM, adaptive Dynamic Global Vegetation Model; eCO<sub>2</sub>, elevated CO<sub>2</sub>; precipitation; RCP, representative concentration pathway . . . . . 33

- 2.5 Consensus biome type under RCP8.5-fCO<sub>2</sub> in 2000–2019 (a), biome changes until 2080–2099 (b) and transitions and fractional cover of biomes (c) simulated by aDGVM. The consensus biome type is the biome simulated by at least three ensemble members of the scenario. Grid cells with an agreement of less than three ensemble members do not have a higher probability than an outcome by chance and are marked as ‘No consensus’. The biomes shown in (b) are the biomes that were simulated for 2080–2099 for grid cells where biome transitions were simulated for the consensus biome. Numbers in each coloured circle (c) represent the percentage of area covered by each biome at the respective time step in the consensus map. Arrows show biome changes with regard to the previous time step. Arrow thickness is proportional to the change in total area. In panel (c), only changes that affected more than 0.5% of the African land surface are shown. See Appendix A Figure S7 for RCP4.5-fixed [CO<sub>2</sub>] (fCO<sub>2</sub>). aDGVM, adaptive Dynamic Global Vegetation Model; fCO<sub>2</sub>, CO<sub>2</sub> fixed at 400 ppm; precipitation; RCP, representative concentration pathway . . . . . 34
- 2.6 Change in African area covered by each biome in each GCM simulation and ensemble medians (box plots) under RCP4.5 and RCP8.5 with eCO<sub>2</sub> and fCO<sub>2</sub> simulated by aDGVM. Change is the difference in area covered between the time periods 2000–2019 and 2080–2099 in percentage points (left axis) and km<sup>2</sup> (right axis). aDGVM, adaptive Dynamic Global Vegetation Model; eCO<sub>2</sub>, elevated CO<sub>2</sub>; fCO<sub>2</sub>, CO<sub>2</sub> fixed at 400 ppm; GCM, general circulation model; RCP, representative concentration pathway . . . . . 35

- 2.7 Mean tree biomass change in relation to mean NPP change for eCO<sub>2</sub> (a, b) and fCO<sub>2</sub> (c, d) under RCP4.5 (a, c) and RCP8.5 (b, d) simulated by aDGVM. Change is represented by the ratio between 2000–2019 and 2080–2099. Hence, values greater than 1 indicate increase and values less than 1 indicate decrease. Black lines are regression lines for all data points of the mean of a scenario. Coloured lines are regression lines for the respective biomes in 2000–2019 of the mean of a scenario. The regression lines for biomes are marked with a symbol at the top right of each line with colour and shape of the respective biome. Each point represents the mean for a simulated grid cell, and colour and shape represent the grid cell's consensus biome type in 2000–2019. The mean of each scenario is based on the six GCM simulations in each time period. Note that the scales of x- and y-axes differ. aDGVM, adaptive Dynamic Global Vegetation Model; eCO<sub>2</sub>, elevated CO<sub>2</sub>; fCO<sub>2</sub>, CO<sub>2</sub> fixed at 400 ppm; GCM, general circulation model; NPP, net primary production; RCP, representative concentration pathway . . . . 36
- 2.8 Agreement of ensemble members in 2000–2019, under eCO<sub>2</sub> (a) and change in agreement until 2080–2099 under eCO<sub>2</sub> (b) and fCO<sub>2</sub> (c) for RCP8.5 in aDGVM simulations. The number of ensemble members simulating the consensus type is denoted as 'Agreement'. Grid cells with an agreement of less than three ensemble members are marked as 'No consensus'. We only displayed the number of ensemble members simulating the consensus type in 2000–2019 for eCO<sub>2</sub> in (a), because agreement is almost identical for eCO<sub>2</sub> and fCO<sub>2</sub> (see Appendix A Figures S8b and S9b). The consensus biome type is the biome simulated by at least three ensemble members of the scenario. See Appendix A Figure S10 for RCP4.5. aDGVM, adaptive Dynamic Global Vegetation Model; eCO<sub>2</sub>, elevated CO<sub>2</sub>; fCO<sub>2</sub>, CO<sub>2</sub> fixed at 400 ppm; RCP, representative concentration pathway . . . . 37

- 2.9 Probability of biome change between 2000–2019 and 2080–2099 simulated by aDGVM. The proportion of the six GCM ensemble members per scenario — here RCP8.5, eCO<sub>2</sub> (a) and fCO<sub>2</sub> (b) — that showed a biome change from 2000–2019 to 2080–2099 was used as a measure of probability of biome change. The more ensemble members projected a biome change per grid cell, the higher its probability of biome change. High probability of biome change — all six simulations project biome changes; medium probability of biome change — four or five simulations with biome changes; low probability of biome change — three simulations with biome changes; no change — zero to two simulations with changes. Grid cells with two or fewer simulations with biome changes do not have a higher probability than an outcome by chance and were therefore regarded as ‘No change’. Whether the ensemble members simulated the same type of biome transition was not considered here. See Appendix A Figure S11 for RCP4.5. aDGVM, adaptive Dynamic Global Vegetation Model; eCO<sub>2</sub>, elevated CO<sub>2</sub>; fCO<sub>2</sub>, CO<sub>2</sub> fixed at 400 ppm; GCM, general circulation model; RCP, representative concentration pathway . . . . . 38



- 3.2 (a) Climate-driven change in tree cover in protected areas (derived from adaptive dynamic global vegetation model based on results from Martens *et al.* [2021]) and (b) socioeconomic pressures in 10-km zones around protected areas by region under SSP2–RCP4.5 (SSP, shared socioeconomic pathways; RCP, representative concentration pathways) and SSP5–RCP8.5 scenarios (defined in Table 3.1 and text) (p.p., percentage points; pop., population; LU, land use; horizontal lines, median; box ends, 25% and 75% quantile; ends of whisker lines, smallest or largest value, respectively,  $\geq$  or  $\leq$  1.5 times the interquartile range beyond the box ends of protected areas in each group; \* continental scale medians from the Africa panel for each pressure and scenario combination). Regions are based on regions defined by the African Union (Appendix B S6). Absolute values for tree-cover change from 2000–2019 to 2080–2099 are used because both negative and positive tree-cover changes represent climate-driven vegetation changes. The socioeconomic pressures population (based on Gao [2017]) and land use (based on Hurtt *et al.* [2020]) in 10-km zones around the protected areas were rescaled from 0 to 10 (Equation 3.1; Appendix B S3) based on Venter *et al.*'s (2016) scheme. Pressures for protected areas by biome and region under both scenarios are in Appendix B S7 . . . . . 62



- 3.4 Climate-driven (a, b) tree-cover change in protected areas and population pressure in 10-km zones surrounding protected areas and (c, d) population pressure change in 10-km zones surrounding protected areas for (a, c) SSP2–RCP4.5 and (b, d) SSP5–RCP8.5 scenarios (defined in Table 3.1 and text) and habitat loss by region and biome (p.p., percentage points; cross, continental mean across protected areas; polygons, convex hulls of subgroups of protected areas; solid lines and filled circles, subgroups of protected areas projected to show habitat loss and their means; dashed lines and circles, subgroups of protected areas without habitat loss and their means). Tree-cover change derived from simulations with the adaptive dynamic global vegetation model (Martens *et al.*, 2021). Population density (based on Gao [2017]) in 10-km zones surrounding protected areas was scaled from 0 to 10 based on an adapted scheme from Venter *et al.* (2016). Pressure plots showing all individual protected areas and regions for SSP2–RCP4.5 and SSP5–RCP8.5, respectively, are in Appendices B S13 and B S14. Pressure-change plots showing individual protected areas and regions for SSP2–RCP4.5 and SSP5–RCP8.5, respectively, are in Appendices B S15 and B S16 . . . . . 67

- 3.5 Climate-driven (a, b) tree-cover change in protected areas and land-use pressure in 10-km zones surrounding protected areas and (c, d) land-use pressure change in 10-km zones surrounding protected areas for (a, c) SSP2–RCP4.5 and (b, d) SSP5–RCP8.5 scenarios (defined in Table 3.1 and text) and habitat loss by region and biome (p.p., percentage points; cross, continental mean across protected areas; polygons, convex hulls of subgroups of protected areas; solid lines and filled circles, subgroups of protected areas projected to show habitat loss and their means; dashed lines and circles, subgroups of protected areas without habitat loss and their means). Tree-cover change derived from simulations with the adaptive Dynamic Global Vegetation Model (Martens *et al.*, 2021). Land-use (based on Hurtt *et al.* [2020]) pressure factors in 10-km zones surrounding protected areas were scaled from 0 to 10 based on an adapted scheme from Venter *et al.* (2016). Pressure plots showing all individual protected areas and regions for SSP2–RCP4.5 and SSP5–RCP8.5, respectively, are in Appendices B S17 and B S18. Pressure change plots showing individual protected areas and regions for SSP2–RCP4.5 and SSP5–RCP8.5, respectively, are in Appendices B S19 and B S20

4.1 Eddy covariance flux tower sites that are registered with FLUXNET2015 or FLUXNET and their distribution across continents and biomes. The figure was taken from <https://fluxnet.org/sites/site-summary/> which was accessed on September 13, 2022 at 14:35. . . . .

4.2 Nama Karoo vegetation at the leniently grazed Middelburg eddy covariance flux tower site. Dwarf shrubs are the dominant life form (a, E. Falge, October 2015). Main dwarf shrub species include *Eriocephalus spinescens*, *Ruschia intricata* (b, C. Martens, October 2016), and *Eriocephalus ericoides* (c, C. Martens, October 2016) .

4.3 Daily net ecosystem exchange ( <i>NEE</i> ), gross primary production ( <i>GPP</i> ), and ecosystem respiration ( <i>Reco</i> ) at the leniently grazed eddy covariance flux tower site in Middelburg derived from tower measurements and from simulations with a base version of the adaptive dynamic global vegetation model 2 (aDGVM2). By convention, negative <i>NEE</i> values represent a carbon sink. For plotting purposes, <i>GPP</i> is shown as negative fluxes. For both measurements and simulations, a 30-day sliding average was used to smooth the data. The grey horizontal line indicates 0. . . . .	97
4.4 Net ecosystem exchange ( <i>NEE</i> ), gross primary production ( <i>GPP</i> ), and ecosystem respiration ( <i>Reco</i> ) at the leniently grazed eddy covariance flux tower site in Middelburg derived from tower measurements and from simulations with the adaptive dynamic global vegetation model 2 (aDGVM2) with different simulation setups. In panels on the left (a, c & e), results from adapted aDGVM2 versions with individual changes are shown (' <i>GPP/3</i> ', <i>GPP</i> reduced by factor of 1/3; 'Niche sep.', niche separation for soil water access; 'Soil thickn.', decreased soil layer thickness). In panels on the right (b, d & f), combinations of changes in the aDGVM2 are shown ('Comb. 1': <i>GPP/3</i> , niche separation, and soil thickness; 'Comb. 2': <i>GPP/3</i> and niche separation). Depicted aDGVM2 results are the mean of 20 simulations. The y axes scales differ for each sub plot. For both measurements and simulations, a 30-day sliding average was used to smooth the data. By convention, negative <i>NEE</i> values represent carbon uptake. The grey horizontal lines indicate 0. . . . .	99

- 4.5 Ecosystem respiration ( $Reco$ ) at the leniently grazed eddy covariance flux tower site in Middelburg derived from tower measurements and from simulations with the adaptive dynamic global vegetation model 2 (aDGVM2). For simulated  $Reco$ , the contributing components growth respiration ( $Rgr$ ), maintenance respiration ( $Rmt$ ), and heterotrophic respiration ( $Rhet$ ) are shown. For this simulation, aDGVM2 was modified so that  $GPP$  was reduced by a factor of 1/3 and the niche for soil water access was separated ( $sim_{comb2}$ ). Depicted aDGVM2 results are the mean across 20 simulations. For both measurements and simulations, a 30-day sliding average was used to smooth the data. . . . . 102
- 4.6 Soil moisture and soil temperature at the leniently grazed eddy covariance flux tower site in Middelburg derived from tower measurements and from simulations with the adaptive dynamic global vegetation model 2 (aDGVM2). For aDGVM2, results for different model setups are shown. aDGVM2 setups included the base version ‘Base’, setups with individual changes (‘ $GPP/3$ ’,  $GPP$  reduced by factor of 1/3; ‘Niche sep.’, niche separation for soil water access; ‘Soil thickn.’, decreased soil layer thickness), and setups with combinations of changes (‘Comb. 1’,  $GPP/3$ , niche separation, and soil thickness; ‘Comb. 2’,  $GPP/3$  and niche separation). Note that for (b) soil temperature simulation results for ‘Comb. 1’ and ‘Soil thickn.’ as well as for ‘Base’, ‘Comb. 2’, ‘ $GPP/3$ ’, and ‘Niche sep.’ are almost identical. Depicted aDGVM2 results are the mean across 20 simulations. For both measurements and simulations, a 30-day sliding average was used to smooth the data. . . . . 104



# List of Tables

2.1 Area (%) of Africa affected by biomass change and biome change between 2000–2019 and 2080–2099 and agreement of simulation results per scenario. Change for aboveground biomass (AGB) is given as the percentage of area with AGB increases or decreases. Where AGB increases and decreases did not sum to 100%, the remaining percentage of land area did not experience AGB changes. For biome change, proportions of area with no consensus biome in either period were not included. For agreement of biome state, only areas where all six ensemble members of a scenario agreed on simulated biome in 2080–2099 were included. The respective percentages refer to the total area of the African continent. . . . .	30
2.2 Change in aboveground biomass (AGB) and in WUE from 2000–2019 to 2080–2099. Change in carbon in AGB was calculated for all six ensemble members for each RCP-CO <sub>2</sub> scenario. The range of minimum and maximum change rate for the six ensemble members for each scenario are presented here. See Table S4 for change rates for each ensemble member. . . . .	30
2.3 Effect size of explanatory variables for change in carbon stored in aboveground biomass and WUE between 2000–2019 and 2080–2099. The table presents $\omega^2$ for the dependent variables aboveground biomass change (in Pg C) and WUE change (in gC/kgH <sub>2</sub> O) and explanatory variables CO <sub>2</sub> scenario, RCP scenario and GCM. Two-way interaction effects are included in the model and are denoted with ‘:’. . . . .	31

3.1	Shares of overall protected area in 2000-2019, and 2080-2099 and of projected habitat loss for each biome. . . . .	59
3.2	Spearman's rank correlation ( $\rho$ ) of pressures in and around protected areas for both SSP–RCP <sup>a</sup> scenarios at continental scale and on regional level . . . . .	63
4.1	Vegetation composition and biomass observed at the leniently grazed Middelburg eddy covariance flux tower site. Information on the October 2016 measurement campaign can be found in Appendix C. . . . .	85
4.2	Alternative functions for annual decomposition rate $k_a$ (1), temperature ( $T$ ) (2a-b) and soil moisture ( $SMC$ ) response modifier (3a-c) for heterotrophic respiration in the Yasso soil carbon model coupled with the aDGVM2. (1) is the original function in the Yasso soil carbon model. (2a-b) and (3a-c) were tested for the described simulation setup with daily time steps. Respective parameter values can be found in the cited literature. . . . .	92
4.3	Standard deviation (SD) for meteorological data from the eddy covariance flux tower for the leniently grazed site in Middelburg and the general circulation model GFDL-ESM2M (original and debiased data). The debiasing approach for meteorological data with gaps from Vuichard & Papale (2015) was used. . . . .	94

4.4 Root mean square error (RMSE) for simulated net ecosystem exchange ( <i>NEE</i> ), gross primary production ( <i>GPP</i> ), and ecosystem respiration ( <i>Reco</i> ) in comparison to measurements at an eddy covariance flux tower at a leniently grazed site in Middelburg, South Africa. Simulations were implemented with the adaptive dynamic global vegetation model 2 (aDGVM2). Observations and simulations covered November 2015 to October 2021. Results for six different simulation setups in aDGVM2 are shown: <i>sim<sub>base</sub></i> , simulations with a base version of aDGVM2; <i>sim<sub>GPP/3</sub></i> , <i>GPP</i> reduced by factor of 1/3; <i>sim<sub>niche</sub></i> , niche separation for soil water access; <i>sim<sub>soil</sub></i> , decreased soil layer thickness; <i>sim<sub>comb1</sub></i> , combination of <i>GPP/3</i> , niche separation, and decreased soil thickness; <i>sim<sub>comb2</sub></i> , combination of <i>GPP/3</i> and niche separation. aDGVM2 results were the mean across 20 simulations. . . . .	98
4.5 Annual balances for net ecosystem exchange ( <i>NEE</i> ), gross primary production ( <i>GPP</i> ), and ecosystem respiration ( <i>Reco</i> ) derived from an eddy covariance (EC) flux tower at a leniently grazed site in Middelburg, South Africa and simulations with the adaptive dynamic global vegetation model 2 (aDGVM2) from 2016 to 2020. In the aDGVM2 setup <i>sim<sub>niche</sub></i> , niche separation for soil water access is implemented. In <i>sim<sub>comb2</sub></i> , <i>GPP</i> reduced by a factor of 1/3 is combined with niche separation. aDGVM2 results for <i>sim<sub>comb2</sub></i> and <i>sim<sub>niche</sub></i> were each the mean across 20 simulations. . . . .	101

4.6 Vegetation structure and aboveground biomass simulated by aDGVM2 for the leniently grazed eddy covariance flux tower site in Middelburg. Values are means and standard deviation for the simulated time period November 2015 to October 2021. Results from adapted aDGVM2 versions in comparison to its base version ( $sim_{base}$ ) are shown. Individual changes included,  $GPP$  reduced by factor of 1/3 ( $sim_{GPP/3}$ ), niche separation for soil water access ( $sim_{niche}$ ), decreased soil layer thickness ( $sim_{soil}$ ). Simulations with combinations of changes in the aDGVM2 were  $sim_{comb1}$  ( $GPP/3$ , niche separation, and soil thickness) and  $sim_{comb2}$  ( $GPP/3$  and niche separation). aDGVM2 results for each simulation setup were the mean of 20 simulations. ‘–’ signifies that the respective plant functional type did not survive in aDGVM2. See Tab. 4.1 for observed values. . . 103

## Chapter 1

# Introduction

It is a truth, though not universally but widely acknowledged, that a single species, homo sapiens, in possession of good rationality must be in want of climate action today.\* This statement and this thesis is motivated by the fact that today's climate is changing at rates unprecedented in recent human history. Global surface temperature increased over the last 50 years at a rate not seen over the last 2000 years and the global mean temperature from 2011-2020 was warmer than any multi-century period since the last interglacial 125 000 years ago. As consolidated by the Intergovernmental Panel on Climate Change (IPCC), it is unequivocal that this change is largely driven by anthropogenic greenhouse gas emissions such as CO<sub>2</sub>. In Africa, increases in hot temperature extremes have been observed across the whole continent with high confidence in human contribution to these changes. Heavy precipitation events as well as agricultural and ecological drought have been observed especially in southern Africa (Arias *et al.*, 2022).

Terrestrial ecosystems are an important sink of atmospheric CO<sub>2</sub> and remove part of the anthropogenic CO<sub>2</sub> emissions from the atmosphere (Friedlingstein *et al.*, 2022). Dryland ecosystems have been found to be the key driver of the interannual variability and the trend of this global terrestrial carbon sink. However, the contribution of dryland ecosystems to driving the global variability vary. In Africa, savannas drove this variability whereas other African semi-arid ecosystems, such as the Nama Karoo in southern Africa, contributed less to the global variability (Ahlström *et al.*, 2015). Yet, uncertainties in modelling dryland vegetation and carbon cycle dynamics remain (Wang *et al.*, 2022) and our ability to simulate future climate change effects on dryland ecosystems lags behind more mesic systems (Osborne *et al.*, 2022). Understanding the response of land ecosystems and their carbon sink and source dynamics under climate change and increasing atmospheric CO<sub>2</sub> concentrations, including the antagonistic processes of carbon assimilation and heterotrophic respiration from decomposition (Prentice *et al.*, 2000), is key to understanding the potential buffering effects of ecosystems on the climate system by removing CO<sub>2</sub> from the atmosphere (Canadell *et al.*, 2007). A good grasp of dryland ecosystem responses to climate change is all the more critical, as many people's livelihoods depend on drylands and their ecosystem services (EMG, 2011).

---

\*Adapted from the first sentence in Austen (1813): "It is a truth universally acknowledged, that a single man in possession of a good fortune, must be in want of a wife."

Anthropogenic climate change already degraded ~13% of global dryland, which affects 213 million people who live mostly in low to middle income countries (Burrell *et al.*, 2020). The vast majority of Africa is covered by drylands (Wang *et al.*, 2022) and savannas are the dominant ecosystem on the continent (Scholes & Walker, 1993). Savannas are highly dynamic systems in which fire and herbivory are important ecosystem-shaping disturbances (Sankaran *et al.*, 2005). Links and feedbacks between vegetation, fire, climate, and atmospheric CO<sub>2</sub> may result in regionally varying climate change impacts in savannas (IPBES, 2019a). In the past, African savannas have already experienced both expansion (Gonzalez *et al.*, 2012) into previously more humid regions and increased woody cover in existing savanna ecosystems (Stevens *et al.*, 2017). However, ancient savannas and grasslands with their rich biodiversity (Bond, 2016) are slow to establish (Veldman *et al.*, 2015a). Thus, biome changes due to climate change may lead to loss of biodiversity and communities, which cannot easily be replaced by newly established savannas under climate change.

For southern Africa's semi-arid Nama Karoo, large uncertainties on ecosystem processes such as carbon dynamics (Rybchak *et al.*, 2023) and climate change impacts on ecosystem functioning (Henschel *et al.*, 2018) persist. At the same time, most parts of the Nama Karoo, which is a mixture of dwarf shrubs and grasses, is used for livestock production (du Toit *et al.*, 2018). Therefore, a good understanding of feedbacks between ecosystem dynamics, herbivory and climate in the Nama Karoo are also important for land use planning. The naturally high variability of environmental conditions and particularly of precipitation in semi-arid ecosystems (e.g., Kew *et al.*, 2021 for eastern Africa and du Toit & O'Connor, 2014 for precipitation variability in the eastern Nama Karoo) complicates the development of a good understanding for the Nama Karoo and potential climate-change impacts. These uncertainties are also reflected in the difficulties of modelling the Nama Karoo and other Southern African biomes, that are not represented on the forest-savanna-grassland spectrum, and potential biome transitions and shifts under climate change with dynamic vegetation models (DVMs, Moncrieff *et al.*, 2015).

Soil moisture was found to be the main driving force of vegetation changes (Higgins *et al.*, 2023b) and carbon dynamics for semi-arid ecosystems (Liu *et al.*, 2023). In these ecosystems,

water availability limits plant growth (Venter, 2001) and drives carbon release from decomposition processes in the soil (Zhou *et al.*, 2021). However in semi-arid regions, response times and strengths differ for assimilation through photosynthesis (gross primary production, *GPP*) and carbon release through respiration from both above and below-ground processes (Poulter *et al.*, 2014). The net carbon balance, measured as net ecosystem exchange (*NEE*), is often close to zero and can switch between being a carbon source or sink from one year to the next in semi-arid ecosystems (Dannenberg *et al.*, 2023). At local scale, eddy covariance flux towers improve our understanding of spatial and temporal ecosystem carbon dynamics by measuring *NEE* and thus recording carbon exchange dynamics between the atmosphere and the local ecosystem (Chapin III *et al.*, 2011, p.208). However, only few eddy covariance measurement sites across Africa and its semi-arid ecosystems are available (Abdi *et al.*, 2019; Valentini *et al.*, 2014). In addition, this data is rarely used for testing and benchmarking of modelled carbon fluxes in process-oriented modelling studies for Africa (Valentini *et al.*, 2014) or dryland regions (Mac-Bean *et al.*, 2021). In Middelburg, Eastern Cape, South Africa in the Nama Karoo, two eddy covariance flux towers were installed in October 2015. These measurements can contribute to an improved understanding of carbon and ecosystem dynamics in the Nama Karoo (Rybchak *et al.*, 2023) and climate change impacts.

Brook *et al.* (2008) highlighted the importance of investigating climate change in combination with other factors threatening biodiversity. Land use change, resource exploitation, pollution and invasion of alien species are other important components of global change that drive large changes in biodiversity (Brook *et al.*, 2008). A combination of these drivers can reinforce each other's effects (IPBES, 2019b). For sub-Saharan Africa, Leisher *et al.* (2022) found crops, logging and wood harvesting, and hunting as main threats to biodiversity conservation, currently outranking the threats from climate change. Conversion and degradation of habitats due to land use have caused global declines in biodiversity with major declines in the Sahel, the west African coast, east Africa, and southern Africa (Newbold *et al.*, 2015). In consequence, Africa's biodiversity is increasingly restricted to protected areas (e.g., Pacifici *et al.*, 2020, for mammal species). The pressure on biodiversity is expected to intensify with a growing, more affluent

human population in the future (Powers & Jetz, 2019). These developments and prognoses motivated the adoption of the target to protect at least 30% of both land and sea areas by 2030 under the Kunming-Montreal global biodiversity framework of the Convention on Biological Diversity (CBD COP, 2022).

In this thesis, I used DVMs to investigate future scenarios of climate change impacts on ecosystems and carbon cycles in Africa and uncertainties associated with these DVM simulations and projections. In combination with projections for human population and land use, I used DVM projections to analyse the co-occurrence of potential future global change pressures on African protected areas. I investigated challenges associated with simulating a semi-arid niche ecosystem and its carbon cycle with a DVM using the example of the Nama Karoo. To provide thematic background for my thesis, I present introductions to key cross-cutting topics in the following sections. This includes information on the CO<sub>2</sub> fertilisation effects and ecosystem dynamics in savannas (Section 1.1.1), on DVMs (Section 1.1.2), and on scenarios for future climate change and societal developments (1.1.3). Finally, I present the main research questions and a short overview of this thesis (Section 1.2).

## 1.1 Background

### 1.1.1 CO<sub>2</sub> fertilisation and ecosystem-fire dynamics in African savannas

Rising atmospheric CO<sub>2</sub> concentrations are a main driver of climatic and environmental changes. The role of CO<sub>2</sub> as a greenhouse gas that drives climate change is well established and highlighted in assessment reports of the IPCC (Arias *et al.*, 2022). Apart from the indirect effect of greenhouse-gas-driven impacts of climate change on ecosystems, changes in CO<sub>2</sub> concentrations also have a direct impact on plant physiology stimulating plant photosynthesis and carbon assimilation (De Kauwe *et al.*, 2014), especially in plants with the C<sub>3</sub> photosynthetic pathway. In the associated, so-called CO<sub>2</sub> fertilisation effect, it is assumed that increased assimilation rates drive increases in vegetation biomass. However, it is unclear if and under which conditions the increased assimilation translates into increased biomass production (e.g., Körner

*et al.*, 2007). Tissue growth rather than assimilation may be the limiting factor of biomass production (Körner, 2015). Limited availability of nutrients such as nitrogen or phosphorus was found to attenuate the effect of elevated CO<sub>2</sub> concentrations on plant growth (e.g., Jiang *et al.*, 2020a; Luo *et al.*, 2004).

CO<sub>2</sub> is an essential substrate required for photosynthesis and the current atmospheric CO<sub>2</sub> concentration remains below saturation levels of the photosynthetic reaction for C<sub>3</sub> plants (Fig. 1.1). For plants with C<sub>4</sub> photosynthetic pathway, photosynthesis levels have already plateaued at current atmospheric CO<sub>2</sub> concentrations, but for C<sub>4</sub> crops some stimulating effects of elevated CO<sub>2</sub> have also been found (Körner *et al.*, 2007). In experimental setups that tested individual plant responses to elevated CO<sub>2</sub>, generally the response of C<sub>3</sub> plants was stronger than that of C<sub>4</sub> plants, fast-growing plants were stimulated more than slow-growing plants, and nitrogen-fixing plants responded more than non-fixing plants. However, these responses are weakened in multi-species communities (Potvin *et al.*, 2007). For example, the presence of C<sub>4</sub> grass competition but also simulated herbivory reduced growth responses of seedlings of the prolific C<sub>3</sub> tree *Vachellia karoo*, a common encroaching species in southern African savanna (Raubenheimer & Ripley, 2022).

In addition to increasing assimilation rates, elevated CO<sub>2</sub> reduces stomatal conductance (Eamus, 1991). Variations in the level of reduction of stomatal conductance under elevated CO<sub>2</sub> concentrations are driven by soil moisture availability (De Kauwe *et al.*, 2021). Decreased stomatal conductance rates in combination with increased assimilation rates result in an increased water use efficiency of plants (De Kauwe *et al.*, 2021), where water use efficiency reflects the trade-off between carbon uptake and water loss for vegetation (Liu *et al.*, 2020). In line with this in Australian savanna, increases in ambient CO<sub>2</sub> concentrations over a 33 year measurement period from 1982 to 2014 have led to an increased water use efficiency. Precipitation trend was an important additional driver and droughts led to declines in water use efficiency in forests in southern Australia (Liu *et al.*, 2020). It is not clear yet if rising CO<sub>2</sub> concentrations can ameliorate plant water stress in water-limited conditions (De Kauwe *et al.*, 2021; Wang *et al.*, 2022).

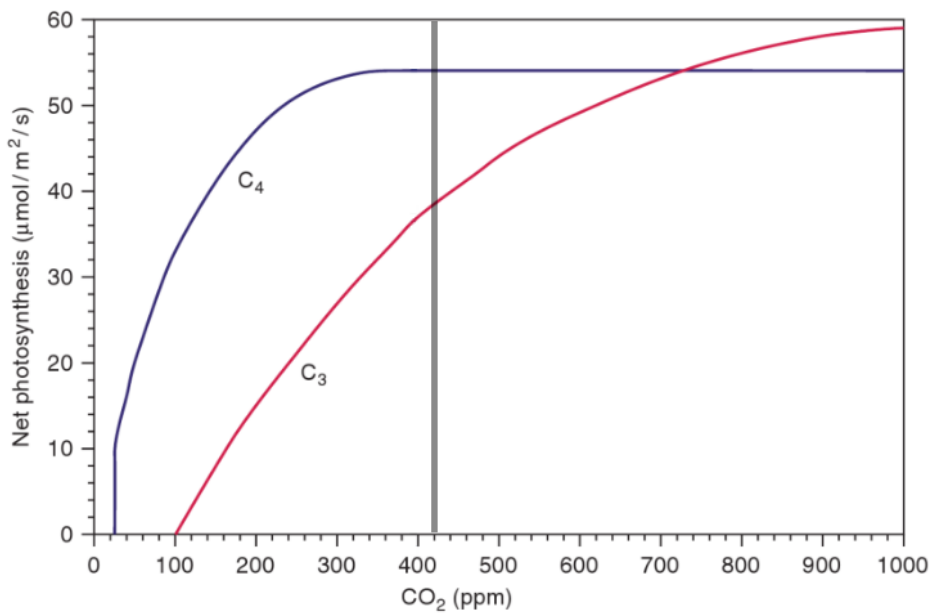


FIGURE 1.1: Schematic response of C<sub>3</sub> and C<sub>4</sub> photosynthesis to atmospheric CO<sub>2</sub> concentrations, adapted from Newman (2011, p. 76). The vertical grey line marks atmospheric CO<sub>2</sub> concentrations at 420 ppm, the approximate concentration measured in Mauna Loa, Hawaii, in March 2023 (<https://gml.noaa.gov/ccgg/trends/mlo.html>, accessed on March 17, 2023).

Seedlings of woody C<sub>3</sub> species grow faster under elevated atmospheric CO<sub>2</sub> concentrations. This does not necessarily mean that the plants will accumulate more biomass in their lifespan (Körner *et al.*, 2007). However, faster growth can provide woody plants with a critical advantage in African grassy ecosystems with fire disturbance, such as savannas (Fig. 1.2). Fires can lead to the death of aboveground biomass including stem biomass for trees, the so-called topkill (Higgins *et al.*, 2000), keeping the ecosystem open (Bond, 2008). With CO<sub>2</sub>-stimulated growth, C<sub>3</sub> trees can grow taller than the fire zone more quickly. Thus, the likelihood that they escape the fire trap increases (Kgope *et al.*, 2010). When more trees are alive with aboveground biomass after a fire, tree canopy cover increases. Light availability for grasses decreases with increased tree canopy cover suppressing grass growth, because of the high shade intolerance of C<sub>4</sub> grasses (Lehmann *et al.*, 2011). In Africa these feedback loops are especially relevant in regions with mean annual precipitation between 1000 mm and ~2500 mm, where fire differentiates between savanna and forest as alternative stable states (Staver *et al.*, 2011b).

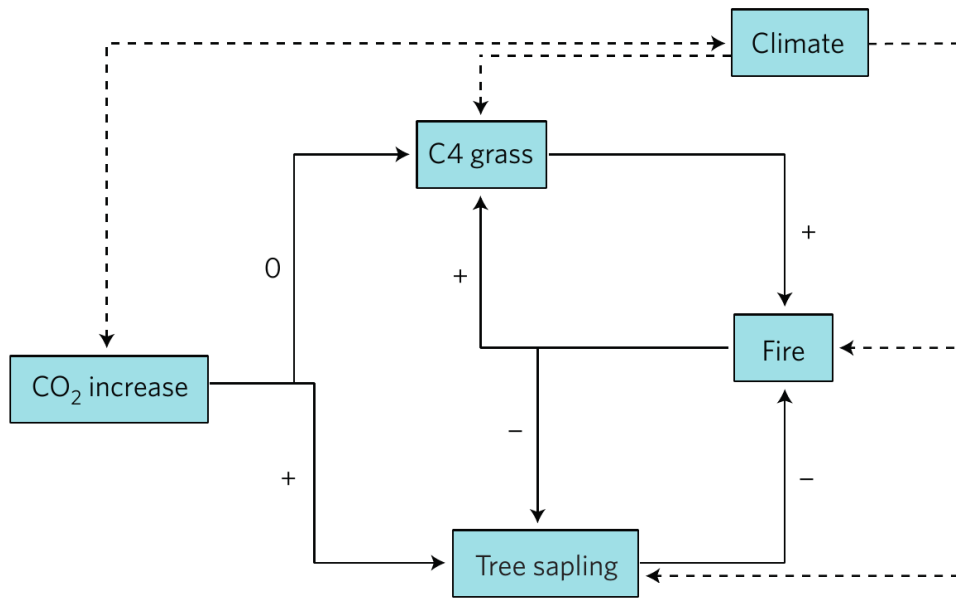


FIGURE 1.2: Interactions and feedbacks of atmospheric CO<sub>2</sub> concentration, growth of C<sub>4</sub> grasses and C<sub>3</sub> trees, and fire, adapted from Midgley & Bond (2015). '+', '0', and '-' signify enhancing, neutral, and inhibiting effects, respectively. Climate consists of multiple components such as temperature and precipitation that also drive these dynamics, but that are not elaborated here.

Africa's savanna fires are mostly characterised by small, frequent, low-intensity fires that are grass-fuelled (Archibald *et al.*, 2013). Therefore, less grass biomass implies less fuel biomass for fires and thus a lower fire occurrence. Less fire additionally promotes the establishment of trees (Midgley & Bond, 2015). This feedback loop with demographic changes towards more tree-dominated ecosystems leads to biomass increases (Bond & Midgley, 2012). This is in line with findings that rising CO<sub>2</sub> may lead to changes in plant community structure, especially in highly dynamic ecosystems, which may lead to changes in ecosystem biomass. Species composition and climate variables, e.g., precipitation, are critical factors influencing whether ecosystem biomass increases under elevated CO<sub>2</sub> (Potvin *et al.*, 2007). Herbivory is another major ecosystem-shaping disturbance in African savanna limiting tree cover (Midgley & Bond, 2015) but is not a main focus in this thesis. It is therefore not described in detail here.

### 1.1.2 Dynamic vegetation models

Observations of ecosystems and experimental manipulations are valuable methods that increase the understanding of ecosystem functioning and key processes, but their scope is limited in time and space. Modelling approaches help to combine and integrate ecological information from different sources (Prentice *et al.*, 2007) and to test derived hypotheses and our understanding of ecosystem components (Schulze *et al.*, 2019, p. 514). Approaches of vegetation models range from, e.g., empirical to mechanistic and stochastic to deterministic and vary in their spatial and temporal scale. Dynamic vegetation models (DVMs) are suitable when investigating climate change impacts on ecosystems, because they allow studying dynamic, transient behaviour of ecosystems to external drivers. As mechanistic models, they try to emulate ecosystem processes and interactions between different ecosystem components (Schulze *et al.*, 2019, p. 514-515). Simulated processes range from photosynthesis at leaf level, to plant phenology and demographic processes such as mortality at plant level, to competition at stand level. Environmental input data such as meteorological variables, atmospheric CO<sub>2</sub> concentrations, or soil physical properties drive processes in DVMs. Provided projections of climate variables are available, DVMs can be used to investigate future climate change impacts on vegetation under different climate change scenarios (Prentice *et al.*, 2007).

DVM developers typically make use of so-called plant functional types (PFTs) to represent main growth forms and plant functions of ecosystems (Prentice *et al.*, 2007). PFTs are artificial constructs that are based on functional plant traits that are linked to plant functions. These functional traits can be morphological, ecophysiological, biochemical, demographical or phenomenological. They are considered to reflect adaptations to environmental conditions and tradeoffs between different plant functions such as acquisition of light versus acquisition of water. Growth forms represent many tradeoffs in functional traits and have been used as basis for creating PFT classifications in DVMs (Lavorel *et al.*, 2007). State variables of a PFT or its simulated individuals such as size of plant biomass compartments, leaf area index, or plant height change dynamically throughout a simulation. In DVMs, different PFTs usually co-occur and compete with each other (Prentice *et al.*, 2007).

The adaptive dynamic global vegetation model (aDGVM) is an individual-based DVM. It was originally developed for tropical vegetation with a focus on Africa (Scheiter & Higgins, 2009), but was also applied to other tropical regions such as parts of Australia, South America and South Asia (Kumar & Scheiter, 2019; Moncrieff *et al.*, 2016; Scheiter *et al.*, 2015). Next to well-established implementations for photosynthesis, respiration, and evapotranspiration (Arora, 2002; Ball *et al.*, 1987; Collatz *et al.*, 1991, 1992; Farquhar *et al.*, 1980; Ronda *et al.*, 2001; Schulze *et al.*, 1994), the aDGVM includes modules for phenology and carbon allocation that adapt to changing environmental conditions for simulated plant individuals. The implemented fire model (Higgins *et al.*, 2000, 2008) simulates the effect of fire on individual trees (Scheiter & Higgins, 2009).

In aDGVM, vegetation is represented by two growth forms, grasses and trees. Trees can either grow as fire-resistant, shade-intolerant savanna trees or fire-sensitive, shade-tolerant forest trees. Grasses can have C<sub>3</sub> or C<sub>4</sub> photosynthetic pathways (Scheiter *et al.*, 2012). Trees are simulated as plant individuals, while grasses are simulated as superindividuals that either grow under or between tree canopies (Scheiter & Higgins, 2009). Thus, 4 different PFTs (2 grass types each represented by 2 superindividuals and 2 tree types) are simulated in aDGVM.

Fire is an important ecosystem-shaping disturbance in tropical grass-tree ecosystems such as savannas and keeps them open (Bond *et al.*, 2005). The implementation in aDGVM was specifically developed to account for these dynamics and simulates fire effects for individual trees (Scheiter & Higgins, 2009). In observations of the topkill effect, trees shorter than a certain height, with smaller stem diameters and bark thicknesses die, whereas taller trees are usually not affected (Hoffmann & Solbrig, 2003). In aDGVM, a combination of height, fuel moisture, and wind influences fire intensity and thus, in combination with an individual's carbon balance, topkill survival probability of tree individuals (Scheiter & Higgins, 2009).

The aDGVM2 was developed with the objective of including concepts from community assembly theory and coexistence theory into vegetation modelling. It implements a more flexible, trait-based approach as opposed to PFTs with fixed plant traits (Scheiter *et al.*, 2013). This takes into account that considerable variation in trait values occurs within a life form (Lavorel

*et al.*, 2007). The simulated plant community in aDGVM2 assembles based on the performance of each plant with its individual combination of trait values under given environmental conditions such as water availability. Tradeoffs between the traits ensure that only plants with realistic trait combinations establish and different strategies of trait combination within, e.g., a woody PFT evolve and coexist. Basic structures and implementations of aDGVM2 are based on processes in the aDGVM (Scheiter *et al.*, 2013).

Individual plants in aDGVM2 can have individual sets of trait combinations. Plant growth and competition between plant individuals is defined by these trait combinations for each plant. Trait combinations that are favourable under the given environmental conditions enable plant individuals to prosper and grow so that they eventually produce seeds. Seeds inherit the traits of the plant individual that produced them. This results in trait filtering, where only trait combinations from reproductive individuals are passed on to new plant individuals. Traits from a reproductive individual can also cross-over with traits from other reproductive individuals and adopt their value. In addition in seed production, individual traits of a reproductive individual can randomly be mutated, which introduces new trait combinations into the community (Scheiter *et al.*, 2013). This implementation also allows a more flexible representation of biodiversity in a DVM. In aDGM2, plant individuals can be grouped into PFTs in post-processing of simulation results and PFTs can thus be tailored to specific research questions (Scheiter *et al.*, 2013).

Both aDGVM and aDGVM2 originally only included grass and tree growth forms. Because large parts of Africa apart from the tropical rainforest and the deserts are at least partially covered by shrubs (Tuanmu & Jetz, 2014), Gaillard *et al.* (2018) developed a shrub sub-module for aDGVM2. In this shrub model, woody plant individuals can either grow multi-stemmed or single-stemmed. This implements a trade-off between water-uptake capacity and height-growth. Single-stemmed trees can grow higher and are thus more competitive in a light-limited environment. Multi-stemmed shrubs have higher sapwood area in relation to single-stemmed trees with the same stem biomass. In aDGVM2, the efficiency in water uptake increases with sapwood area. Thus, the more efficient water uptake provides multi-stemmed shrubs with a

competitive advantage in water-limited environments. Stem number is a trait for woody plant individuals that is constant throughout their life span and can be modified in seeds by mutation or cross-over. Through trait-filtering, the trade-off between water uptake efficiency and height growth leads to the dominance of woody plant individuals that are better adapted to water- or light-limited environmental conditions (Gaillard *et al.*, 2018).

### 1.1.3 Scenarios for future climate change and societal developments

Climate is one of the controlling factors of vegetation and ecosystem processes and states. Therefore, future ecosystem states depend on future climate. Because climate depends on the chemical composition of the atmosphere and surface properties (Chapin III *et al.*, 2011, pp. 14, 23), different climate futures are possible depending on anthropogenic drivers such as greenhouse-gas emissions and land-use. To test the impact on future climate but also on, e.g., future ecosystem states, alternative future scenarios and development paths for these drivers have been developed in the context of the IPCC (O'Neill *et al.*, 2016).

Currently, there are two sets of scenarios relevant for climate change and climate-change impact projections until 2100, the representative concentration pathways (RCPs) and the shared socioeconomic pathways (SSPs). The RCPs provide information on components of radiative forcing such as greenhouse-gas emissions and land use that are required for climate modeling. Radiative forcing is the change in energy flux in the atmosphere which drives changes in climate. The naming of the scenarios follows the respective radiative forcing level in 2100, e.g., RCP8.5 corresponds to  $8.5 \text{ W/m}^2$  radiative forcing. The RCP scenarios that were originally developed for the IPCC's Fifth Assessment Report covered RCP2.6, RCP4.5, RCP6, and RCP8.5  $\text{W/m}^2$  (van Vuuren *et al.*, 2011).

In the SSPs, narratives for socioeconomic futures were developed, which include assumptions and quantitative descriptions of factors such as population, economic growth and urbanisation until 2100. The SSP narratives cover SSP1 - "sustainability" with low challenges to mitigation and adaptation, SSP2 - "middle of the road" with medium challenges to mitigation and adaptation, SSP3 - "regional rivalry" with high challenges to mitigation and

adaptation, SSP4 - “inequality” with low challenges to mitigation and high challenges to adaptation, and SSP5 - “fossil-fueled development” with high challenges for mitigation and low challenges to adaptation (Fig. 1.3). Basic projections around these narratives are used as input for so-called integrated assessment models (IAM) that cover more complex projections for, e.g., energy systems, land-use changes, and associated greenhouse-gas emissions. Different IAMs use different assumptions and approaches to implement a specific SSP narrative and vary in their projections of, e.g., greenhouse-gas emissions. The RCP and SSP scenarios can be combined to SSP-RCP scenarios, where different assumptions and implementations in IAMs for an individual SSP scenario can achieve different radiative forcings for RCP scenarios. Not all SSP and RCP scenarios are compatible with each other and feedbacks from the climate system on the socioeconomic system are not incorporated in the IAM implementations of SSP scenarios (Riahi *et al.*, 2017).



FIGURE 1.3: Shared socioeconomic pathways (SSPs) that are based on different combinations of challenges for climate mitigation and adaptation from O’Neill *et al.* (2017).

These scenarios describe anthropogenic drivers of climate change consistent with socioeconomic developments and allow to assess impacts on ecosystems and societies (O'Neill *et al.*, 2016). Spatially explicit land use projections from the IAMs (Hurtt *et al.*, 2020) and population projections (Gao, 2019) facilitate the analysis of potential consequences of different societal developments. Climate change projections based on the RCP scenarios can be used to project vegetation dynamics into the future with DVMs (Prentice *et al.*, 2007).

## 1.2 Scope and overview of this thesis

The main motivation for this thesis was to contribute to an improved understanding of ecosystem processes and the impacts of climate change and global change on African ecosystems. As DVMs are particularly suitable for future projections under climate change and analysing individual processes, they are the main tool applied to answer the following main research questions that guided this thesis:

1. How does climate change affect African ecosystems and carbon stocks until the end of the 21<sup>st</sup> century?
2. Where may climate change impacts and the global change drivers human population density and land use co-occur and exert pressure on African protected areas until the end of the 21<sup>st</sup> century?
3. Which uncertainties do these future projections entail? Can the simulations be used to make detailed projections for individual ecosystems and their carbon dynamics or for individual protected areas?
4. How well do we understand and reproduce carbon cycle dynamics in semi-arid niche ecosystems such as the Nama Karoo?

This thesis is based on two publications, Martens *et al.* (2021, Chapter 2) and Martens *et al.* (2022, Chapter 3), and an unpublished manuscript (Chapter 4). The publications are included as published with minor formatting changes.

The focus of Chapter 2 lies on vegetation change projections with aDGVM for Africa until the end of the 21<sup>st</sup> century. Uncertainties associated with climate input data, chosen climate change scenario, and CO<sub>2</sub> fertilisation effect were analysed. The analysis was focused on biome changes and changes in the water use efficiency of simulated vegetation and addresses research questions 1 and 3.

In Chapter 3, the potential, future co-occurrence of the global change drivers climate change, human population growth, and land-use change were analysed for African protected areas. The aDGVM projections for climate-change impacts on vegetation from Chapter 2 were combined with data on human population densities and land use until the end of the 21<sup>st</sup> century to address research question 2. The discussion of uncertainties associated with this analysis adds an additional aspect for research question 3.

In Chapter 4, the focus shifts to a smaller scale zooming in on the challenges of simulating and reproducing ecosystem dynamics in South Africa's Nama Karoo dwarf shrub ecosystem. Data from an eddy covariance flux tower on ecosystem carbon fluxes and vegetation structure were the basis for reparameterising the aDGVM2 and benchmarking of simulation results. This analysis was used to derive knowledge gaps in the process understanding of the Nama Karoo and the representation of dwarf shrubs, its main vegetation component, in aDGVM2. In this chapter, I focused on research question 4 and delved further into research question 3 and the uncertainties associated with simulating a specific African ecosystem and its carbon dynamics.

The research questions are reviewed in Chapter 5 based on a synthesis of the presented research and are put into a wider context. Based on the presented research, potential avenues of future research are suggested.



## Chapter 2

# Large uncertainties in future biome changes in Africa call for flexible climate adaptation strategies

Carola Martens, Thomas Hickler, Claire Davis-Reddy, Francois Engelbrecht, Steven I. Higgins,  
Graham P. von Maltitz, Guy F. Midgley, Mirjam Pfeiffer and Simon Scheiter \*†

---

\*This chapter is published as Martens *et al.* (2021) Large uncertainties in future biome changes in Africa call for flexible climate adaptation strategies, *Global Change Biology*, 27: 340–358. <https://doi.org/10.1111/gcb.15390>. Supporting information can be found in Appendix A.

†Author contributions: CM, SS and TH conceived the study. CM designed and conducted the analysis of simulation results and led the writing of this article. SS conducted the simulations for this study. SS and TH contributed to the analysis of simulation results. CDR and FE provided the climate forcing data used in this article. GFM provided valuable support for the implementation of this study. TH, FE, SIH, GPvM, GFM, MP and SS contributed to the writing of this article.

## 2.1 Abstract

Anthropogenic climate change is expected to impact ecosystem structure, biodiversity and ecosystem services in Africa profoundly. We used the adaptive Dynamic Global Vegetation Model (aDGVM), which was originally developed and tested for Africa, to quantify sources of uncertainties in simulated African potential natural vegetation towards the end of the 21<sup>st</sup> century. We forced the aDGVM with regionally downscaled high-resolution climate scenarios based on an ensemble of six General Circulation Models (GCMs) under two Representative Concentration Pathways (RCPs 4.5 and 8.5). Our study assessed the direct effects of climate change and elevated CO<sub>2</sub> on vegetation change and its plant-physiological drivers. Total increase of carbon in aboveground biomass in Africa until the end of the century was between 18-43% (RCP4.5) and 37-61% (RCP8.5) and was associated with woody encroachment into grasslands and increased woody cover in savannas. When direct effects of CO<sub>2</sub> on plants were omitted, woody encroachment was muted and carbon in aboveground vegetation changed between (-8)-11% (RCP4.5) and (-22)-(-6)% (RCP8.5). Simulated biome changes lacked consistent large-scale geographical patterns of change across scenarios. In Ethiopia and the Sahara/Sahel transition zone, the biome changes forecast by the aDGVM were consistent across GCMs and RCPs. Direct effects from elevated CO<sub>2</sub> were associated with substantial increases in water use efficiency, primarily driven by photosynthesis enhancement, which may relieve soil moisture limitations to plant productivity. At the ecosystem level, interactions between fire and woody plant demography further promoted woody encroachment. We conclude that substantial future biome changes due to climate and CO<sub>2</sub> changes are likely across Africa. Because of the large uncertainties in future projections, however, adaptation strategies must be highly flexible. Focused research on CO<sub>2</sub> effects, and improved model representations of these effects will be necessary to reduce these uncertainties.

## 2.2 Introduction

Climate change is expected to drive changes in ecosystem structure and functioning as well as geographical shifts of ecosystems and biomes (Engelbrecht & Engelbrecht, 2016; Hoegh-Guldberg *et al.*, 2018; Niang *et al.*, 2014). Such ecosystem changes will impact the potential for future land uses and the livelihoods of people in Africa, where agriculture accounts for 50% of employment in 2019 (ILO, 2019). The critical ecosystem services provided vary for different biomes (Chapin III *et al.*, 2011, p.428), such as carbon sequestration (forests), and pasture for grazing (grasslands and savannas, Naidoo *et al.*, 2008). Biome changes and shifts therefore impact ecosystem services (Gonzalez *et al.*, 2010). Furthermore, many animal species are strongly associated with certain biome types (Jetz & Fine, 2012), which together with vegetation changes implies large potential impacts on prevailing biodiversity.

Biome shifts attributed to climate change have already been observed in Africa (Niang *et al.*, 2014), but do not show a consistent pattern. For instance, declines in tree density and changes in species composition have led to a southward shift of the savanna vegetation zone in West Africa (Gonzalez *et al.*, 2012) into previously more humid areas. At the same time, increased woody cover in savannas has been reported at many sites across Africa, including West Africa. Increasing atmospheric CO<sub>2</sub> concentrations ([CO<sub>2</sub>]), changes in land management and altered rainfall patterns were identified as likely drivers of this woody vegetation increase (Stevens *et al.*, 2017).

With the widespread mixture of grasses with C<sub>4</sub> photosynthesis and woody plants with C<sub>3</sub> photosynthesis across African savannas, plant physiological effects of increasing [CO<sub>2</sub>] might change the competitive balance between grasses and trees and thus play a key role for future ecosystem changes (Bond & Midgley, 2000; Midgley & Bond, 2015; Osborne *et al.*, 2018). Furthermore, changes in plant growth interact with changes in fire regimes, and direct enhancement of tree sapling growth rates under elevated [CO<sub>2</sub>] (eCO<sub>2</sub>) increases the likelihood that young tree individuals escape the “firetrap”. This might lead to a positive feedback, where an

initial increase in woody vegetation suppresses grasses, thereby reduces fire activity, which in turn benefits woody plants (Bond & Midgley, 2012; Midgley & Bond, 2015).

However, the magnitude of eCO<sub>2</sub> effects both, directly on plant growth through CO<sub>2</sub> fertilisation of photosynthetic efficiency (Long *et al.*, 2004), and indirectly on ecosystem hydrology (through a reduction of stomatal conductance, g<sub>s</sub>; Ainsworth & Rogers, 2007; Medlyn *et al.*, 2001), is still debated (Körner, 2015; Medlyn *et al.*, 2015; Zaehle *et al.*, 2014). Free-Air Carbon dioxide Enrichment (FACE) experiments suggest that an increase in carbon assimilation in C<sub>3</sub> plants does not necessarily scale to increased plant growth (e.g. Körner *et al.*, 2005; Medlyn *et al.*, 2015), particularly when limited by nutrient availability (e.g. Jiang *et al.*, 2020a,b; Norby *et al.*, 2010). For ecosystem hydrology and water use efficiency (WUE), eCO<sub>2</sub> effects translate into a balance of decreased transpiration and water demand due to reduced g<sub>s</sub> (De Kauwe *et al.*, 2013) and increased water demand following increased net primary production (NPP, Warren *et al.*, 2011).

Dynamic Global Vegetation Models (DGVMs) are a widely used tool to project future ecosystem changes and to attribute ongoing changes to different drivers and mechanisms (Prentice *et al.*, 2007). DGVMs simulate ecophysiological processes, such as photosynthesis and plant growth, vegetation dynamics and structure, geographical distribution of plant biomes, and biogeochemical cycles (e.g. water and carbon), in particular in response to climate change (e.g. Prentice *et al.*, 2007; Sitch *et al.*, 2008). However, the effects of eCO<sub>2</sub> on plants and interactions with nutrient limitations in DGVMs are still uncertain (Hickler *et al.*, 2015; Medlyn *et al.*, 2015). If key plant demographic processes such as mortality, recruitment of tree saplings, and fire impacts on plant individuals, are implemented in DGVMs (Fisher *et al.*, 2018), they can capture complex dynamics in savanna ecosystems.

In this study, we simulated the impacts of climate change and eCO<sub>2</sub> on carbon stocks, WUE, and biome distribution of potential natural vegetation (PNV) in Africa using the adaptive Dynamic Global Vegetation Model (aDGVM, Scheiter & Higgins, 2009). The aDGVM was originally developed for Africa and its savanna (Scheiter & Higgins, 2009) and has been applied and tested in several Africa-focused case studies (e.g. Scheiter *et al.*, 2018; Scheiter & Savadogo,

2016). It simulates woody plant demography for individual trees and this allows fire impacts to be conditioned on individual tree size. Advancing on earlier studies with the aDGVM, we used an ensemble of Regional Climate Model (RCM) data based on six downscaled General Circulation Models (GCMs, Archer *et al.*, 2018; Davis-Reddy *et al.*, 2017; Engelbrecht *et al.*, 2015) and two Representative Concentration Pathway (RCP) scenarios (RCPs 4.5 and 8.5 Stocker *et al.*, 2013). This is the first time that this ensemble of downscaled GCM data has been used as climate driver for a DGVM covering Africa. We ran the aDGVM with and without eCO<sub>2</sub> effects enabled to assess uncertainty related to plant-physiological CO<sub>2</sub> effects and to identify important drivers of vegetation change. Our study quantifies how uncertainty in projections caused by CO<sub>2</sub>, in particular concerning CO<sub>2</sub> effects on WUE and biomass, interacts with uncertainty due to the choice of GCM and RCP.

## 2.3 Materials and methods

### 2.3.1 The aDGVM

For this study, we used the well-tested adaptive Dynamic Global Vegetation Model (aDGVM), a regionally adapted DGVM (e.g. Scheiter & Higgins, 2009; Scheiter *et al.*, 2015; Scheiter & Savadogo, 2016). The aDGVM was developed for tropical and subtropical grass-tree ecosystems (for details see Scheiter & Higgins, 2009; Scheiter *et al.*, 2012). It incorporates ecophysiological processes that are commonly implemented in DGVMs (Prentice *et al.*, 2007). State variables such as photosynthetic rates, biomass or height are simulated for individual plants depending on environmental conditions. For each plant the aDGVM dynamically simulates leaf phenology and flexibly determines carbon allocation to plant biomass compartments (roots, stem or leaf biomass). aDGVM prioritises carbon allocation to compartments that are most limiting for plant growth based on the constraining factors water, light or photosynthesis. Physiological processes, such as photosynthesis, stomatal conductance ( $g_s$ ) and transpiration, are simulated for each individual plant based on environmental and plant individual state variables such as light availability. Stomatal conductance  $g_s$  is represented by the model from Ball

*et al.* (1987) and is directly proportional to relative humidity, and the ratio of photosynthesis and [CO<sub>2</sub>] at the leaf surface (Medlyn *et al.*, 2001).

The aDGVM simulates 1ha plots that are assumed to be representative for the simulated grid cell. Grasses with C<sub>3</sub> and C<sub>4</sub> photosynthesis are each implemented as two types of super-individuals that represent grasses growing beneath tree canopies and in tree canopy gaps. The aDGVM distinguishes savanna and forest trees (Scheiter *et al.*, 2012) as two distinct tree types that differ in their fire and shade tolerance (Bond & Midgley, 2001; Ratnam *et al.*, 2011). In the model, savanna trees are shade-intolerant and more fire-resistant as adult trees (>2m). Modelled forest trees are shade-tolerant but fire-sensitive in all age classes. Each tree individual competes for light with neighbouring plants and for water with all plants simulated per 1ha plot.

Fire in the aDGVM is determined by fuel load and fuel moisture, both dependent on biomass growth and thus indirectly influenced by climate, and wind speed following Higgins *et al.* (2008). Ignitions are simulated as random events decoupled from climatic or regional factors. Fire disturbance is therefore one of the factors causing some stochasticity in the model results. Whether fire spreads after a stochastic ignition event depends on fire intensity and a previously determined likelihood that a fire will spread (Scheiter & Higgins, 2009).

In contrast to many other DGVMs, simulating individual trees in aDGVM allows accounting for fire effects on individual plants and vegetation structure as a function of individual plant height (Scheiter & Higgins, 2009). Height influences if trees survive grass fires because only tall enough trees can escape the flame or topkill zone of a fire (Higgins *et al.*, 2000). In addition, in contrast to forest trees, grasses and savanna trees in aDGVM are able to resprout after fire damage (Bond & Midgley, 2001). Population composition evolves dynamically in the model as a result of interactions of, e.g., fire and [CO<sub>2</sub>]. Random events in demography sub-routines for tree populations add to the stochasticity in model results.

### 2.3.2 Regional climate model simulations

Climate input data consisted of an ensemble of six downscaled GCM projections under two mitigation scenarios generated with the variable-resolution conformal-cubic atmospheric model (CCAM, McGregor, 2005). The simulations were performed at the Council for Scientific and Industrial Research (CSIR) in South Africa (Archer *et al.*, 2018; Davis-Reddy *et al.*, 2017; Engelbrecht *et al.*, 2015). The GCM projections formed part of the Coupled Model Intercomparison Project Phase 5 (CMIP5; Table S1, Stocker *et al.*, 2013). The downscaling procedure involved CCAM being integrated globally at a quasi-uniform resolution of about 50km in the horizontal, forced at its lower boundary by sea-ice concentrations and bias-corrected sea-surface temperatures from the host GCMs (Engelbrecht *et al.*, 2015). The CCAM simulations were performed for the period 1961-2099 and for the low mitigation scenario RCP8.5 and modest-high mitigation scenario RCP4.5.

The downscaled climate data sets were bias-corrected to the monthly climatologies of temperature and rainfall from CRU TS3.1 data for the period 1961-1990 (Engelbrecht *et al.*, 2015; Engelbrecht & Engelbrecht, 2016). Previously, the CCAM downscalings have been shown to realistically represent present-day climate over southern Africa (e.g. Engelbrecht *et al.*, 2009, 2013, 2015).

CCAM output is available on a latitude-longitude grid of 0.5° resolution and at a daily time step. We used daily precipitation, daily minimum and maximum temperature, daily wind speed and daily relative humidity from the CCAM data set to force aDGVM (see Appendix A Figure S1 for mean annual precipitation (MAP) and temperature maps). As projected radiation data was not available, we derived present day radiation from sunshine percentage (Allen *et al.*, 1998) from New *et al.* (2002) data set. Thus, our vegetation simulations are based on an ensemble of climate data providing a range of GCM-projected climate change under two emission scenarios at high spatial and temporal resolution.

### 2.3.3 Simulation design

We simulated vegetation dynamics in Africa from 1971 to 2099 at 0.5° resolution by forcing the aDGVM with the climate ensemble described above and soil data from the Global Soil Data Task Group (2000). A model spin-up of 210 years was simulated to allow vegetation to reach equilibrium with environmental forcing. To that end, we used a random series of climate data from the period 1971-1979. In our experimental setup, we combined changes in climatic conditions with increases of [CO<sub>2</sub>] (eCO<sub>2</sub>) for two greenhouse gas emission scenarios, RCPs 4.5 and 8.5. To estimate the extent of the eCO<sub>2</sub> effect and its uncertainties, we repeated the same simulations with climate conditions following the two RCP scenarios, but with [CO<sub>2</sub>] rising only to 400ppm and then keeping [CO<sub>2</sub>] fixed (fCO<sub>2</sub>).

Stochastic effects within DGVMs can be factored in when conducting replicate runs for each ensemble member. Due to high computing times for continental-scale high-resolution simulations, for each GCM only one simulation was conducted per RCP-CO<sub>2</sub> scenario. In a previous study with the aDGVM at regional scale, more than 60% of replicate simulations agreed with respect to biome projections for the year 2100 for large parts of the simulated area, the Limpopo province in South Africa (Scheiter *et al.*, 2018). As opposed to Scheiter *et al.* (2018), the use of daily climate input data for our simulations helped to avoid generation of daily climate time series with the aDGVM and thus removed the associated stochasticity. In addition, the high spatial resolution of our simulations effectively acts as a replication in space with smooth simulation patterns in space indicating low aDGVM-caused variability in the simulation.

### 2.3.4 Analysis of simulation results

Aboveground carbon dynamics and plant-physiological effects of eCO<sub>2</sub> were analysed in more detail. We defined stand WUE as the ratio of NPP and plant transpiration, following the definition by De Kauwe *et al.* (2013) for FACE results. We used NPP, transpiration and WUE to isolate which processes – CO<sub>2</sub> fertilisation of photosynthesis or increased WUE via reduced transpiration through reduced g<sub>s</sub> – are driving plant-physiological responses to eCO<sub>2</sub>.

We created time series for total aboveground carbon and WUE in Africa for the four RCP-CO<sub>2</sub>-scenario combinations (RCP4.5/8.5 with fCO<sub>2</sub>/eCO<sub>2</sub>) with annual time steps for 2000-2099. We used the ensemble mean and standard deviation (SD) of the six ensemble members for each of the four scenario combinations in each year. For other analyses, model results were averaged over 20-year periods to focus on long-term climate-driven trends (Stocker *et al.*, 2013) and to reduce the influence of model-inherent stochastic processes on model output. Two time windows were used for comparison: 2000-2019 and 2080-2099. Maps of aboveground biomass were generated, based on the mean across all 24 simulation runs in 2000-2019, because the different scenarios did not deviate much from another. For 2080-2099, we used the ensemble mean of each of the four scenarios. In addition, changes in mean aboveground biomass from the present (2000-2019) until 2080-2099 were mapped for the four scenarios. For the change in total aboveground vegetation carbon and in WUE (from 2000-2019 to 2080-2099), we used the omega squared ( $\omega^2$ ) measure to quantify the effect size of explanatory variables (see supplementary material for R code; R Core Team, 2015). CO<sub>2</sub> scenario, RCP scenario, and GCM and their two-way interactions were used to explain differences of the dependent variables. Using  $\omega^2$  to estimate the proportion of variance explained (Olejnik & Algina, 2003), we quantitatively evaluate the magnitude of the differences between the ensemble members (White *et al.*, 2014). As computational limitations restricted us from implementing replicate runs, analysing for three-way interactions between the three explanatory variables was not possible.

To study potential future biome distributions and biome changes, we classified the simulated vegetation into seven biome types: desert, C<sub>3</sub> grassland, C<sub>4</sub> grassland, C<sub>3</sub> savanna, C<sub>4</sub> savanna, woodland and forest. The classification scheme is based on simulated tree cover, grass biomass and composition of tree and grass types (Scheiter *et al.*, 2012) with minimum grass biomass levels for grassland classifications (Scheiter *et al.*, 2018, see Table S2). In this definition scheme, the main difference between savannas and woodlands is the predominance of savanna or forest tree types, which is in turn an indicator of fire activity.

Based on this biome classification scheme, we identified biomes for the above-listed time periods for Africa for each RCP-CO<sub>2</sub>-scenario (RCP4.5/8.5 with eCO<sub>2</sub>/fCO<sub>2</sub>). The biomes identified for all GCM simulations per scenario were used to derive consensus biome maps for each scenario. For each grid cell, the biome type that was most common in the ensemble member maps was used to derive each scenario's consensus biome map. According to the binomial distribution, two ensemble members agreeing in the simulated biome do not have a higher probability than an outcome by chance. Such grid cells therefore were denominated as having 'No consensus'. In addition, we plotted the number of ensemble members that simulated the consensus vegetation type for each time period as an indicator of agreement within the simulated ensemble.

We used the number of ensemble members per RCP-CO<sub>2</sub>-scenario combination that showed a biome change from 2000-2019 to 2080-2099 (maximum six ensemble members) as an indicator for the probability of biome change under future climatic conditions. We therefore derived a measure of uncertainty from the number of simulated biome changes within a scenario. The type of biome change, i.e., whether ensemble members simulate the same or different biome transitions, was not considered in this uncertainty assessment.

To illustrate the overall potential consequences (i.e. areal increase or decrease) of biome changes for each biome type, we determined each biome's change in total area covered [%] between 2000-2019 and 2080-2099 based on the consensus biome maps for all four scenarios. In addition, we plotted the changes of total area covered by each biome type for two time steps (2000-2019, 2080-2099).

Atmospheric CO<sub>2</sub> effects on WUE and g<sub>s</sub> were analysed for each RCP-CO<sub>2</sub> scenario, based on the relative change of ensemble means from 2000-2019 to 2080-2099 for each grid cell. As a proxy for water availability, NPP change and MAP change were plotted against each other as relative change for each RCP-CO<sub>2</sub> scenario combination. NPP change against tree biomass change per grid cell was used to illustrate possible effects of population dynamics on biomass. For these figures, biomes in 2000-2019 were depicted on a per grid cell basis to assess different responses for different biomes.

## 2.4 Results

### 2.4.1 Current aboveground biomass and future projections

The spatial pattern of simulated biomass in 2000-2019 compared reasonably well with an observation-based biomass distribution (Avitabile *et al.*, 2016, Figure 2.1 a,b). Our simulations of potential natural biomass underestimated the high aboveground biomass in the Congo basin, while overestimating biomass in areas more distant to the equator (Figure 2.1a). While Avitabile *et al.*'s (2016) map included both intact and nonintact vegetation, aDGVM only simulated PNV, thus intact vegetation. aDGVM, therefore, overestimated simulated biomass and actual carbon stocks in areas of high land-use, such as agricultural land. The mean carbon stored in simulated total aboveground biomass for Africa between 2000 and 2010 amounted to 52.2 PgC ( $\pm 0.36$ , all 24 ensemble members, Figure 2.2a). This is within the range of estimates derived from satellite and inventory plot data (48.3-64.5 PgC, Figure 2.2a, Avitabile *et al.*, 2016; Baccini *et al.*, 2012; Liu *et al.*, 2015; Saatchi *et al.*, 2011, extent varies from tropical Africa to continental Africa).

When comparing current (2000-2019) and future (2080-2099) aboveground biomass, both RCP-eCO<sub>2</sub> scenarios showed similar spatial patterns of increasing and decreasing biomass, but areas with increasing biomass predominated (Figure 2.1c-d; Appendix A Figure S2a,b; Table 2.1). Both RCP-eCO<sub>2</sub> scenarios showed small biomass decreases in a narrow belt along the equator. North and south of the equator both RCP scenarios showed a general pattern towards woody encroachment, with higher biomass increases for RCP8.5.

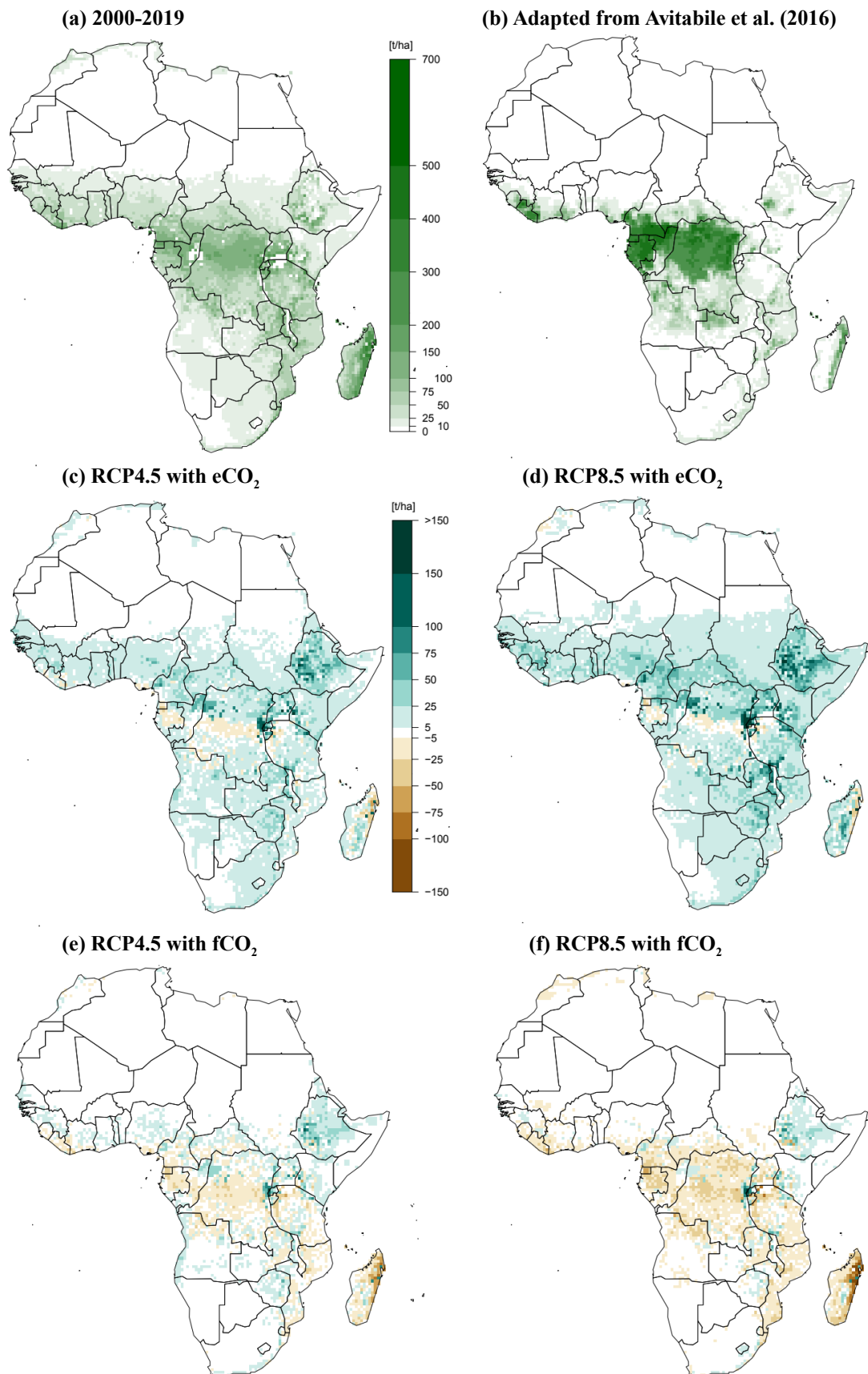


FIGURE 2.1: Simulated and observation-derived aboveground biomass in Africa and simulated change in biomass. Current aboveground biomass in Africa (t/ha) is derived from the ensemble mean across all 24 ensemble members of aDGVM-simulated biomass (2000–2019, a) and Avitabile *et al.* (2016, b). Change in aboveground biomass between 2000–2019 and 2080–2099 under RCP4.5 and 8.5 with eCO<sub>2</sub> (c, d) and with fCO<sub>2</sub> (e, f) is based on the mean of all six ensemble members of the respective scenario. aDGVM, adaptive Dynamic Global Vegetation Model; eCO<sub>2</sub>, elevated CO<sub>2</sub>; fCO<sub>2</sub>, CO<sub>2</sub> fixed at 400 ppm; RCP, representative concentration pathway

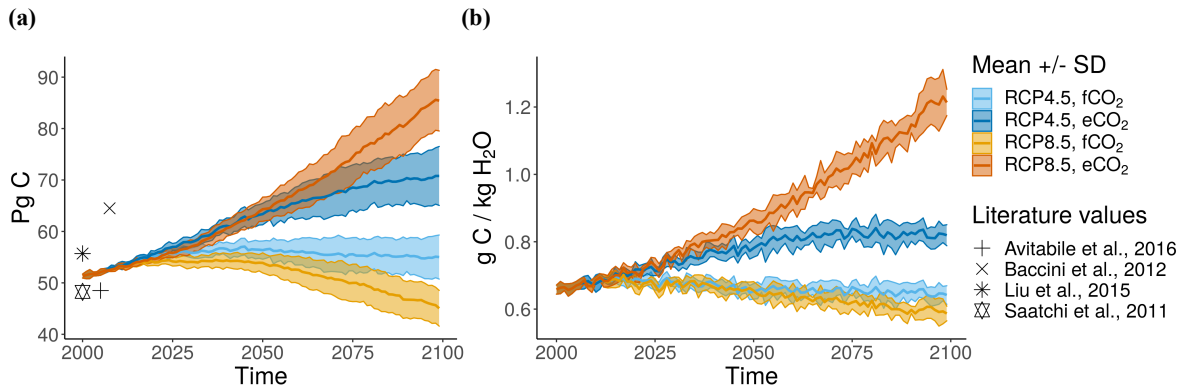


FIGURE 2.2: Mean total aboveground carbon and WUE in Africa in 2000–2099 under RCP4.5 and RCP8.5 with eCO<sub>2</sub> and fCO<sub>2</sub> simulated by the aDGVM. Thick lines are the mean over all six ensemble members per scenario. Shaded areas are the mean  $\pm$  standard deviation (SD) of the six ensemble members per scenario. In (a), aboveground carbon for tropical Africa (64.5 Pg C, Baccini *et al.*, 2012), sub-Saharan Africa (Avitabile *et al.* 2016, and 48.3 Pg C, Saatchi *et al.*, 2011) and Africa (55.7 Pg C, Liu *et al.*, 2015) are depicted for comparison. See Appendix A Figure S3 for aboveground carbon time series of all individual ensemble members. Water use efficiency (WUE, b) is defined as the ratio of net primary production and transpiration. See Table S3 for more details on the variability of aboveground carbon and WUE in 2080–2099. aDGVM, adaptive Dynamic Global Vegetation Model; eCO<sub>2</sub>, elevated CO<sub>2</sub>; fCO<sub>2</sub>, CO<sub>2</sub> fixed at 400 ppm; RCP, representative concentration pathway

Spatial patterns of biomass change in the fCO<sub>2</sub> scenarios were more variable. Increases prevailed over decreases under RCP4.5 and decreases prevailed under RCP8.5 (Table 2.1 and Figure 2.1c-f). The Ethiopian Highlands were the only larger area that showed mean biomass increases for all four RCP-CO<sub>2</sub> scenarios. However, these increases were weaker under fCO<sub>2</sub> than under eCO<sub>2</sub>. This biomass increase is in line with precipitation increases predicted for this region (Appendix A Figure S1). Both RCP-eCO<sub>2</sub> scenarios showed an appreciable carbon sink for Africa by the end of the 21<sup>st</sup> century in all GCM simulations (Figure 2.2a & S3). The increase under RCP8.5 was more pronounced, whereas under RCP4.5 mean total aboveground carbon started to saturate towards the end of the century (81.3 PgC and 70.0 PgC in 2080-2099, respectively, see Table 2.2 for % change). Saturating biomass increases under RCP4.5-eCO<sub>2</sub> followed the projected mid-century peak in greenhouse gas emissions for RCP4.5 (Stocker *et al.*,

TABLE 2.1: Area (%) of Africa affected by biomass change and biome change between 2000–2019 and 2080–2099 and agreement of simulation results per scenario. Change for aboveground biomass (AGB) is given as the percentage of area with AGB increases or decreases. Where AGB increases and decreases did not sum to 100%, the remaining percentage of land area did not experience AGB changes. For biome change, proportions of area with no consensus biome in either period were not included. For agreement of biome state, only areas where all six ensemble members of a scenario agreed on simulated biome in 2080–2099 were included. The respective percentages refer to the total area of the African continent.

Scenario	% area with AGB increase	% area with AGB decrease	% area with biome changes	% area with agreement in biome state in all ensemble members in 2080–2099
RCP4.5, eCO <sub>2</sub>	84.3	15.3	23.4	45.6
RCP8.5, eCO <sub>2</sub>	80.2	19.1	27.7	45.7
RCP4.5, fCO <sub>2</sub>	64.5	35.2	17.5	50.3
RCP8.5, fCO <sub>2</sub>	31.8	67.5	18.6	53.7

AGB, aboveground biomass; eCO<sub>2</sub>, elevated CO<sub>2</sub>; fCO<sub>2</sub>, CO<sub>2</sub> fixed at 400 ppm; RCP, representative concentration pathway

2013). Variability within each RCP ensemble due to differences between the six GCMs ( $\pm$ SD,  $2 \times$ SD=9.7 and 11.2 PgC, respectively for RCPs 4.5 and 8.5) was similar to the difference of the means of the two eCO<sub>2</sub> RCP scenarios (11.2 PgC, see Table S3).

TABLE 2.2: Change in aboveground biomass (AGB) and in WUE from 2000–2019 to 2080–2099. Change in carbon in AGB was calculated for all six ensemble members for each RCP-CO<sub>2</sub> scenario. The range of minimum and maximum change rate for the six ensemble members for each scenario are presented here. See Table S4 for change rates for each ensemble member.

Scenario	AGB change	WUE change
RCP4.5, eCO <sub>2</sub>	18 to 43%	15 to 25%
RCP8.5, eCO <sub>2</sub>	37 to 61%	61 to 74%
RCP4.5, fCO <sub>2</sub>	-8 to -11%	-1 to -9%
RCP8.5, fCO <sub>2</sub>	-6 to -22%	-9 to -16%

AGB, aboveground biomass; eCO<sub>2</sub>, elevated CO<sub>2</sub>; fCO<sub>2</sub>, CO<sub>2</sub> fixed at 400 ppm; RCP, representative concentration pathway; WUE, water use efficiency

Under fCO<sub>2</sub>, simulated total biomass in 2099 was lower than under eCO<sub>2</sub> (Figure 2.2a). For RCP8.5 under fCO<sub>2</sub>, vegetation became a carbon source by the 2050s and biomass in 2080–2099 (47.1 PgC, see Tab 2 for % change) was less than in 2000. For RCP4.5-fCO<sub>2</sub>, the ensemble mean biomass in 2080–2099 was 55.2 PgC. It depended on the downscaled GCM whether a small source or a small sink was projected for RCP4.5 under fCO<sub>2</sub> (Appendix A Figure S3). The  $\omega^2$  metric indicated that variation in total carbon between all 24 ensemble members was mainly explained by the CO<sub>2</sub> scenarios, followed by interaction effects of CO<sub>2</sub> and RCP scenarios (Table 2.3; see Table S5 for corresponding F-values from ANOVA).

### 2.4.2 Future projections of WUE and underlying plant physiological processes

Changes in WUE, here defined as the ratio of NPP and transpiration, until 2080-2099 were similar to the trends simulated for aboveground biomass for all four RCP-CO<sub>2</sub> scenarios (Figure 2.2b; Table 2.2). Yet, under RCP4.5-eCO<sub>2</sub>, WUE leveled off earlier than carbon in aboveground biomass. Both fCO<sub>2</sub> scenarios showed a decrease in mean WUE. For NPP and WUE, the shape of the timeseries was almost identical for each individual scenario (Figure 2.2b & Appendix A Figure S4a). For transpiration on the other hand, all four scenarios showed increases (Appendix A Figure S4b). Within an RCP, transpiration was lower for fCO<sub>2</sub> than for eCO<sub>2</sub>.

TABLE 2.3: Effect size of explanatory variables for change in carbon stored in aboveground biomass and WUE between 2000–2019 and 2080–2099. The table presents  $\omega^2$  for the dependent variables aboveground biomass change (in Pg C) and WUE change (in gC/kgH<sub>2</sub>O) and explanatory variables CO<sub>2</sub> scenario, RCP scenario and GCM. Two-way interaction effects are included in the model and are denoted with ':'.

Independent variables and interaction effects	$\omega^2$	
	AGB	WUE
CO <sub>2</sub>	0.794	0.692
RCP	0.005	0.105
GCM	0.069	0.009
RCP:CO <sub>2</sub>	0.123	0.190
CO <sub>2</sub> :GCM	0.002	0.000
GCM:RCP	0.005	0.000

AGB, aboveground biomass; GCM, general circulation model; RCP, representative concentration pathway; WUE, water use efficiency

WUE increased in most of the simulated grid cells between 2000-2019 and 2080-2099 in eCO<sub>2</sub> simulations, and relative change ratios were higher than in fCO<sub>2</sub> simulations (Figure 2.3a). With a stronger decrease under eCO<sub>2</sub> than fCO<sub>2</sub> and for RCP8.5 than for RCP4.5,  $g_s$  showed the opposite trend (Figure 2.3b). Although  $g_s$  decreased with increasing [CO<sub>2</sub>], transpiration increased for all four RCP-CO<sub>2</sub> scenarios (Appendix A Figure S4b). NPP was more sensitive to MAP changes under RCP8.5 than RCP4.5, with a steeper slope for eCO<sub>2</sub> (Figure 2.3c). We found increased NPP in both eCO<sub>2</sub> scenarios even for grid cells where MAP decreased. Variation in WUE was largely explained by CO<sub>2</sub> scenarios, followed by the interaction between CO<sub>2</sub>, and

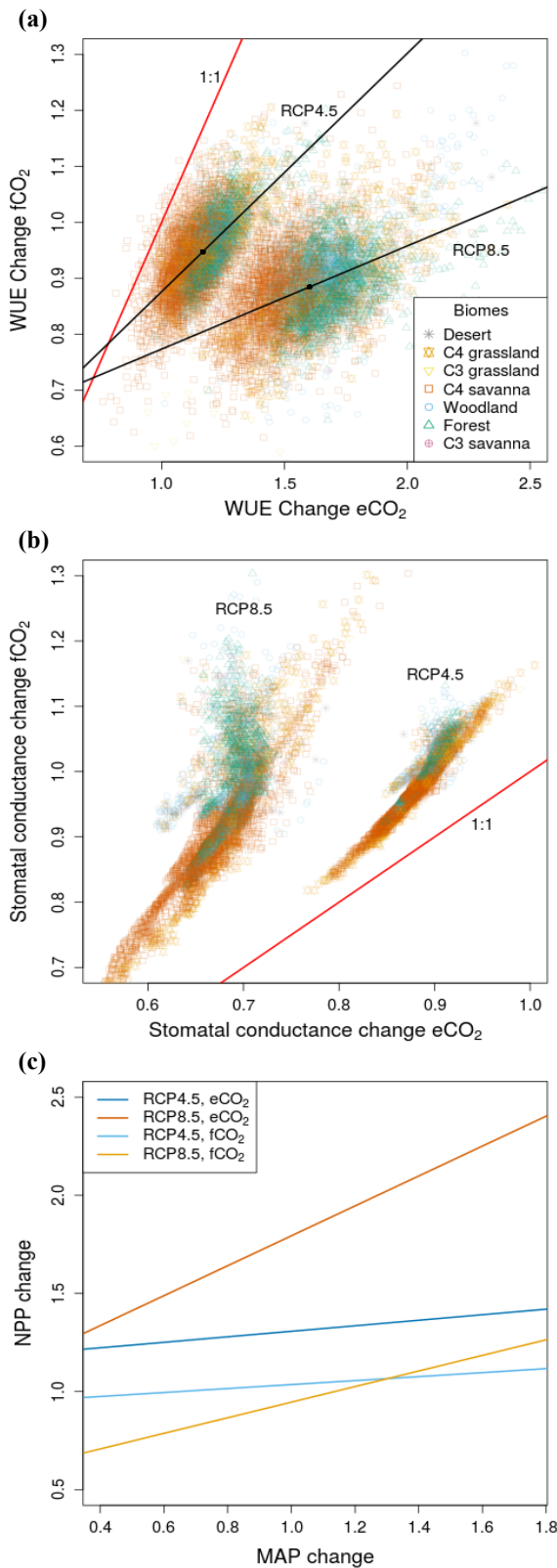


FIGURE 2.3: Change in WUE (a) and stomatal conductance  $g_s$  (b) under  $e\text{CO}_2$  and  $f\text{CO}_2$ , and change in NPP versus change in MAP (continental scale, c) between 2000–2019 and 2080–2099 simulated by the aDGVM. Changes are represented by the ratio between values for 2000–2019 and 2080–2099 for each simulated grid cell. Values greater than 1 indicate an increase, values less than 1 indicate a decrease. Black lines in (a) are linear regressions for the respective RCP scenarios with the continental-scale mean of the scenario shown as a black point. Red lines represent the 1:1 lines. Each point represents a grid cell and is shape- and colour-coded according to its assigned biome type in 2000–2019. Lines in (c) are continental-scale regression lines for the four RCP- $\text{CO}_2$  scenario combinations. Appendix A Figure S5 for data points used to derive the MAP-NPP change regression lines for each scenario. Note that x- and y-axes do not have the same scale. aDGVM, adaptive Dynamic Global Vegetation Model;  $e\text{CO}_2$ , elevated  $\text{CO}_2$ ;  $f\text{CO}_2$ ,  $\text{CO}_2$  fixed at 400 ppm; MAP, mean annual precipitation; NPP, net primary production; RCP, representative concentration pathway; WUE, water use efficiency

RCP, and the RCP scenario (Table 2.3). The effect of RCP scenario on WUE was stronger than its effect on carbon in aboveground biomass.

#### 2.4.3 Projected biome changes and population dynamics

For all 24 ensemble members, aDGVM simulated biome shifts (change of spatial location of biomes) and biome transitions (changes in biome type at a given location) from 2000-2019 to 2080-2099 (Figures 2.4 and 2.5 for RCP8.5 and Appendix A Figures S6 and S7 for RCP4.5). This implied considerable changes in area covered by each biome (Figure 2.6).

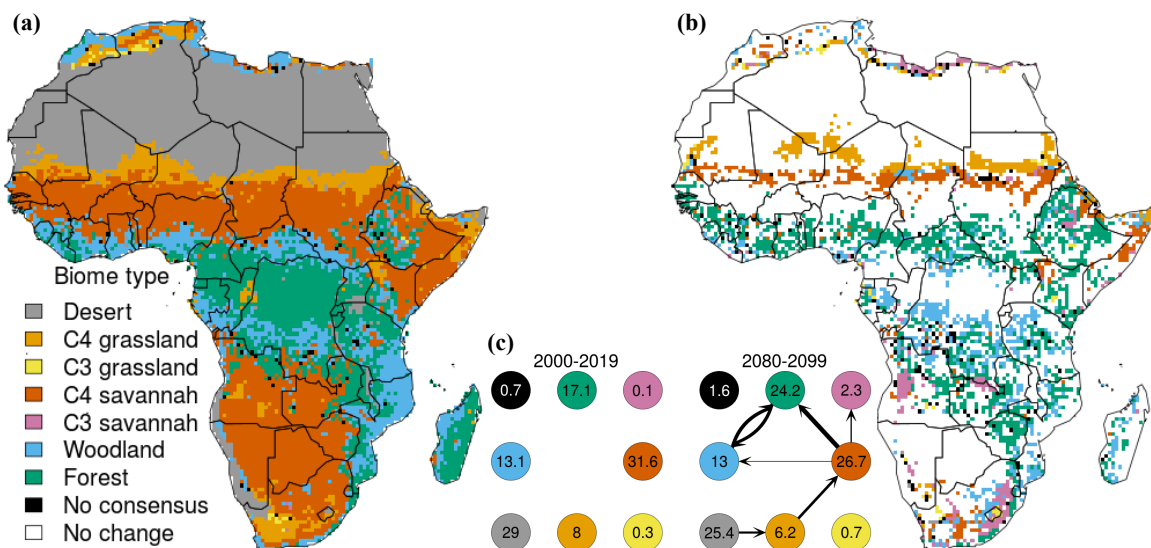


FIGURE 2.4: Consensus biome type under RCP8.5-eCO<sub>2</sub> in 2000–2019 (a), biome changes until 2080–2099 (b) and transitions and fractional cover of biomes (c) simulated by aDGVM. The consensus biome type is the biome simulated by at least three ensemble members of the scenario. Grid cells with an agreement of less than three ensemble members do not have a higher probability than an outcome by chance and are marked as ‘No consensus’. The biomes shown in (b) are the biomes that were simulated for 2080–2099 for grid cells where biome transitions were simulated for the consensus biome. Numbers in each coloured circle (c) represent the percentage of area covered by each biome at the respective time step in the consensus map. Arrows show biome changes with regard to the previous time step. Arrow thickness is proportional to the change in total area. In panel (c), only changes that affected more than 0.5% of the African land surface are shown. See Appendix A Figure S6 for RCP4.5-eCO<sub>2</sub>. aDGVM, adaptive Dynamic Global Vegetation Model; eCO<sub>2</sub>, elevated CO<sub>2</sub>; precipitation; RCP, representative concentration pathway

Under eCO<sub>2</sub>, in line with simulated biomass increase, biome transitions from non-woody biomes to woody biomes dominated for both RCP scenarios (Figure 2.4). The area covered by

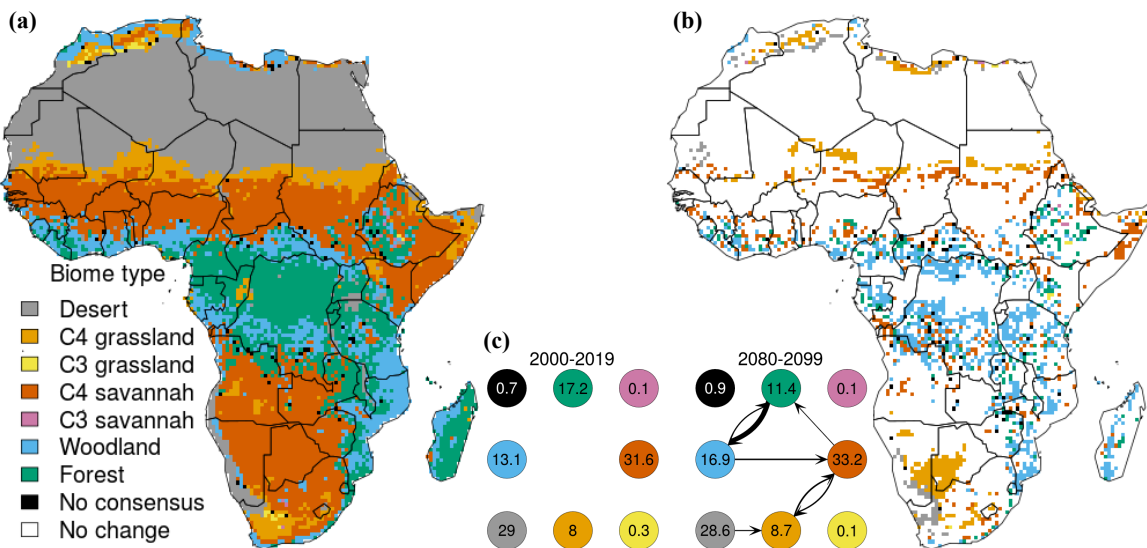


FIGURE 2.5: Consensus biome type under RCP8.5-fCO<sub>2</sub> in 2000–2019 (a), biome changes until 2080–2099 (b) and transitions and fractional cover of biomes (c) simulated by aDGVM. The consensus biome type is the biome simulated by at least three ensemble members of the scenario. Grid cells with an agreement of less than three ensemble members do not have a higher probability than an outcome by chance and are marked as ‘No consensus’. The biomes shown in (b) are the biomes that were simulated for 2080–2099 for grid cells where biome transitions were simulated for the consensus biome. Numbers in each coloured circle (c) represent the percentage of area covered by each biome at the respective time step in the consensus map. Arrows show biome changes with regard to the previous time step. Arrow thickness is proportional to the change in total area. In panel (c), only changes that affected more than 0.5% of the African land surface are shown. See Appendix A Figure S7 for RCP4.5-fCO<sub>2</sub>. aDGVM, adaptive Dynamic Global Vegetation Model; fCO<sub>2</sub>, CO<sub>2</sub> fixed at 400 ppm; precipitation; RCP, representative concentration pathway

forest increased for both RCP-eCO<sub>2</sub> scenarios at the expense of desert, grasslands and savannas, with stronger effects for RCP8.5 (Figure 2.6). Non-desert biomes shifted towards mid-latitudes (Figure 2.4a,b; Appendix A Figure S6a,b). However, in line with simulated biomass reductions, woodland replaced forests in some areas close to the equator (Figure 2.1c,d). [CO<sub>2</sub>] increase and climatic change are stronger in RCP8.5, therefore the aDGVM simulated that larger areas changed biome state than under RCP4.5 (Table 2.1). Large areas showed transitions from C<sub>4</sub> savanna to forest, especially under RCP8.5 (Figure 2.4c).

As opposed to the eCO<sub>2</sub> scenarios, a decrease in forests dominated biome cover changes in the fCO<sub>2</sub> scenarios (Figure 2.5). In total, under fCO<sub>2</sub> a smaller area was projected to experience biome transitions (Table 2.1). For RCP8.5, we found a strong decrease of forest cover (5.8 percentage points) and an increase of C<sub>4</sub>-dominated biomes. Forests mainly shifted to woodlands

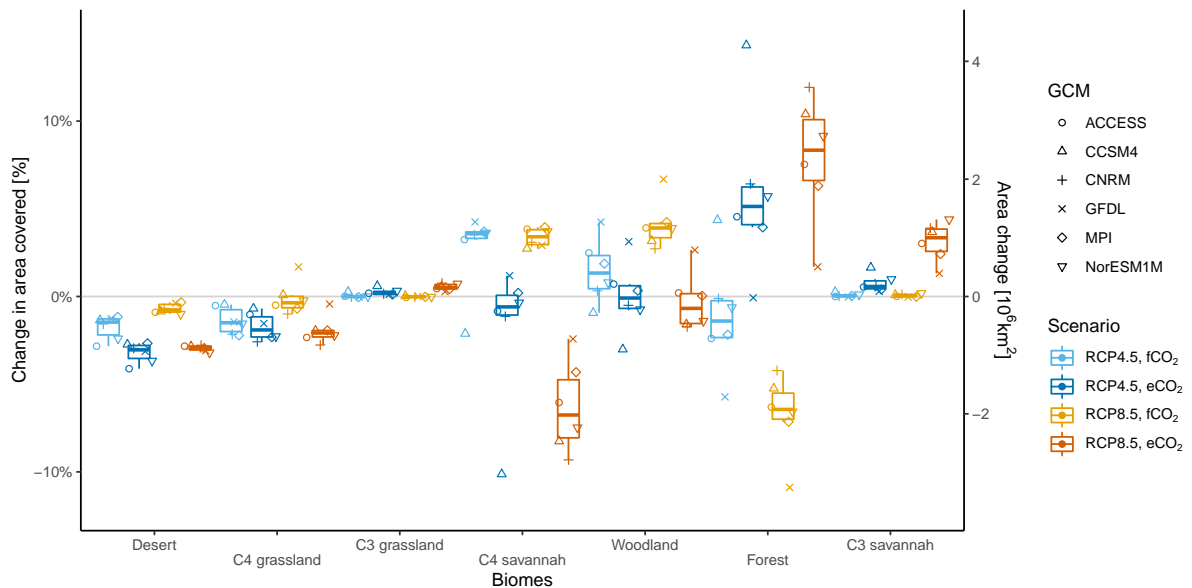


FIGURE 2.6: Change in African area covered by each biome in each GCM simulation and ensemble medians (box plots) under RCP4.5 and RCP8.5 with eCO<sub>2</sub> and fCO<sub>2</sub> simulated by aDGVM. Change is the difference in area covered between the time periods 2000–2019 and 2080–2099 in percentage points (left axis) and km<sup>2</sup> (right axis). aDGVM, adaptive Dynamic Global Vegetation Model; eCO<sub>2</sub>, elevated CO<sub>2</sub>; fCO<sub>2</sub>, CO<sub>2</sub> fixed at 400 ppm; GCM, general circulation model; RCP, representative concentration pathway

in both RCP scenarios (Figure 2.5c; Appendix A Figure S7c). Under RCP8.5-fCO<sub>2</sub>, the core savanna area in 2080-2099 in southern Africa was smaller and located further north than in the other three scenarios (Appendix A Figures S8e,f and S9e,f), with a pronounced transition from C<sub>4</sub> savanna to C<sub>4</sub> grasslands in the Kalahari region (Figure 2.5a,b). Under RCP4.5 the cover fractions of biome types did not change as much, with transitions in favour of C<sub>4</sub> savanna and woodlands.

Rates of tree biomass change were biome-specific and varied between CO<sub>2</sub> scenarios (Figure 2.7). Under eCO<sub>2</sub>, C<sub>4</sub> savannas showed a stronger relative increase in tree biomass change rates than woodlands and forests for both RCP scenarios, hinting at population dynamics effects (Figure 2.7a,b). Tree biomass change in C<sub>4</sub> savannas was more sensitive to NPP change than in other woody biomes for both eCO<sub>2</sub> scenarios. With fCO<sub>2</sub>, an increase of NPP often did not lead to an increase in tree biomass, especially for RCP8.5 and forest biomes.

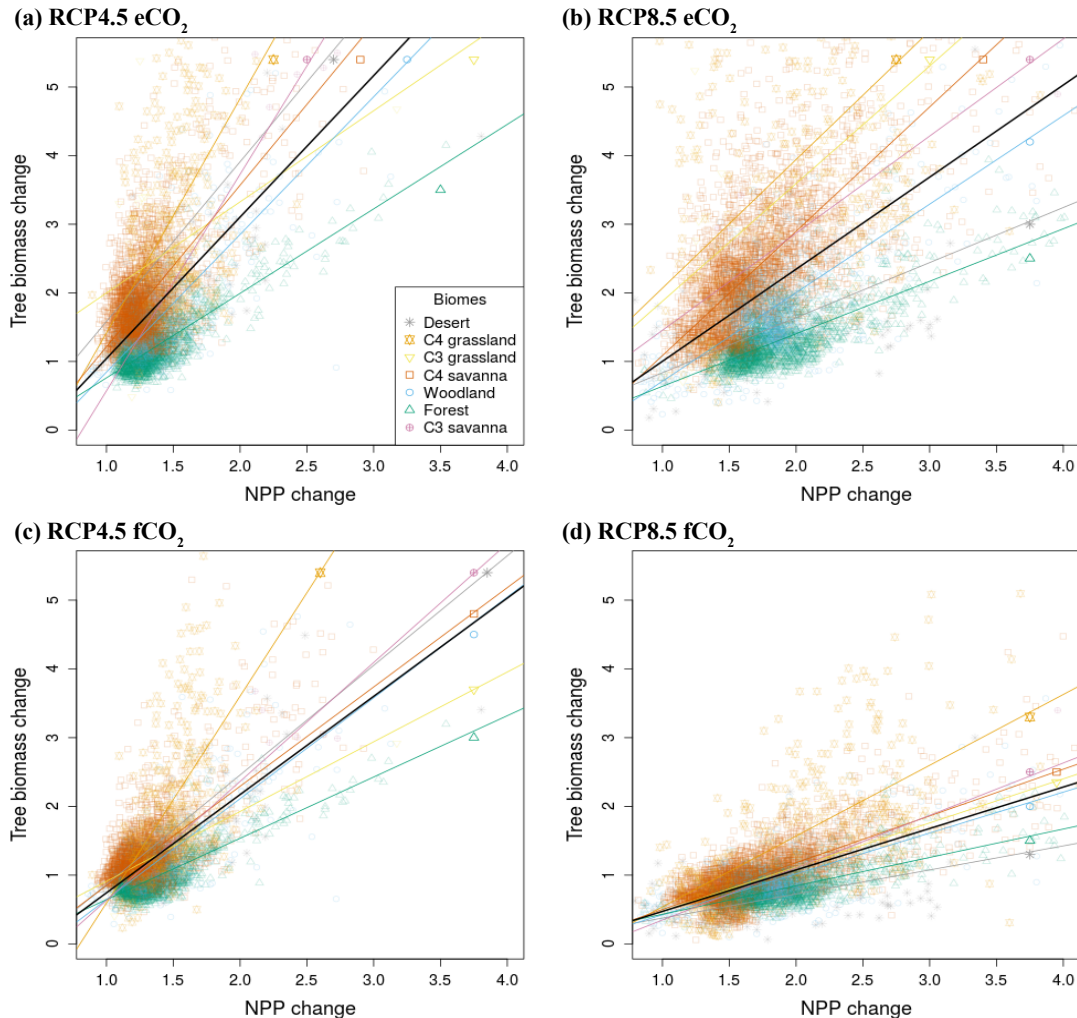


FIGURE 2.7: Mean tree biomass change in relation to mean NPP change for eCO<sub>2</sub> (a, b) and fCO<sub>2</sub> (c, d) under RCP4.5 (a, c) and RCP8.5 (b, d) simulated by aDGVM. Change is represented by the ratio between 2000–2019 and 2080–2099. Hence, values greater than 1 indicate increase and values less than 1 indicate decrease. Black lines are regression lines for all data points of the mean of a scenario. Coloured lines are regression lines for the respective biomes in 2000–2019 of the mean of a scenario. The regression lines for biomes are marked with a symbol at the top right of each line with colour and shape of the respective biome. Each point represents the mean for a simulated grid cell, and colour and shape represent the grid cell's consensus biome type in 2000–2019. The mean of each scenario is based on the six GCM simulations in each time period. Note that the scales of x- and y-axes differ. aDGVM, adaptive Dynamic Global Vegetation Model; eCO<sub>2</sub>, elevated CO<sub>2</sub>; fCO<sub>2</sub>, CO<sub>2</sub> fixed at 400 ppm; GCM, general circulation model; NPP, net primary production; RCP, representative concentration pathway

#### 2.4.4 Uncertainty of biome projections

The simulated biomes for the six ensemble members of all four RCP-CO<sub>2</sub> scenarios agreed well at the beginning of the simulations (2000-2019) in the equatorial forests, the Sahara desert along the Tropic of Cancer, and in more open C<sub>4</sub> savanna areas (Figs 8a, S10a). In the transition zones between these biome types the ensemble members agreed less well and agreement was low in grasslands, closed savannas and woodlands.

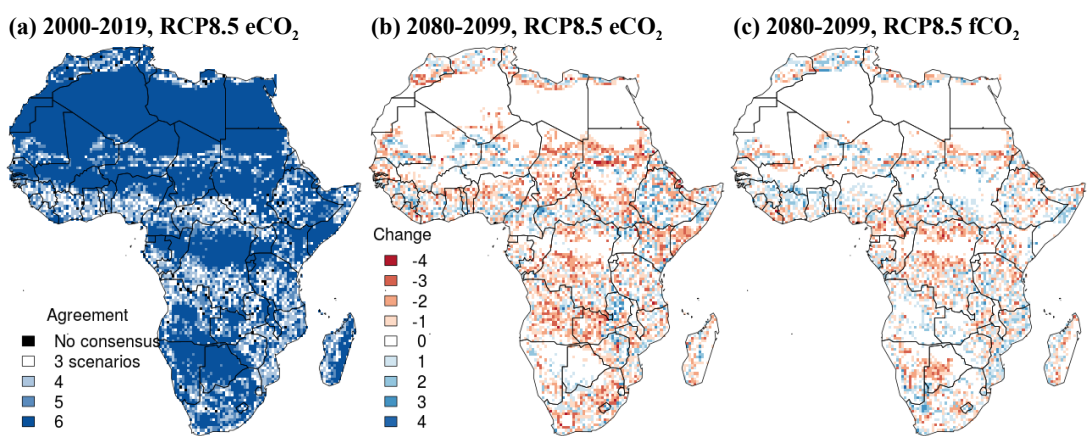


FIGURE 2.8: Agreement of ensemble members in 2000–2019, under eCO<sub>2</sub> (a) and change in agreement until 2080–2099 under eCO<sub>2</sub> (b) and fCO<sub>2</sub> (c) for RCP8.5 in aDGVM simulations. The number of ensemble members simulating the consensus type is denoted as ‘Agreement’. Grid cells with an agreement of less than three ensemble members are marked as ‘No consensus’. We only displayed the number of ensemble members simulating the consensus type in 2000–2019 for eCO<sub>2</sub> in (a), because agreement is almost identical for eCO<sub>2</sub> and fCO<sub>2</sub> (see Appendix A Figures S8b and S9b). The consensus biome type is the biome simulated by at least three ensemble members of the scenario. See Appendix A Figure S10 for RCP4.5. aDGVM, adaptive Dynamic Global Vegetation Model; eCO<sub>2</sub>, elevated CO<sub>2</sub>; fCO<sub>2</sub>, CO<sub>2</sub> fixed at 400 ppm; RCP, representative concentration pathway

Agreement of the six ensemble members per scenario decreased towards the end of the 21<sup>st</sup> century, especially for eCO<sub>2</sub> scenarios (Figure 2.8b,c; Appendix A Figure S10b,c). The core areas of forest, C<sub>4</sub> savanna and desert, where all six ensemble members still showed high agreement within a scenario, decreased. Agreement was higher for fCO<sub>2</sub> scenarios, where only climate change influenced vegetation changes (Table 2.1; Figure 2.8b,c; Appendix A Figure S10b,c).

Under eCO<sub>2</sub>, the projections for the transition zones between forest and C<sub>4</sub> savanna, and C<sub>4</sub> savanna and desert showed increasing disagreement between ensemble members for each RCP scenario (Figure 2.8b; Appendix A Figure S10b), with the desert-grassland-savanna transition

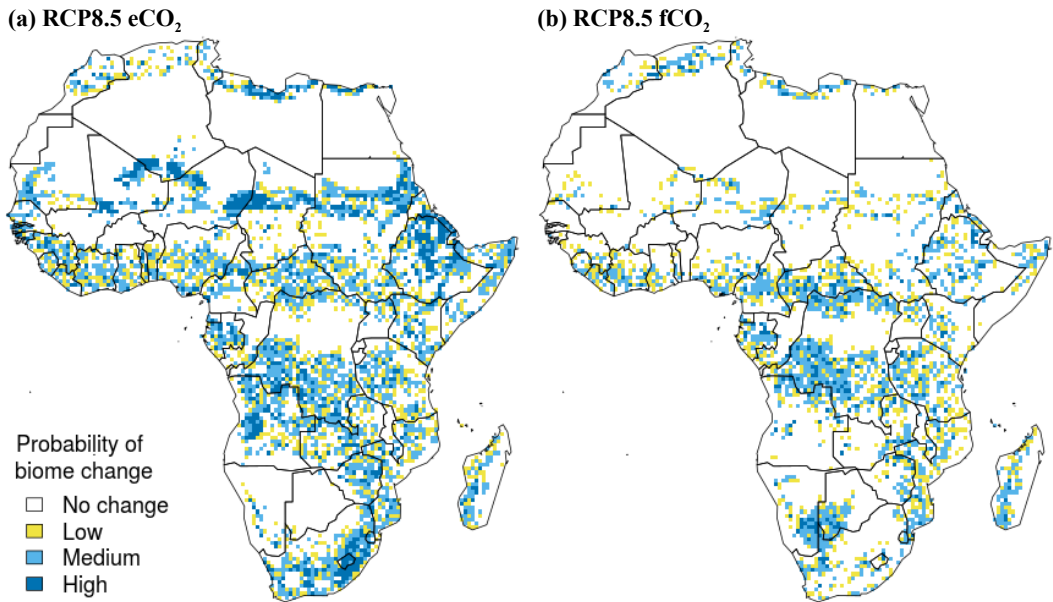


FIGURE 2.9: Probability of biome change between 2000–2019 and 2080–2099 simulated by aDGVM. The proportion of the six GCM ensemble members per scenario — here RCP8.5, eCO<sub>2</sub> (a) and fCO<sub>2</sub> (b) — that showed a biome change from 2000–2019 to 2080–2099 was used as a measure of probability of biome change. The more ensemble members projected a biome change per grid cell, the higher its probability of biome change. High probability of biome change — all six simulations project biome changes; medium probability of biome change — four or five simulations with biome changes; low probability of biome change — three simulations with biome changes; no change — zero to two simulations with changes. Grid cells with two or fewer simulations with biome changes do not have a higher probability than an outcome by chance and were therefore regarded as ‘No change’. Whether the ensemble members simulated the same type of biome transition was not considered here. See Appendix A Figure S11 for RCP4.5. aDGVM, adaptive Dynamic Global Vegetation Model; eCO<sub>2</sub>, elevated CO<sub>2</sub>; fCO<sub>2</sub>, CO<sub>2</sub> fixed at 400 ppm; GCM, general circulation model; RCP, representative concentration pathway

zone north of the equator at a medium to high probability of biome transition in our simulations, especially under RCP8.5 (Figure 2.9a; Appendix A Figure S11a). Further hotspots of medium to high probability of biome transitions for both RCP-eCO<sub>2</sub> scenarios were found in eastern Africa, areas north and south of the equator in the humid and moist sub-humid tropics, and for RCP8.5 in southern Africa with an increased dominance of C<sub>3</sub> plants (Figure 2.4b and 9a).

In fCO<sub>2</sub> scenarios, biomes were projected to have a lower probability of change (Figure 2.9b; Appendix A Figure S11b). The hotspot of likely biome transitions south of the equator under eCO<sub>2</sub> was also simulated under fCO<sub>2</sub> for both RCP scenarios. Conversely, unlike in the eCO<sub>2</sub> scenarios, the southern Kalahari was projected to change with medium to high probability

under RCP8.5-fCO<sub>2</sub>. Overall for both CO<sub>2</sub> scenarios, under RCP8.5 a larger area in Africa had a medium to high probability for biome transitions than under RCP4.5 (Figure 2.9; Appendix A Figure S11).

## 2.5 Discussion

The aim of this study was to provide projections of climate- and [CO<sub>2</sub>]-driven vegetation changes in Africa until the end of the century using a regionally adapted DGVM and regionally downscaled climate data. We analysed plant-physiological and vegetation dynamics responses to eCO<sub>2</sub> and quantified the impact of three sources of uncertainty on vegetation projections: the influence of climate models (GCM implementations), future global socio-economic development (RCP scenario) and strength of CO<sub>2</sub> effects on plant growth (CO<sub>2</sub> scenarios). We found that large regions in Africa are likely to experience changes in biomes and carbon stocks, especially with eCO<sub>2</sub> response scenarios. The extent of the projected changes depended on the chosen scenario and patterns were less clear for biome changes. Projected change in above-ground biomass was driven primarily by CO<sub>2</sub> fertilisation and showed that assumptions concerning CO<sub>2</sub> effects (eCO<sub>2</sub> or fCO<sub>2</sub>) caused the strongest variability in future projections (Table 2.3; Figure 2.2; Appendix A Figure S3). Even medium-impact scenarios (RCP4.5, irrespective of CO<sub>2</sub> scenario) suggested considerable ecosystem change (Figure 2.6; Appendix A Figure S6b,c).

### 2.5.1 Plant-physiological effects of eCO<sub>2</sub> and drivers of woody encroachment

Elevated CO<sub>2</sub> led to strong woody encroachment in our projections and was accompanied by enhanced WUE. Increases in NPP clearly drove WUE enhancement, although both photosynthesis (increase of NPP via more efficient CO<sub>2</sub> fixation) and g<sub>s</sub> (decrease) are affected by eCO<sub>2</sub> in aDGVM. We therefore conclude that increased WUE, intensification of carbon sinks and woody encroachment are mainly driven by CO<sub>2</sub> fertilisation of photosynthesis in aDGVM. This finding seems to contradict observational studies that found that increased intrinsic WUE in mature tropical and subtropical trees did not translate into growth enhancement and often even resulted in declining tree growth rates (Peñuelas *et al.*, 2011; Silva & Anand, 2013; van der Sleen *et al.*,

2015). However, our simulated biomass increases in savannas are driven by a combination of demographic processes and CO<sub>2</sub> fertilisation effects on tree seedlings and saplings, which are sub-mature, unlike most empirical studies (Figure 2.7).

Similar to observations reported from FACE experiments in young forest stands (Warren *et al.*, 2011), the effects of increased NPP and vegetation cover on transpiration outweigh the effects of decreased  $g_s$  under eCO<sub>2</sub> with increased transpiration having a dampening effect on WUE. For RCP8.5, this leads to an increased positive relation between NPP and MAP change with a steeper slope under eCO<sub>2</sub>. The increased sensitivity of NPP to MAP under RCP8.5 implies stronger limitation of plant growth by soil moisture availability. This limitation is driven by a combination of higher demand for water by more productive vegetation, higher transpiration (Appendix A Figure S4b), temperature increases, and regionally decreasing MAP (Appendix A Figure S1). However, the  $g_s$  model implemented in the aDGVM might not represent eCO<sub>2</sub>-responses adequately in these increasingly water-limited ecosystems (Medlyn *et al.*, 2001).

Our results confirm results from previous DGVM studies that plant-physiological CO<sub>2</sub> effects strongly impact projections of future vegetation states (Cramer *et al.*, 2001; Hickler *et al.*, 2015; Huntingford *et al.*, 2013; Rammig *et al.*, 2010; Sato & Ise, 2012). The ensemble modelling results are useful to estimate potential lower and upper bounds of potential eCO<sub>2</sub> effects. Disabled eCO<sub>2</sub> effect scenarios serve as a surrogate for low physiological sensitivity of plants to eCO<sub>2</sub>, represent an artificial lower bound of change. It is, however, unlikely that eCO<sub>2</sub> effects on plants will be negligible in systems composed of C<sub>3</sub> and C<sub>4</sub> plants, where feedbacks between CO<sub>2</sub> fertilisation and fire disturbance affecting the competitive balance between C<sub>3</sub> and C<sub>4</sub> plants have been postulated (Midgley & Bond, 2015). However, DGVMs such as aDGVM might not adequately represent carbon sink-source processes and other non-photosynthetic growth limitations (Körner, 2015), though empirical work by Kgope *et al.* (2010) strongly implicate sink:source effects in controlling the demographic process under elevated CO<sub>2</sub>, as simulated by aDGVM. The first sub-models that consider long-term physiological acclimation effects in plants to eCO<sub>2</sub> are now being implemented in DGVMs (Haverd *et al.*, 2018).

Nutrient dynamics in plants and ecosystems can stimulate or reduce eCO<sub>2</sub> effects on plants, but are not represented in aDGVM. Low nutrient availability, e.g. nitrogen and phosphorus deficits, limits the growth-enhancing effects of eCO<sub>2</sub> and therefore on aboveground biomass (e.g. Jiang *et al.*, 2020a; Peñuelas *et al.*, 2011). Vegetation models including nutrient cycling frequently predict smaller eCO<sub>2</sub> effects (Fleischer *et al.*, 2019; Hickler *et al.*, 2015). Field data suggests that tree encroachment might further reduce nitrogen availability in African savannas, which might lead to a negative feedback on CO<sub>2</sub>-induced tree encroachment (Higgins *et al.*, 2015). The ability of trees to benefit from eCO<sub>2</sub> under nutrient limitation depends on their association with different mycorrhizal types and a tree's ability to fix atmospheric nitrogen (Terrer *et al.*, 2018) with nitrogen-fixing trees from the Fabaceae-family having high abundances in African savannas (Stevens *et al.*, 2017). Under nitrogen limitation, tree species associated with arbuscular mycorrhizae, the dominant type in the tropics, benefit less than trees associated with ectomycorrhizae or N<sub>2</sub>-fixers (Terrer *et al.*, 2016, 2018).

Based on extrapolation of 138 eCO<sub>2</sub> experiments, Terrer *et al.* (2019) confirmed substantial biomass increases due to CO<sub>2</sub> fertilisation in past decades and likely in the future, even when accounting for nutrient limitation. They estimated 12±3% and 12.5±3% increases in global and tropical biomass, respectively, as a result of a 250ppm increase in [CO<sub>2</sub>] from 375ppm by 2100. This is less than the increase of 26.9% in aDGVM-projected aboveground biomass for eCO<sub>2</sub>-compared to fCO<sub>2</sub>-scenarios in 2080-2099 for RCP4.5 ( $\Delta\text{CO}_2 \sim 135\text{ppm}$ , Figure2a), but Terrer *et al.*'s results clearly ignore demographic effects that result in biome structural shifts. Next to missing nutrient limitations in aDGVM, another explanation for this mismatch could be that empirical eCO<sub>2</sub> experiments do not account for ecological feedback mechanisms proposed for savannas that might foster woody encroachment and increase biomass stocks (Midgley & Bond, 2015), nor does Terrer *et al.*'s meta analysis explicitly (but indirectly) include N<sub>2</sub>-fixation and the associated eCO<sub>2</sub> response. Indeed, Stevens *et al.* (2017) found that recent patterns of woody encroachment in savannas in Africa are often due to N-fixing species. Thus, large uncertainties in vegetation response remain with a significant response to be expected in tropical areas. For representation in DGVMs, the FUN2.0 model offers a mechanism that considers a

range of processes for nitrogen acquisition (e.g. different mycorrhizal strategies, active uptake, resorption from senescent leaves; Shi *et al.*, 2016).

Belowground carbon, including roots and soil carbon, are estimated to make up 77% of Sub-Saharan Africa's carbon stocks (161Pg C of 209Pg C total C stocks, Bombelli *et al.*, 2009). We acknowledge that root biomass and soil carbon are crucial for a full representation of the terrestrial carbon cycle, especially as carbon and nitrogen cycles are highly interdependent. Soil and vegetation responses to climate change and eCO<sub>2</sub> may vary and may impact carbon cycling significantly (Dietzen *et al.*, 2019; Dufresne *et al.*, 2002).

Long-term FACE experiments (AmazonFACE, OzFACE; Norby *et al.*, 2016; Stokes *et al.*, 2005) in African ecosystems in combination with eCO<sub>2</sub> experiments such as open-top chamber experiments with savanna plants (pers. comm. BS Ripley, March 2019) may provide further insights regarding the long-term effects of eCO<sub>2</sub> in Africa. Consolidated results from these experiments will contribute to a comprehensive understanding of the effects of rising [CO<sub>2</sub>] on African plant communities and can be used to revise process implementation in DGVMs.

## 2.5.2 Climate change impacts on biome patterns

Projected biome changes towards woody vegetation under eCO<sub>2</sub> are consistent with results from previous studies on regional (Conradi *et al.*, 2020; Doherty *et al.*, 2010) and continental scale (Gonzalez *et al.*, 2010; Higgins & Scheiter, 2012; Niang *et al.*, 2014; Scholze *et al.*, 2006; Sitch *et al.*, 2008). The transition of grassland and savanna biomes, i.e. C<sub>4</sub>-dominated biomes, to more woody biomes, i.e., C<sub>3</sub>-dominated biomes, in eCO<sub>2</sub> simulations corroborates findings that savannas and grasslands are particularly vulnerable to biome changes under eCO<sub>2</sub> (Higgins & Scheiter, 2012; Osborne *et al.*, 2018; Scheiter *et al.*, 2018). Woody encroachment into grasslands and savannas in Africa is a major threat to their biodiversity (Bond, 2016).

Tropical forests are less stable in our simulations than suggested by Gonzalez *et al.* (2010), Scholze *et al.* (2006) and Sitch *et al.* (2008). Climatic changes outweigh eCO<sub>2</sub> effects in a belt south of the equator with decreasing biomass in both CO<sub>2</sub> scenarios by 2080-2099, which is similar to DGVM-results by Sato & Ise (2012) and projections of carbon sinks saturating in African

tropical forests by 2040 (Hubau *et al.*, 2020). In our simulations, this decrease in regional carbon stocks in forests is outweighed on the continental scale by increases in other tropical forest areas as well as savanna and grassland areas that were not included in Hubau *et al.* (2020). Feedbacks between population dynamics and combined fire-eCO<sub>2</sub> effects in the aDGVM also explain this discrepancy. While Hubau *et al.* (2020) used linear regression models both to project predictor variables, such as mean annual temperature, and then based on these to project carbon changes into the future, here the process-based aDGVM was driven with downscaled GCM data. Increases in aboveground biomass and transitions to forest biomes in East Africa under both eCO<sub>2</sub> and present-day [CO<sub>2</sub>] levels (400ppm, fCO<sub>2</sub>) for both RCP scenarios are the result of higher water availability due to increased precipitation in these areas (Appendix A Figure S1e,f; Archer *et al.*, 2018; Doherty *et al.*, 2010; Engelbrecht *et al.*, 2015; Niang *et al.*, 2014).

Large proportions of simulated biome changes under eCO<sub>2</sub> occur in the moist sub-humid and humid tropics where woodland and C<sub>4</sub> savanna biomes were found in 2000-2019 (Figure 2.4a,b). This is opposed to previous studies where most changes occurred further north and south of the equator in regions with more open savannas (Gonzalez *et al.*, 2010; Higgins & Scheiter, 2012).

Explanations for differences in biome change projections between different studies include the use of different modelling approaches (e.g., species distribution models, Conradi *et al.*, 2020), different climate data sets, (e.g., GCM data or interpolated data such as ISIMIP instead of RCM data), different DGVMs (Doherty *et al.*, 2010; Gonzalez *et al.*, 2010), and that precipitation changes until 2100 were not accounted for (Higgins & Scheiter, 2012). In addition, utilisation of different biome classification schemes can influence if and where vegetation changes are simulated (Scheiter *et al.*, 2020) and create mismatches between different vegetation models that impede comparison of simulated biomes. Nonetheless, the different studies agree on a potential increase in the area covered by woody biomes under future climatic conditions.

Where MAP decreases and temperatures increase, C<sub>4</sub> plants can maintain their competitive advantage over C<sub>3</sub> plants even under eCO<sub>2</sub> (Higgins & Scheiter, 2012). We found such behaviour in southwestern Africa, where the CCAM ensemble predicts a decrease in MAP, and a

temperature increase to levels unprecedented in recent history. Trends of bush encroachment observed in this region in the recent past were explained by a combination of [CO<sub>2</sub>] increase, precipitation increase, and land use practices such as live stock grazing (O'Connor *et al.*, 2014). However, future projections of precipitation in our forcing data for this region showed a trend towards substantial precipitation decreases, i.e. opposed to increases in the past, whereas land use was not considered in our study. In particular, the shift from C<sub>4</sub> savanna to C<sub>4</sub> grasslands by 2080-2099 in the Kalahari under RCP8.5 with fCO<sub>2</sub> is due to the competitive advantage of C<sub>4</sub> plants under drier conditions at lower [CO<sub>2</sub>]. Differences between Higgins & Scheiter (2012) and our result in this region, illustrate that it is crucial to include precipitation changes in vegetation projections under climate change. Increasing likelihood or severity of droughts under future climate conditions may offset the eCO<sub>2</sub> effect, as plant responses to eCO<sub>2</sub> are hampered by low soil water availability (Nowak *et al.*, 2004; Reich *et al.*, 2014). On the other hand, advantages of C<sub>4</sub> grasses over C<sub>3</sub> grasses in dry habitats may be reduced under drought conditions (Taylor *et al.*, 2011).

### **2.5.3 Uncertainties of vegetation projections**

In our simulations, direct eCO<sub>2</sub> effects on plants are the primary determinants of the future carbon sink or source, WUE and biome states in Africa (Figures 2.2 and 2.6; Table 2.3). This is consistent with the results from Rammig *et al.* (2010) for the Amazon and Huntingford *et al.* (2013) for the global tropics. Direct eCO<sub>2</sub> effects are very likely, but considerable uncertainty remains with respect to the strength of the effect. Thus, the effect sizes in Table 2.3 only allow comparison of CO<sub>2</sub> effects and climate input data as simulated by the aDGVM. Nevertheless, our results suggest that improving our understanding of plant-physiological CO<sub>2</sub> effects is crucial to achieve realistic future ecosystem projections.

Areas with high uncertainty in projected biome transitions only partially agree with patterns reported by Gonzalez *et al.* (2010). Uncertainty is often higher in our study (Figure 2.9a). Both studies agree on high uncertainty for biome changes in the western parts of the transition zone between the Sahel and the Sahara. The uncertainty of biome change we inferred in this study

was similar or smaller than in Scholze *et al.*'s (2006) projections. Low agreement of projected biome changes in grassland, closed savanna, and woodland areas in our ensemble can be explained by alternative vegetation states related to fire occurrence typical for Africa (Hoffmann *et al.*, 2012; Moncrieff *et al.*, 2014; Staver *et al.*, 2011b) and variability in climatic drivers derived from GCMs, in particular uncertainty regarding precipitation.

Uncertainty in future projections is increased by the interplay of eCO<sub>2</sub>, fire and feedbacks caused by population dynamics. Enhanced tree sapling growth under eCO<sub>2</sub> may eventually reduce grass biomass and fine fuel availability, which in turn reduces fire frequency and intensity. In combination with climate changes, this feedback mechanism can lead to rapid woody encroachment in savanna ecosystems (Figure 2.7, Midgley & Bond, 2015). Fire disturbance is a factor shaping ecosystems (e.g. Bond & Midgley, 2012; Midgley & Bond, 2015; Scheiter *et al.*, 2012) leading to multiple stable states for the same climate zones (e.g. Higgins & Scheiter, 2012; Staver *et al.*, 2011b). Fire has been shown to influence and delay projected biome changes and can delay transitions to woody biomes and thus stabilisation of ecosystem states after changes in environmental drivers stabilised (e.g. [CO<sub>2</sub>], Scheiter *et al.*, 2020). Even when ecophysiological processes have already saturated (e.g. here expressed via NPP), ecosystem states continue to change (e.g., biomass, Figure 2.2a; Appendix A Figure S4a), because they have not reached an equilibrium state under changed environmental conditions. In addition, stochastic processes in the aDGVM fire model and differences in GCM climate projections can produce varying fire occurrences in different ensemble members and thus explain uncertainty in projections, especially in fire-shaped ecosystems like savannas. Other disturbances not included here, such as herbivory, and their interactions with fire and eCO<sub>2</sub> are additional factors of uncertainty in vegetation projections.

Despite of the uncertainties in regional patterns, the projections of substantial biome changes across all scenarios of the ensemble suggest substantial future changes in habitat structure and biodiversity. These potentially large changes in climate and biomes sharply contrast with relative stability in past climates and disturbance regimes in Africa, which probably contributed to its high biodiversity (Midgley & Bond, 2015).

## **2.5.4 Socio-economic development and flexible adaptation**

The stronger impacts under RCP8.5 compared to RCP4.5, irrespective whether eCO<sub>2</sub> or fCO<sub>2</sub> is assumed, entail that today's decisions from individual to policy level shape the degree to which climate, ecosystems and livelihoods will change. The strong carbon sink simulated here under RCP8.5-eCO<sub>2</sub> might suggest regional potential for land-based climate mitigation, but the associated conversion of grassy biomes to more encroached biomes is a threat to their biodiversity. Increased woody cover in grassy biomes might lead to losses of their ecosystem services, such as arable and range land (Parr *et al.*, 2014; Bond *et al.*, 2019).

The range of possible climate change impacts in Africa presented in our study can support policy makers and stakeholders in Africa in planning for alternative climate futures in climate change adaptation measures (Müller *et al.*, 2014) even though the study was not specifically designed to address policy questions. Our PNV simulations, for example, could help to guide good practice in nature conservation and land-use planning (Loidi & Fernández-González, 2012) or to avoid afforestation activities in non-forest ecosystems (Bond *et al.*, 2019; Brancalion *et al.*, 2019; Veldman *et al.*, 2015b). Stakeholders such as NGOs and state agencies can use projections of PNV to raise awareness for possible climate change impacts. To inform policy makers and stakeholders, it will also be necessary to include land management practices such as live-stock and fire management in model simulations (e.g. Pfeiffer *et al.*, 2019; Scheiter & Savadogo, 2016; Scheiter *et al.*, 2019) and to implement DGVM ensemble simulations with greenhouse gas emissions and land-use scenarios of different Shared Socio-Economic Pathways (SSPs, Popp *et al.*, 2017).

As the large differences between the different scenarios imply large uncertainties, adaptation strategies must be highly adaptive and flexible. Over time, observations of climate change and impacts on ecosystems will provide an improved knowledge base (Fletcher *et al.*, 2019). As opposed to using vegetation projections only, Bayesian statistics combined with a stochastic dynamic programming approach allow an upfront assessment of the opportunity of this increased knowledge base in the future (Fletcher *et al.*, 2019; Yousefpour *et al.*, 2012). Thus, trade-offs between investing in highly flexible measures compared to potentially simpler but less

flexible measures can be weighed against each other (Fletcher *et al.*, 2019). In combination with updated information on population developments and land-use change via continued monitoring, this method may support stakeholders in the development of adequate management plans. However, implementing this method requires close and iterative exchange between stakeholders and scientists, so that specific policy and planning questions and their uncertainties can be assessed using vegetation projections as an exploratory tool adjusted to the specific question (Weaver *et al.*, 2013).

Combining DGVMs with land use, SSPs and population development would give deeper insights into the vulnerability of different regions in Africa to climate change. However, knowledge of PNV states is a basis for future conservation planning and provides an estimate of ecosystem and plant types that could persist and thrive under future climatic conditions. When considering human population development and future potential land use, information on PNV is essential to feed into development policies. Especially in regions with higher uncertainty regarding the impact of climate change on future PNV, a diverse set of climate change adaptation measures needs to be included in development strategies, such as diversification of income and flexibility in production methods, to account for this uncertainty (Müller *et al.*, 2014). Policies need to embrace the opportunities of continuous knowledge gain about climate change impacts (Fletcher *et al.*, 2019) based on latest monitoring results, empirical research and updated models with scientists and policy makers collaborating closely in the decision making process.

## 2.6 Acknowledgements

This study and CM were funded under the SPACES - Science Partnerships for the Assessment of Complex Earth System Processes - under the German Federal Ministry of Education and Research (BMBF)'s framework programme (Project EMSAfrica, grant number 01LL1801B). MP thanks the BMBF SPACES initiative for funding South African Limpopo Landscapes Network (SALLnet) project, grant 01LL1802B. GFM acknowledges support under a Humboldt Research Award, and funding under the NRF Global Change Grand Challenge Grant number (11859).

SS thanks the DFG Emmy Noether programme for funding (grant SCHE 1719/2-1). The authors thank the SBiK-F modelling centre research group and the ARS AfricaE and EMSAfrica research consortia for valuable insights.

## 2.7 Data Sharing and Accessibility

The aDGVM code that was used to produce the results in this publication is available on Github ([https://github.com/540aDGVM/aDGVM1\\_CCAM](https://github.com/540aDGVM/aDGVM1_CCAM)). aDGVM simulation results are accessible through the SASSCAL database ([http://data.sasscal.org/metadata/view.php?view=library&process\\_step&id=6379&ident=118872017185729320](http://data.sasscal.org/metadata/view.php?view=library&process_step&id=6379&ident=118872017185729320)).

## Chapter 3

# Combined impacts of future climate-driven vegetation changes and socioeconomic pressures on protected areas in Africa

*Carola Martens, Simon Scheiter, Guy F. Midgley, and Thomas Hickler<sup>\*†</sup>*

---

<sup>\*</sup>This chapter is published as Martens *et al.* (2022) Combined impacts of future climate-driven vegetation changes and socioeconomic pressures on protected areas in Africa, *Conservation Biology*, 36, e13968. <https://doi.org/10.1111/cobi.13968>. Supporting information can be found in Appendix B.

<sup>†</sup>Author contributions: C.M., T.H. and S.S. conceived the study. C.M. designed and conducted the analysis of simulation results. S.S. and T.H. contributed to the analysis of simulation results. C.M. led the writing of this article with contributions from all authors.

### **3.1 Abstract**

Africa's protected areas (PAs) are the last stronghold of the continent's unique biodiversity, but they appear increasingly threatened by climate change, substantial human population growth, and land-use change. Conservation planning is challenged by uncertainty about how strongly and where these drivers will interact over the next few decades. We investigated the combined future impacts of climate-driven vegetation changes inside African PAs and human population densities and land use in their surroundings for 2 scenarios until the end of the 21<sup>st</sup> century. We used the following 2 combinations of the shared socioeconomic pathways (SSPs) and representative greenhouse gas concentration pathways (RCPs): the "middle-of-the-road" scenario SSP2–RCP4.5 and the resource-intensive "fossil-fueled development" scenario SSP5–RCP8.5. Climate change impacts on tree cover and biome type (i.e., desert, grassland, savanna, and forest) were simulated with the adaptive dynamic global vegetation model (aDGVM). Under both scenarios, most PAs were adversely affected by at least 1 of the drivers, but the co-occurrence of drivers was largely region and scenario specific. The aDGVM projections suggest considerable climate-driven tree cover increases in PAs in today's grasslands and savannas. For PAs in West Africa, the analyses revealed climate-driven vegetation changes combined with hotspots of high future population and land-use pressure. Except for many PAs in North Africa, future decreases in population and land-use pressures were rare. At the continental scale, SSP5–RCP8.5 led to higher climate-driven changes in tree cover and higher land-use pressure, whereas SSP2–RCP4.5 was characterized by higher future population pressure. Both SSP–RCP scenarios implied increasing challenges for conserving Africa's biodiversity in PAs. Our findings underline the importance of developing and implementing region-specific conservation responses. Strong mitigation of future climate change and equitable development scenarios would reduce ecosystem impacts and sustain the effectiveness of conservation in Africa.

## 3.2 Introduction

African protected areas (PAs) are strongholds of Africa's unique biodiversity (Pacifici *et al.*, 2020) and are fundamental to safeguarding it. A proposed key global goal is to protect 30% of terrestrial area (action target 3, Convention on Biological Diversity [2021]), but there is increasing evidence that under climate change this target may not be ambitious enough to protect biodiversity (Hannah *et al.*, 2020). Even today, PAs and the biodiversity they conserve are increasingly under pressure from global change drivers such as climate change (Hannah, 2008), human population growth, and land-use change (Geldmann *et al.*, 2014).

Climate-driven vegetation changes in African PAs have already been observed. Woody encroachment into African savannas in PAs has probably at least partly been driven by fertilization effects of increased atmospheric CO<sub>2</sub> on woody plants (Stevens *et al.*, 2017). Changes in tree cover and thus vegetation structure in savanna and forest biomes imply habitat loss and decreased biodiversity (Aleman *et al.*, 2016; Midgley & Bond, 2015), which impairs the potential of PAs for biodiversity conservation under climate change. Under future climate change, dynamic vegetation models (DVMs) have projected woody encroachment into African grasslands and savannas driven by increasing atmospheric CO<sub>2</sub> and its potential effects on plant physiology and vegetation structure (Martens *et al.*, 2021; Scheiter & Higgins, 2009). In dynamic vegetation simulations for areas with at least 50% protected area, only 2% of Africa remains refugia for biodiversity under climate change (Eigenbrod *et al.*, 2015).

At the beginning of the 21<sup>st</sup> century, human population growth within the perimeters of African PAs was limited (Geldmann *et al.*, 2019). However, until the end of the century, the human population in sub-Saharan Africa is projected to increase substantially, in contrast to all other global regions (United Nations, Department of Economic and Social Affairs, Population Division, 2019). Urbanization in the vicinity of PAs is projected to increase more than 8-fold from 2000 to 2030 across Africa, which implies vast, dynamic changes in future socioeconomic pressures on biodiversity and PAs (Güneralp *et al.*, 2017). In the past, agricultural expansion inside

African PAs was stronger than in similar unprotected regions (Geldmann *et al.*, 2019). Deforestation, logging, and fire in the immediate vicinity of PAs often drive changes within PAs (e.g., through ecological edge effects and by predisposing the PA to similar land-use-driven changes) (Laurance *et al.*, 2012). In the future, pressure from commercial agriculture in the vicinity of PAs is expected to increase and intensify (DeFries *et al.*, 2007), likely driven by the expected human population growth and socioeconomic developments.

Increased pressure from a combination of drivers such as human population and intensive agriculture on the majority of African PAs has already been reported for the recent past, although pressure was reduced for several other PAs in Africa (Jones *et al.*, 2018). However, there have been few studies on relationships between climate change impacts (e.g., tree-cover changes) and pressure from socioeconomic drivers (e.g., human population density and agricultural and pasture land use) as they relate to African PAs in the future. Asamoah *et al.* (2021) estimated that by 2050, ~27% of PAs globally are expected to be in areas with large climate and land-use changes. PAs in tropical moist forests and tropical savanna and grassland biomes are expected to be particularly affected (Asamoah *et al.*, 2021). Both land-use and climate change have been projected to continuously drive a decline of African plant biodiversity in the future for most regions and scenarios (Di Marco *et al.*, 2019).

To assess global change pressure on PAs in Africa until the end of the 21<sup>st</sup> century, we used projections for climate-driven tree-cover change, human population density, and land use, including urban, agricultural, pasture, and natural land, under 2 shared socioeconomic pathway (SSP) and representative concentration pathway (RCP) marker scenarios (SSP2-RCP4.5 and SSP5-RCP8.5). For each SSP–RCP scenario, we investigated up to the end of the 21<sup>st</sup> century which PAs and biomes in PAs were projected to be most affected by climate-change-driven vegetation and habitat loss; which PAs were projected to be particularly affected by population and land-use pressure in their surroundings; and whether population and land-use pressures were projected to co-occur with each other and with climate-change-driven vegetation changes. We also investigated whether the global-change scenarios we considered suggest differing strategies for conservation in different PAs in Africa.

The SSP2–RCP4.5 is the “middle-of-the-road” (O’Neill *et al.*, 2017) scenario in which global inequalities in development and income growth continue with some regional improvements and medium climatic changes (Riahi *et al.*, 2017). In SSP5RCP8.5, rapid economic and social development is driven by fossil fuel exploitation and associated strong climate change and technological development (“fossil-fueled development”) (Kriegler *et al.*, 2017). We simulated climate-driven vegetation changes with the adaptive dynamic global vegetation model (aDGVM) and used projections of population density (Gao, 2019) and land use (Hurtt *et al.*, 2020) and their respective changes in the surroundings of PAs as proxies for future socioeconomic pressures directly or indirectly exerted on PAs.

### 3.3 Methods

#### 3.3.1 Scenarios

The RCP and SSP scenarios describe alternative future developments of anthropogenic climate change and its drivers. Emissions associated with possible societal development (SSP) are used as input for RCP scenarios. Radiative forcing from RCP scenarios is used as input for climate model projections. The SSP–RCP scenarios that we used in our analysis, SSP2–RCP4.5 and SSP5–RCP8.5, are designated marker scenarios and part of the Scenario Model Intercomparison Project (ScenarioMIP) for phase 6 of the Coupled Model Intercomparison Project (O’Neill *et al.*, 2016).

The selection of scenario combinations was limited to SSP2–RCP4.5 and SSP5–RCP8.5 by the available climate data for vegetation simulations. Under SSP2–RCP4.5, population is projected to increase by ~157% from 2010 until 2100 for Africa (KC & Lutz, 2017). Cropland is expected to expand by ~51% (~154Mha) and pastures to decrease by ~7% (58Mha) from 2020 to 2090 in Africa (based on land-use harmonization [LUH2] data) (Hurtt *et al.*, 2020) (see land-use section under “Data sets and data processing” section). Climatic changes are modest to high and mean

annual temperature from 2000–2019 to 2080–2099 is projected to increase by 2.0 °C at the continental scale in Africa (derived from Engelbrecht *et al.* [2015] and Martens *et al.* [2021]) (details below in “aDGVM and simulation design” section).

Under SSP5–RCP8.5, the evolving global energy-intensive lifestyle and associated greenhouse gas emissions lead to strong climate changes, with mean annual temperature increasing by 4.5 °C from 2000–2019 to 2080–2099 in Africa (based on Engelbrecht *et al.* [2015] and Martens *et al.* [2021]). Africa’s population in 2100 is projected to be 77% higher than in 2010 (KC & Lutz, 2017). Even though population increase for SSP5–RCP8.5 is only about half the increase for SSP2–RCP4.5, the increased food and feed demand of the changed lifestyle (Hurtt *et al.*, 2020) leads to a similar expansion in cropland (~42%, ~131 Mha) and decrease in pastures (~−7%, ~58 Mha, LUH2 data) from 2020 to 2090 in Africa.

### 3.3.2 aDGVM and simulation design

The aDGVM is a DVM and was originally developed for tropical vegetation and treegrass dynamics in Africa. It includes dynamic climate–vegetation–fire feedback processes (Scheiter & Higgins, 2009), which influence tree cover and thus habitats and biome changes in Africa (Midgley & Bond, 2015). Implemented processes at the plant level include photosynthesis, transpiration, and carbon allocation to different plant compartments based on limiting factors, such as light and water availability (Scheiter & Higgins, 2009). Simulated trees compete for light with neighboring trees and for water with all plants at stand scale. Trees are represented as individuals of forest or savanna tree types. Forest trees are shade tolerant but do not cope well with fire, whereas savanna trees are fire tolerant, but shade intolerant. Grasses are represented by superindividuals with C<sub>4</sub> or C<sub>3</sub> photosynthesis growing either below or between tree canopies. Shrubs are not included in aDGVM and thus ecosystems such as the Succulent Karoo or Fynbos in South Africa are not well represented. Fire disturbance occurs in aDGVM depending on available fuel biomass from grasses and tree leaf litter and their moisture content. Ignition events occur randomly. A full model description is in Scheiter & Higgins (2009) and Scheiter *et al.* (2012).

We used results for potential natural vegetation (i.e., no human land use) from aDGVM simulations in Martens *et al.* (2021). The aDGVM was forced with an ensemble of climate input from 6 different general circulation models (GCMs) (i.e., ACCESS, CCSM4, CNRM, GFDL, MPI, NorESM1M [Archer *et al.*, 2018]) that were downscaled for Africa with the conformal-cubic atmospheric model (CCAM) (McGregor, 2005) to  $0.5^\circ$  resolution. The mechanistic model CCAM was forced with bias-corrected sea-surface temperature and sea-ice data from the GCMs (Engelbrecht *et al.*, 2015) for RCP4.5 and RCP8.5. Soil properties were derived from Global Soil Data Task Group's (2000) soil data. The aDGVM was run for a spin-up period of 210 years to allow simulated vegetation to reach an equilibrium state. Spin-up was followed by a transient phase with the CCAM climate data for 1971–2099. For each  $0.5^\circ$  grid cell, vegetation in aDGVM was simulated in a 1-ha stand. We scaled the simulation results up to the  $0.5^\circ$  grid by assuming vegetation is homogeneous in each grid cell and that the simulated 1-ha stand is representative for the grid cell. We used the mean across the ensemble of 6 aDGVM simulations for each RCP scenario for our analyses.

### 3.3.3 Data sets and data processing

We derived geographical location and administrative boundaries of PAs in Africa from the World Database on Protected Areas (WDPA) (UNEP-WCMC & IUCN, 2019). An overview figure of data sets used is in Appendix B S1. We excluded PAs smaller than  $5 \text{ km}^2$  from the analysis. Hence, many of the PAs considered in the analysis are smaller than the resolution of the other data sets used ( $0.5^\circ$  for vegetation,  $0.25^\circ$  for LUH2). Vegetation in smaller PAs is often characterized by small-scale local microclimatic and topographic conditions, such as steep valleys, that cannot be captured in DVM simulations due to the coarse resolution of climate forcings. We used QGIS 3.10 (QGIS Development Team, 2021) to select African terrestrial PAs of an area greater than  $5 \text{ km}^2$  for the analysis, fill holes in PAs, and identify and fix invalid geometries, such as self-intersecting polygons in the original data set, with the fix geometries algorithm in QGIS. The PAs without spatial polygon data available were excluded from this study as well as PAs with a designation status of proposed or not reported. Coastal PAs

that were not covered by the aDGVM data, due to the resolution of simulations, were also removed. In total, 5121 PAs were used for this analysis (72.0% of terrestrial PAs with spatial data and 99.9% of their total PA [Appendix B S2]).

Human population pressure was based on Gao's 2019 downscaled projections for SSPs 2 and 5 at 1 km<sup>2</sup> resolution (Gao, 2017). We used climate data operators' (CDO) remapcon algorithm for first-order conservative remapping (Schulzweida, 2019) to regrid these projections to 0.25° resolution to match the resolution of the LUH2 data set (see below). For each grid cell, decadal population (pop.) densities for 2020 and 2090 were rescaled from 0 to 10 so land-use and population would be on comparable scales. This rescaling assumes a steep increase of population pressure at low population densities that saturates at a population density of 1000/km<sup>2</sup> (Venter *et al.*, 2016):

$$pop.\text{pressure} = \begin{cases} 3.333 * \log_{10}(\text{pop. density} + 1) & \text{pop. density} < 1000/\text{km}^2 \\ 10 & \text{pop. density} \geq 1000/\text{km}^2. \end{cases} \quad (3.1)$$

To estimate land-use pressure, we used annual data for 2020 and 2090 from SSPRCP marker scenarios SSP2–RCP4.5 and SSP5–RCP8.5 from the LUH2 data set (Hurtt *et al.*, 2020) at 0.25° resolution. The LUH2 data were simulated with different integrated assessment models (IAMs) that combine economic and energy models with agricultural and land-use models and environmental impacts (Hurtt *et al.*, 2020). The SSP2–RCP4.5 data were simulated with the IAM MESSAGE-GLOBIOM and SSP5–RCP8.5 with REMIND-MAgPIE (Hurtt *et al.*, 2020). Each IAM implementation is the marker scenario for the respective SSP and recommended for use in analyses of climate change impact (Riahi *et al.*, 2017).

We grouped the different land-use types in LUH2 into 5 classes (primary vegetation, secondary vegetation, pasture, cropland, urban) and assigned each class a land-use pressure factor from 0 to 10 (Appendix B S3) based on an adapted scheme from Venter *et al.* (2016). We grouped secondary natural vegetation into young, intermediate, and mature vegetation based on stand age classes (Newbold *et al.*, 2015), where land-use pressure was lower for mature vegetation

stands and higher for young stands. In the LUH2 data set, the fractional cover of each land-use type in a grid cell is given. The overall land-use pressure in a grid cell is based on the weighted mean of pressure factors of land-use fractions. A land-use level of 4 is equivalent to pasture. Levels of 4 and higher are considered human dominated (Watson *et al.*, 2016).

### 3.3.4 Data analysis

Based on simulated tree cover and aboveground biomass, we classified vegetation into desert, grassland, savanna, and forest biomes (simplified from Martens *et al.*, 2021) (Appendix B S4). The savanna–forest threshold was chosen at 70% tree cover to reflect observations from remote sensing on the fire- and rainfall-driven bimodality of savanna and forest showing that intermediate tree cover levels of 50–75% rarely occur in Africa (Staver *et al.*, 2011a). Subtropical deserts are treeless (Chapin III *et al.*, 2011); therefore, we used biomass to distinguish grasslands from deserts. Biome classification for a PA was based on means for tree cover and aboveground biomass in the PA. Because habitat loss is an important driver of biodiversity loss, we used changes in tree cover as an indicator of habitat loss in forest, savanna (Aleman *et al.*, 2016), and grassland. Tree-cover change does not represent habitat loss and climate-driven vegetation changes well for desert biomes; therefore, we used change in aboveground biomass as indicator of habitat loss in the desert biome (Appendix B S5).

Analyses of the impacts of the different drivers on PAs in Africa were conducted in R (R Core Team, 2020). For climate change impacts on PAs, we analyzed simulated vegetation and vegetation changes within PAs and used the R package raster (Hijmans, 2020)) to crop data to the boundaries of PAs. Ensemble means of aDGVM simulation results were averaged over 2, 20-year periods, 2000–2019 and 2080–2099, to represent long-term climate-driven vegetation states for both RCP scenarios. We used population and land use within a specified area surrounding PAs (i.e., buffers) (Wittemyer *et al.*, 2008) as a proxy for potential pressures resulting from socioeconomic states and indirect drivers, such as deforestation or overexploitation of ecosystem resources near PAs. We assumed that population and land-use drivers mainly act from outside PAs and omitted communities and land use inside PAs. Population and land use for grid cells

intersecting with buffers and the size of the intersecting area were used to derive average pressures from outside a PA. Based on a previous study (Wittemyer *et al.*, 2008) and our minimum PA size of 5 km<sup>2</sup>, we chose 10-km buffers around each PA, but also tested 50-km buffers. Buffer areas were created in QGIS.

To investigate the impacts of climate-driven vegetation changes on biomes in PAs, we compared each biome's share of the total area protected in 2000–2019 and in 2080–2099 and looked at shares of their initial extent affected by habitat loss. To investigate regional differences in the drivers and impacts on PAs, we grouped the PAs by regions of the African Union (Organization of African Unity, 1976) (Appendix B S6) and compared them in a box plot. Changes in socioeconomic pressures were calculated as the difference between pressure factors in 2090 and 2020. To determine whether PAs in certain regions were projected to be particularly affected by multiple drivers simultaneously, we plotted population pressure, land-use pressure (and their changes), and climate-driven tree-cover change from 2000–2019 to 2080–2099 against each other for different regions and projected habitat loss of PAs by convex hulls. We investigated relationships between the socioeconomic pressures, population and land use (and their changes), and climate-driven tree-cover change with Spearman's rank correlation for each scenario at continental and regional scale. These analyses required a single indicator of climate change impact on vegetation in PAs. For this purpose, we chose change in mean simulated tree cover because tree cover was also used for the classification of 3 out of the 4 biomes used. Absolute values of tree-cover change were used for Spearman's rank correlation because both negative and positive tree-cover changes represent climate-driven vegetation changes. For population and land-use pressure, actual change values in the buffers were used because increasing values represented increasing pressure. A strong relationship between the different pressure factors may also occur when pressures are low. To analyze differences between the SSP–RCP scenarios, we compared the respective results from the above analyses.

## 3.4 Results

### 3.4.1 Climate-driven vegetation changes

Model results showed large increases in tree cover until 2080–2099 (Figure 3.1a,e), which often implied habitat loss in PAs in savanna and grassland regions under both scenarios (Figure 3.1b,f). The savanna and grassland areas in PAs decreased, and more than 50% of these biomes were projected to lose habitat until the end of the century under both scenarios (Table 3.1). Forest area in PAs increased under both scenarios (Table 3.1) and was projected to be less affected by habitat loss (Table 3.1; Figure 3.1b,f). Modeled tree cover increases and decreases in PAs were more pronounced under SSP5–RCP8.5 than under SSP2–RCP4.5 (Figure 3.2a). For both scenarios, tree-cover change in the majority of PAs in Southern and West Africa exceeded the median tree-cover change at the continental scale (Figure 3.2a).

TABLE 3.1: Shares of overall protected area in 2000-2019, and 2080-2099 and of projected habitat loss for each biome.

	Desert	Grassland	Savanna	Forest
<b>SSP2-RCP4.5</b>				
2000-2019	13.7%	9.4%	51.2%	25.7%
2080-2099	9.4%	8.2%	46.4%	36.0%
habitat loss <sup>b</sup>	39.0%	56.7%	67.3%	15.0%
<b>SSP5-RCP8.5</b>				
2000-2019	16.2%	7.0%	51.3%	25.5%
2080-2099	13.9%	5.4%	40.1%	40.7%
habitat loss <sup>b</sup>	19.3%	64.2%	71.8%	21.2%

<sup>a</sup> Simulated with the adaptive dynamic global vegetation model. Results from Martens *et al.* (2021) were classified into biomes based on the scheme in Appendix B S4. Definitions: SSP2–RCP4.5, intermediate scenario in which global inequalities in development and income growth cont with some regional improvements and medium climatic changes (Riahi *et al.*, 2017); SSP5–RCP8.5, rapid economic and social development driven by fossil fuel exploitation and associated strong climate change and technological development (Kriegler *et al.*, 2017).

<sup>b</sup> Based on the scheme to determine habitat loss in Appendix B S5.

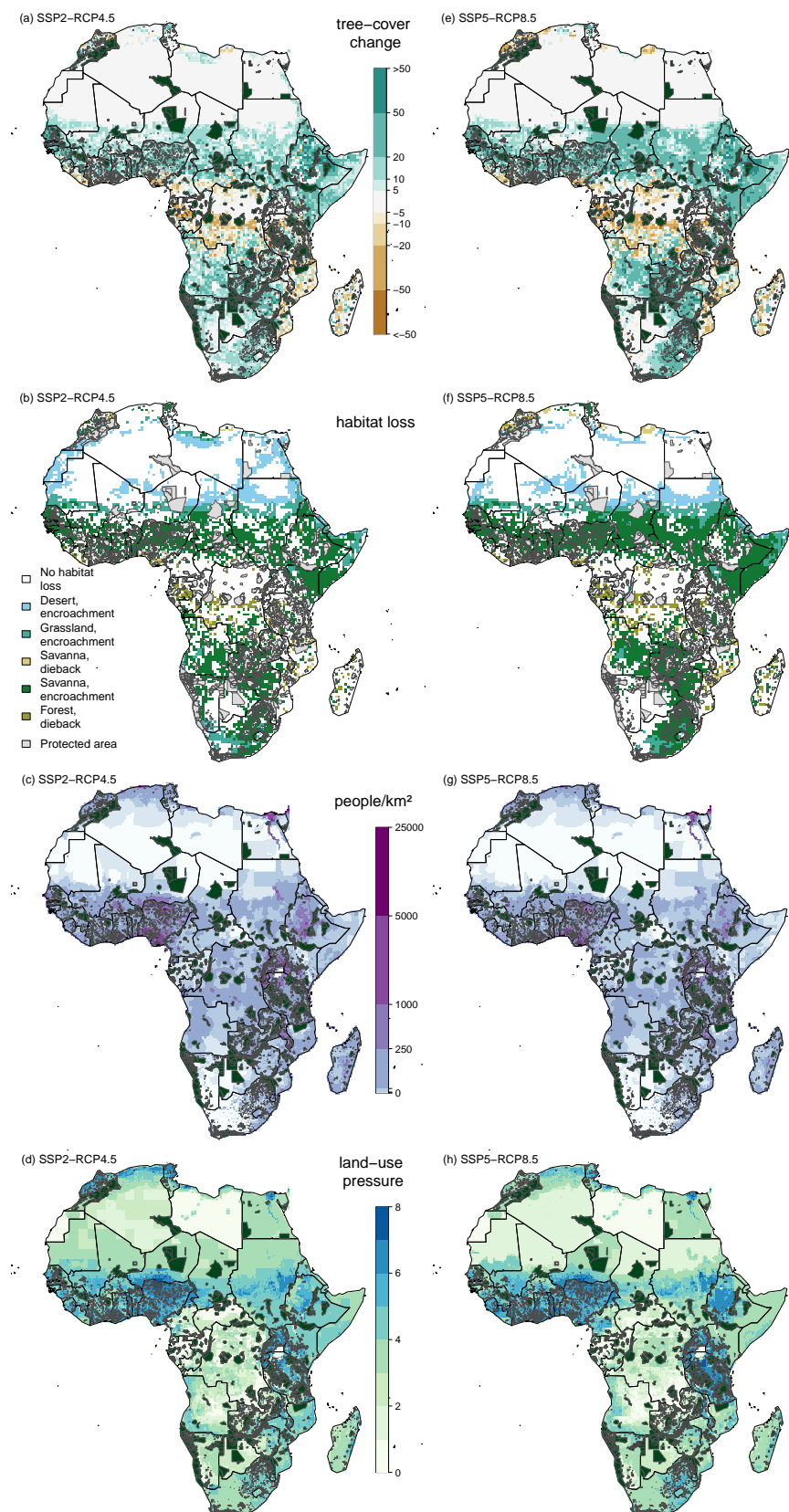


FIGURE 3.1: Projected (a, e) climate-driven change in tree cover in percentage points, (b, f) habitat loss, (c, g) population density in people per square kilometers, and (d, h) land-use pressure in Africa and protected areas for scenarios (a–d) SSP2–RCP4.5 and (e–h) SSP5–RCP8.5 (RCP, representative concentration pathways; SSP, shared socioeconomic pathways). Projected tree-cover changes (a, e) and derived habitat loss (b, f) (derived from the adaptive dynamic global vegetation model) show the difference between 2000–2019 and 2080–2099 (based on Martens *et al.* [2021]). For deserts, encroachment was defined as aboveground biomass increase  $>0.5$  t/ha. For grasslands and savannas, encroachment was defined as an increase in tree cover  $>5$  percentage points (p.p.) and  $>10$  p.p., respectively. Dieback for savanna and forest was defined by reductions of tree cover of ( $>10$  and  $>20$  p.p., respectively). Population (based on Gao [2017]) and land-use (based on Hurtubise *et al.* [2020]) pressure are shown for 2090. Land-use pressure factors were based on an adapted scheme from Venter *et al.* (2016), in which higher numbers represent higher land-use pressure. Protected areas used in this study are mapped on top for each panel. Maps of population density and land-use pressures in 2020 and their projected changes up to 2090 for both SSP–RCP scenarios are in Appendix B S8

### 3.4.2 Future socioeconomic pressures

At the continental scale, PAs were projected to experience higher population pressure in buffers in 2090 under SSP2–RCP4.5 than under SSP5–RCP8.5 (Figure 3.2b); regional patterns were similar (Figure 3.1c,g). For the majority of PAs in North and Southern Africa, population densities decreased by the end of the century under SSP5–RCP8.5 (Figure 3.2b). Continental-scale projections of land-use pressure generally showed higher pressure under SSP5–RCP8.5 than under SSP2–RCP4.5 in 2090 (Figure 3.2b). However, in North Africa future land-use pressure in the buffers of PAs was generally lower under SSP5–RCP8.5 than under SSP2–RCP4.5 (Figures 3.1d,h & 3.2b). Projected land-use pressure in 2090 for PAs in East and West Africa was high (Figure 3.1d,h). Increases in land-use pressure for the majority of PAs in Central, East, and West Africa exceeded the continental-scale median increase (Figure 3.2b). Most PAs in Central Africa were projected to experience lower future population and land-use pressure in their buffers than the continental-scale medians, whereas PAs in East and West Africa were projected to be particularly exposed to both pressures in their buffers under both SSP–RCPs (Figure 3.2b).

### 3.4.3 Co-occurrence of climate-driven vegetation changes and future socioeconomic pressures

At the continental scale, 7.1% of PAs under SSP2–RCP4.5 and 8.2% under SSP5–RCP8.5 were projected to experience high future pressure from all 3 global-change drivers

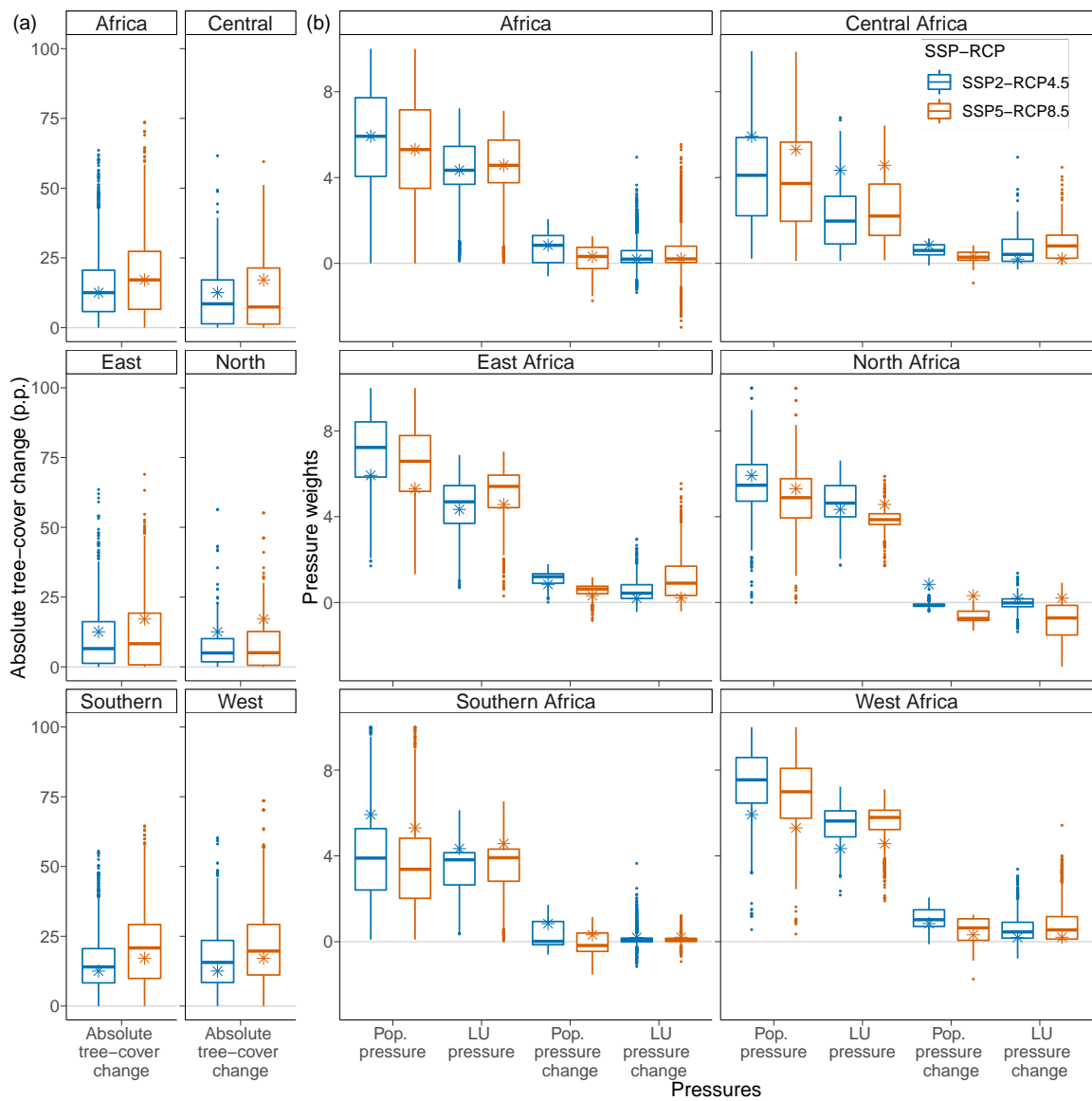


FIGURE 3.2: (a) Climate-driven change in tree cover in protected areas (derived from adaptive dynamic global vegetation model based on results from Martens *et al.* [2021]) and (b) socioeconomic pressures in 10-km zones around protected areas by region under SSP2-RCP4.5 (SSP, shared socioeconomic pathways; RCP, representative concentration pathways) and SSP5-RCP8.5 scenarios (defined in Table 3.1 and text) (p.p., percentage points; pop., population; LU, land use; horizontal lines, median; box ends, 25% and 75% quantile; ends of whisker lines, smallest or largest value, respectively,  $\geq$  or  $\leq$  1.5 times the interquartile range beyond the box ends of protected areas in each group; \* continental scale medians from the Africa panel for each pressure and scenario combination). Regions are based on regions defined by the African Union (Appendix B S6). Absolute values for tree-cover change from 2000–2019 to 2080–2099 are used because both negative and positive tree-cover changes represent climate-driven vegetation changes. The socioeconomic pressures population (based on Gao [2017]) and land use (based on Hurtt *et al.* [2020]) in 10-km zones around the protected areas were rescaled from 0 to 10 (Equation 3.1; Appendix B S3) based on Venter *et al.*'s (2016) scheme. Pressures for protected areas by biome and region under both scenarios are in Appendix B S7

(Figure 3.3a,b; PAs with population and land-use pressure levels >6 and habitat loss). Future population and land-use pressure were positively correlated with each other for both scenarios at the continental scale and for most regions (Table 3.2), but future changes in population and land-use pressure on buffers of PAs were only weakly correlated under SSP5–RCP8.5 (Table 3.2). Climate-driven tree-cover changes in PAs were not correlated with future population, land-use pressures, or their changes (Table 3.2).

TABLE 3.2: Spearman's rank correlation ( $\rho$ ) of pressures in and around protected areas for both SSP–RCP<sup>a</sup> scenarios at continental scale and on regional level

Pressure and scenario <sup>b</sup>	Continental (5121 <sup>c</sup> )	Central Africa (187 <sup>c</sup> )	East Africa (1017 <sup>c</sup> )	North Africa (279 <sup>c</sup> )	Southern Africa (1979 <sup>c</sup> )	West Africa (1659 <sup>c</sup> )
<b>TCC &amp; population</b>						
SSP2-RCP4.5						
$\rho$	-0.06	-0.11	-0.31	0.37	0.01	0.01
p	<0.0005	0.137	<0.0005	<0.0005	0.647	0.598
SSP5-RCP8.5						
$\rho$	-0.05	-0.14	-0.29	0.51	0.19	-0.07
p	<0.0005	0.055	<0.0005	<0.0005	<0.0005	0.007
<b>TCC &amp; population change</b>						
SSP2-RCP4.5						
$\rho$	-0.04	-0.14	-0.15	-0.16	-0.09	-0.01
p	0.002	0.062	<0.0005	0.006	<0.0005	0.837
SSP5-RCP8.5						
$\rho$	-0.02	-0.17	-0.20	-0.14	0.02	0.00
p	0.109	0.024	<0.0005	0.020	0.286	0.988
<b>TCC &amp; land use</b>						
SSP2-RCP4.5						
$\rho$	0.02	0.02	-0.16	0.30	-0.03	-0.01
p-value	0.167	0.795	<0.0005	<0.0005	0.212	0.811
SSP5-RCP8.5						
$\rho$	-0.02	0.05	-0.08	0.08	0.00	-0.10
p	0.112	0.542	0.008	0.163	0.911	<0.0005
<b>TCC &amp; land use change</b>						
SSP2-RCP4.5						
$\rho$	0.03	0.17	0.01	0.12	0.02	0.01
p-value	0.019	0.024	0.776	0.039	0.384	0.566
SSP5-RCP8.5						
$\rho$	-0.10	0.00	0.11	-0.57	-0.15	-0.11
p	<0.0005	0.938	0.001	<0.0005	<0.0005	<0.0005

*continued*

Pressure and scenario <sup>b</sup>	Continental (5121 <sup>c</sup> )	TABLE 3.2: (continued)					
		Central Africa (187 <sup>c</sup> )	East Africa (1017 <sup>c</sup> )	North Africa (279 <sup>c</sup> )	Southern Africa (1979 <sup>c</sup> )	West Africa (1659 <sup>c</sup> )	
<b>Population &amp; land use</b>							
SSP2-RCP4.5							
$\rho$	0.70	0.57	0.69	0.63	0.17	0.69	
p	<0.0005	<0.0005	<0.0005	<0.0005	<0.0005	<0.0005	
SSP5-RCP8.5							
$\rho$	0.67	0.60	0.44	0.18	0.12	0.56	
p	<0.0005	<0.0005	<0.0005	0.002	<0.0005	<0.0005	
<b>Population change &amp; land use change</b>							
SSP2-RCP4.5							
$\rho$	0.33	0.22	-0.35	0.07	0.19	-0.23	
p	<0.0005	0.003	<0.0005	0.243	<0.0005	<0.0005	
SSP5-RCP8.5							
$\rho$	0.11	-0.05	-0.28	0.36	-0.46	-0.51	
p	<0.0005	0.470	<0.0005	<0.0005	<0.0005	<0.0005	

<sup>a</sup> Shared socioeconomic pathway (SSP) and representative concentration pathway (RCP). Pathways are defined in Table 3.1 and text. Correlations for SSP–RCP scenario combinations SSP2–RCP4.5 and SSP5–RCP8.5 were derived.

<sup>b</sup> TCC, tree-cover change simulated with the adaptive dynamic global vegetation model (Martens *et al.*, 2021) for which absolute change values from 2000–2019 to 2080–2099 were used because both negative and positive tree-cover changes represent climate-driven vegetation changes; population, projections derived from Gao (2017); land-use pressure, projections derived from Hurtt *et al.* (2020). For population and land use, values for 2090 and change from 2020 to 2090 were derived from areas surrounding protected areas.

<sup>c</sup> Number of protected areas considered.

In West Africa, PAs were projected to experience climate-driven habitat loss in combination with elevated future population and land-use pressure in their buffers under both scenarios (Figure 3.3a,b). These included PAs in savannas and forests of West Africa, where current socioeconomic pressures are already high (Appendix B S7). For PAs in East Africa, climate-driven tree-cover change was negatively correlated with future population pressure and its change under both scenarios (Table 3.2). Future population and land-use changes in East Africa were negatively correlated (Table 3.2). For Central Africa, future population pressure was lower under both scenarios for PAs affected by habitat loss than for those without (Figure 3.4a,b), but future land-use pressure was, on average, higher (Figure 3.5a,b). Future changes in population pressure were generally lower for PAs in Central Africa affected by habitat loss (Figure 3.4c,d). Many PAs in Southern Africa were subject to habitat loss with low to intermediate future socioeconomic pressures under both scenarios (Figure 3.3). Under SSP5–RCP8.5, for

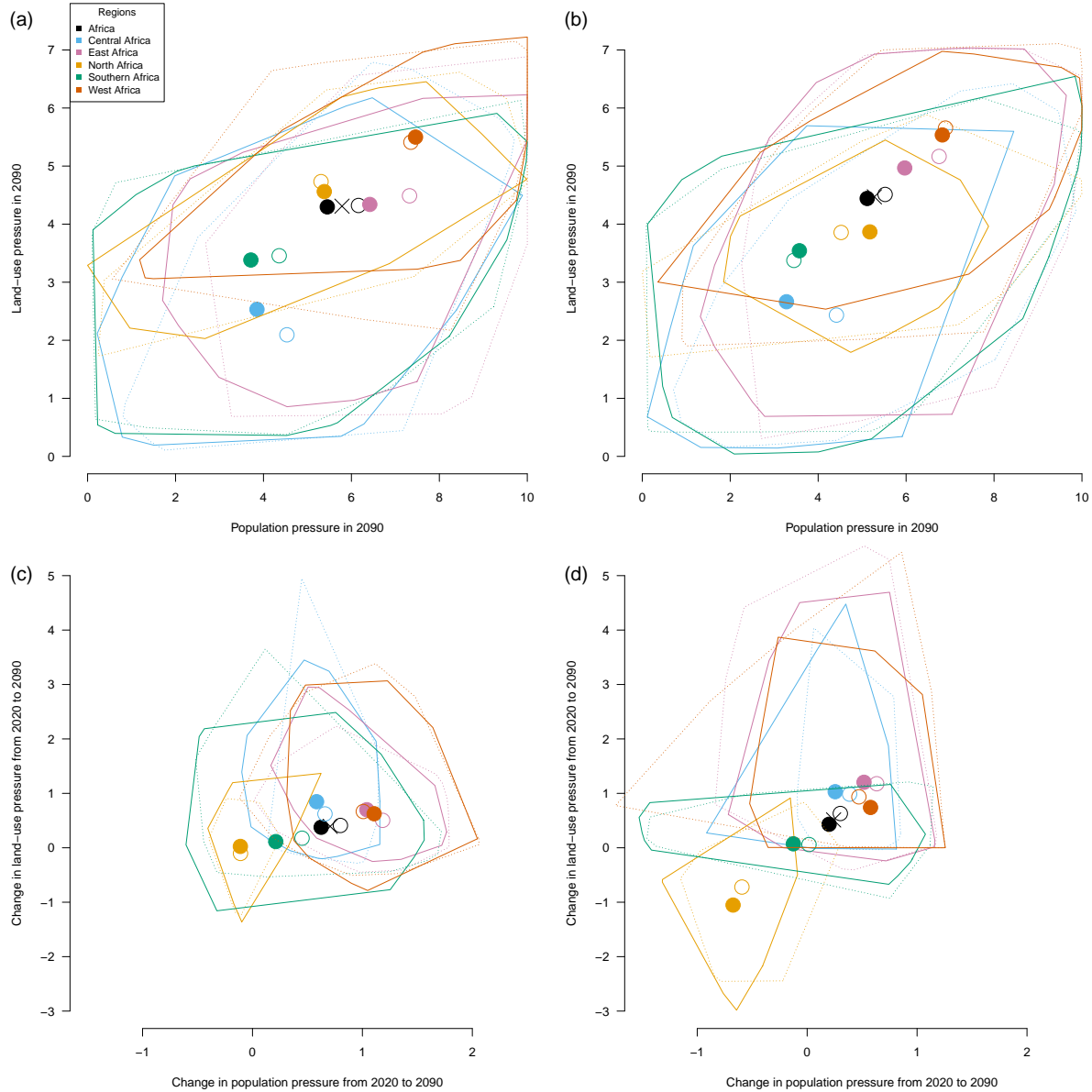


FIGURE 3.3: (a, b) Population and land-use pressure in 10-km zones around protected areas and (c, d) their change for (a, c) SSP2–RCP4.5 and (b, d) SSP5–RCP8.5 scenarios (defined in Table 3.1 and text) and habitat loss by region and biome (p.p., percentage points; cross, continental mean across protected areas; polygons, convex hulls of subgroups of protected areas; solid lines and filled circles, subgroups of protected areas projected to show habitat loss and their means; dashed lines and circles, subgroups of protected areas without habitat loss and their means). Land use (based on Hurt et al. [2020]) and population density (based on Gao [2017]) pressures in 10-km zones surrounding protected areas were scaled based on an adapted scheme from Venter et al. (2016). Pressure plots showing all individual protected areas and regions for SSP2–RCP4.5 and SSP5–RCP8.5 are in Appendices B S9 and B S10. Pressure-change plots showing individual protected areas and regions for SSP2–RCP4.5 and SSP5–RCP8.5 are in Appendices B S11 and B S12.

Southern Africa changes in future population pressure were negatively correlated with changes in future land-use pressure (Table 3.2). Under SSP2–RCP4.5, PAs with habitat loss in Southern Africa were projected to experience lower population pressure and lower population increases in their buffers than PAs without habitat loss (Figure 3.4a,c).

North Africa was the only region where many PAs were projected to experience a decrease in both socioeconomic pressures in their buffers and no habitat loss under both scenarios (bottom left quadrants in Figure 3.3c,d). In North Africa, climate-driven tree-cover changes under both scenarios particularly affected PAs that also experienced elevated future population pressure and under SSP2–RCP4.5 land-use pressures in their buffers (Table 3.2). However, increases in land-use pressure were negatively correlated with climate-driven tree-cover changes in North Africa under SSP5–RCP8.5 (Table 3.2).

When considering the combination of all 3 pressures (Figure 3.3a,b), the continental-scale patterns were broadly the same between the 2 SSP–RCP scenarios. Under both scenarios, many PAs were affected by climate-change-associated habitat loss but experienced regionally varying combinations of future socioeconomic pressures. Under SSP5–RCP8.5, climate-change impacts and future land-use pressure were often higher for PAs and their buffers (Figure 3.2). In contrast, PAs across all regions experienced higher future population pressure in their buffers under SSP2–RCP4.5. Despite similar spatial patterns, there was a tendency for SSP5–RCP8.5 to have higher overall pressure considering all drivers at the continental scale.

### 3.5 Discussion

Our results suggest that the majority of overall PA with grassland and savanna vegetation will be affected by climate-driven increases in tree cover and habitat loss. At the continental scale, the projected climate-driven tree-cover changes were not correlated with socioeconomic pressures under both scenarios. Except for many PAs in North Africa, PAs across Africa were generally projected to experience increasing pressure from at least 1 of the investigated global change pressures under both SSP–RCP scenarios. Particularly strong pressure from all 3 drivers was

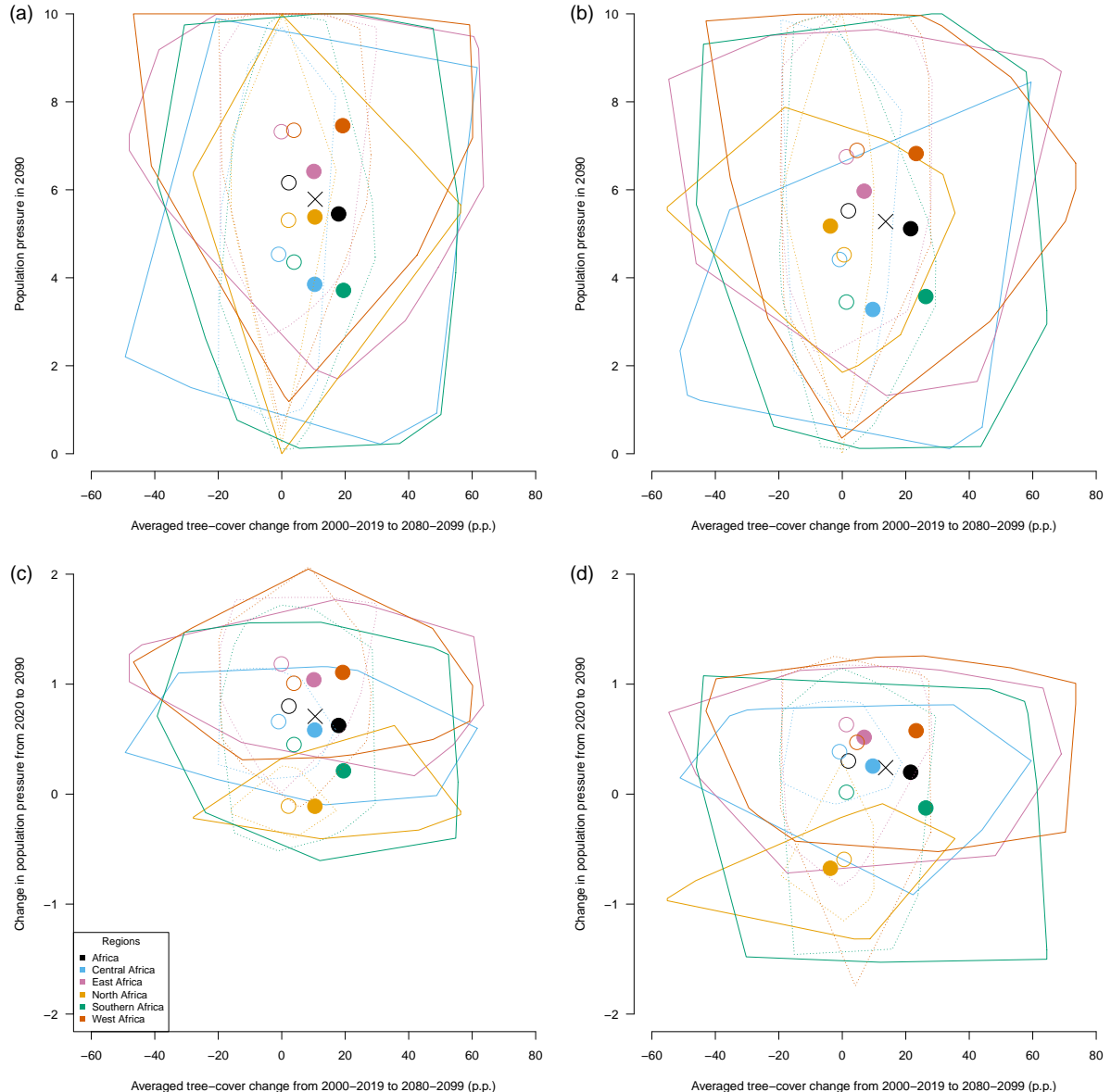


FIGURE 3.4: Climate-driven (a, b) tree-cover change in protected areas and population pressure in 10-km zones surrounding protected areas and (c, d) population pressure change in 10-km zones surrounding protected areas for (a, c) SSP2–RCP4.5 and (b, d) SSP5–RCP8.5 scenarios (defined in Table 3.1 and text) and habitat loss by region and biome (p.p., percentage points; cross, continental mean across protected areas; polygons, convex hulls of subgroups of protected areas; solid lines and filled circles, subgroups of protected areas projected to show habitat loss and their means; dashed lines and circles, subgroups of protected areas without habitat loss and their means). Tree-cover change derived from simulations with the adaptive dynamic global vegetation model (Martens *et al.*, 2021). Population density (based on Gao [2017]) in 10-km zones surrounding protected areas was scaled from 0 to 10 based on an adapted scheme from Venter *et al.* (2016). Pressure plots showing all individual protected areas and regions for SSP2–RCP4.5 and SSP5–RCP8.5, respectively, are in Appendices B S13 and B S14. Pressure-change plots showing individual protected areas and regions for SSP2–RCP4.5 and SSP5–RCP8.5, respectively, are in Appendices B S15 and B S16

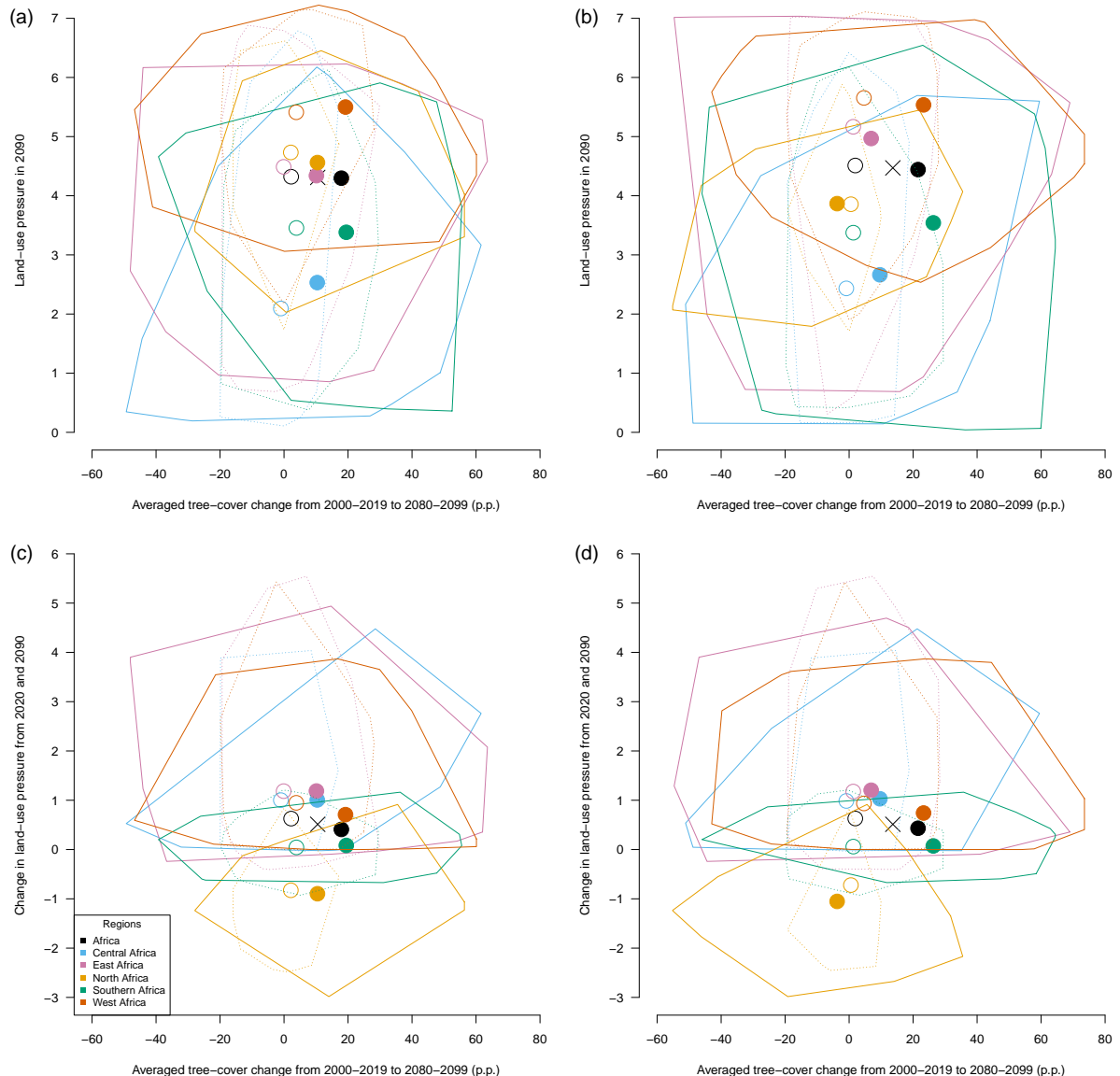


FIGURE 3.5: Climate-driven (a, b) tree-cover change in protected areas and land-use pressure in 10-km zones surrounding protected areas and (c, d) land-use pressure change in 10-km zones surrounding protected areas for (a, c) SSP2–RCP4.5 and (b, d) SSP5–RCP8.5 scenarios (defined in Table 3.1 and text) and habitat loss by region and biome (p.p., percentage points; cross, continental mean across protected areas; polygons, convex hulls of subgroups of protected areas; solid lines and filled circles, subgroups of protected areas projected to show habitat loss and their means; dashed lines and circles, subgroups of protected areas without habitat loss and their means). Tree-cover change derived from simulations with the adaptive Dynamic Global Vegetation Model (Martens *et al.*, 2021). Land-use (based on Hurt et al. [2020]) pressure factors in 10-km zones surrounding protected areas were scaled from 0 to 10 based on an adapted scheme from Venter *et al.* (2016). Pressure plots showing all individual protected areas and regions for SSP2–RCP4.5 and SSP5–RCP8.5, respectively, are in Appendices B S17 and B S18. Pressure change plots showing individual protected areas and regions for SSP2–RCP4.5 and SSP5–RCP8.5, respectively, are in Appendices B S19 and B S20

projected for PAs in West Africa. Overall, impacts from SSP5–RCP8.5 were slightly stronger than under SSP2–RCP4.5, even though increases in population pressure were generally lower under SSP5–RCP8.5.

### 3.5.1 Climate change impacts on PAs

The aDGVM results suggested high vulnerability of grasslands and savannas to climate- and CO<sub>2</sub>-driven habitat loss in African PAs; effects were stronger under SSP5–RCP8.5, which is consistent with continental-scale biome change projections of Martens *et al.* (2021). This previous analysis also showed that physiological effects of increasing atmospheric CO<sub>2</sub> have a large impact on simulated climate-driven vegetation changes and are a main source of uncertainties in the simulations (Martens *et al.*, 2021).

The high vulnerability of grasslands and savannas also confirms Eigenbrod *et al.*'s (2015) results: protected tropical grasslands and tropical woodlands are among the global biomes most vulnerable to climate-driven biome shifts. Differences between our results and Eigenbrod *et al.* (2015) included a lower vulnerability of forests in PAs to climate-driven vegetation changes in our results. This may be due to differences in climate input data and DVMs, in climate change impacts on simulated future vegetation states at global scale compared with the African scale, and in applied biome classification schemes. In addition, we focused on habitat loss rather than biome change, where habitat loss may occur without a biome change and vice versa.

In our DVM-based projections of vegetation changes under climate change, habitat loss in PAs was more widespread under SSP5–RCP8.5 than SSP2–RCP4.5. This is consistent with projections from species distribution models (SDMs) (e.g., Hannah *et al.*, 2020), which are the basis for calls to limit climate change and expand the PA network to reduce species extinction risk. The widespread habitat loss projected for all biomes in our simulations supports the view that the current extent of African PAs might not be sufficient to prevent species loss. Using DVM results as input for SDMs could improve representation of climate change impacts and ecosystem feedbacks among fire dynamics, CO<sub>2</sub> fertilization of C<sub>3</sub> photosynthesis, and related tipping points (Midgley & Bond, 2015) for species and their habitat.

### **3.5.2 Socioeconomic change impacts on PAs**

The projected general increase in population density in the vicinity of most African PAs until the end of this century under both scenarios (Gao, 2017) is consistent with urbanization trends projected to 2030 (Güneralp *et al.*, 2017). Although rural to urban migration may reduce pressure on PAs, increased food and resource demands (Güneralp *et al.*, 2017) (e.g., through resource-intensive lifestyles under SSP5–RCP8.5) can lead to increased land-use pressure on PAs. This particularly affects PAs in urban catchments and near good transportation links to cities (Rudel, 2013). Increases in human population in combination with socioeconomic development may also increase societal pressure to downgrade PAs to allow, for example, human settlements and livestock herding (Lindsey *et al.*, 2017) or renewable energy facilities (Rehbein *et al.*, 2020) in PAs. This is expected to increase conflicts between achieving conservation goals and meeting human needs (DeFries *et al.*, 2007). In IAMs, PAs are usually excluded from conversion into cropland or pastures (Stehfest *et al.*, 2019) and land-use types from industrial activities are not explicitly included apart from urban land (Hurtt *et al.*, 2020). We used the developments of human population and land use in the vicinity of PAs as a proxy for these types of developments and associated impacts on PAs.

The co-occurrence of population and land-use pressure under both scenarios is in line with population pressure being a key driving force of land-cover change in West Africa (Herrmann *et al.*, 2020). However, for changes in these socioeconomic pressures, co-occurrences were variable: positive, negative, and no correlation depending on region and scenario. This can be attributed to a combination of scenario-dependent local patterns of population pressure, the physical environment, socioeconomic conditions, policies (Herrmann *et al.*, 2020), and links to international markets (Kriegler *et al.*, 2017).

### 3.5.3 Combined socioeconomic and climate change impacts on PAs

At the continental scale, no clear overall patterns in relationships between climate-driven vegetation changes and socioeconomic pressures emerged from our analysis. This is not surprising because climate-driven vegetation changes and socioeconomic drivers are spatially independent global change drivers and socioeconomic developments vary regionally such that different regions will be subject to different combinations of pressures. The majority of PAs in West Africa might face challenges coping with elevated pressures from climate change impacts together with population and land-use pressure. In East Africa, socioeconomic pressure factors will need to be considered in management plans of PAs. In Southern Africa, climate change adaptation in PAs will be the main challenge, whereas socioeconomic pressures are weaker than in other regions.

Our results largely confirmed regional patterns of climate and land-use change under SSP5–RCP8.5 in African PAs identified by Asamoah *et al.* (2021). However, our climate-driven DVM simulations included dynamic fire–vegetation feedbacks and plant-physiological effects of increasing atmospheric CO<sub>2</sub> concentrations. As Martens *et al.* (2021) showed, CO<sub>2</sub> fertilization may partially compensate for adverse climate-change impacts on vegetation. This explains why climate-change impacts on forest PAs in Central Africa in our analysis were weaker than those presented by Asamoah *et al.* (2021).

Patterns of increased land-use pressure until 2090 in our analysis for SSP5–RCP8.5 are in line with Di Marco *et al.*'s (2019) LUH2-driven statistical modeling projections of declining plant biodiversity persistence until 2050. Compared with these global land-use-only projections, climate-change impacts increased the number of species estimated to go extinct by a factor of 4.5 (Di Marco *et al.*, 2019), which underlines the importance of combining climate and socioeconomic projections when analyzing global-change impacts on ecosystems and PAs. Even under the high mitigation SSP1–RCP2.6 scenario, impacts on biodiversity from land use alone were projected to increase by a factor of 3.7 when climate change impacts were included (Di Marco *et al.*, 2019).

### 3.5.4 Study limitations

Our data were derived from model projections. Models inherently come with assumptions and uncertainties, such as the implementation of the CO<sub>2</sub>-fertilization effect (Martens *et al.*, 2021), country- or regional-level assumptions for population or land use (Riahi *et al.*, 2017), and limited data resolution, and can only be evaluated against observational data (e.g., Scheiter & Higgins [2009] for aDGVM). To study potential future dynamics at larger scales, models are, however, the only feasible option. We included PAs that were smaller than the size of grid cells in the data sets we used. Hence, heterogeneity of, for example, environmental conditions within PAs or differences inside and outside of smaller PAs were not represented. This simplification allowed us to study regional patterns of pressures for PAs rather than providing specific estimates for individual PAs.

In conservation science, the effectiveness of PAs is often analyzed using a matching approach, in which environmental states in a PA are compared with those of a matching site outside the PA (e.g., Geldmann *et al.*, 2019). We used buffers as proxies for potential future socioeconomic influences on PAs because this study was based entirely on model results and could not be tested against observational data. Land-use and population changes in PAs depend on factors, such as management capacities, resource availability, and socioeconomic level (Lindsey *et al.*, 2017), that are difficult to project into the future across larger scales. We argue that PAs are usually not isolated from their surrounding areas, neither ecologically nor socioeconomically. Using the matching approach to identify sites similar to the PA would introduce additional parameters to our analysis and increase uncertainty.

We acknowledge uncertainties of the applied buffer approach. Where the ecosystem in a PA is very different from the surrounding area, developments in the buffer do not adequately represent developments of the PA (Joppa & Pfaff, 2011). Therefore, we do not assume that the developments in buffer areas are representative of developments within PAs, but rather that they represent potential indirect socioeconomic influences on PAs as well as the potential isolation of PAs from other natural areas. We expected that the size of the buffer may influence

our results; however, the analysis with 50-km instead of 10-km buffers yielded similar results (Appendix B S21).

Future studies could also include other SSP–RCP scenario combinations, including a high mitigation sustainability scenario to give a wider overview of consequences of societal pathways and could thus help motivate policies beneficial for conservation. For example, high climate change mitigation under SSP2–RCP2.6 (Riahi *et al.*, 2017) may come at the cost of large increases in bioenergy croplands, which would affect biodiversity (Hof *et al.*, 2018). These biodiversity impacts can have similar magnitudes, as in a scenario with higher climate change but lower land-use impacts (SSP2–RCP6.0; Hof *et al.*, 2018).

### 3.5.5 Implications for conservation and management

The high vulnerability of grasslands and savannas in PAs to climate- and CO<sub>2</sub>-driven habitat loss may require well-conceived conservation measures. Active management practices that include fire and browsing to maintain grasslands and savannas (Midgley & Bond, 2015) may help safeguard their unique, ancient biodiversity (Bond, 2016). Where future environmental conditions do not support grasslands and savannas in their current locations, intensive management might not be sufficient to conserve these ecosystems. Therefore, future anthropogenic climate and CO<sub>2</sub> change may lead to the loss of these old-growth ecosystems and their biodiversity. The controversial method of managed translocation of species to new or other PAs (Corlett & Westcott, 2013) to recreate old-growth grassland communities might not be appropriate for these systems because old-growth grasslands are very slow to establish and are distinct from secondarily established grasslands (Veldman *et al.*, 2015a). Managed translocation also bears the risk of potentially introducing invasive species to local ecosystems (Schwartz *et al.*, 2012). In addition, over time costs of maintaining PAs and their connectivity under climate change increase and their effectiveness decreases (Hannah, 2008). We conclude that limiting climate change is the most promising path to conserving these unique ecosystems.

Projected associations of multiple pressures for African PAs differed by region and biome as well as by socioeconomic and climate change scenario. This implies that challenges for conservation differ by region and biome, depending on socioeconomic and climatic developments. To account for these differences, conservation strategies need to be regionally and locally adapted. A solid understanding of the individual socioeconomic and ecological conditions as well as existing or potential conflicts builds an important foundation for planning (DeFries *et al.*, 2007). Developing regional narratives in the context of the global SSP scenarios (Palazzo *et al.*, 2017) can ensure that projections and policy development are based on regionally appropriate and relevant scenarios.

For PAs with high population pressure in heavily fragmented regions, fencing together with sufficient resources and management capacities can effectively prevent increasing human influence within PAs and human–wildlife conflicts (Lindsey *et al.*, 2017). Multiuse buffer areas with low-intensity land use and community engagement that surround the main PAs can also support conservation goals and local communities (Wittemyer *et al.*, 2008). At the same time, introducing buffer zones around PAs with high population density or intensive land use often leads to local imbalances of power, land, and resource access and to conflicts due to relocation and evictions (Neumann, 1997).

For PAs with communities that rely heavily on local food and energy resources in their vicinity, the main challenge for conservation remains to develop livelihood alternatives that improve human well-being, reduce pressure on natural resources (DeFries *et al.*, 2007), and thus reduce pressure on the PA. Under the scenarios we investigated, socioeconomic pressures in the vicinity of PAs increased, which emphasizes that future conservation strategies need to account for the socioeconomic situation and changes in the surroundings of PAs. Community-managed PAs (Grantham *et al.*, 2020) with a strong focus on long-term awareness strategies (Nzau *et al.*, 2020), participatory decision-making processes, and benefit sharing that consider socioeconomic and power structures and interests of local communities (Neumann, 1997) are important to develop strategies that account for conservation and community needs. Indigenous knowledge, which is increasingly being lost, formal education, awareness raising, and equitable

access to resources are important contributing factors for the success of these strategies (Nzau *et al.*, 2020).

Despite the large variation between scenarios and regions, it can be concluded that climate-change impacts on vegetation will likely be exacerbated by socioeconomic pressures for most PAs and regions in Africa. This combination of pressures challenges conservation aspirations, such as protecting 30% of land areas (post-2020 global biodiversity framework; Convention on Biological Diversity, 2021). Our results suggest that efforts to strongly mitigate climate change combined with measures that promote equitable, wealth-distributing, and sustainable development (Crist *et al.*, 2017) are key for the success of ecosystem conservation in this century.

### 3.6 Acknowledgments

This study and C.M. were funded under the SPACES program (Science Partnerships for the Assessment of Complex Earth System Processes) under the German Federal Ministry of Education and Research (BMBF)'s framework program (Project EMSAfrica, grant number 01LL1801B). S.S. acknowledges funding under the DFG Emmy Noether program with grant SCHE 1719/2-1.

Open Access funding enabled and organized by Projekt DEAL.

### 3.7 Supporting Information

Additional supporting information can be found online in the Supporting Information section at the end of this article.



## Chapter 4

# Towards carbon accounting in southern Africa's Nama Karoo ecosystem

*Carola Martens\**

---

\*Supporting information can be found in Appendix C.

## 4.1 Abstract

Semi-arid ecosystems are the main driver of variability of the global carbon sink. However, the contribution of southern Africa's semi-arid Nama Karoo dwarf-shrubland to this variability is less clear. In addition, climate change impacts on the Nama Karoo carbon dynamics, its grass dwarf-shrub balance, and its sheep farming system are uncertain. To assess carbon and vegetation dynamics under climate change, dynamic vegetation models (DVMs) are key tools. Here, I applied the adaptive dynamic global vegetation model 2 (aDGVM2) with its shrub submodule to a site in the Nama Karoo. I evaluated the simulated carbon fluxes against carbon flux measurements from an eddy covariance flux tower and compared simulated and observed vegetation structure. Soil water access, soil depth, and photosynthesis were reparameterised to test which model setups improve simulation results. Simulated carbon fluxes and biomass for the Nama Karoo were vastly overestimated in all simulation setups. Compared to a base version, the different simulation setups improved the agreement for individual flux components or biomass, but none of the implemented reparametrisations of the model was able to represent dwarf shrub morphology and carbon fluxes and their intra- and interannual dynamics. Soil moisture levels were overestimated in all simulations. Nonetheless, simulations with limited soil water access led to the extinction of shrubs. In simulations where shrubs established, they grew too tall with heights of 1.5–3.2 m which are common for savanna shrubs. The discrepancies of the aDGVM2 simulations highlighted that dwarf shrub ecology is not represented by the existing shrub-module. To simulate the vegetation in the Nama Karoo in aDGVM2, an implementation of dwarf shrubs by a distinct plant functional type may be necessary. Further field research on the ecophysiology and processes driving the dynamics of Nama Karoo vegetation and soil moisture is required to parameterise DVMs. If this is addressed, DVMs can be a powerful tool for much needed research on climate-change impacts on its ecology but also regional livelihoods.

## 4.2 Introduction

Semi-arid ecosystems contributed around 20% to the global net primary productivity at the beginning of the 21<sup>st</sup> century (Ahlström *et al.*, 2015). Yet, Africa's role in the global carbon balance and whether Africa is a source or a sink still carries large uncertainties (Valentini *et al.*, 2014). From the 1980s until 2011, variability in the global carbon sink was mainly driven by semi-arid ecosystems in the southern hemisphere. Southern African semi-arid ecosystems together with Australian and temperate South American semi-arid regions explained most of the variability in global net primary productivity (NPP) (Poulter *et al.*, 2014). However, among the southern African semi-arid ecosystems, the contribution varied and savannas contributed positively to the global variability whereas the Karoo shrublands were neutral or contributed negatively depending on chosen simulation model (Ahlström *et al.*, 2015).

At the same time, climate change in Southern Africa has manifested in increases in mean air temperatures and extreme heat, in decreases of mean precipitation, and in increases of droughts. These trends continue in projections of future climate change (Arias *et al.*, 2022). Semi-arid ecosystems such as South Africa's Nama Karoo dwarf-shrubland exhibit high natural variability in the environmental conditions, particularly precipitation, which makes it more difficult to detect and associate climate-change-driven trends and changes (du Toit & O'Connor, 2014). At the same time, ecological change in semi-arid ecosystems such as the Nama Karoo is often slow (Hoffman *et al.*, 2018). This means that projecting climate change impacts on vegetation and carbon cycling in the Nama Karoo into the future is a challenge (Walker *et al.*, 2018). However, there is sparse research on climate change impacts on ecosystem functioning of the Nama Karoo (Henschel *et al.*, 2018) and large uncertainties in the carbon dynamics remain (Rybchak *et al.*, 2023).

Eddy covariance flux tower measurements contribute to an improved understanding of carbon cycle dynamics and net ecosystem carbon exchange (NEE), but only a limited number of (long-running) towers and data sets across Africa (Valentini *et al.*, 2014) and in semi-arid ecosystems (Fig. 4.1) are available. In the eddy covariance flux tower technique, rapidly repeated local

measurements of the vertical wind speed and the atmospheric CO<sub>2</sub> concentration above an ecosystem are used to derive net CO<sub>2</sub> flux for the local ecosystem (Chapin III *et al.*, 2011, p. 209). At local scales, these in-situ measurements are key to understanding and monitoring ecosystem dynamics (Valentini *et al.*, 2014), especially in relation to environmental variables and local drivers of NEE variability such as soil moisture content (SMC) or temperature (Chapin III *et al.*, 2011, p. 209). These NEE measurements can also be used to derive estimates for gross primary production (GPP) and ecosystem respiration (*Reco*). However, extrapolation from these limited, local measurements to regional, country or continental scale are associated with high uncertainties (Valentini *et al.*, 2014), especially in semi-arid regions (Jung *et al.*, 2020).

For larger scale estimates of carbon dynamics, remote sensing derived NEE can be used, but these products have uncertainties for drylands because processes of soil and plant respiration are difficult to detect for satellites (Dannenberg *et al.*, 2023). Carbon dynamics at larger scales can also be derived from simulations with dynamic vegetation models (DVMs) (Prentice *et al.*, 2007). The application of DVMs allows investigating future scenarios, potential drought impacts and potential interactions between changes in multiple environmental variables and are thus well suited for research on climate change impacts on ecosystems. However, continental or regional DVM simulations require parameters that might not be appropriate for individual ecosystems, such as the Nama Karoo (Moncrieff *et al.*, 2015). In addition, locally dominant plant functional types such as dwarf shrubs are often not implemented in DVMs (Moncrieff *et al.*, 2015). DVMs provide the opportunity to integrate knowledge on the Nama Karoo ecosystem from different disciplines (Hoffman *et al.*, 2018). Local scale eddy covariance flux tower measurements can be used to evaluate DVM simulations (Prentice *et al.*, 2007; Valentini *et al.*, 2014) and to investigate the sensitivity of data-model agreement to the implementation and parametrisation of different processes. Only few DVM studies have used local eddy covariance flux tower data to evaluate the quality of modelled carbon fluxes in Africa (Valentini *et al.*, 2014) or in dryland regions (MacBean *et al.*, 2021). The representation of dryland vegetation dynamics and carbon fluxes in DVMs remains poor in comparison with remote-sensing based estimates (MacBean *et al.*, 2021).

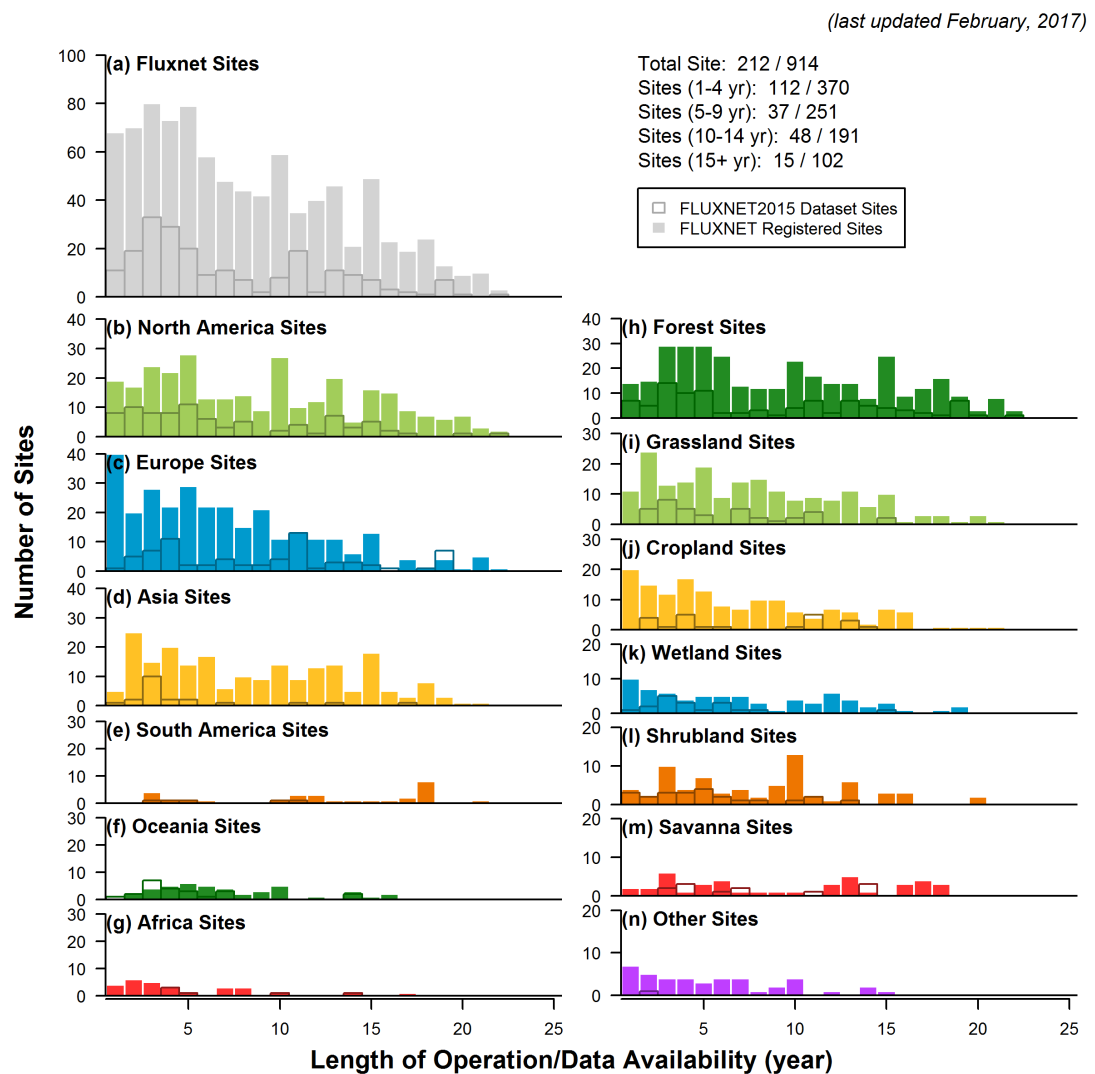


FIGURE 4.1: Eddy covariance flux tower sites that are registered with FLUXNET2015 or FLUXNET and their distribution across continents and biomes. The figure was taken from <https://fluxnet.org/sites/site-summary/> which was accessed on September 13, 2022 at 14:35.

In this chapter, ecosystem characteristics of the semi-arid Nama Karoo dwarf-shrubland in southern Africa are described. These are put into context of previous research on its carbon cycle and modelling vegetation of the Karoo. By applying the state-of-the-art DVM adaptive dynamic global vegetation model 2 (aDGVM2) (Scheiter *et al.*, 2013) to an eddy covariance flux tower site in the Nama Karoo and testing the sensitivity of the simulation results to changes in the aDGVM2, I showcased the challenges of simulating the Nama Karoo with a DVM. Based on the presented simulation results, knowledge gaps in ecosystem functioning of the Nama Karoo and requirements for the representation of dwarf shrubs in DVMs were highlighted. In the end, opportunities for future research with DVMs on the Nama Karoo were developed.

## **4.3 Ecosystem characteristics of the Nama Karoo**

### **4.3.1 General ecosystem characteristics**

The Nama Karoo vegetation is a mix of dwarf shrubs with C<sub>3</sub> and crassulacean acid metabolism (CAM) photosynthesis and C<sub>3</sub> and C<sub>4</sub> grasses mixed with geophytes and annual forbs. From West to East following an increase in mean annual precipitation and a shift from winter rainfall in the neighbouring Succulent Karoo in the West to summer rainfall in the Nama Karoo, the abundance of grasses increases and the abundance of succulent shrubs decreases. Unlike other South African ecosystems such as the Succulent Karoo or the Fynbos it has low numbers of local endemics. Naturally present grazers, migratory ungulates, were gradually replaced in the landscape by sheep and goat farming since the 19th century (Mucina *et al.*, 2006, p. 329-331).

### **4.3.2 Site description**

The site for the case study in the Nama Karoo ecosystem lies in paddocks of a decades-long grazing trial ran by the Grootfontein Agricultural Development Institute (GADI) in the Eastern Upper Karoo (Mucina *et al.*, 2006, p. 341) approximately 8 km north of Middelburg, Eastern

Cape at approximately 1310 m.a.s.l. (31°25'S 25°01'E, Berger *et al.*, 2019). The mean annual precipitation in the period 1981-2010 was 413 mm with an approximate range from 180 to 725 mm (du Toit & O'Connor, 2014). Mid- to late southern hemisphere summer is the main rainfall season (du Toit & O'Connor, 2014) and March is generally the wettest month (Venter & Mebrhatu, 2005). Temperatures vary from daytime temperatures of 30-35 °C in summer to night-time temperatures of -4-4 °C in winter (du Toit & O'Connor, 2014). The soils at the site are classified as loam soils (Roux (1993) in du Toit & O'Connor (2020)).

Two eddy covariance flux towers are located in grazing paddocks of different grazing management schemes. In this study, I focused on the site with a lenient grazing scheme because more data on ecological structure and from field experiments was available. The vegetation is characterised by a grassy dwarf shrubland which is constituted by perennial, small-leaved C<sub>3</sub> shrubs that usually do not grow much taller than 50 cm and annual and perennial C<sub>4</sub> grasses with bare ground in between (du Toit & O'Connor, 2014, Fig. 4.2, Tab. 4.1). The dominant shrub species include *Eriocephalus ericoides*, *Eriocephalus spinescens*, and *Ruschia intricata* which are accompanied by grasses such as *Digitaria eriantha* (field data collected in October 2016 with Dr. Nicola Stevens). Dwarf shrubs cover approximately 1/5 of the ground (Tab. 4.1) with large parts of bare ground in between. Aboveground biomass of the ecosystem was estimated to be 2.5-4.3 t/ha in a study executed nearby (Tab. 4.1, Roux (1988) in Milton (1990)). More recent estimates were not available. Since the 1970s, this site has been grazed by sheep and cattle two weeks at a time followed by a resting period of 24-26 weeks (stocking rates of approximately 0.0625 animal units per hectare, du Toit (2002) in Rybchak *et al.* (2023)).



(a) Nama Karoo eddy covariance flux tower with vegetation



(b) Nama Karoo vegetation during a field experiment with bare ground in between (c) *Eriocephalus ericoides* during photosynthesis measurements

FIGURE 4.2: Nama Karoo vegetation at the leniently grazed Middelburg eddy covariance flux tower site. Dwarf shrubs are the dominant life form (a, E. Falge, October 2015). Main dwarf shrub species include *Eriocephalus spinescens*, *Ruschia intricata* (b, C. Martens, October 2016), and *Eriocephalus ericoides* (c, C. Martens, October 2016)

TABLE 4.1: Vegetation composition and biomass observed at the leniently grazed Middelburg eddy covariance flux tower site. Information on the October 2016 measurement campaign can be found in Appendix C.

Variable	value	source & comments
Aboveground bio-mass [t/ha]	2.5-4.3	Roux (1988) in Milton (1990); measurements close to Middelburg on slopes
Mean shrub cover [%] $\pm$ SD	$19.18 \pm 0.05$	measurements conducted with Dr. Nicola Stevens in October 2016
Mean shrub canopy area [ $m^2$ ] $\pm$ SD	$0.11 \pm 0.11$	based on measurements conducted with Dr. Nicola Stevens in October 2016 assuming an elliptical canopy shape
Mean shrub height [m] $\pm$ SD	$0.24 \pm 0.10$	measurements conducted with Dr. Nicola Stevens in October 2016
Shrub life-span [a]	25-70	assumptions by Wiegand <i>et al.</i> (1995)

## 4.4 Carbon balance and previous steps towards carbon accounting for the Nama Karoo

### 4.4.1 Ecosystem carbon balance and its components

The carbon balance of an ecosystem can be expressed as net ecosystem production (*NEP*), which is the balance of *GPP*, the carbon fixed by photosynthesis, and *Reco*, the ecosystem respiration:

$$NEP = GPP - Reco. \quad (4.1)$$

*Reco* is composed of autotrophic respiration (*Raut*) from plants and heterotrophic respiration (*Rhet*) from microbes and animals. Because *NEP* is difficult to measure, net ecosystem exchange (*NEE*) is often used to approximate *NEP*. *NEE* is measured by eddy covariance flux towers in the atmosphere above an ecosystem and is defined as CO<sub>2</sub> flux from the ecosystem to the atmosphere. Therefore, *NEE* for an ecosystem acting as a carbon sink is negative. Carbon losses through, e.g., leaching and other non-gaseous processes or from non-CO<sub>2</sub> carbon components such as methane are not accounted for in *NEE* CO<sub>2</sub> measurements (Chapin III *et al.*, 2011, p. 208-214).

#### 4.4.2 Eddy covariance flux towers in Middelburg

The number of eddy covariance flux tower measurement sites in South Africa has increased in recent years: Two eddy covariance flux towers in the Nama Karoo in Middelburg were established in the projects Adaptive Resilience of Southern African Ecosystems (ARS AfricaE) and Ecosystem Management Support for Climate Change in Southern Africa (EMSAfrica) in 2015 alongside two other towers in northeastern South Africa. South Africa's Expanded Freshwater and Terrestrial Environmental Observation Network (EFTEON, <https://efteon.saeon.ac.za/>) is in the process of establishing more observation sites that include eddy covariance flux measurements. *NEE* measurements from eddy covariance flux towers can be used to derive *GPP* and *Reco* estimates (Chapin III *et al.*, 2011, p. 209) in the footprint of the tower. A footprint is the area surrounding a tower that is included in measurements and its size increases with sensor height above the vegetation surface and wind (Schmid, 2002). Carbon balances (*NEE*) at the two Nama Karoo eddy covariance flux tower sites in Middelburg were close to neutral and fluctuated with a slight tendency towards a small source ( $26 \pm 39 gCm^{-2}$  at the leniently grazed site and  $-5 \pm 42 gCm^{-2}$  at the second site) over the 6-year measurement period from November 2015 to October 2021. At the onset of rains in November and December, *Reco* responded with an immediate increase to major precipitation events. For *GPP*, the response at the beginning of the growing season was delayed by about 1 to 4 weeks. Therefore, the Nama Karoo at these sites first becomes a carbon source at the onset of rains and slowly switches to a carbon sink (Rybchak *et al.*, 2023).

#### 4.4.3 Previous modelling approaches

In previous vegetation modelling approaches that focused on the Nama Karoo or an Israeli dwarf-shrub-dominated ecosystem (Malkinson & Jeltsch, 2007), dwarf shrubs were simulated at monthly (Wiegand *et al.*, 1995) or annual (Beukes *et al.*, 2002; Hahn *et al.*, 2005; Malkinson & Jeltsch, 2007) time steps. The model by Venter (2001) and Venter (2002) is an exception with daily time steps. These models scaled shrub production expressed in stem growth, either in length (Malkinson & Jeltsch, 2007) or as growth rate in relation to optimal conditions (Venter,

2001, 2002), biomass (Beukes *et al.*, 2002), or shrub canopy cover (Hahn *et al.*, 2005; Wiegand *et al.*, 1995) based on empirical statistical relationship with annual precipitation (Beukes *et al.*, 2002; Hahn *et al.*, 2005; Malkinson & Jeltsch, 2007; Venter, 2001, 2002; Wiegand *et al.*, 1995). In Wiegand *et al.* (1995), this relationship was modulated by age (Wiegand *et al.*, 1995). Only Wiegand *et al.* (1995) and Malkinson & Jeltsch (2007) simulated shrubs as individuals and included processes such as death, seed production, germination and establishment. In some models, competition between simulated plant species or individuals was included and affected growth or establishment (Hahn *et al.*, 2005; Wiegand *et al.*, 1995). Grass production was only simulated in Beukes *et al.* (2002).

While these models adequately reproduced shrub production for their specific research questions, which were sometimes focused on economic or subsistence grazing systems (Beukes *et al.*, 2002; Hahn *et al.*, 2005), they did not explicitly simulate ecophysiological processes such as photosynthesis and did not include environmental factors such as temperature or atmospheric CO<sub>2</sub> concentrations. In implementations of DVMs, these additional environmental drivers are accounted for and competitive interactions between shrub and grass individuals can be included (Prentice *et al.*, 2007). The representation of shrubs is a challenge when simulating the Nama Karoo with DVMs (Moncrieff *et al.*, 2015), as ecological differences between shrubs and trees are not yet fully understood (Zizka *et al.*, 2014) especially outside of African savannas (Gaillard *et al.*, 2018). This also includes the implementation of soil water dynamics and competition between grasses and shrubs (Moncrieff *et al.*, 2015).

## 4.5 Dynamic vegetation modelling experiment for Nama Karoo vegetation

### 4.5.1 Methods

#### 4.5.1.1 Eddy covariance flux measurements for model evaluation

Data from the eddy covariance flux tower in Middelburg were provided by EMSAfrica project partners from the Thünen Institute of Climate-Smart Agriculture in Braunschweig (contact

persons Oksana Rybchak and Dr. Christian Brümmer). They provided meteorological data from the eddy covariance flux tower and gap-filled carbon fluxes at daily resolution from 1 November 2015 to 31 October 2021. Flux and meteorological measurements at the Middelburg eddy covariance flux tower had several unavoidable data gaps due to instrument failure. Processing and filtering for, e.g., bad data quality further reduced the number of data points (Rybchak *et al.*, 2020). These were filled with standard daytime gap-filling techniques (Lasslop *et al.*, 2010).

In a preliminary analysis of the precipitation data from the eddy covariance flux tower, the following issues stood out: periods with missing data could not be distinguished from periods of 0 mm precipitation; inconsistencies in the precision of measurements after a longer period ( $> 1$  year) of 0 mm precipitation. This confirmed the assessment from Dr. Justin du Toit, a local researcher from GADI maintaining the Middelburg eddy covariance flux towers, that the precipitation measurements at the tower sites are not reliable. Dr. Justin du Toit runs a privately operated rain gauge, which does not provide daily precipitation information but accumulated records over multiple days. These were used to derive annual precipitation sums.

#### 4.5.1.2 aDGVM2

The DVM aDGVM2 is based on the aDGVM (Scheiter & Higgins, 2009) which was originally developed for tropical grass-tree ecosystems. In aDGVM2, individuals from the vegetation types grass and woody plant are simulated with flexible, individual plant trait combinations (Langan *et al.*, 2017; Scheiter *et al.*, 2013). Simulated vegetation types in aDGVM2 vary in their life-history strategies such as C<sub>3</sub> or C<sub>4</sub> photosynthetic pathways and annual or perennial strategies for grasses, and deciduous or evergreen phenology and single or multi-stemmed for woody plants (Gaillard *et al.*, 2018; Kumar *et al.*, 2021a; Langan *et al.*, 2017; Pfeiffer *et al.*, 2019; Scheiter *et al.*, 2013). The simulated vegetation types in aDGVM2 are similar to plant functional types (PFTs) in other DVMs, but do not have fixed, predefined vegetation traits across all individuals of a vegetation type. Plant trait values for individuals from the same vegetation type in aDGVM2 vary from one individual to another and are inheritable. These inheritable

trait values are drawn from a uniform random distribution with predefined bounds for each trait of an individual at initialisation of a simulation. Inheritable traits are fixed throughout an individual's lifetime (Langan *et al.*, 2017; Scheiter *et al.*, 2013).

The inheritable traits influence growth, reproduction and mortality and include, e.g., carbon allocation to different plant compartments such as roots or leaves. The allocation varies between individuals but follows mass conservation rules, where a higher allocation to one plant compartment implies a lower allocation to other compartments. Traits for plant architecture (e.g. root or canopy form) and leaf and plant economics (e.g. matric potential at 50% loss of xylem conductance,  $P_{50}$ ) are also inheritable (Langan *et al.*, 2017). Trade-offs between these traits are implemented for mass conservation, plant mechanics (e.g., stem stability versus height growth) and empirically measured trade-offs, where processes are not explicitly simulated in the model such as cavitation resistance versus hydraulic efficiency. Processes are driven by meteorological and soil input data. Neighbouring plants compete for light resources and all plants compete for soil water resources (Langan *et al.*, 2017; Scheiter *et al.*, 2013). Photosynthetic rates are sensitive to factors such as leaf temperature, light availability, and water availability (Scheiter & Higgins, 2009). State variables such as stem biomass, height or crown area change throughout the lifetime of a simulated individual (Scheiter *et al.*, 2013).

Reproductive individuals pass their traits on to their seeds and only trait combinations of successful, reproductive individuals are passed on to new plant individuals. Thus, trait filtering occurs and individuals with trait combinations that are not well adapted to the environmental conditions are filtered out. Cross-over of traits between reproductive individuals and development of new trait values through mutation allow changes of the trait values of reproductive plants and thereby adaptation of plant communities to changing conditions. PFTs can be derived by classification and post-processing of simulated plants and their trait values (Scheiter *et al.*, 2013).

In the original version of the included shrub module (Gaillard *et al.*, 2018), woody plants can either grow as single-stemmed trees or as multi-stemmed shrubs. However, because of shallow soils and low precipitation, trees generally do not grow in the Nama Karoo (Mucina *et al.*,

2006, p. 329). Therefore, I excluded tree architecture of 3 stems or fewer from the simulations. Although fires occur in irregular intervals in the Nama Karoo and in the region around Middelburg, they are rare and vegetation responses are not well known (du Toit *et al.*, 2015). Therefore, fire was switched off in the aDGVM2 to simplify the simulation setup. Although C<sub>3</sub> grasses occur in the Nama Karoo (Midgley & van der Heyden, 2004; Mucina *et al.*, 2006, p. 330), they were also switched off in the simulations to focus on the dynamics between the main vegetation types of the ecosystem, C<sub>4</sub> grasses and C<sub>3</sub> shrubs (du Toit & O'Connor, 2020).

Carbon fluxes *GPP* and *Raut*, which consists of maintenance respiration (*Rmt*) and growth respiration (*Rgr*), are components of the ecosystem carbon balance that aDGVM2 simulates and that are directly required to derive plant growth. *Reco* is the sum of *Raut* and *Rhet* from soil microbes decomposing dead plant material, where *Rhet* is simulated using the Yasso soil model (see section 4.5.1.3) in aDGVM2. *Rhet* from animals is not considered.

Simulations were implemented for the Middelburg site for stands of 1 ha. Results for the 1-ha-stand were assumed to be representative of the vegetation in the footprint of the eddy covariance flux tower. The spin-up duration was chosen at 2500 years to bring traits, model state variables, and soil carbon pools into equilibrium. The climate forcing for the spin-up period was derived by randomly sampling years of meteorological data between 1951 and 1980 from the Inter-Sectoral Impact Model Intercomparison Project (ISIMIP2a, see section 4.5.1.4). The spin-up was followed by a transient run from 1981 to 2025. Simulations were repeated 20 times to account for stochastic processes such as trait initialisation, cross-over, and mutation in the aDGVM2. The mean of the 20 runs was used to represent a specific simulation setup.

#### 4.5.1.3 Yasso soil model

The Yasso soil carbon model was originally developed for forest soils (Liski *et al.*, 2005). However, in a previous study *NEE* and *Reco* fluxes in Australian savanna ecosystems were reproduced well by a version of aDGVM which was coupled with the Yasso model, but soil carbon pools and individual *Reco* components such as *Rhet* were not analysed (Scheiter *et al.*, 2015). In

addition, Tuomi *et al.* (2009) showed with an updated version that the model is globally applicable. The Yasso model (Liski *et al.*, 2005) uses three litter input pools, non-woody, fine woody, and coarse woody litter, and simulates decomposition of organic carbon. In the decomposition process, carbon is released as CO<sub>2</sub> to the atmosphere and transferred to five decomposition pools (extractives, celluloses, lignin-like components, humus and recalcitrant humus).

Liski *et al.*'s (2005) Yasso model uses annual decomposition rates. For these simulations, I derived daily decomposition rates  $k_d$  from annual decomposition rates  $k_a$

$$k_d = 1 - (1 - k_a)^{\frac{1}{365}}. \quad (4.2)$$

In the original Yasso model, decomposition rates are influenced by the water budget of the summer months (precipitation minus potential evapotranspiration) in relation to a standard water budget ((1) in Tab. 4.2). When simulating daily carbon fluxes, the daily variability in decomposition is not reflected in this moisture modifier for decomposition rates. Adapting this scheme with daily precipitation and potential evapotranspiration is associated with uncertainties, because the standard water budget only represents summer months. Therefore, a different soil moisture response function was chosen. This also required to change the structure of the equation for  $k_d$ 's sensitivity from a sum (Liski *et al.*, 2005) to a product and thus, to change the soil temperature modifier. The decomposition rates modified by temperature and SMC  $k_{sens}$  of the different litter and soil carbon pools were implemented as

$$k_{sens} = k_d * mod_{SMC} * mod_T \quad (4.3)$$

with the soil moisture modifier  $mod_{SMC}$  and the temperature modifier  $mod_T$ .  $mod_{SMC}$  was based on a non-linear function driven by SMC (Kucharik *et al.*, 2000; Zhou *et al.*, 2021)

$$mod_{SMC} = e^{\frac{-(SMC-0.6)^2}{0.08}}. \quad (4.4)$$

$mod_{SMC}$  reaches its maximum value 1 for  $SMC = 0.6$ , i.e., 60% soil moisture. Following Krinner *et al.* (2005),  $mod_T$  depends on temperature  $T$  ( $^{\circ}\text{C}$ )

$$mod_T = 2^{\frac{(T-30)}{10}}. \quad (4.5)$$

Other temperature (Tuomi *et al.*, 2009; Vuichard *et al.*, 2019) and soil moisture response functions (Zhou *et al.*, 2021) were also tested (Tab. 4.2, 2a-b and 3a-c), but produced similar or worse results for this simulation setup.

TABLE 4.2: Alternative functions for annual decomposition rate  $k_a$  (1), temperature ( $T$ ) (2a-b) and soil moisture ( $SMC$ ) response modifier (3a-c) for heterotrophic respiration in the Yasso soil carbon model coupled with the aDGVM2. (1) is the original function in the Yasso soil carbon model. (2a-b) and (3a-c) were tested for the described simulation setup with daily time steps. Respective parameter values can be found in the cited literature.

	Function	reference
(1)	$k_a = k_{a0}(1 + s_j\beta(T - T_0) + \gamma(D - D_0))$	Liski <i>et al.</i> (2005)
(2a)	$mod_T = e^{(\beta_1 T + \beta_2 T^2)}$	Tuomi <i>et al.</i> (2009)
(2b)	$mod_T = e^{\frac{0.69(T-30)}{10}}$	Vuichard <i>et al.</i> (2019)
(3a)	$mod_{SMC} = \left( \frac{1.7 - SMC}{1.15} \right)^{6.6481} \left( \frac{SMC - 0.007}{0.557} \right)^{3.22}$	Zhou <i>et al.</i> (2021), CABLE model
(3b)	$mod_{SMC} = 0.25 + 0.75 * SMC$	Zhou <i>et al.</i> (2021), LPJ model
(3c)	$mod_{SMC} = \begin{cases} 5 * SMC & SMC < 0.2 \\ 1 & SMC \geq 0.2 \end{cases}$	Zhou <i>et al.</i> (2021), TECO model

#### 4.5.1.4 Input data

Soil properties for the aDGVM2 were generally derived from Global Soil Data Task Group (2000). For soil texture, local information was available and did not agree with the data set. Therefore, the soil texture class was set to loam soil (Roux (1993) in du Toit & O'Connor (2020)). For climate input data, DVMs require continuous time series. Data from climate

models from the ISIMIP2a ensemble for climate-impacts simulations (Rosenzweig *et al.*, 2017) provided all meteorological variables required as input for aDGVM2. The ISIMIP2a climate data also covered the historic period as well as future projections and therefore allow for climate change impact simulations.

Because the Nama Karoo is mostly a water-limited ecosystem (Desmet & Cowling, 2004; Jonard *et al.*, 2022; Rybchak *et al.*, 2023), I used precipitation measures to select a general circulation model (GCM) from the ISIMIP2a ensemble. For precipitation, the GFDL-ESM2M data agreed best with the long-term mean from 1981-2010 for Grootfontein with a mean annual precipitation of 459 mm and agreed second best for minimum and maximum annual precipitation (287 mm and 676 mm, respectively). The mean of the GFDL-ESM2M data set is higher than the measured mean annual precipitation and minimum and maximum are less extreme. In the GFDL-ESM2M simulations, data covered a historical period from 1950 to 2005. For the years 2006 to 2025, I used GFDL-ESM2M data from the representative concentration pathway (RCP) 8.5, for which mean, minimum and maximum agreed best with the measured precipitation data. The ISIMIP meteorological data had a 0.5° resolution.

Evaluating DVM-simulated carbon fluxes with locally measured carbon fluxes requires local meteorological data. However, as mentioned the meteorological data from the eddy covariance flux towers have data gaps that range from days to months. To fill these data gaps in meteorological flux tower data for modelling purposes, Vuichard & Papale (2015) used globally available, continuous, simulated meteorological data. As these global data are not accurate at local scale, they developed a method that applies slope and intercept of a linear regression between flux tower meteorological data and climate model data for bias correction in the simulated meteorological data. As the timing of precipitation events in model data is not expected to agree with observations (Vuichard & Papale, 2015), especially in semi-arid regions with less predictable rainfall events (Cowling & Hilton-Taylor, 2004), they use a simple rescaling approach for precipitation data based on total precipitation in the measurement period.

When I applied the Vuichard & Papale (2015) algorithms to the input data, standard deviation of the GFDL-ESM2M data was reduced for most variables and decreased agreement with the

flux tower meteorological data standard deviation, except for long-wave radiation, short-wave radiation, and wind speed (Tab. 4.3). For the Middelburg study site in the Nama Karoo, an ecosystem driven by inter- and intra-annual climate variability (Cowling & Hilton-Taylor, 2004), the debiasing removed an important, ecosystem-defining characteristic from the climate data for most variables. In addition, the largest part of the climate input data for the aDGVM2 is not in the observation period of a few years from the Middelburg eddy covariance flux tower. This includes the 30 years of data used for the aDGVM2 spin-up. A switch from GFDL-ESM2M data to flux tower meteorological data, where both data sets differ in standard deviation, may lead to unpredictable model behaviour. Therefore, GFDL-ESM2M data was used as meteorological input for aDGVM2.

TABLE 4.3: Standard deviation (SD) for meteorological data from the eddy covariance flux tower for the leniently grazed site in Middelburg and the general circulation model GFDL-ESM2M (original and debiased data). The debiasing approach for meteorological data with gaps from Vuichard & Papale (2015) was used.

variable	SD flux tower	SD GFDL-ESM2M	SD debiased GFDL-ESM2M
air pressure [Pa]	426.2	395.4	118.4
long-wave radiation [W/m <sup>2</sup> ]	37.5	44.1	43.6
mean temperature [K]	5.8	6.1	3.5
relative humidity [%]	17.8	18.4	3.3
short-wave radiation [W/m <sup>2</sup> ]	88.7	81.7	83.3
wind speed [m/s]	1.2	0.8	0.9

#### 4.5.1.5 Sensitivity analysis

To compare simulated vegetation with observed vegetation, I compared ecosystem characteristics such as vegetation biomass, shrub height, shrub canopy cover, and carbon fluxes from literature and measurements with simulation results. The simulated carbon fluxes net ecosystem exchange ( $NEE_{sim}$ ), gross primary production ( $GPP_{sim}$ ), and ecosystem respiration ( $Reco_{sim}$ ) were compared to  $NEE_{EC}$ ,  $GPP_{EC}$ , and  $Reco_{EC}$  from eddy covariance flux tower measurements. The  $Reco_{sim}$  components  $Rgr_{sim}$ ,  $Rhet_{sim}$ , and  $Rmt_{sim}$  were put into context of  $Reco_{EC}$  and  $Reco_{sim}$ , because measurement derived counterparts did not exist. SMC as driver of  $Reco$  but also  $GPP$  and soil temperature ( $T_{soil}$ ) as driver of heterotrophic respiration ( $Rhet$ ) were also

compared between field measurements at the eddy covariance flux tower ( $SMC_{EC}$ ,  $T_{soil_{EC}}$ ) and simulation results ( $SMC_{sim}$ ,  $T_{soil_{sim}}$ ). 30-day sliding averages were used to smooth data from measurements and modelling.

Initial test simulations with a base version of aDGVM2 ( $sim_{base}$ ) have shown that  $GPP_{sim}$  and especially  $Reco_{sim}$  exceed  $GPP_{EC}$  and  $Reco_{EC}$  at the investigated Middelburg eddy covariance flux tower site (Fig. 4.3). Because  $Reco_{sim}$  was more than 10 times bigger than  $Reco_{EC}$  compared to  $GPP_{sim}$  which was about 2-3 times bigger than  $GPP_{EC}$ ,  $NEE_{sim}$  was a strong carbon source compared to an almost neutral carbon balance  $NEE_{EC}$ . Aboveground biomass was almost 30 times higher than estimates from field observations (Tab. 4.1).

To improve the representation of the carbon fluxes in the aDGVM2 in comparison to eddy covariance flux tower measurements, I tested the sensitivity of simulation results to changes in different aDGVM2 components. I compared time series, the root mean square error (RMSE), and annual carbon fluxes between simulations and measurements. aDGVM2 components that were adapted ranged from photosynthesis, water balance and soil to establishment and competition. Changes in the photosynthesis and plant production included:

- (a) Reducing the plant leaf area index (LAI) limit for allocation to leaf biomass to 2 instead of 5 to limit an individual's total plant photosynthesis. A side-effect may be that more assimilated carbon is allocated to other plant compartments such as stem biomass and thus total biomass is increased.
- (b) Reducing the maximum LAI limit for an evergreen individual for flushing leaves from 7 to 2, also with the idea of limiting allocation to leaf biomass and limiting total plant photosynthesis.
- (c) Increasing a light extinction parameter to decrease a shrub's light use efficiency. In theory with a lower light use efficiency, a smaller fraction of light can be used for photosynthesis.
- (d) Reducing photosynthesis by a factor of 1/3 to test how this influences the overall carbon balance.

In the water balance, the following were adapted to test their impact on the simulation results:

- (e) Water input into the soil was decreased in a simple implementation of surface runoff with the objective of decreasing  $SMC$  and reducing water availability for plants.
- (f) Evaporation underneath plants was increased by considering half of the area covered by plants as bare ground with the intention of decreasing  $SMC$  and thus water availability for plants.

Adapted soil components included:

- (g) A decrease in soil layer thickness to 5 cm per layer and an overall depth of 60 cm to better represent actual soil depth.
- (h) Setting soil temperature equal to air temperature, because measured soil temperatures had a larger annual amplitude with a higher maximum than simulated soil temperatures. Soil temperature is critical for decomposition and  $R_{het}$ .

In plant competition, I tested the following:

- (i) A niche separation in soil water access, where grasses were only able to access water in the top 2 soil layers and shrubs soil layers 2 and below. Thus, soil layer 2 was shared by grasses and shrubs.
- (j) The effects of lowering germination probability of seeds from 100% to 50% for woody plants and perennial grasses. The motivation behind this was to decrease the number of plants that establish and to decrease the overall productive biomass. This could also increase the fraction of bare ground.

Simulations were implemented with each of the modifications described in (a) to (j) separately. Some of these modifications to the aDGVM2 did not improve the agreement between measurements and simulations. These modifications were excluded from further analysis. In additional simulations, modifications from (a) to (j) were combined. In the following, only simulation results for individual aDGVM2 changes that improved the agreement and the two combinations

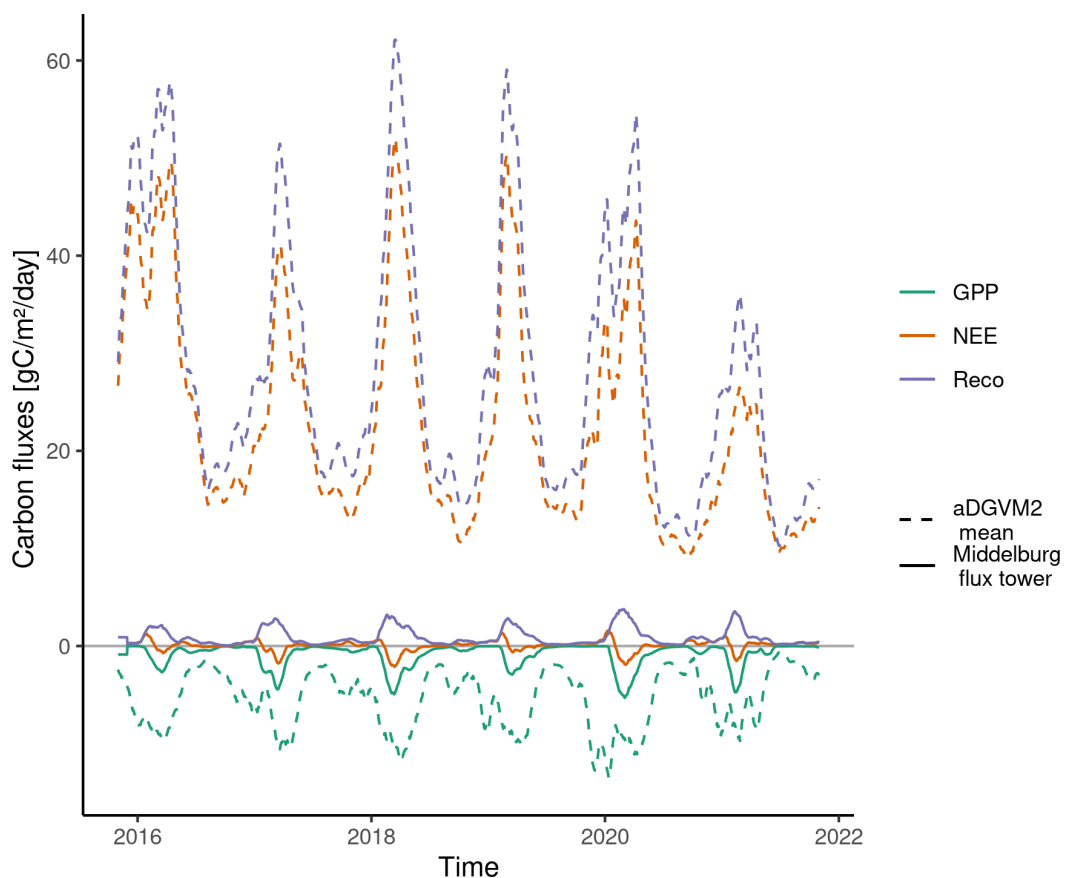


FIGURE 4.3: Daily net ecosystem exchange (NEE), gross primary production (GPP), and ecosystem respiration (Reco) at the leniently grazed eddy covariance flux tower site in Middelburg derived from tower measurements and from simulations with a base version of the adaptive dynamic global vegetation model 2 (aDGVM2). By convention, negative NEE values represent a carbon sink. For plotting purposes, GPP is shown as negative fluxes. For both measurements and simulations, a 30-day sliding average was used to smooth the data. The grey horizontal line indicates 0.

with the best agreement with the measurements are presented (d, g, i). The presented, modified aDGVM2 versions include reducing  $GPP$  by a factor of 1/3 ( $sim_{GPP/3}$ ), niche separation of soil water access for grasses and shrubs ( $sim_{niche}$ ), and the decrease in soil layer depths ( $sim_{soil}$ ). The aDGVM2 simulations where individual model changes were combined included the combination of all three changes ( $sim_{comb1}$ ) and the combination of only reducing  $GPP$  by 1/3 and niche separation of soil water access ( $sim_{comb2}$ ).

## 4.5.2 Nama Karoo simulation results

### 4.5.2.1 Carbon fluxes

All three simulation setups with individual changes, improved the agreement of the simulated carbon fluxes with the measurements (Figs 4.3, 4.4a, c & e) and reduced the RMSE (Tab. 4.4). The order of magnitude of  $NEE_{sim}$  was closest to  $NEE_{EC}$  for  $sim_{niche}$  with the smallest RMSE, followed by  $sim_{GPP/3}$  (Fig. 4.4a, Tab. 4.4).  $sim_{soil}$  showed only a small improvement in  $NEE$  agreement and RMSE. None of the three simulation setups reproduced the intraannual patterns well.  $sim_{GPP/3}$  and  $sim_{soil}$  showed seasonal patterns but these patterns did not agree well with  $NEE_{EC}$ . For  $sim_{niche}$ , no clear intraannual pattern emerged.

TABLE 4.4: Root mean square error (RMSE) for simulated net ecosystem exchange ( $NEE$ ), gross primary production ( $GPP$ ), and ecosystem respiration ( $Reco$ ) in comparison to measurements at an eddy covariance flux tower at a leniently grazed site in Middelburg, South Africa. Simulations were implemented with the adaptive dynamic global vegetation model 2 (aDGVM2). Observations and simulations covered November 2015 to October 2021. Results for six different simulation setups in aDGVM2 are shown:  $sim_{base}$ , simulations with a base version of aDGVM2;  $sim_{GPP/3}$ ,  $GPP$  reduced by factor of 1/3;  $sim_{niche}$ , niche separation for soil water access;  $sim_{soil}$ , decreased soil layer thickness;  $sim_{comb1}$ , combination of  $GPP/3$ , niche separation, and decreased soil thickness;  $sim_{comb2}$ , combination of  $GPP/3$  and niche separation. aDGVM2 results were the mean across 20 simulations.

Simulation setup	RMSE $NEE$ [gC/m <sup>2</sup> /day]	RMSE $GPP$ [gC/m <sup>2</sup> /day]	RMSE $Reco$ [gC/m <sup>2</sup> /day]
$sim_{base}$	25.7	5.7	30.6
$sim_{comb1}$	2.2	3.0	3.8
$sim_{comb2}$	1.9	4.0	2.9
$sim_{GPP/3}$	5.9	2.5	7.4
$sim_{niche}$	3.2	6.4	6.0
$sim_{soil}$	23.1	7.7	29.5

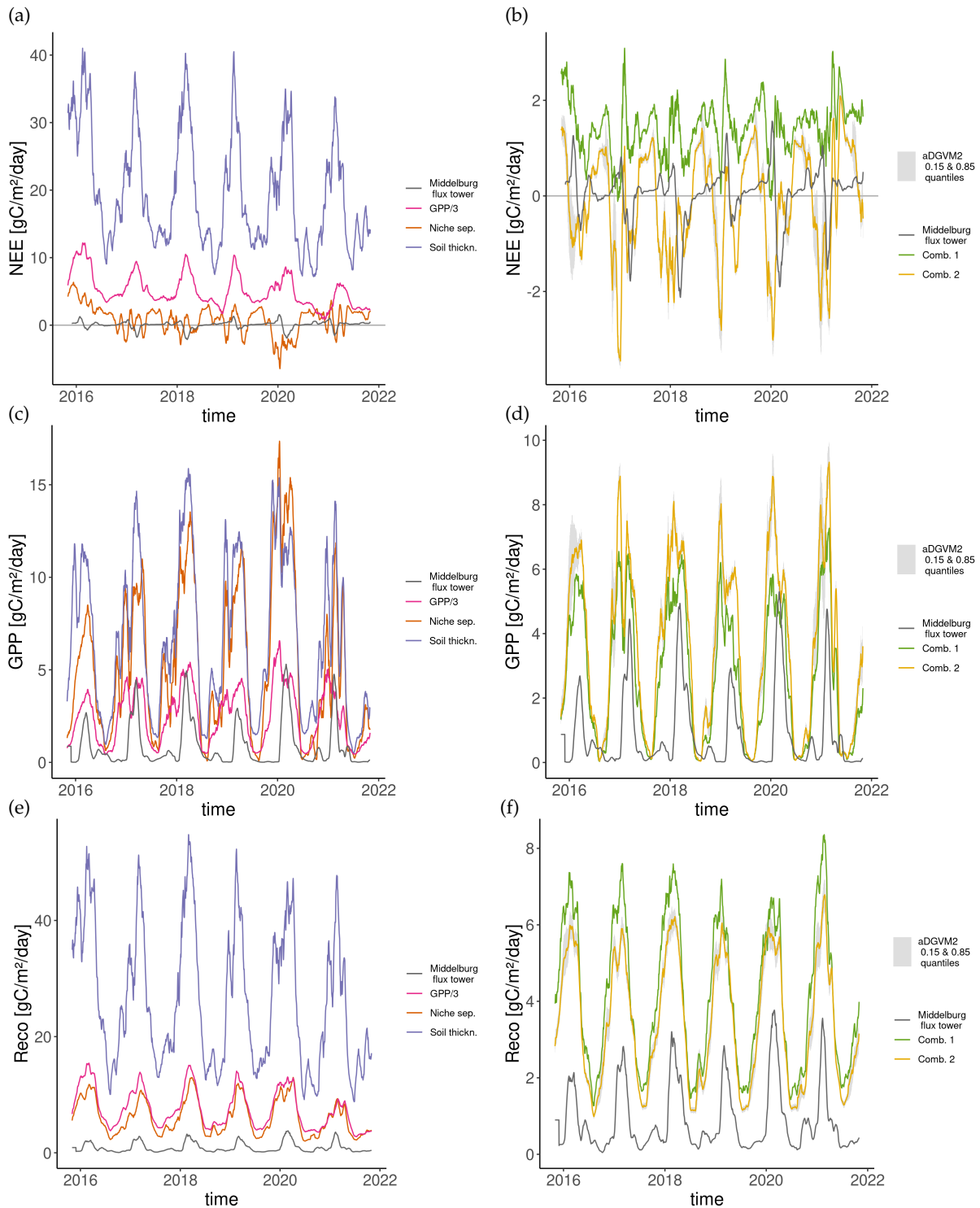


FIGURE 4.4: Net ecosystem exchange ( $NEE$ ), gross primary production ( $GPP$ ), and ecosystem respiration ( $Reco$ ) at the leniently grazed eddy covariance flux tower site in Middelburg derived from tower measurements and from simulations with the adaptive dynamic global vegetation model 2 (aDGVM2) with different simulation setups. In panels on the left (a, c & e), results from adapted aDGVM2 versions with individual changes are shown (' $GPP/3$ ',  $GPP$  reduced by factor of 1/3; 'Niche sep.', niche separation for soil water access; 'Soil thickn.', decreased soil layer thickness). In panels on the right (b, d & f), combinations of changes in the aDGVM2 are shown ('Comb. 1':  $GPP/3$ , niche separation, and soil thickness; 'Comb. 2':  $GPP/3$  and niche separation). Depicted aDGVM2 results are the mean of 20 simulations. The y axes scales differ for each subplot. For both measurements and simulations, a 30-day sliding average was used to smooth the data. By convention, negative  $NEE$  values represent carbon uptake. The grey horizontal lines indicate 0.

For the two simulation setups  $sim_{comb1}$  and  $sim_{comb2}$  with combinations of changes in the model, the agreement of simulated with measured fluxes also improved (Figs 4.3, 4.4b, d, f, Tab. 4.4). Of all simulations,  $NEE_{sim}$  for  $sim_{comb2}$  was closest to  $NEE_{EC}$  with the smallest RMSE (Figs 4.4a & b). Simulations with niche separation in soil water access ( $sim_{niche}$ ,  $sim_{comb1}$  and  $sim_{comb2}$ ) had more variable  $NEE_{sim}$  with a less pronounced seasonality than  $NEE_{EC}$ . A broad intraannual seasonal pattern emerged but the timing and frequency of maxima and minima did not match well with  $NEE_{EC}$ .

Intraannual  $NEE_{EC}$  patterns usually started with carbon release (positive values, maxima) at the beginning of the warm summer rain season and larger rainfall events followed by a switch to carbon uptake (negative values, minima). In the colder, drier winter periods, low levels of exchange that were almost neutral or a small carbon source followed. None of the implemented aDGVM2 simulations were able to reproduce this pattern, especially not the more inactive winter period. While  $NEE_{EC}$  at annual scales switched between small sources and sinks,  $NEE_{sim}$  was mostly a carbon source from 2016 to 2021 except for  $sim_{comb2}$  and  $sim_{niche}$  (Figs 4.4a, b & Tab. 4.5). These simulation setups did not reproduce the interannual variability of annual  $NEE_{EC}$ .

For  $GPP$ , the intraannual pattern was largely reproduced, but the productive summer period in aDGVM2 usually started earlier and was longer (Fig. 4.4c, d). In the colder, drier winters,  $GPP_{sim}$  was hardly ever close to 0 unlike  $GPP_{EC}$  which usually showed an extended period of vegetation inactivity.  $sim_{GPP/3}$  showed the best agreement between  $GPP_{sim}$  and  $GPP_{EC}$  (Tab.

TABLE 4.5: Annual balances for net ecosystem exchange ( $NEE$ ), gross primary production ( $GPP$ ), and ecosystem respiration ( $Reco$ ) derived from an eddy covariance (EC) flux tower at a leniently grazed site in Middelburg, South Africa and simulations with the adaptive dynamic global vegetation model 2 (aDGVM2) from 2016 to 2020. In the aDGVM2 setup  $sim_{niche}$ , niche separation for soil water access is implemented. In  $sim_{comb2}$ ,  $GPP$  reduced by a factor of 1/3 is combined with niche separation. aDGVM2 results for  $sim_{comb2}$  and  $sim_{niche}$  were each the mean across 20 simulations.

Year	$NEE$ [ $\text{gC/m}^2/\text{year}$ ]			$GPP$ [ $\text{gC/m}^2/\text{year}$ ]			$Reco$ [ $\text{gC/m}^2/\text{year}$ ]		
	EC	$sim_{comb2}$	$sim_{niche}$	EC	$sim_{comb2}$	$sim_{niche}$	EC	$sim_{comb2}$	$sim_{niche}$
2016	62.1	-177.8	600.5	221.6	1443.3	1689.7	265.0	1265.5	2290.2
2017	-15.4	-77.6	317.5	347.3	1330.6	1849.7	317.1	1253.1	2167.2
2018	-54.9	-120.8	152.9	424.7	1406.3	2236.5	370.0	1285.5	2389.4
2019	78.1	-26.5	87.1	216.9	1300.0	2415.2	290.6	1273.5	2502.3
2020	3.4	-76.9	-62.3	443.5	1300.0	2200.0	435.5	1223.0	2137.7

4.4). Under  $sim_{GPP/3}$ , the interannual variability in the amplitude of  $GPP_{EC}$  was roughly reproduced in  $GPP_{sim}$ .  $sim_{comb1}$  and  $sim_{comb2}$  also approached  $GPP_{EC}$  and  $sim_{comb1}$  agreed better than  $sim_{comb2}$  with a smaller RMSE (Fig. 4.4d, Tab. 4.4). The other simulation setups had peaks up to three times higher than  $GPP_{EC}$ .

None of the simulation setups achieved  $Reco_{sim}$  in the same order of magnitude as  $Reco_{EC}$  (Fig. 4.4e, f).  $sim_{comb2}$  came closest but was still up to three times larger than  $Reco_{EC}$  for peak respiration. In addition, none of the  $Reco_{sim}$  had values close to 0 in winter as opposed to  $Reco_{EC}$ . Small  $Reco_{EC}$  peaks in winter were lower than the minimum values of  $Reco_{sim}$  in winter. Similar to  $GPP_{sim}$ ,  $Reco_{sim}$  had very short periods of low activity. Periods of higher activity in  $Reco_{sim}$  started earlier than in  $Reco_{EC}$  and lasted longer. In the dry winter season, the main source of simulated respiration was  $Rhet_{sim}$  which contributed the largest part to  $Reco_{sim}$  as was shown exemplarily for  $sim_{comb2}$  (Fig. 4.5).  $Rgr_{sim}$  and  $Rmt_{sim}$  were smaller than  $Rhet_{sim}$  and approached 0 in the winter season similar to  $Reco_{EC}$ . The sum of  $Rgr_{sim}$  and  $Rmt_{sim}$ , i.e.,  $Raut$ , was roughly in the order of magnitude of  $Reco_{EC}$  and sometimes exceeded it.

#### 4.5.2.2 Biomass and vegetation structure

In comparison to  $sim_{base}$ , agreement of simulated aboveground biomass with observation-derived estimates improved for all simulations with adapted aDGVM2 versions and simulated aboveground biomass decreased (Tabs 4.1 & 4.6). Estimates for the observation period for

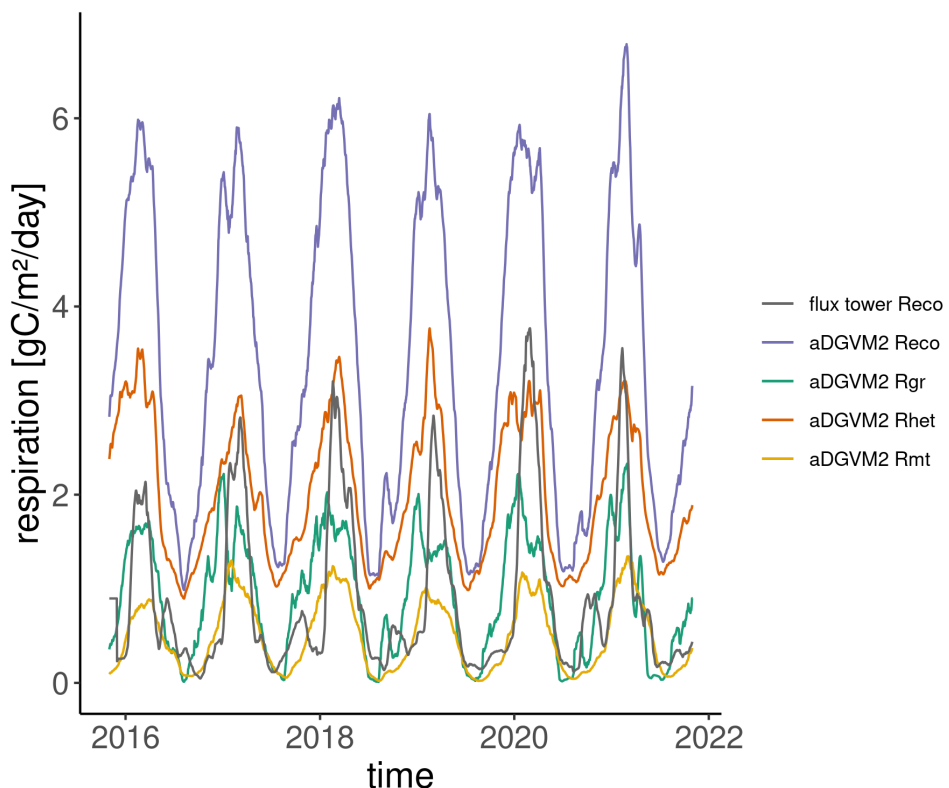


FIGURE 4.5: Ecosystem respiration (*Reco*) at the leniently grazed eddy covariance flux tower site in Middelburg derived from tower measurements and from simulations with the adaptive dynamic global vegetation model 2 (aDGVM2). For simulated *Reco*, the contributing components growth respiration (*Rgr*), maintenance respiration (*Rmt*), and heterotrophic respiration (*Rhet*) are shown. For this simulation, aDGVM2 was modified so that *GPP* was reduced by a factor of 1/3 and the niche for soil water access was separated (*sim<sub>comb2</sub>*). Depicted aDGVM2 results are the mean across 20 simulations. For both measurements and simulations, a 30-day sliding average was used to smooth the data.

$sim_{comb1}$ ,  $sim_{niche}$  and  $sim_{comb2}$  were in the range of observations. At the same time, these were the aDGVM2 simulations where shrubs did not grow during the measurement period under the given environmental conditions and plant biomass was based on grass individuals only.

TABLE 4.6: Vegetation structure and aboveground biomass simulated by aDGVM2 for the leniently grazed eddy covariance flux tower site in Middelburg. Values are means and standard deviation for the simulated time period November 2015 to October 2021. Results from adapted aDGVM2 versions in comparison to its base version ( $sim_{base}$ ) are shown. Individual changes included, GPP reduced by factor of 1/3 ( $sim_{GPP/3}$ ), niche separation for soil water access ( $sim_{niche}$ ), decreased soil layer thickness ( $sim_{soil}$ ). Simulations with combinations of changes in the aDGVM2 were  $sim_{comb1}$  (GPP/3, niche separation, and soil thickness) and  $sim_{comb2}$  (GPP/3 and niche separation). aDGVM2 results for each simulation setup were the mean of 20 simulations. ‘-’ signifies that the respective plant functional type did not survive in aDGVM2. See Tab. 4.1 for observed values.

Simulations	age [a]		biomass [t/ha] aboveground	crown area [ $m^2$ ] shrubs	height [m] shrubs
	grasses	shrubs			
$sim_{base}$	$6.3 \pm 0.8$	$46.9 \pm 1.3$	$93.9 \pm 5.9$	$17.5 \pm 0.8$	$3.2 \pm 0.1$
$sim_{GPP/3}$	$17.7 \pm 1.8$	$17.1 \pm 0.5$	$15.1 \pm 2.1$	$6.6 \pm 0.6$	$1.5 \pm 0.1$
$sim_{niche}$	$26.6 \pm 3.2$	-	$2.7 \pm 2.0$	-	-
$sim_{soil}$	$17.3 \pm 1.6$	$33.4 \pm 1.5$	$69.5 \pm 6.1$	$17.6 \pm 0.7$	$2.8 \pm 0.2$
$sim_{comb1}$	$43.0 \pm 0.7$	-	$5.3 \pm 1.1$	-	-
$sim_{comb2}$	$66.4 \pm 2.0$	-	$2.2 \pm 1.4$	-	-

For the two adapted aDGVM2 versions where shrubs persisted ( $sim_{GPP/3}$  and  $sim_{soil}$ ), simulated shrubs were bigger than plants growing on-site (Tabs 4.1 and 4.6). For  $sim_{GPP/3}$ , crown area and shrub height decreased compared to  $sim_{base}$  and  $sim_{soil}$ , but were still not close to observed vegetation. Simulated shrub individuals rather resembled tree-like savanna shrubs in their heights and crown areas (Zizka *et al.*, 2014) and were around 1 order of magnitude taller with a crown area up to 2 orders of magnitude larger than dwarf shrubs found on site (Tab. 4.1, Fig. 4.2). Mean shrub age was within the range of shrub life spans used in Wiegand *et al.*’s (1995) model for aDGVM2 simulation setups in which shrubs persisted (Tab. 4.1).

#### 4.5.2.3 Soil moisture and soil temperature

$SMC_{sim}$  was higher than  $SMC_{EC}$  for all simulations including  $sim_{base}$  (Fig. 4.6a). Under  $sim_{soil}$ ,  $SMC_{sim}$  came closest to  $SMC_{EC}$  and was most variable, but minimum values of  $SMC_{sim}$  were only in the range of maximum values of  $SMC_{EC}$ . For  $sim_{comb1}$ , which included the reduced soil

layer thickness in aDGVM2, the variability of  $SMC_{sim}$  was similar but values were higher than for  $sim_{soil}$ . All other simulations had a simpler, less variable seasonal cycle.

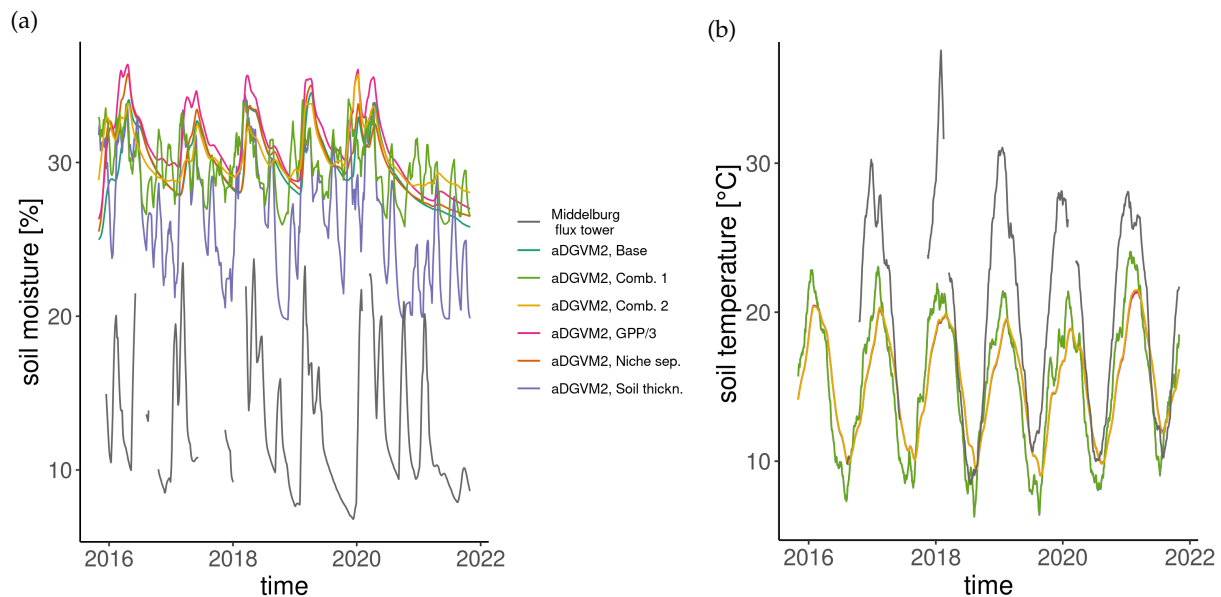


FIGURE 4.6: Soil moisture and soil temperature at the leniently grazed eddy covariance flux tower site in Middelburg derived from tower measurements and from simulations with the adaptive dynamic global vegetation model 2 (aDGVM2). For aDGVM2, results for different model setups are shown. aDGVM2 setups included the base version 'Base', setups with individual changes ('GPP/3', GPP reduced by factor of 1/3; 'Niche sep.', niche separation for soil water access; 'Soil thickn.', decreased soil layer thickness), and setups with combinations of changes ('Comb. 1', GPP/3, niche separation, and soil thickness; 'Comb. 2', GPP/3 and niche separation). Note that for (b) soil temperature simulation results for 'Comb. 1' and 'Soil thickn.' as well as for 'Base', 'Comb. 2', 'GPP/3', and 'Niche sep.' are almost identical. Depicted aDGVM2 results are the mean across 20 simulations. For both measurements and simulations, a 30-day sliding average was used to smooth the data.

For all simulations, the amplitude of  $T_{soil_{sim}}$  was smaller than for  $T_{soil_{EC}}$  (Fig. 4.6b). Minima were in the range of  $T_{soil_{EC}}$  and the seasonal cycle was reproduced well. Maxima were up to 5 to 10 °C smaller than for  $T_{soil_{EC}}$ . Simulations with decreased soil layer thickness ( $sim_{comb1}$  and  $sim_{soil}$ ) increased the amplitude of  $T_{soil_{sim}}$  with smaller minima and bigger maxima, but maxima were still smaller than for  $T_{soil_{EC}}$ .

### 4.5.3 Discussion

The case study for the Nama Karoo at the Middelburg eddy covariance flux tower site showed that the aDGVM2 currently does not adequately simulate this semi-arid dwarf shrub ecosystem. After basic reparametrisation, calibration, and changes in aDGVM2, observed vegetation structure and carbon fluxes were still not reproduced by simulations. In simulations where  $NEE_{sim}$  approximated  $NEE_{EC}$  ( $sim_{comb2}$  and  $sim_{niche}$ ), the simulated grassy vegetation and absence of shrubs did not agree with the observed vegetation. Because of the mismatch of  $GPP_{sim}$  and  $Reco_{sim}$  with  $GPP_{EC}$  and  $Reco_{EC}$ , the intraannual  $NEE_{EC}$  patterns are not reproduced well by  $NEE_{sim}$ . In simulations where shrubs established, individuals were bigger both in size and canopy cover than dwarf shrubs at the study site and the simulated carbon balance was at least an order of magnitude higher than the measurements.  $SMC$  was overestimated by aDGVM2.

#### 4.5.3.1 Limitations of the eddy covariance flux tower data and field measurements

The gap-filled eddy covariance flux tower data and especially the components  $Reco_{EC}$  and  $GPP_{EC}$  come with uncertainties. Sources of uncertainty in the gap-filled data include decisions in the quality control filtering,  $NEE$  gap-filling techniques, and techniques of partitioning fluxes into  $Reco_{EC}$  and  $GPP_{EC}$  (Wutzler *et al.*, 2018). For example, in the daytime gap-filling technique (Lasslop *et al.*, 2010), both  $Reco_{EC}$  and  $GPP_{EC}$  are based on a model and they do not balance out to exactly  $NEE_{EC}$  (Wutzler *et al.*, 2018). Measurements are ongoing and longer time series can help to compensate data gaps in future analyses. In addition, regular servicing of the tower can reduce the occurrence of data gaps or unreliable data caused by instrument failure.

Precipitation events and soil moisture are important drivers of carbon fluxes in semi-arid ecosystems (Archibald *et al.*, 2009; Merbold *et al.*, 2009) such as the Nama Karoo. Especially, the timing and the amount of rainfall shape intraannual flux patterns (Hao *et al.*, 2020). As explained in section 4.5.1.1, measured local precipitation data at daily time steps were not available. The timing of the GFDL-ESM2M precipitation data that were used here cannot be expected to agree accurately with precipitation events at the eddy covariance flux tower (Vuichard

& Papale, 2015). GFDL-ESM2M data also have a much lower resolution than the eddy covariance flux tower footprint. Next to the difficulties of simulating the dwarf shrub vegetation, this may explain some of the differences of patterns and timing of peaks of carbon fluxes in aDGVM2-simulated and flux-tower-derived carbon fluxes. Obtaining continuous meteorological data that agree well with the original weather conditions during the carbon flux measurement period is important for simulating and recreating intraannual ecosystem carbon flux patterns.

Independent measurements of the *Reco* components *Raut* and *Rhet* can be used to test the implementation of respiration processes in DVMs (Luyssaert *et al.*, 2007). To improve the understanding of respiration processes in the Nama Karoo, soil respiration was measured during a soil watering experiment with measurement chambers by a team from CzechGlobe for a week in October 2016 (contact person Dr. Eva Dařenová). A challenge for working with these data was that soil respiration is a combination of *Raut* from plant roots and *Rhet*. Therefore, the components that are simulated in DVMs are not measured separately. This hinders identifying processes that are not implemented well in DVMs or deriving ecosystem-specific decomposition rates that could be used to parameterise *Rhet* in DVM soil models. In addition in this specific case study, the range of measured *SMC* (4-20%) during the soil respiration measurements was much lower than *SMC<sub>sim</sub>*. Any derived decomposition rates or equations to use in the aDGVM2 would need to be extrapolated and applied for *SMC* values well outside of the range of measured values.

#### 4.5.3.2 Challenges in simulating the Nama Karoo with the aDGVM2 and knowledge gaps

The regular switch of annual  $NEE_{EC}$  between carbon source and sink throughout the measurement period is characteristic of dryland sites (Dannenberg *et al.*, 2023). Although the simulation setups showed interannual variability, the switch between source and sink was not reproduced by any of the simulation setups. The measured carbon flux response to precipitation events throughout the growing season of the Nama Karoo in Middelburg is in line with semi-arid grassland research (Hao *et al.*, 2020). In the initial response to the first larger rainfall

events at the beginning of the summer growing season, a prompt increase in  $Reco_{EC}$  increased the ecosystem's carbon source. A delayed increase in  $GPP_{EC}$  led to a subsequent switch to a carbon sink in the eddy covariance flux tower measurements. This delayed response of  $GPP_{EC}$  to SMC increases but also subsequent decreases in  $Reco_{EC}$  due to drying of upper soil layers (Parton *et al.*, 2012) is not represented well in aDGVM2. The delayed  $GPP_{EC}$  response of 1 to 4 weeks (Rybchak *et al.*, 2023) could be used to reparameterise the phenology switch and its time dependence in aDGVM2 so that the transition of a plant individual to an active state at the beginning of larger rainfall events is delayed accordingly. Detailed analyses of the responses of carbon flux components in Middelburg to individual precipitation events could be used to derive a minimum size of a precipitation event that triggers a  $GPP_{EC}$  response in the ecosystem (Parton *et al.*, 2012) or to investigate activity durations of  $GPP_{EC}$  and  $Reco_{EC}$  following precipitation events (Hao *et al.*, 2020). In addition, carbon flux measurements in the savanna in Kruger National Park in South Africa have shown that the intensity and duration of dry spells before precipitation events may cause lags in carbon flux responses (Williams *et al.*, 2009). The results from these analyses could be used to parameterise the photosynthesis and respiration responses in aDGVM2.

My simulations in combination with previous results (Gaillard *et al.*, 2018) showed that dwarf shrubs and their ecology are not represented well by the shrub model in aDGVM2. The shrubs implemented in the aDGVM2 and thus in my simulations represented savanna-type shrubs that can grow to the size of small to medium trees (see Gaillard *et al.*, 2018). These tree-like shrubs differ in their morphology from the dwarf shrubs under the semi-arid conditions in the Nama Karoo. The main focus of Gaillard *et al.*'s (2018) aDGVM2 shrub module was to implement a trade-off between adapting to water-limited or light-limited conditions based on stem number. The plant physiology did not differ for shrub and tree individuals. The simulations have shown that the existing representation of shrubs does not suffice to simulate the Nama Karoo ecosystem, because the shrub individuals do not survive or the architecture of the dwarf shrubs is not reproduced.

Growth of Karoo dwarf shrubs is limited by water availability (Venter, 2001), but soil water dynamics in the aDGVM2 currently do not represent the observed patterns and ranges at the Middelburg site well. In an experiment with the Karoo species *E. ericoides*, soil moisture levels greater than 10% led to stomatal conductance greater than optimal stomatal conductance rates. In the field, *E. ericoides* individuals rapidly use soil water resources and thus reduce soil water availability for other competitors (Midgley & Moll, 1993), which is in line with the spiteful water use theory (Blonder *et al.*, 2023). In addition, an experiment in semi-arid Argentina did not confirm the implemented type of niche separation for soil water access for an evergreen shrub species and grasses (Peláez *et al.*, 1994). Therefore the implemented niche separation for soil water access in aDGVM2 might not represent Nama Karoo processes well because simulated competitors have exclusive access to soil water resources in some of the soil layers. In addition,  $SMC_{sim}$  levels did not drop to the levels that were observed in field measurements and were always higher than 10%. In the simulations where  $SMC$  access for plants was restricted, the implemented shrubs did not grow. This indicates that processes in aDGVM2 may not reflect the coping mechanisms of Nama Karoo shrubs for limited water resources well and more field research on root systems in the Nama Karoo is required.

In an ecosystem, where water limitation is a key driver of ecosystem dynamics and carbon fluxes, the  $SMC_{sim}$  levels in the current aDGVM2 implementation provide  $Rhet$  processes with more  $SMC$  than is available in reality. Thus,  $Reco_{sim}$  is higher than derived by measurements. In addition, Zhou *et al.* (2021) showed that the selection of the moisture-response function is a key source of uncertainty in simulating soil  $Rhet$ . In combination with an adequate dwarf shrub representation, an appropriate implementation of  $Rhet$  responses to soil moisture pulses and temperatures will be key to achieve the typical, pulsed  $Reco$  (Rybchak *et al.*, 2023) in simulations.

In this case study, grazing was ignored to remove an additional layer of complexity. Yet, herbivory is an important disturbance in the Nama Karoo (van der Merwe & Milton, 2019; Wiegand *et al.*, 1995). Grazing trials in Middelburg have shown that the timing and the duration of grazing influence dwarf shrub abundance, where continuous grazing throughout the year and

summer grazing led to higher shrub densities (Mureva & Ward, 2016). Once the ecophysiology of dwarf shrubs is implemented adequately in aDGVM2, including grazing and herbivory into simulations using a previously implemented grazing model (Pfeiffer *et al.*, 2019) would be important to fully represent the Nama Karoo and its key ecosystem processes.

The analysis in this chapter was focused on carbon fluxes and shrub representation in aDGVM2. However, the mix of grasses and shrubs is an important characteristic of the Nama Karoo (p. 330 Mucina *et al.*, 2006). To ensure that all key components of the Nama Karoo vegetation are represented adequately, especially when grazing effects are considered, simulated grass vegetation, currently only C<sub>4</sub> grasses, would need to be analysed in more detail and should also include C<sub>3</sub> grasses. Ideally, simulated vegetation would reflect changes in annual and perennial grass and dwarf shrub abundances as well as changes in palatability of grasses following different grazing treatments. This would also allow testing the implementation of annual and perennial grasses in aDGVM2 and the grazing module in which palatability of grasses is based on specific leaf area (SLA, the inverse of leaf dry mass per leaf area) as a proxy (Pfeiffer *et al.*, 2019).

Even though shrubs with the CAM-type photosynthesis are usually not dominant in the Nama Karoo, they are an important part of the vegetation. For example, in Middelburg *Ruschia intricata* is a common succulent from the *Ruschia* genus (du Toit *et al.*, 2015). Facultative CAM, i.e., environmentally triggered CAM, was shown for many succulent shrub species including other *Ruschia* species (Winter, 2019) and likely also plays a role in the metabolism of *Ruschia intricata*. Currently in aDGVM2, woody plants can only have C<sub>3</sub> and grasses C<sub>3</sub> or C<sub>4</sub> photosynthetic pathways. Future developments of aDGVM2 could therefore, include an implementation of CAM for woody plants.

Nutrient cycling and nitrogen in particular is currently not implemented in aDGVM2. At the same time, the role of nutrients in the Nama Karoo is uncertain (Whitford, 2004). Measurements in the Namibian Nama Karoo hinted at nitrogen limitation (Büdel *et al.*, 2009). Nutrient availability and mobilisation in Nama Karoo soils seem to be periodic, where

dead roots from annual plants after productive years lead to nutrient immobilisation and nutrient availability is higher after a prolonged drought (Milton & Dean, 2004; Whitford, 2004). Representing these mechanisms in aDGVM2 adequately may prove to be challenging, because of the variable availability of nutrients but also the potential role of soil crusts (Büdel *et al.*, 2009). The role of termites for nutrients in Karoo soils is unresolved (Whitford, 2004) and termites are not represented in aDGVM2.

The challenges of simulating the Nama Karoo were also shown in simulations with the DVM Lund-Potsdam-Jena General Ecosystem Simulator (LPJ-GUESS) for southern Africa. The globally parameterised LPJ-GUESS overestimated net primary production in the Nama Karoo when compared to satellite-derived MODIS net primary productivity estimates (Thavhana *et al.*, 2023). For a global DVM, Thavhana *et al.* (2023) highlight that a regional parameterisation with shrub PFTs would be key to improve the representation of the Nama Karoo. At the same time physiological characteristics of shrubs in general (Moncrieff *et al.*, 2015) and of dwarf shrubs in particular and how they differ from trees are still unclear. The aDGVM2 simulations in this study have shown that developing an appropriate parameterisation of shrubs to adequately represent the Nama Karoo's typical semi-arid dwarf shrubs is challenging.

#### 4.5.4 Requirements for the representation of dwarf shrubs in aDGVM2

An extension of the aDGVM2 may be required to simulate the shrubs in the Nama Karoo ecosystem. A new representation of dwarf shrubs would need to represent the slow growth and small size typical of Karoo dwarf shrubs (van der Merwe & Milton, 2019), where ungrazed shrubs usually reach their maximum canopy size within a decade (Wiegand *et al.*, 1995). Low growth rates and thus smaller leaf surface areas come with a lower risk of damage during times of low water availability and droughts, especially for seedlings (Esler & Phillips, 1994). In combination with their small size, the dwarf shrubs are also characterised by their small leaves. As an adaptation to the semi-arid growing conditions, Karoo shrubs also feature the ability to revive after longer dry periods, where they show elevated growth rates with low water-use efficiency (Venter, 2004).

In this chapter's simulations in which shrubs disappeared, their disappearance was caused by carbon mortality, i.e., plant individuals died because of a negative carbon balance. The main components of the carbon balance in aDGVM2 are water- and light-limited photosynthesis, representing carbon uptake, and  $R_{mt}$  and  $R_{gr}$ , representing carbon losses. Leaf and root turnover also decrease the carbon balance which includes biomass turnover in case of a prolonged period of water stress. As long as a certain threshold of water limitation is exceeded, each day an individual loses a fixed fraction of its alive leaf and root biomass, thus decreasing its carbon balance. To simulate the dwarf shrubs in the Nama Karoo, the simulated susceptibility to dry stress could be reduced for dwarf shrubs. By decreasing the daily rate of leaf and root biomass that dies for dwarf shrub individuals in case of water limitation, they would lose less leaf and root biomass. This would also lead to higher remaining leaf and root biomass at the end of a dry spell which would also facilitate the subsequent recovery of dwarf shrubs.

Currently, the daily biomass turnover rate is a fixed model parameter which is equal for all woody individuals (shrubs and trees). In an aDGVM2 implementation that accounts for dwarf shrubs, this parameter could vary between woody individuals and could be lower for drought-resilient dwarf shrubs. Ideally, this parameter for drought resilience would be implemented with trade-offs against other plant traits. A simple approach could be to couple the daily turnover rate under drought stress to the number of stems of an individual, where the daily turnover rate decreases with the number of stems. The daily turnover rate could also be implemented as a trade-off with growth rates. Plants with lower growth rates such as dwarf shrubs could have lower turnover rates in drought situations. This implementation would provide shrubs with slow growth rates a competitive advantage over fast-growing shrubs, because the stress caused by dry spells would be lower.

The daily biomass turnover rate is a fixed model parameter that is currently not parameterised based on measured data. The TRY data base (Kattge *et al.*, 2020) contains globally available turnover data, but lacks data for dwarf shrubs. A sensitivity analysis and benchmarking of model results with data on plant morphology and carbon fluxes could be used to constrain the parameter for woody vegetation and dwarf shrubs specifically.

Some traits from the leaf economics spectrum (Wright *et al.*, 2004), such as SLA and leaf longevity (the inverse of leaf turnover), and some trade-offs between traits are implemented in aDGVM2 (Scheiter *et al.*, 2013). According to the leaf economics spectrum, plants with lower SLA, i.e., with higher leaf construction costs, have a higher leaf longevity (Wright *et al.*, 2004), which is typical for slow-growing species (Lambers & Poorter, 1992) such as the Nama Karoo dwarf shrubs and supports the above suggestion of reducing leaf turnover rates. In aDGVM2, trade-offs between SLA and leaf longevity have been implemented in the past (Langan *et al.*, 2017; Scheiter *et al.*, 2013). However in subsequent model development and thereby in the applied version of aDGVM2, leaf longevity was not tied to SLA anymore. Including this trade-off may be key for appropriate dwarf shrub representation.

Growth rates are also linked to maximum photosynthetic rates (Chapin III *et al.*, 2011, p. 144), where dwarf shrubs tend to have lower maximum photosynthetic rates and thus lower growth rates (Schulze & F.S. Chapin, 1987). To lower  $GPP_{sim}$  with a process-oriented scheme rather than a tuning parameter as was implemented in  $sim_{GPP/3}$ , investigating the role of maximum carboxylation rates might be promising. Sakschewski *et al.* (2015) implemented a trade-off in the DVM LPJmL (Lund-Potsdam-Jena managed Lands) where area-based maximum carboxylation rates increased for leaves with decreasing SLAs such as the slow-growing Nama Karoo dwarf shrubs. At first glance, this is in contrast to the lower photosynthetic rates for dwarf shrubs in Chapin III *et al.* (2011, p. 144) and Schulze & F.S. Chapin (1987) and points towards the complexity of this relationship. However based on leaf mass, the maximum carboxylation rates of plants with small SLAs may nonetheless be lower than those for high-SLA plants (Sakschewski *et al.*, 2015). In a sensitivity analysis and optimisation study with the Ecosystem Demography (EDv2.2) model for a shrub PFT developed for the North American sagebrush steppe, SLA limits were lower than currently implemented in aDGVM2 ( $3\text{--}9\ m^2kg^{-1}$  and  $4.5\text{--}20.3\ m^2kg^{-1}$ , respectively; Pandit *et al.*, 2019). In the optimisation, their range limits for maximum carboxylation rate per leaf area were also lower than the range limits implemented in

aDGVM2 ( $14\text{--}21.5 \mu\text{mol m}^{-2}\text{s}^{-1}$  and  $17.5\text{--}37 \mu\text{mol m}^{-2}\text{s}^{-1}$ , respectively). However, traits cannot be compared directly between aDGVM2 and EDv2.2, because the process implementations differ in the two models and the optimisation in Pandit *et al.* (2019) was implemented for sagebrush steppe. To lower SLA range limits in aDGVM2, range limits for matric potential at 50% loss of xylem conductance,  $P_{50}$ , would need to be lowered. Field measurements with  $\text{CO}_2$ -response curves of photosynthesis for typical Nama Karoo shrubs can be used to derive maximum carboxylation rates to parameterise the aDGVM2 (De Kauwe *et al.*, 2016).

Leaf size is not explicitly simulated as inheritable trait in aDGVM2. Leaf length is currently a fixed parameter that is used in aDGVM2 to scale leaf hydraulic conductivity for woody individuals and thus influences water availability for plant individuals and their photosynthesis. For dwarf shrubs, leaf length could be reduced compared to single- and multi-stemmed tree and shrub individuals. Thus, the characteristic, small leaves of Karoo shrubs could be taken into account. The complex dynamics of leaf physiology in aDGVM2, including photosynthesis and stomatal conductance sub-models, make it difficult to predict the effect that this change would have on simulated vegetation. Preliminary test simulations and analyses can show, if additional model development is necessary to implement leaf size as a trait that varies by vegetation type or by individual plants in aDGVM2. This will also show if the simulated effects of smaller leaf size agree with results in the literature, where, for arid, warm environments, plants with smaller leaves are better adapted to achieve transpirational cooling when water resources are limited (Wright *et al.*, 2017).

To improve the representation of dwarf shrubs, aDGVM2 parameters for crown architecture could also be adapted. One of the parameters characterising crown architecture of woody plants in aDGVM2 is the height of the bottom end of the crown. For trees and shrubs, the crown does not start at the bottom of the stem. This does not represent the crown architecture of dwarf shrubs in Middelburg well (Fig. 4.2), although shrubs with a more inverse conical shape are also typical in the Karoo (Whitford, 2004). For dwarf shrubs, the range limits for the height of the bottom of the crown, an inheritable aDGVM2 trait, could be lowered so that the crown can start close to the ground. In addition, parameter ranges for aDGVM2 parameters

that relate plant height to biomass could be adjusted to limit height growth of individuals. High degrees of branching with many small-diameter twigs is typical for the Nama Karoo shrubs in Middelburg and play a role in plant water dynamics decreasing water potential in leaves and growing shoots. This could be a factor limiting height growth (Wilson, 1995) and would require further model development and refinement of an existing branching sub-module in aDGVM2.

The inadequate representation of dwarf shrubs and the need to improve existing PFTs or introducing new PFTs can also be found in other DVMs or for other world regions. For example, for the North American semi-arid sagebrush steppe, a new PFT was developed for EDv2.2 (Pandit *et al.*, 2019) and an existing Mediterranean shrub PFT was adapted and optimised in LPJ-GUESS (Renwick *et al.*, 2019). In simulations with the Sheffield dynamic global vegetation model for Namibia, the Namibian Nama Karoo was classified based on thresholds for deciduous broad-leaved trees and grass biomass without considering a shrub or a dwarf shrub PFT (Thuiller *et al.*, 2006). Similar to this chapter, Horvath *et al.* (2021) faced difficulties with the DVM community land model 4.5 bio-geo-chemical cycles and dynamical vegetation (CLM4.5BGCDV) in simulations for Norway, although PFTs in their simulations were developed for boreal regions and thus different climatic zones. The existing boreal shrub PFT in CLM4.5BGCDV was developed for larger-sized shrubs and do not represent dwarf shrubs well.

In these models, shrub PFTs are defined by bioclimatic limits and fixed parameters (Horvath *et al.*, 2021; Pandit *et al.*, 2019; Renwick *et al.*, 2019). Maximum growth limitations, e.g., in terms of maximum annual growth or maximum biomass values, are also used to restrain the growth of a PFT (Horvath *et al.*, 2021). Some of the traits and parameter values that were used in other DVMs to parameterise shrubs would require model development in aDGVM2, because the traits currently do not exist in aDGVM2 (e.g., growing degree-day sum) or the traits are implemented with different equations and trade-offs (e.g., SLA and maximum carboxylation rate). Nonetheless, implementations in other DVMs can shed light on critical processes and parameters to consider when implementing dwarf shrubs in aDGVM2.

For the Nama Karoo, test simulations with the suggested changes in aDGVM2 can show if driven by environmental input data and the newly implemented trade-offs dwarf shrubs emerge

in the woody vegetation type. If dwarf shrubs do not emerge, some key trade-offs may still be missing. However, larger ecophysiological differences between dwarf shrubs and larger woody plants, such as trees and savanna shrubs, that cannot be represented by trade-offs alone, could also be an explanation for this. This may then point to the need of an implementation of dwarf shrubs as a new, separate vegetation type in aDGVM2. An important prerequisite for these simulations would be that soil water processes in aDGVM2 are adapted so that they represent soil water dynamics in the Nama Karoo more closely.

## 4.6 Further considerations and future research opportunities

The analysis in this chapter showed that further field research on the ecophysiology and processes driving the dynamics of Nama Karoo vegetation and soils is required. For example, the Nama Karoo C<sub>3</sub> shrubs predominantly grow in spring (August - September) and autumn (March - May), but generally throughout the whole year (du Toit & O'Connor, 2020). The driving processes behind this pattern are unclear. For the case study site in the Nama Karoo, experimental temperature increases had a growth enhancing impact on stem lengths for the C<sub>3</sub> shrub *E. ericoides* (Edwardes, 2018), indicating that both water and temperature limitation might contribute to this growth pattern. More extensive field experiments are required to relate growth rates and photosynthetic rates to each other and to investigate the effect of molecular (e.g., carbon-expensive photorespiration) and structural (e.g., reduced light-use efficiency) photoprotection on carbon balance (Fernández-Marín *et al.*, 2020). Because of slow changes in community composition in the Nama Karoo ecosystem, especially for the slow-growing shrubs (van der Merwe & Milton, 2019), long-term ecological observations are important to get a better understanding of drivers of ecological change (Hoffman *et al.*, 2018) and potential climate change impacts. This will increase understanding of key processes driving vegetation dynamics and improving their representation in DVMs.

Nama Karoo grasses are much faster in their response to grazing pressure and changes in precipitation than Nama Karoo shrubs. In the past, increased precipitation led to an increased grass abundance in the Nama Karoo close to Middelburg (du Toit *et al.*, 2018). Increased grass

abundance, and hence increased fuel load, could increase the likelihood of fire occurrence. Therefore, if the precipitation trend continues, the fire dynamics in the Nama Karoo could change (du Toit *et al.*, 2018). In the past, fires were rare in the semi-arid eastern Nama Karoo dwarf shrublands. In one of the rare fires that occurred about 1 km away from the Middelburg eddy covariance flux tower from this case study, the dominant shrub species *E. ericoides* and *R. intricata* were extirpated by the fire (du Toit *et al.*, 2015). If fire occurrence increases in the future, this could benefit resprouting plants and fast-growing grasses as opposed to slow-growing shrubs. Therefore, when investigating climate change impacts on the Nama Karoo in the future, it would be critical to include fire in the simulation setup. Thus, feedbacks and tipping point effects, where increased grass abundance and increased fire occurrence facilitate each other and extirpate dwarf shrubs, could be investigated. This would lead to a transition from Nama Karoo to a grassland biome.

The differing responses of species with C<sub>3</sub> or C<sub>4</sub> photosynthesis to changes in environmental drivers such as warming or increases in atmospheric CO<sub>2</sub> concentration further complicate these dynamics. At first glance, observations of increased growth for a C<sub>3</sub> shrub but not C<sub>4</sub> grasses under experimental heating treatments at the Middelburg site (Edwardes, 2018) may be surprising, because C<sub>4</sub> grasses tend to cope better with warmer climates than C<sub>3</sub> plants (Collatz *et al.*, 1998). This behaviour may be explained by the requirement of sufficient soil moisture for C<sub>4</sub> grasses to grow well. Climate change simulations with an appropriate implementation of dwarf shrubs in aDGVM2 would allow investigating potential effects of warming in combination with elevated atmospheric CO<sub>2</sub> concentrations on the implemented vegetation types and growth forms and their dynamic interactions. Climate change effects such as bush encroachment of larger-sized shrubs and the potential interplay of grasses, dwarf shrubs, and bigger shrubs could be investigated. However, precipitation projections for the Nama Karoo are still uncertain but current projections point towards a reduction in precipitation (Arias *et al.*, 2022).

Grazing and browsing also shape the Nama Karoo vegetation, but effects are often dwarfed by the influence of precipitation (du Toit *et al.*, 2018). When combining grazing and browsing models with vegetation dynamics, socio-economic impacts of droughts and future climate changes

could be investigated to fill an important research gap (Hoffman *et al.*, 2018). In a previously published aDGVM2 sub-module for cattle grazing (Pfeiffer *et al.*, 2019, 2022), the biomass demand required for each livestock unit would need to be reparameterised to implement grazing simulations for sheep. Because palatable dwarf shrub species contribute to feed for livestock, the grazing model would ideally be extended to include browsing of leaves from dwarf shrubs. Combined with an economic model previously developed for the aDGVM (Scheiter *et al.*, 2018), ecological and socioeconomic Nama Karoo systems can be coupled. Estimates for the economic value of sheep and cattle in the Nama Karoo could be derived in collaboration with researchers from e.g., GADI in Middelburg with their long-term research and experience (du Toit *et al.*, 2018; Hoffman *et al.*, 2018). To assess ecological and socio-economic dynamics, future studies could also couple the aDGVM2 with an agent-based model that simulates animal behaviour (Fust & Schlecht, 2018; Grillot *et al.*, 2018) or human decision processes (Dressler *et al.*, 2019). Thus, interactions of different components in the socio-ecological system and how decisions on, e.g., grazing strategy affect the ecosystem state (Pfeiffer *et al.*, 2022) in the Nama Karoo could be analysed. This could support the decision processes in the development of management strategies (Fust & Schlecht, 2018).

Based on a socioeconomically coupled version of aDGVM2, climate change impacts on Nama Karoo vegetation and its grazing system as well as human livelihoods under different shared socioeconomic pathways (SSP) and climate change scenarios (representative concentration pathways, RCPs) (O'Neill *et al.*, 2016) could be investigated. Potential woody encroachment under scenarios of climate change and increased atmospheric CO<sub>2</sub> concentrations (see Chapter 2 and Figure 2.1, Martens *et al.*, 2021) could also be considered in the economic model. In the case of encroachment of larger shrubs, the removal of encroaching biomass may generate economic opportunities, e.g., by its use for charcoal production as it is currently done in Namibia (Shikangalah & Mapani, 2020) or generation of electricity (Stafford *et al.*, 2017). Thus, climate-driven changes and potential losses in grazing, an important ecosystem service in the Nama Karoo, can be put into perspective of emerging economic opportunities. This economic incentive could support intervention efforts of clearing larger shrubs to keep the Nama Karoo an open dwarf

shrub ecosystem. Ecologically, a fully encroached ecosystem, where the encroaching species led to a change in dominant plant functional type, cannot easily be reverted to its previous state at a timescale of several decades (Scholes, 2009), especially in a slow-growth ecosystem such as the Nama Karoo. Benefits of clearing activities to restore an encroached Nama Karoo landscape can also include water-related ecosystem services and by avoiding local biodiversity loss could provide benefits on multiple levels (Stafford *et al.*, 2017).

Livestock farming is the predominant land use in the Nama Karoo with regionally important economic significance. At the same time competing non-agricultural land uses such as renewable energy and mining increasingly put pressure on the Nama Karoo ecosystem (Walker *et al.*, 2018). In combination with the uncertainty of the contribution of the Nama Karoo to the interannual variability and trend of the global land carbon balance (Ahlström *et al.*, 2015), this emphasises the need for a solid understanding of the ecosystem components and processes of the Nama Karoo and potential impacts and consequences of these land uses and land use changes. At the same time, DVMs are currently the only tools for investigating impacts of future climate change and dynamic feedback effects between ecosystem components (Prentice *et al.*, 2007). However, this study has shown that simulating the Nama Karoo with a DVM is still challenging and that further model development and field research are essential for making meaningful projections for climate change impacts on the Nama Karoo.

## Chapter 5

# Synthesis

## 5.1 Overview

African ecosystems provide the livelihoods and ecosystem services for approximately 1.4 billion people (United Nations, Department of Economic and Social Affairs, Population Division, 2022) and the habitat for a unique biodiversity (Midgley & Bond, 2015). Semi-arid ecosystems, which cover large parts of Africa, drive trends and variability of global terrestrial carbon dynamics (Ahlström *et al.*, 2015). However, the African continent is highly vulnerable to climate change due to intersections between environmental, socioeconomic and political factors. The majority of people in sub-Saharan Africa work in agriculture, where 95% of croplands are rainfed (Trisos *et al.*, 2022). At the same time, the human population in sub-Saharan Africa is projected to grow and potentially more than double by the end of the 21<sup>st</sup> century in contrast to all other world regions (United Nations, Department of Economic and Social Affairs, Population Division, 2022). This population growth and the associated changes in land use and land cover are challenges for the conservation of Africa's biodiversity (IPBES, 2018b). Understanding ecosystem and carbon cycle dynamics and potential climate change impacts in Africa and uncertainties associated with vegetation projections is critical for the planning of climate change adaptation measures (Müller *et al.*, 2014). These prospects motivated the research in this thesis with a focus on future climate change impacts on ecosystems and carbon dynamics in Africa and where they may co-occur with the global change drivers population and land use. In addition, I investigated uncertainties of DVM projections and how the representation of the Nama Karoo as a niche ecosystem and its carbon cycle could be improved. I showed opportunities but also limitations and uncertainties of simulations and climate change projections with the DVMs aDGVM and aDGVM2 for African ecosystems and their carbon balance and the combination of DVM projections with global change projections. In the following section, I first respond to the research questions presented in Chapter 1 based on the presented research. Then, avenues of future research are presented including potentials of model development and the application of DVMs in climate impact attribution research and for assessing nature-based solutions, before drawing final conclusions.

### 5.1.1 How does climate change affect African ecosystems and carbon stocks until the end of the 21<sup>st</sup> century?

The projections for African ecosystems until the end of the 21<sup>st</sup> century in Martens *et al.* (2021, Chapter 2) show that changes in biomes and carbon stocks are likely for large areas in Africa. Effects were stronger under RCP8.5 than RCP4.5, but even the medium-impact scenario RCP4.5 suggested considerable ecosystem change across Africa. Elevated atmospheric CO<sub>2</sub> concentrations resulted in enhanced water use efficiency (WUE) and strong woody encroachment into C<sub>4</sub>-dominated savannas and grasslands and their transition to more C<sub>3</sub>-dominated, woody biomes. This confirms the vulnerability of savanna and grassland biomes (Bond, 2016) to woody encroachment under elevated atmospheric CO<sub>2</sub> concentrations, which threaten their biodiversity (Midgley & Bond, 2015). At the same time tropical forests in a belt south of the equator were less stable in our simulations than found by Gonzalez *et al.* (2010), Scholze *et al.* (2006) and Sitch *et al.* (2008).

At first glance, the combination of increased WUE and increased biomass production contrasts with analyses that did not find increased tree growth when WUE was increased under elevated CO<sub>2</sub> (e.g., Peñuelas *et al.*, 2011). However, in our simulations the biomass increase is linked to demographic effects and changes in vegetation structure in grassland and savanna ecosystems. Feedbacks between CO<sub>2</sub> fertilisation and fire disturbance alter the competitive balance between C<sub>3</sub> trees and C<sub>4</sub> grasses in favour of C<sub>3</sub> trees and their saplings (Midgley & Bond, 2015). Recent experiments with an encroaching southern African savanna tree have confirmed that elevated CO<sub>2</sub> concentrations stimulate growth in the critical recruitment phase and seedlings reach a critical size threshold faster, which allows them to survive herbivory (Ripley *et al.*, 2022). Even though demographic effects in Martens *et al.* (2021) were only influenced by fire dynamics, these findings corroborate the importance of demographic effects in African savanna ecosystems. When herbivory or C<sub>4</sub> grass competition occur during the initial recruitment phase, the stimulating effect of elevated CO<sub>2</sub> concentration on the growth of C<sub>3</sub> tree seedlings is removed (Raubenheimer & Ripley, 2022). Nonetheless during the tree seedling recruitment phase, the CO<sub>2</sub>-stimulated growth of tree saplings decreases the probability of fatal herbivory (Ripley

*et al.*, 2022). Next to fire, herbivory is an essential ecosystem-shaping disturbance in African savannas (Bond *et al.*, 2005). This underlines that including representation of herbivory (e.g., Pfeiffer *et al.*, 2019) in future projections is key to reflect ecosystem dynamics in African savannas under a changing climate and increasing atmospheric CO<sub>2</sub>.

Mean annual precipitation in central African tropical forest is close to a postulated lower viability threshold for humid tropical forest of 1500 mm (Malhi *et al.*, 2013; Zelazowski *et al.*, 2011). This agrees with analyses where the tropical forest region in the Congo basin is not characterised as deterministic forest but rather as bistable, where savanna is a possible alternative vegetation state (Staver *et al.*, 2011b). Our findings of high vulnerability of African tropical forest to vegetation change driven by climate change by the end of the 21<sup>st</sup> century in Martens *et al.* (2021) supports these findings. The CO<sub>2</sub> fertilisation effect only partially counteracted these climate-change driven developments. However, a recent analysis challenges the previously assumed extent of possible alternative vegetation states (Staver *et al.*, 2011b), including central African forests (Higgins *et al.*, 2023a). They argue that alternative states are less prevalent and that often micro-environments resulting from, e.g., topographic gradients create local climates that mainly determine the local ecosystem state (Higgins *et al.*, 2023a).

### **5.1.2 Where may climate change impacts and the global change drivers human population density and land use co-occur and exert pressure on African protected areas until the end of the 21<sup>st</sup> century?**

The combination of projections for vegetation change, human population and land use in Martens *et al.* (2022, Chapter 3) showed that most African protected areas and their biodiversity are projected to be adversely affected by at least one of these three global change drivers until the end of the 21<sup>st</sup> century. The co-occurrence of the three drivers was mostly specific to a region or one of the two investigated scenarios, SSP2-RCP4.5 and SSP5-RCP8.5. At the continental scale, no clear overall patterns in relationships between climate-driven vegetation changes and socioeconomic pressures emerged from our analysis. This is not surprising because climate-driven vegetation changes and socioeconomic drivers are spatially independent

global change drivers. Different regions will be subject to different combinations of pressures as socioeconomic developments vary regionally. Protected areas in West Africa were projected to be affected by climate-driven vegetation changes in combination with high levels of future population density and land-use pressure in their vicinity. Except for North Africa, future decreases in population density and land-use pressure in the vicinity of protected areas were rare. Both SSP-RCP scenarios implied increasing challenges for conserving Africa's biodiversity in protected areas.

Consistent with the continental scale biome projections in Martens *et al.* (2021, Chapter 2), the investigation in Martens *et al.* (2022) suggests high vulnerability of protected areas with grasslands and savannas to future climate- and CO<sub>2</sub>-driven habitat loss. This confirms previous results, where protected tropical grasslands and tropical woodlands were among global biomes most vulnerable to climate-driven biome changes (Eigenbrod *et al.*, 2015). Habitat loss in our projections was more widespread under SSP5-RCP8.5 than SSP2-RCP4.5, which is consistent with projections from species distribution models (e.g., Hannah *et al.*, 2020). The widespread projected habitat loss in protected areas raises the question, if the current extent and network of protected areas in Africa is sufficient to prevent species loss. Under climate change, connectivity of protected areas may be essential to facilitate climate-induced movement between protected areas (Dobrowski *et al.*, 2021). Yet, this connectivity is currently not given underlining the need for conservation and land management strategies that allow for species range shifts (Parks *et al.*, 2023). Conservation targets of increasing the cover of protected land areas to at least 30% under the Kunming-Montreal global biodiversity framework of the Convention on Biological Diversity (CBD COP, 2022) are in line with this need for increased connectivity.

At the same time, the projected increases in human population and land use in the vicinity of many protected areas may be interpreted as proxies for additional pressure on the protected areas (Martens *et al.*, 2022). For instance, the likelihood for the downsizing of big protected areas increases with local population densities (Symes *et al.*, 2016). Societal pressure to down-grade protected areas to allow, for example, human settlements and livestock herding (Lindsey *et al.*, 2017) or renewable energy facilities (Rehbein *et al.*, 2020) in protected areas is expected

to increase conflicts between achieving conservation goals and meeting human needs (DeFries *et al.*, 2007). Thus, the goals of biodiversity protection and climate mitigation through protected areas are competing with, e.g., food production. Despite the large variation between scenarios and regions, we concluded that socioeconomic pressures will likely exacerbate climate-change impacts on vegetation for most protected areas and regions in Africa. Our findings also underline the importance of developing and implementing region-specific conservation responses (Martens *et al.*, 2022). Other global change factors such as invasive species, that are known to be a great threat for protected areas (Sieck *et al.*, 2011) or other proxies for human pressure such as electricity and road infrastructure (Sanderson *et al.*, 2002) could expand future analyses of pressures on protected areas.

In the two investigated scenarios, all three investigated pressures showed medium to strong increases in pressures for most protected areas in Africa and point to increasing difficulties to sustain the effectiveness of conservation in Africa (Martens *et al.*, 2022). Hence, an increase in coverage to 30% will also need to be accompanied by an improved effectiveness of protected areas. For protected areas in China, socio-economic status was an important predictor for the effectiveness of protected areas in conserving threatened species (Zhao *et al.*, 2023). Therefore, efforts to strongly mitigate climate change combined with measures that promote equitable, wealth-distributing, and sustainable development (Crist *et al.*, 2017) are key for the success of biodiversity conservation in this century.

### **5.1.3 Which uncertainties do these future projections entail? Can the simulations be used to make detailed projections for individual ecosystems and their carbon dynamics or for individual protected areas?**

Our projections in Martens *et al.* (2021, Chapter 2) with the aDGVM showed that the implementation of the CO<sub>2</sub> fertilisation is key for the simulation results and projected vegetation states. CO<sub>2</sub> fertilisation caused the strongest variability in our future projections compared to RCP scenario and chosen climate model (general circulation model, GCM) and primarily defined the future carbon source or sink behaviour, WUE, and biome states. This importance of

CO<sub>2</sub> fertilisation for simulation outcome is consistent with projections for the Amazon (Rammig *et al.*, 2010) and the global tropics (Huntingford *et al.*, 2013). The simulations with and without increases in atmospheric CO<sub>2</sub> concentration and thus with and without CO<sub>2</sub> fertilisation give an idea of the range of the potential impact of CO<sub>2</sub> fertilisation and future climate change. The aDGVM currently does not include nutrient cycling and therefore no nutrient limitation. DVMs with incorporated nutrient dynamics often project smaller impacts of elevated CO<sub>2</sub> than shown in Martens *et al.* (2021) due to nutrient limitation. Compared to experimental data the aDGVM projections overestimate the CO<sub>2</sub> fertilisation effect (e.g., Fleischer & Terrier, 2022). Especially due to the feedback effects between population and fire dynamics and elevated CO<sub>2</sub> concentrations in savanna ecosystems (Midgley & Bond, 2015) some effects promoting woody encroachment and biomass increases as simulated in Martens *et al.* (2021) are likely.

The ensemble approach in Martens *et al.* (2021) revealed disagreements in the simulated biomes between the different ensemble members especially in the transition zones between biomes. This disagreement increased in the projections of climate change impacts until the end of the 21<sup>st</sup> century. Variability in climatic drivers from GCMs and particularly uncertainty in projected future precipitation (Engelbrecht *et al.*, 2015) explain disagreements between ensemble members. In the transition zones between savanna and forest, stochastic processes in the aDGVM fire model may also partially explain the disagreement between ensemble members, because fire is an important driving factor which differentiates between these two alternative stable biome states, which are possible in large parts of Africa (Staver *et al.*, 2011b). The projections of substantial biome changes across all simulations and scenarios of the ensemble suggest substantial future changes in habitat structure and biodiversity, which contrasts with relative stability of past climates and disturbance regimes in Africa (Midgley & Bond, 2015).

The ecosystem changes simulated at continental scale indicate broad patterns of change in vegetation biomass and biome change under elevated CO<sub>2</sub> concentrations across Africa (Martens *et al.*, 2021) and in African protected areas in particular (Martens *et al.*, 2022). Most of the protected areas included in the study were smaller than the size of grid cells in the vegetation

simulations. This implies that small-scale environmental conditions within protected areas and unique features of protected areas were not represented in the vegetation projections. This simplification hampers estimates for individual protected areas, but allowed the analysis of regional patterns of potential future pressures on protected areas.

The results from Chapter 4 for recent vegetation dynamics at a site in the Nama Karoo in South Africa underline that DVM simulations need to be interpreted cautiously for individual ecosystems and their carbon fluxes. For aDGVM and aDGVM2, this is particularly true for ecosystems not covered by the forest-savanna-grassland spectrum and niche ecosystems because their growth forms and ecophysiological dynamics may not be represented well. Long-term ecological observations with, e.g., eddy covariance flux towers and repeated field surveys in combination with ecophysiological and soil carbon flux experiments help to improve our understanding of these dynamics (Hoffman *et al.*, 2018). Long-term observations are particularly valuable in ecosystems such as the Nama Karoo with its slow-growing shrub community and associated slow changes in community composition (van der Merwe & Milton, 2019) and its high precipitation variability (du Toit *et al.*, 2018). The Grootfontein Agricultural Development Institute (GADI) close to Middelburg, South Africa, with their long-standing research can be an important partner for further research on Nama Karoo processes. In combination with model developments that ensure the representation of typical growth forms, the knowledge gained from long-term observations will facilitate representation of Nama Karoo vegetation dynamics in DVMs. These model developments will enhance projections of future climate change impacts for the Nama Karoo.

In the analysis of future global change pressures for African protected areas, projections in buffers surrounding protected areas were assumed to be proxies for their potential ecological isolation from other natural areas and for potential, indirect, future, socioeconomic influences on protected areas. This approach does not evaluate population and land use pressures inside the protected areas (Martens *et al.*, 2022). This may be particularly problematic for protected areas, where the ecosystems in the protected area differ strongly from the surrounding area,

e.g. because of elevational gradients (Joppa & Pfaff, 2011). In conservation science, an established method to evaluate the effectiveness of a protected area is to compare developments in a protected area with developments in a site with matching environmental states outside of the protected area (e.g., Geldmann *et al.*, 2019). This approach could be adapted to our research of potential future pressures on protected areas by assuming that projections for the matched site are representative of changes within a protected area. However, because Martens *et al.* (2022) was based entirely on model results and future projections, results cannot be tested against observational data. Applying the matching approach for future projections would require assumptions and additional parameters that would entail additional uncertainty for the analysis, especially because factors, such as management capacities, resource availability, and socioeconomic level, that influence land use and population in protected areas (Lindsey *et al.*, 2017) are difficult to project into the future across larger scales. A comparison of results for the matching approach and the buffer approach in future research would shed further light on the influence of the chosen approach on the results.

#### **5.1.4 How well do we understand and reproduce carbon cycle dynamics in semi-arid niche ecosystems such as the Nama Karoo?**

In simulations for the Nama Karoo in Chapter 4, vegetation biomass was largely overestimated in most simulation setups and simulated vegetation structure did not agree with observed vegetation. In their size and accumulated biomass, simulated shrubs resembled savanna shrubs rather than small Nama Karoo dwarf shrubs. The intraannual patterns of the carbon fluxes gross primary production (*GPP*) and ecosystem respiration (*Reco*) was only partially reproduced and the fluxes were generally overestimated. Delayed responses of *GPP* to soil moisture increases and decreases in *Reco* due to drying in upper soil layers (Parton *et al.*, 2012) were not represented well in the aDGVM2 simulations. Because net ecosystem exchange (*NEE*) is derived from *GPP* and *Reco* in aDGVM2, simulated *NEE* did not agree well with observations neither for intraannual patterns nor for annual budgets and their variabilities.

The simulations in Chapter 4 also showed challenges in simulating below-ground water and carbon processes in semi-arid ecosystems. Simulated soil moisture did not drop to observed levels and heterotrophic respiration was overestimated. In semi-arid ecosystems such as the Nama Karoo, water availability limits plant growth (Venter, 2001) and drives heterotrophic respiration (Zhou *et al.*, 2021). Therefore, an appropriate model representation of soil moisture dynamics is key for plant growth and simulated carbon balance. Even though soil moisture levels in aDGVM2 simulations in Chapter 4 were higher than measured values, simulated shrubs died because of a negative carbon balance in simulations where soil water input from precipitation was limited. This points to a high susceptibility of simulated shrubs to dry stress and that coping mechanisms of semi-arid dwarf shrubs are not reflected well in the aDGVM2 implementation of woody vegetation.

Simulations with the aDGVM2 and its approach of inheritable traits and trade-offs between traits provide the opportunity of simulating the emergence of plants with individual trait combinations that are adapted to the environmental conditions. A community can evolve flexibly over time under changing conditions such as changes in climate or land use (Langan *et al.*, 2017; Pfeiffer *et al.*, 2019; Scheiter *et al.*, 2013). Trade-offs between, e.g., SLA and leaf longevity following the leaf economics spectrum (Wright *et al.*, 2004) or between growth rates and turnover rates of leaves and roots could be tested in aDGVM2 in efforts of improving the representation of dwarf shrubs. In addition, adaptation of parameters for, e.g., crown architecture, biomass longevity and maximum carboxylation rates as well as an implementation of high degrees of branching are promising routes of model development to enable representation of semi-arid vegetation dynamics and dwarf shrubs in particular in aDGVM2 simulations.

If simulations with these adaptations are not successful, this could point to physiological differences between dwarf shrubs and larger woody plants that cannot be represented by trade-offs. In this case, a new vegetation type which is explicitly parameterised for dwarf shrubs may be required to simulate semi-arid dwarf shrub ecosystems. Additional field research on turnover rates, root systems and water dynamics of dwarf shrubs could shed further light on the functioning of vegetation dynamics in dwarf shrub ecosystems. In summary, further model

development and field research are essential for making meaningful DVM projections for land use and climate change impacts on vegetation dynamics and carbon cycles in niche ecosystems such as the Nama Karoo and the roles of rising atmospheric CO<sub>2</sub> concentrations but also fire dynamics.

Livestock farming with sheep but also goats and cattle is a main land use and important part of the economy in the Nama Karoo (du Toit *et al.*, 2018; Walker *et al.*, 2018) and an important disturbance in its ecosystem (van der Merwe & Milton, 2019; Wiegand *et al.*, 1995). It has been shown that grazing in the Nama Karoo influences ecosystem composition and the mix of grasses and dwarf shrubs (du Toit *et al.*, 2018). To fully capture dynamics of the Nama Karoo and grassy dwarf-shrub ecosystem in DVMs, it would therefore be essential to include a grazing model, which also captures transitions between annual and perennial grass species (e.g., Pfeiffer *et al.*, 2019). At the same time, changes in precipitation influence community composition and seem to be a more important driver of the grassiness in the eastern Nama Karoo than grazing. Increases in precipitation in the past have led to a transition towards more grassy species and fewer dwarf shrubs. Although some dwarf shrubs in the Nama Karoo are palatable, palatability of many grasses is higher. Economically, this may be beneficial for livestock farming (du Toit *et al.*, 2018). However beyond the ecosystem service of livestock farming, it can be argued that the Nama Karoo ecosystem and its biodiversity, or any ecosystem for that matter, have their own intrinsic value independent of their use to humans (Batavia & Nelson, 2017). This would implicate that the conservation of the Nama Karoo ecosystem and minimising climate change to avoid biome changes are a moral imperative.

## 5.2 Vision for future research with DVMs and aDGVM2 in particular

### 5.2.1 Future avenues of model development to improve ecosystem representation in DVMs

DVM simulations at regional and continental scale as implemented and used in Chapters 2 and 3 are useful to understand broad patterns of change, but results at smaller scale for individual ecosystems must be interpreted cautiously. This especially applies for ecosystems for which the dominant vegetation types are not explicitly represented in DVMs. For aDGVM and aDGVM2 this comprises ecosystems that are not characterised by tree, savanna shrub and grass vegetation types. For South Africa, Moncrieff *et al.* (2015) have shown with the aDGVM that ecosystems outside of the forest-savanna-grassland spectrum are not represented well in simulations. This is underlined by the case study with the aDGVM2 for the Nama Karoo in Chapter 4 and the presented difficulties in representing soil water and carbon dynamics and dwarf shrub growth forms, which highlighted the importance of revisiting plant and soil water dynamics in aDGVM2 for semi-arid ecosystems. Other ecosystems not represented by aDGVM and aDGVM2 include South Africa's unique Fynbos with its shrubs and crown fires and the Succulent Karoo with succulent shrubs and CAM photosynthesis (Moncrieff *et al.*, 2015) as well as facultative CAM photosynthesis in succulent C<sub>3</sub> dwarf shrubs (Winter, 2019). Representation of dryland ecosystems with fog as a main source of moisture as is found in the Namib Desert (Wang *et al.*, 2019) brings multiple challenges. In a dynamic model, they would require an implementation which captures the dynamics of climatic fog formation, fog interception by plant biomass and moisture uptake by plants (Borthagaray *et al.*, 2010). Next to moisture availability for plants, fog and dew also alter soil moisture and are thus important controls of heterotrophic respiration in semi-arid and arid ecosystems (Logan *et al.*, 2022). This could be a key component to improve the representation of their carbon cycles in DVMs.

Large uncertainties related to the implementation of the CO<sub>2</sub> fertilisation effect were presented in Martens *et al.* (2022, Chapter 2). Nutrient dynamics are not implemented in aDGVM and

aDGVM2 but are known to be an important controlling factor of the CO<sub>2</sub> fertilisation effect, especially in the tropics (Fleischer & Terrer, 2022). The implementation of nitrogen and phosphorus cycles have dampened the CO<sub>2</sub> fertilisation responses in DVMs (e.g., Fleischer *et al.*, 2019; Hickler *et al.*, 2015) and are important steps in aDGVM and aDGVM2 model development. Thus, uncertainty in simulated ecosystem variability under climate change and elevated CO<sub>2</sub> concentrations can be reduced. The implementation of nitrogen fixation as an inheritable trait for tree growth forms in aDGVM2 could be a worthwhile extension when simulating African ecosystem dynamics, because observed woody encroachment in African savannas was mainly driven by nitrogen-fixing species (Stevens *et al.*, 2017).

## 5.2.2 Attribution of anthropogenic climate change to observed vegetation change based on ensemble studies

Sensitivity analyses based on ensembles of climate data such as the implementation in Chapter 2 contribute to the identification of uncertainties in simulations with dynamic vegetation models. They can provide insights into the range of possible impacts of anthropogenic climate change on vegetation. In climate change research, ensemble studies have also been used to investigate if observed meteorological events can be attributed to anthropogenic climate change (e.g., Hegerl & Zwiers, 2011; Otto *et al.*, 2013). Attribution of changes to drivers contributes to the evaluation of how anthropogenic climate change is affecting observed changes. It can provide scientific evidence on impacts of climate change today and support the assessment of changing risks due to climate change (Otto *et al.*, 2013).

For vegetation changes, the interaction and compounded occurrence of multiple drivers of change including land use and climate change (IPBES, 2018a) complicates a direct attribution of vegetation changes to individual drivers (Stone *et al.*, 2013). For observed vegetation changes such as woody encroachment (Stevens *et al.*, 2017) or desertification (Burrell *et al.*, 2020), data on land use and climate in the investigated regions have been analysed to attribute different drivers to the observed changes. Rising atmospheric CO<sub>2</sub>, changing land management, and rainfall were identified as likely drivers of encroachment in Africa based on a literature review

and a statistical analysis of published data on woody cover, mean annual precipitation, and the first year of observations (Stevens *et al.*, 2017). In the analysis of drivers of desertification, vegetation change in the past was based on a time series of remote sensing data on peak normalised difference vegetation index (NDVI). The regional strengths of the desertification drivers CO<sub>2</sub> concentration, climate variability, climate change and land use were derived in a statistical analysis. For this analysis a combination of trend analysis of NDVI, data on atmospheric CO<sub>2</sub> concentration, a relationship between GPP and atmospheric CO<sub>2</sub>, and observed and detrended precipitation and temperature was used (Burrell *et al.*, 2020). Higgins *et al.* (2023b) globally detected climate change as a main driver of changes in terrestrial ecosystems over the past 40 years. Soil moisture was the main driver of change in dry and warm locations and changes in temperature mainly drove changes in cooler ecosystems. Their analysis was based on a combination of NDVI, a dynamic growth model for single plants, climate reanalysis data and detrended time series of climate forcings.

To explicitly attribute anthropogenic climate change as driver of ecological changes distinct from natural variability but also external drivers such as volcanic eruptions and solar luminosity (Stone *et al.*, 2013), a combination of analysis steps has been developed. First, a climatic event is attributed to anthropogenic climate change. Next, an ecosystem response outside of its natural variability needs to be detected. Finally, the likelihood that the biological impact is driven by anthropogenic climate change and not by other forcings is analysed (Harris *et al.*, 2020; Rosenzweig *et al.*, 2008). Ecological impact attribution, however, is challenging at species-level because of missing baseline data and naturally high variability in time and space (Harris *et al.*, 2020). A combination of remote sensing data and DVMs could contribute to closing the gap in attribution research on analysing the role of anthropogenic climate change as driver of observed vegetation changes and trends.

DVMs have reproduced trends in past vegetation changes such as greening trends observed in satellite data for the Sahel (Hickler *et al.*, 2005; Seaquist *et al.*, 2009) and for boreal zones (Lucht *et al.*, 2002) in the 1980s and 1990s. Precipitation (Hickler *et al.*, 2005) and temperature (Lucht *et al.*, 2002) were found to be main climatic drivers of vegetation change. However, these studies

did not investigate whether the detected vegetation change can be at least partially attributed to anthropogenic climate change. Following the above approach (Harris *et al.*, 2020), two sets of climate data would be required, where one includes anthropogenic drivers of the climate and the other, the so-called counterfactual, does not. Under the Inter-Sectoral Impact Model Intercomparison Project 3a (ISIMIP) a counterfactual climate data set was developed. However in this counterfactual data set, anthropogenic climate forcing is not isolated from other drivers of climate change such as volcanic eruptions and solar luminosity (Mengel *et al.*, 2021). If a separation of other drivers is required for the desired investigation, a collaboration with climate scientists that develop data sets including counterfactual simulations for the specific case study and analyse anthropogenic climate change attribution, as was done with a focus on central Africa in Otto *et al.* (2013), may provide a solution. Analysis of the observed and the counterfactual climate data set can establish if detected trends in the climate system are outside of the natural variability of the system and attributable to climate change.

Then, simulations with DVMs driven by the observed climate and by the counterfactual data need to be implemented. Time series of satellite-based data such as NDVI can be used to detect if a change in vegetation occurred in the investigated ecosystem and to test if DVM simulations with the observed climate can accurately reproduce observed vegetation dynamics. To detect if vegetation changes larger than the natural variability of the ecosystem occurred, the counterfactual DVM simulations are compared with the DVM simulations with observed climate. If the observed change may not be explained by alternative drivers such as land use, climate change can be derived as a likely driver of change. Other drivers of vegetation change such as land use and their adequate representation in DVMs pose a challenge for this analysis. The investigation could focus on protected areas and other areas with low levels of land use impacts if it is centered around changes in natural vegetation.

In semi-arid regions, which together with dry sub-humid regions cover a third of Africa (Práválie, 2016), studies on attribution of climate change are challenging because the climate exhibits a naturally high variability especially for precipitation (Kew *et al.*, 2021) and ecosystems evolved

adapted to this variability. With an increasing length of observation periods over time, attribution analyses will yield more reliable information for semi-arid ecosystems. Generally, this approach of combining climate models with process-based ecological models, also called joint attribution (Rosenzweig *et al.*, 2008), can increase the understanding of the natural variability in ecosystem states. Especially in semi-arid ecosystems, this understanding is key for reliable future projections of potential impacts of climate change. In addition, this type of climate change attribution study would reveal if observed changes in vegetation are attributable to anthropogenic climate change. If anthropogenic climate forcing is already reflected in observed vegetation changes, this could be powerful information for the communication on climate change. It might help increasing awareness for future challenges that anthropogenic climate change will bring and for mitigating climate change.

### **5.2.3 Dynamic vegetation models and model coupling to support the planning of nature-based solutions**

Nature-based solutions as tools to address both climate change and biodiversity loss while at the same time contributing to sustainable development have gained increasing attention in research, governmental institutions and the private sector (Seddon *et al.*, 2021). They cover actions in ecosystem-based adaptation and mitigation and eco-disaster risk reduction, but also conservation and management actions to reduce greenhouse gas emissions from ecosystems and to store carbon (Seddon *et al.*, 2020). While nature-based solutions have great potentials, possible adverse impacts, especially of large scale approaches or of a simple focus on tree-planting, require caution and solutions need to be well planned and well-thought-out (Seddon *et al.*, 2021). For example, the controversial afforestation suggestions to mitigate climate change presented in Bastin *et al.* (2019) ensued heavy criticism, e.g., for their one-dimensional carbon sink perspective (e.g., Veldman *et al.*, 2019). The suggested afforestation in grassland and savanna regions (Bastin *et al.*, 2019) would result in biodiversity loss. In addition, afforestation-driven decreases in albedo in some regions would feed back on climate and increase climate change and thus counteract the desired climate change mitigation (Veldman *et al.*, 2019). This

underlines that nature-based solutions require a multi-dimensional, interdisciplinary approach and need to consider synergies and trade-offs associated with them (Seddon *et al.*, 2021).

Simulations with DVMs could support the planning process for nature-based solutions in terrestrial ecosystems to investigate their potential and to ensure robust and resilient responses to climate change and to prevent biodiversity loss (Gómez Martín *et al.*, 2021). Ensemble simulations with DVMs similar to the projections in Martens *et al.* (2021, Chapter 2) could be used to investigate the long-term stability of carbon stocks and ecosystems in nature-based solutions under climate change and potential uncertainties associated with nature-based solutions. Delivering benefits to biodiversity is a key component of nature-based solutions (Seddon *et al.*, 2021), because biodiversity supports the provision of ecosystem services and increases the resilience of ecosystems to disturbances (Cardinale *et al.*, 2012). The design of the aDGVM2 provides the unique opportunity to test potential consequences of changes in biodiversity for the stability of ecosystem biomass but also for the resilience towards changes in climate or atmospheric CO<sub>2</sub> concentrations (Langan, 2018; Scheiter *et al.*, 2013). At the same time, potential influences of climate change or different management options for nature-based solutions and their potential impacts on biodiversity can be investigated with the aDGVM2. Simulations with aDGVM2 can thus help to weigh different nature-based solutions for their potential impacts on biodiversity before their implementation.

The combination of vegetation, human population and land-use projections in Martens *et al.* (2022, Chapter 3) allowed the integration of multiple global change facets in the analysis of its impacts on protected areas, an important component of nature-based solutions. Yet in the integrated assessment models that produced the land use projections used in Martens *et al.* (2022), climate-change impacts on socioeconomic systems are currently not implemented (Riahi *et al.*, 2017). Incorporating feedback processes such as climate-change driven changes in land productivity and their impacts on socioeconomic systems in integrated assessment models would on the one hand lead to a more comprehensive representation of socioeconomic and climate

systems (Calvin *et al.*, 2019) and their impacts on protected areas and other nature-based solutions. On the other hand, this coupling adds additional layers of complexity and uncertainty to climate-impact modelling and requires more research and development (Calvin *et al.*, 2019).

The coupling and combination of DVMs with different models opens up more opportunities for investigating potential impacts and feedbacks of nature-based solutions. Future studies for protected areas could additionally use modelled estimates of global invasion threat by alien species (Early *et al.*, 2016) and, thus, include another main driver of change in nature (IPBES, 2019a) in the analysis. The Lund-Potsdam-Jena Dynamic Global Vegetation Model (LPJ) was coupled with a hydrogeological model to estimate the effects of warming on small watersheds in temperate forests (Beaulieu *et al.*, 2016; Kumar *et al.*, 2021b). Earth system models, where general circulation models that simulate climate are coupled with dynamic vegetation models, could shed light on potential feedback effects of nature-based solutions between atmosphere and biosphere (Schaubroeck, 2018). When land use modules such as grazing (e.g., Pfeiffer *et al.*, 2019) or fire management are integrated in DVMs, they can be used to test different land management practices and their potentials and risks for nature-based solutions. The coupling of DVMs with agent-based models could help to improve the representation of animal behaviour or to include processes of decision-making for human agents (Clemen *et al.*, 2021; Pfeiffer *et al.*, 2022). Some of the coupling steps, especially when multiple models are combined or larger ensembles of multiple models are desired, may require international collaborative efforts, similar to the call for global partnerships to achieve kilometer-scale climate simulations by Slingo *et al.* (2022).

As highlighted in Martens *et al.* (2022, Chapter 3) for the planning of protected areas under global change, it is essential that nature-based solutions ensure that local communities and Indigenous Peoples are fully involved in the planning and implementation and that their needs are met (Seddon *et al.*, 2021). In addition, the analyses of simulations under the medium to high emission scenarios RCP4.5 and RCP8.5 in Martens *et al.* (2021, Chapter 2) and the "middle-of-the-road" SSP2-RCP4.5 scenario and the "fossil-fueled development" SSP5-RCP8.5 scenario in Martens *et al.* (2022, Chapter 3) indicated that minimising climate change by cutting fossil fuel

emissions in combination with equitable, sustainable societal developments are key to keeping global change impacts on nature and society manageable. Nature-based solutions can only work in combination with climate action such as decarbonisation of economies and sustainable development where human rights especially of local communities are respected (Seddon *et al.*, 2021).

### 5.3 Conclusion

The investigations in this thesis have shown that climate change under medium to high emission scenarios will likely result in large scale ecosystem and carbon balance changes in Africa. The presented uncertainties in the representation of the CO<sub>2</sub> fertilisation effect, of semi-arid soil moisture dynamics, of carbon fluxes, and of vegetation types in more niche ecosystems such as the Nama Karoo highlight the importance of further field research and DVM development. For the medium emission scenario, uncertainties in the CO<sub>2</sub> fertilisation effect resulted in a smaller range of potential future ecosystem states compared to the high emission scenario. This entails that adaptation strategies and measures likely need to be less complex or extensive, when climate change is minimised. For African protected areas, climate change challenges may be exacerbated by socioeconomic factors to a regionally varying extent. This analysis pointed towards the importance of not only taking climate action but also ensuring equitable, sustainable development to facilitate successful ecosystem conservation. With this thesis, I hope that I was able to make a contribution towards providing scientific evidence on possible climate change impacts on ecosystems and conservation, the complex links with other global change factors, and research gaps in ecosystem representation in DVMs. Based on the plethora of research on climate and global change and their impacts on ecosystems, my hope is that we as a society will step-by-step learn from science and move towards a lifestyle that conserves biodiversity and will leave an earth that is liveable for future generations. For never was a story of more hope, than this of nature and its blue-green globe.\*

---

\* Adapted from the last sentence in Shakespeare (1597): "For never was a story of more woe / Than this of Juliet and her Romeo."



## Appendix A

# Supporting Information for “Large uncertainties in future biome changes in Africa call for flexible climate adaptation strategies”

Carola Martens, Thomas Hickler, Claire Davis-Reddy, Francois Engelbrecht, Steven I. Higgins,

Graham P. von Maltitz, Guy F. Midgley, Mirjam Pfeiffer and Simon Scheiter \*

---

\*This is the supporting information from Martens *et al.* (2021) Large uncertainties in future biome changes in Africa call for flexible climate adaptation strategies, *Global Change Biology*, 27: 340–358. <https://doi.org/10.1111/gcb.15390>

Uncertainty in African vegetation projections

**Large uncertainties in future biome changes in Africa call for  
flexible climate adaptation strategies**

**Supporting Information**

Carola Martens<sup>1,2</sup>, Thomas Hickler<sup>1,2</sup>, Claire Davis-Reddy<sup>3</sup>, Francois Engelbrecht<sup>4</sup>, Steven I. Higgins<sup>5</sup>, Graham P. von Maltitz<sup>6,7</sup>, Guy F. Midgley<sup>7</sup>, Mirjam Pfeiffer<sup>2</sup> and Simon Scheiter<sup>2</sup>

1 Institute of Physical Geography, Goethe University Frankfurt am Main, Altenhöferallee 1,  
60438 Frankfurt am Main, Germany

2 Senckenberg Biodiversity and Climate Research Centre (SBiK-F), Senckenbergenanlage 25,  
60325 Frankfurt am Main, Germany

3 uLwazi Node, South African Environmental Observation Network (SAEON), Cape Town,  
South Africa

4 Global Change Institute, University of the Witwatersrand, Johannesburg, South Africa

5 Plant Ecology, University of Bayreuth, Universitätstraße 30, 95447 Bayreuth, Germany

6 Council for Scientific and Industrial Research (CSIR), Pretoria, South Africa

7 Global Change Biology Group, Stellenbosch University, Stellenbosch 7600, South Africa

Author for correspondence. Email: martens.carola@yahoo.de

### Uncertainty in African vegetation projections

#### R code for $\omega^2$ metric:

The following R code was used to calculate the effect size of the explanatory variables. The R code was derived from <https://stats.stackexchange.com/questions/2962/omega-squared-for-measure-of-effect-in-r> (website accessed on June 03, 2020, 12:55).

```
omega_sq <- function(aov_in, neg2zero=T){  
  aovtab <- summary(aov_in)[[1]]  
  n_terms <- length(aovtab[["Sum Sq"]]) - 1  
  output <- rep(-1, n_terms)  
  SSr <- aovtab[["Sum Sq"]][n_terms + 1]  
  MSr <- aovtab[["Mean Sq"]][n_terms + 1]  
  SSt <- sum(aovtab[["Sum Sq"]])  
  for(i in 1:n_terms){  
    SSm <- aovtab[["Sum Sq"]][i]  
    DFm <- aovtab[["Df"]][i]  
    output[i] <- (SSm-DFm*MSr)/(SSt+MSr)  
    if(neg2zero & output[i] < 0){output[i] <- 0}  
  }  
  names(output) <- rownames(aovtab)[1:n_terms]  
  
  return(output)  
}
```

Uncertainty in African vegetation projections

### **Supplementary Figures and Tables**

Supplementary Table S1: General Circulation Models (GCMs) from the Coupled Model

Intercomparison Project Phase 5 (CMIP5) used in the ensemble experiment and the institutions and countries, where they were developed.

GCM abbreviation	Full name	Institute	Country of origin
ACCESS	Australian Community Climate and Earth System Simulator	Commonwealth Scientific and Industrial Research Organisation/ Bureau of Meteorology	Australia
CCSM4	Community Climate System Model 4	National Center for Atmospheric Research (NCAR)	USA
CNRM	CNRM Climate Model version 5 (CNRM-CM5)	Centre National de Recherches Météorologiques (CNRM)	France
GFDL	GFDL Climate Model version 3 (GFDL-CM3)	Geophysical Fluid Dynamics Laboratory (GFDL)	USA
MPI	MPI Earth System Model (MPI-ESM)	Max Planck Institute (MPI) for Meteorology	Germany
NorESM1M	Norwegian Earth System Model	Bjerknes Centre for Climate Research, Norway Norwegian Meteorological Institute (NCC)	

Uncertainty in African vegetation projections

Supplementary Table S2: Scheme for classifying vegetation into seven different biomes, based on Scheiter et al. (2012 & 2018). Dominant trees or grasses account for >50% of tree cover or grass biomass (peak leaf biomass), respectively. ‘-’ means that a variable was not used for the classification of a certain biome.

Biome	Tree cover	Dominant trees	Grass biomass	Dominant grasses
Desert	<10%	-	<1.5t/ha	-
C <sub>4</sub> grassland	<10%	-	>1.5t/ha	C <sub>4</sub>
C <sub>3</sub> grassland	<10%	-	>1.5t/ha	C <sub>3</sub>
C <sub>4</sub> savanna	10-80%	Savanna tree	-	C <sub>4</sub>
C <sub>3</sub> savanna	10-80%	Savanna tree	-	C <sub>3</sub>
Woodland	10-80%	Forest tree	-	-
Forest	>80%	-	-	-

### Uncertainty in African vegetation projections

Supplementary Table S3: Variability of carbon stored in continental-scale mean total aboveground biomass (in PgC) and variability of WUE (in gC / H<sub>2</sub>O) in 2080-2099. ‘GCM variability’ is 2×SD of the ensemble mean per scenario. ‘RCP variability’ is the difference between the ensemble means of each RCP scenario per CO<sub>2</sub> scenario. ‘CO<sub>2</sub> variability’ is the difference between eCO<sub>2</sub> and fCO<sub>2</sub> scenarios per RCP scenario. ‘x’ designates which scenarios or ensemble members were used to derive the respective variability. ‘–’ means that this category was not considered in the specific case. See Fig. 1 for the according time series.

CO <sub>2</sub> scenario	RCP scenario			GCM variability		RCP variability		CO <sub>2</sub> variability		
	eCO <sub>2</sub>	fCO <sub>2</sub>	4.5	8.5	AGB	WUE	AGB	WUE	AGB	WUE
x	x				9.7	0.048	-	-	-	-
x		x			11.2	0.085	-	-	-	-
	x	x			7.2	0.041	-	-	-	-
	x	x			7.2	0.044	-	-	-	-
x	x	x			-	-	11.2	0.327	-	-
	x	x	x		-	-	8.0	0.048	-	-
x	x	x			-	-	-	-	14.8	0.173
x	x		x		-	-	-	-	34.1	0.548

Uncertainty in African vegetation projections

Supplementary Table S4: Change in aboveground biomass (AGB) and WUE from 2000-2019 to 2080-2099 for the six GCMs in each RCP-CO<sub>2</sub> scenario.

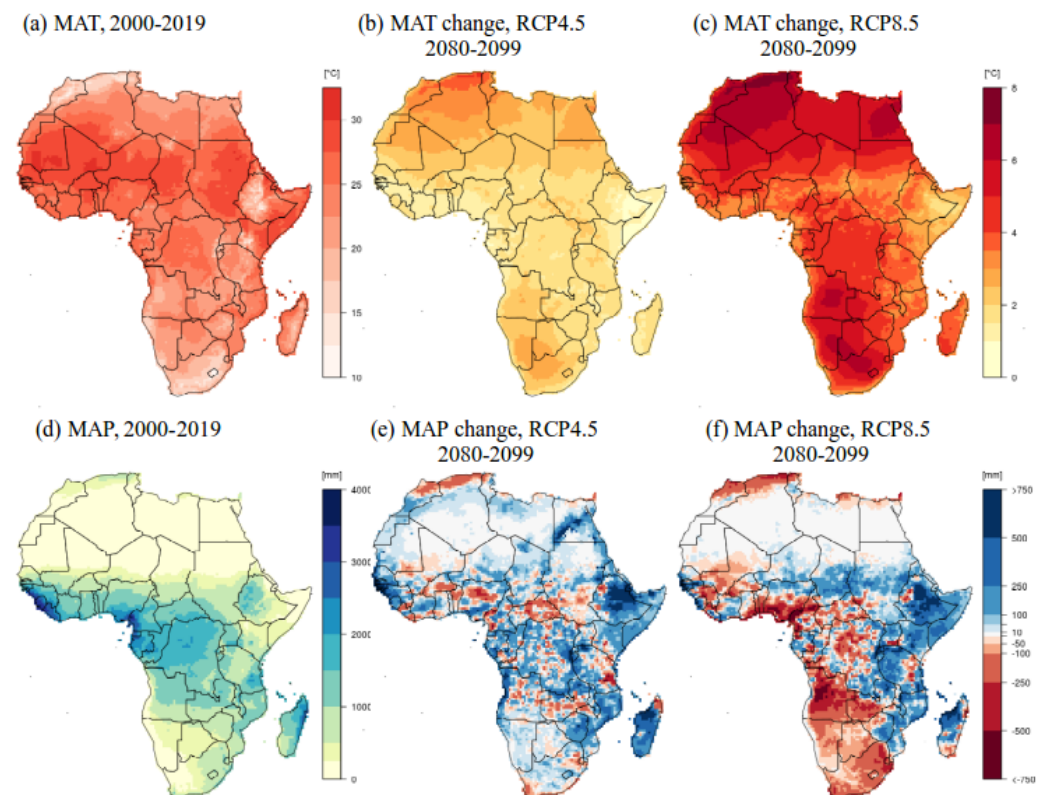
Scenario	GCM	AGB change	WUE change
RCP4.5, eCO <sub>2</sub>	ACCESS	31.0%	20.0%
	CCSM4	43.4%	20.2%
	CNRM	33.3%	22.7%
	GFDL	17.7%	15.3%
	MPI	28.7%	21.4%
	NorESM1M	35.7%	24.7%
RCP8.5, eCO <sub>2</sub>	ACCESS	59.6%	64.0%
	CCSM4	60.1%	72.2%
	CNRM	61.2%	73.0%
	GFDL	36.4%	61.3%
	MPI	48.4%	65.6%
	NorESM1M	55.2%	73.7%
RCP4.5, fCO <sub>2</sub>	ACCESS	3.6%	-4.7%
	CCSM4	11.2%	-4.1%
	CNRM	5.7%	-2.6%
	GFDL	-7.5%	-9.1%
	MPI	2.4%	-3.7%
	NorESM1M	7.5%	-0.9%
RCP8.5, fCO <sub>2</sub>	ACCESS	-6.1%	-12.5%
	CCSM4	-7.4%	-9.4%
	CNRM	-6.0%	-8.8%
	GFDL	-22.2%	-15.7%
	MPI	-13.4%	-12.5%
	NorESM1M	-9.8%	-9.0%

#### Uncertainty in African vegetation projections

Supplementary Table S5: ANOVA for change in carbon in aboveground biomass (AGB) and water use efficiency (WUE) between 2000-2019 and 2080-2099. The table presents F-values from ANOVA for the dependent variables “aboveground biomass change” and “water use efficiency”, and independent variables “CO<sub>2</sub> scenario”, “RCP scenario” and “GCM” that were used for the omega-squared metric. Two-way interaction effects are included in the model and are denoted with ‘:’.

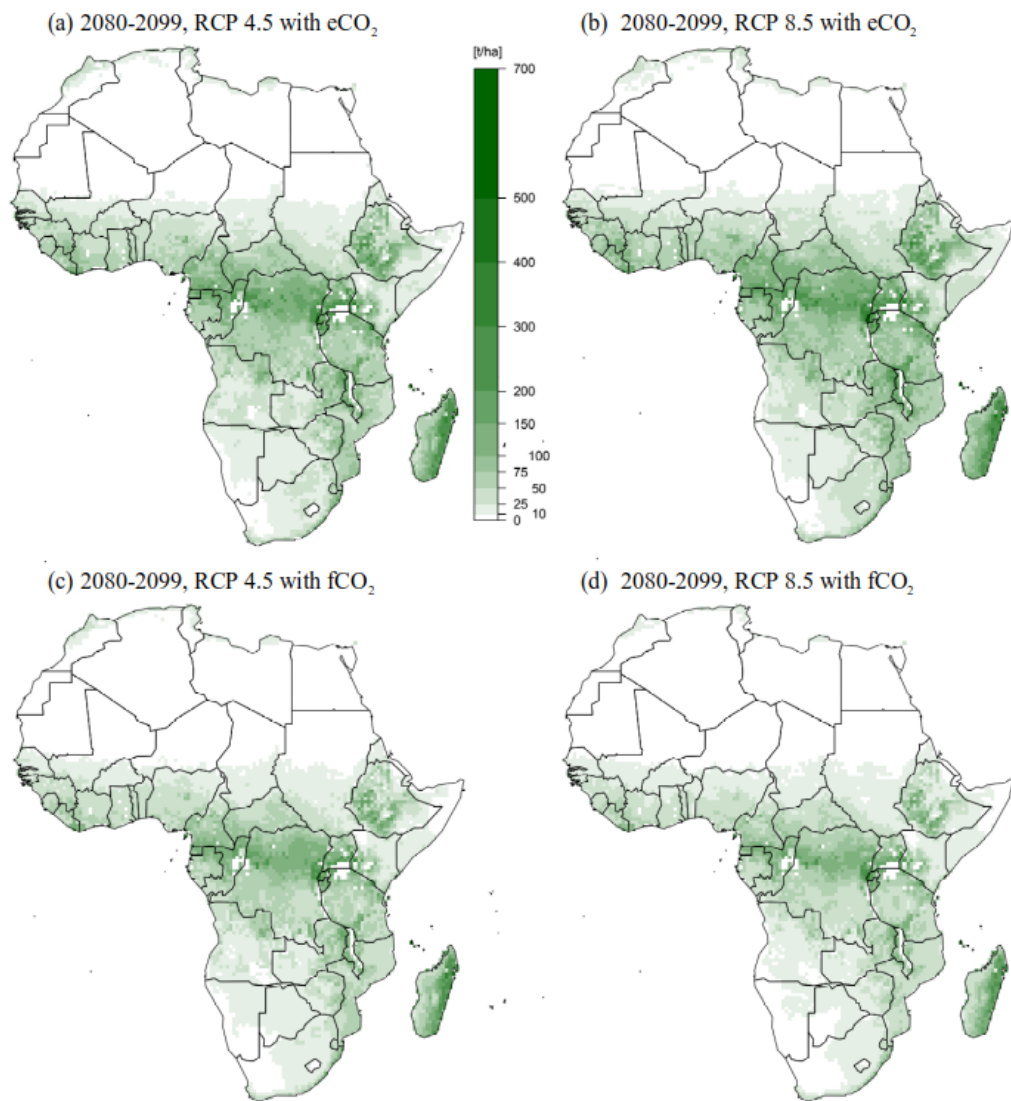
Independent variables & interaction effects	F-value	
	AGB	WUE
CO <sub>2</sub>	8330	7992
RCP	50	1210
GCM	146	23
CO <sub>2</sub> :RCP	1293	2198
CO <sub>2</sub> :GCM	12	3
RCP:GCM	6	2

Uncertainty in African vegetation projections



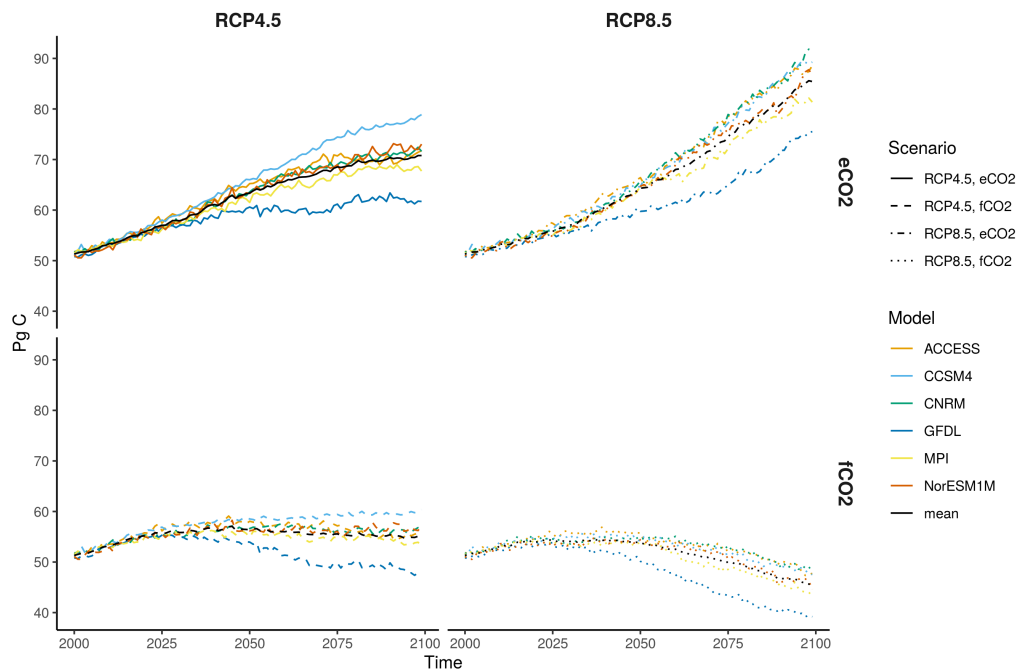
Supplementary Figure S1: Mean annual temperature (MAT) and precipitation (MAP) in 2000-2019 and change by 2080-2099. MAT in 2000-2019 (a) is the mean across all six GCMs under RCP4.5. Change in MAT for RCP4.5 (b) and RCP8.5 (c) is the difference between the periods 2080-2099 and 2000-2019 in °C. MAP in 2000-2019 (d) is the mean across all six GCMs under RCP4.5. Change in MAP for RCP4.5 (e) and RCP8.5 (f) is the difference between the periods 2080-2099 and 2000-2019 in mm.

Uncertainty in African vegetation projections



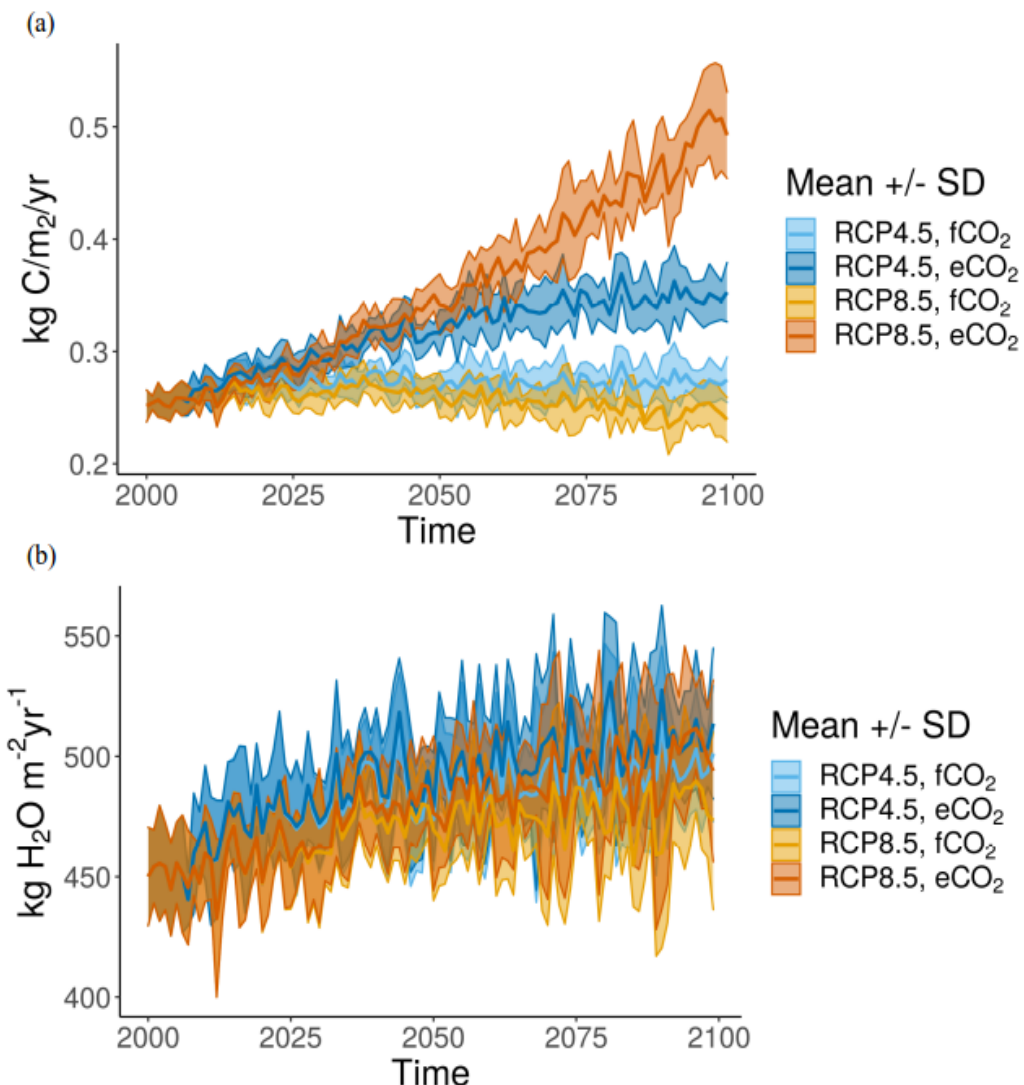
Supplementary Figure S2: Simulated aboveground biomass in t/ha for 2080-2099. The maps show the ensemble mean in 2080-2099 across all six ensemble members under eCO<sub>2</sub> (a, b) and fCO<sub>2</sub> (c, d) with RCP4.5 (a, c) and RCP8.5 (b, d).

Uncertainty in African vegetation projections



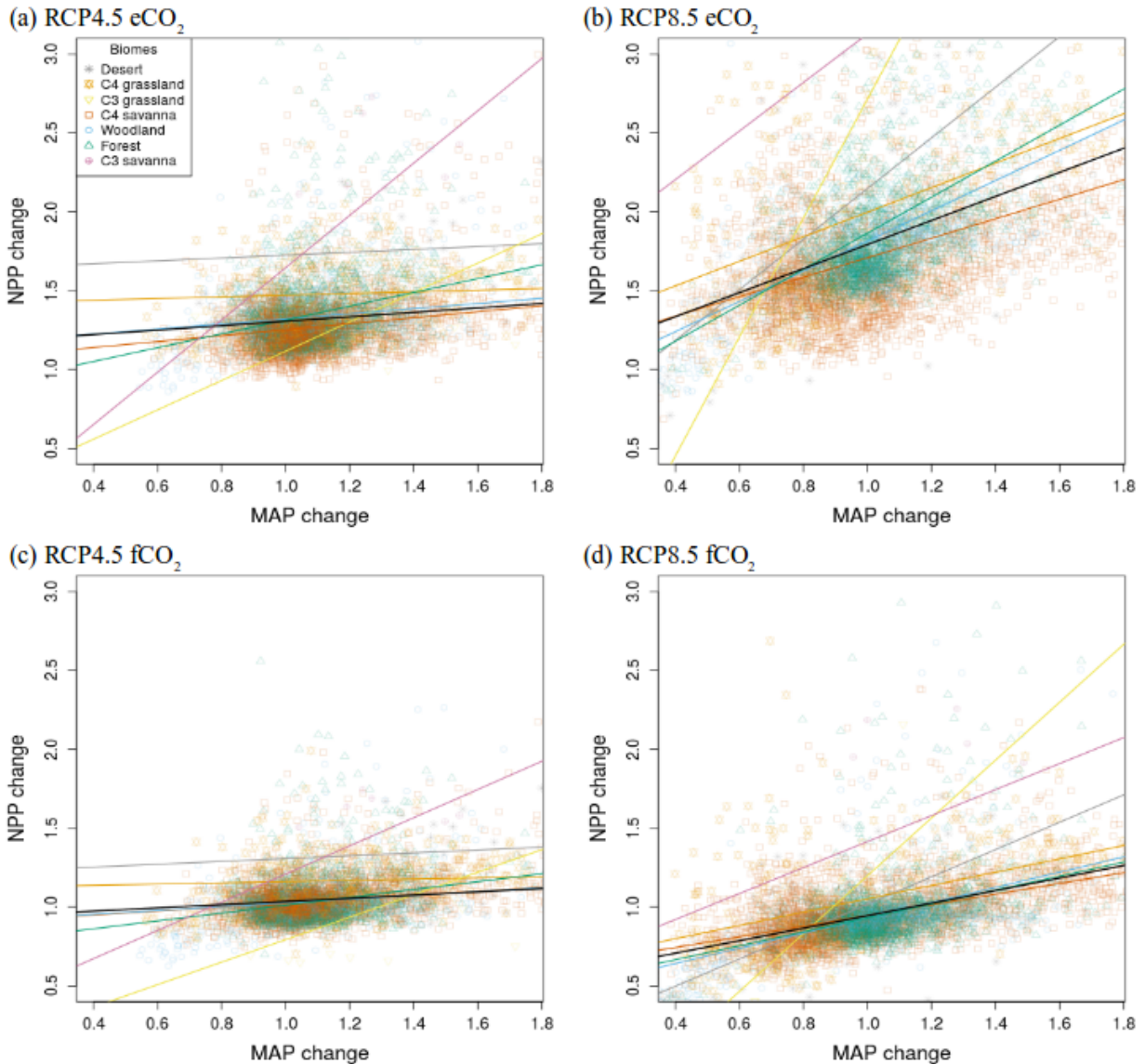
Supplementary Figure S3: Total aboveground carbon in Africa between 2000 and 2099 simulated by all six ensemble members and their mean (black lines) under RCP4.5 and RCP8.5 with eCO<sub>2</sub> and fCO<sub>2</sub>.

Uncertainty in African vegetation projections



Supplementary Figure S4: Mean NPP (a) and mean total transpiration (b) from vegetation in Africa between 2000 and 2099 across all six ensemble members under RCP4.5 and RCP8.5 with eCO<sub>2</sub> and fCO<sub>2</sub>. Shaded areas are the mean +/- standard deviation of the six ensemble members per scenario. NPP and transpiration are used to calculate water use efficiency (WUE).

Uncertainty in African vegetation projections

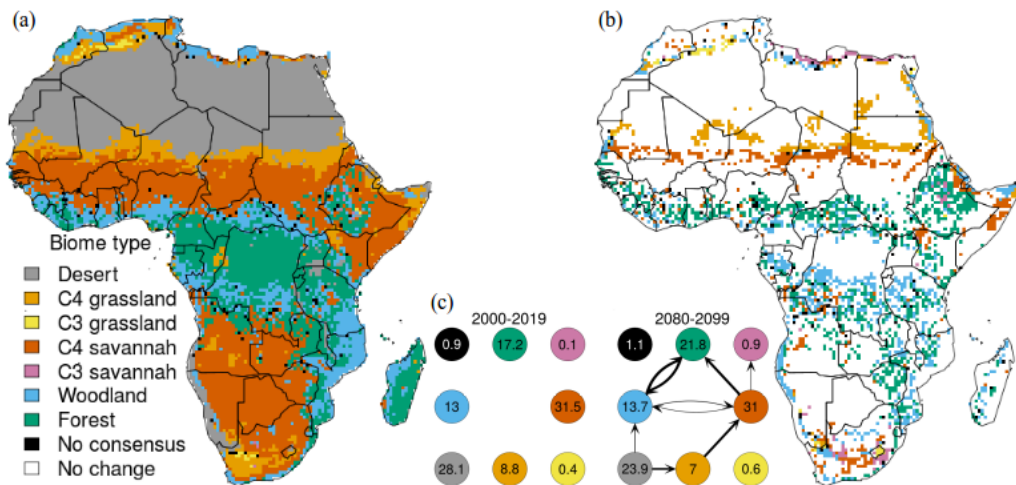


Supplementary Figure S5: MAP change versus NPP change per grid cell between 2000-2019 and 2080-2099 for eCO<sub>2</sub> (a,b) and fCO<sub>2</sub> (c,d) under RCP4.5 (a,c) and RCP8.5 (b,d). Change is the ratio between 2000-2019 and 2080-2099. Black lines are regression lines for all data points of a scenario. Coloured lines are regression lines for the respective biomes per

Uncertainty in African vegetation projections

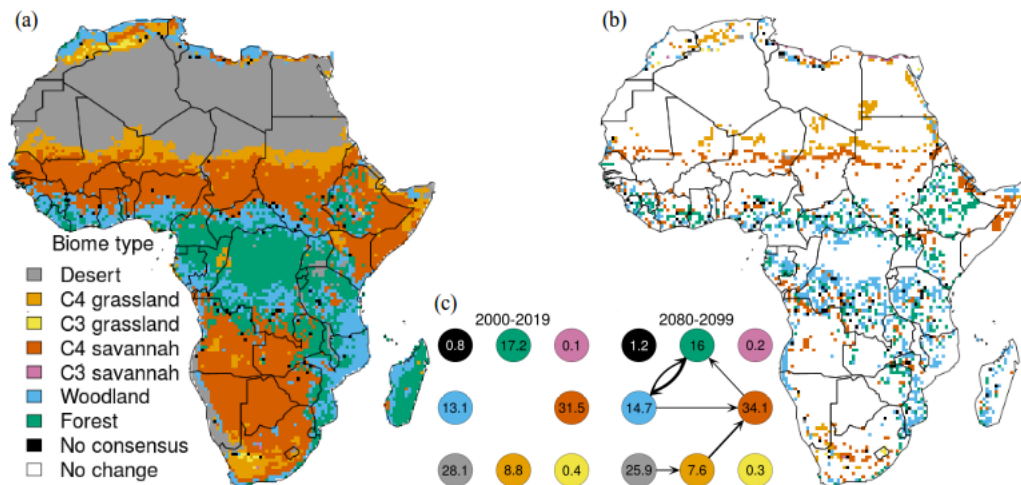
scenario. Points have the colour and shape of the biome in 2000-2019. See Fig. 4 for overall regression lines of MAP-NPP change of all four scenarios in one figure.

Uncertainty in African vegetation projections



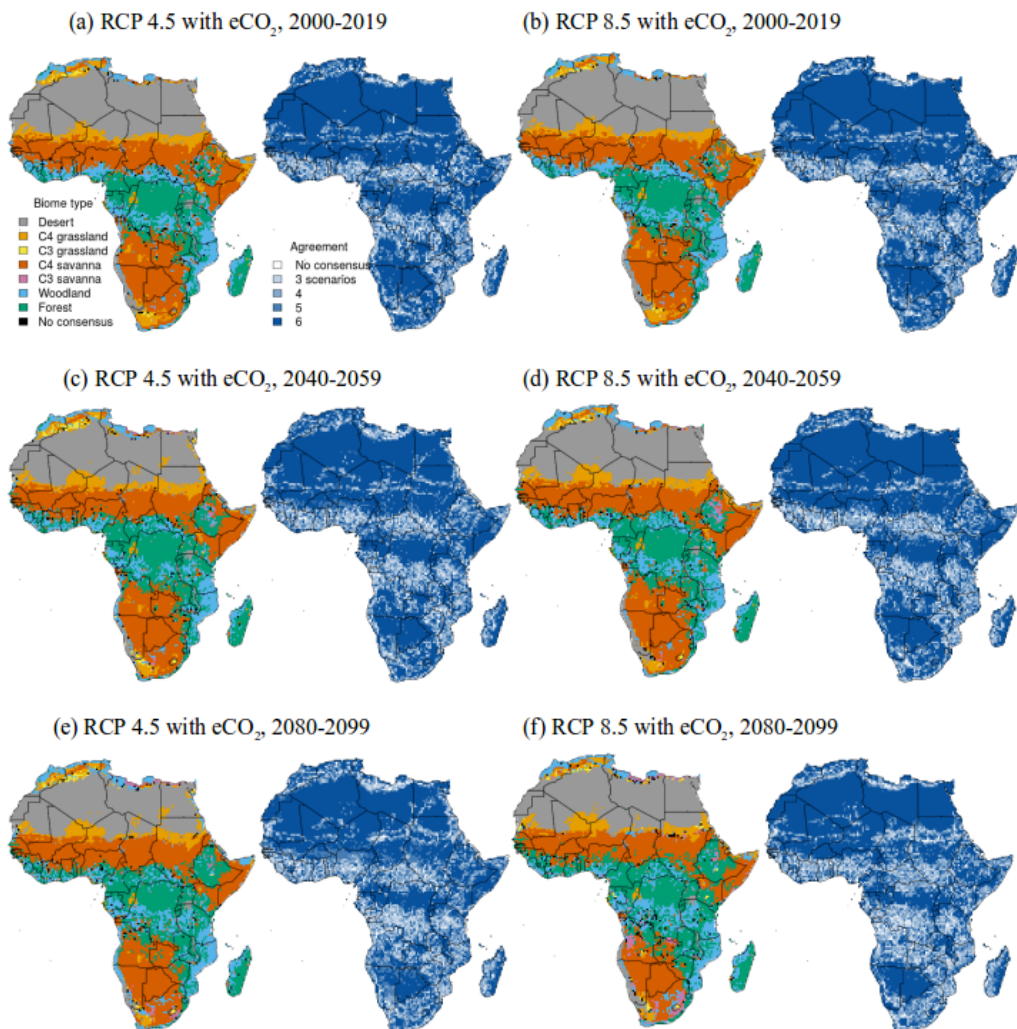
Supplementary Figure S6: Consensus biome type under eCO<sub>2</sub> RCP4.5 in 2000-2019 (a), biome changes in 2080-2099 (b) and transitions and fractional cover of biomes (c). The consensus biome type is the biome simulated by most ensemble members of the scenario. Grid cells with an agreement of less than three ensemble members do not have a higher probability than an outcome by chance and are marked as ‘No consensus’. The biomes shown in (b) are the biomes that were simulated for 2080-2099, shown only for grid cells where biome transitions were simulated for the consensus biome. Numbers in each coloured circle (c) represent the percentage of area covered by each biome at the respective time step in the consensus map. Arrows show biome changes with regard to the previous time step. Thicker arrows indicate that a higher proportion of the total area changed. In panel (c), only changes that affect more than 0.5% of the African land surface are shown. See Fig. 5 for RCP8.5.

### Uncertainty in African vegetation projections



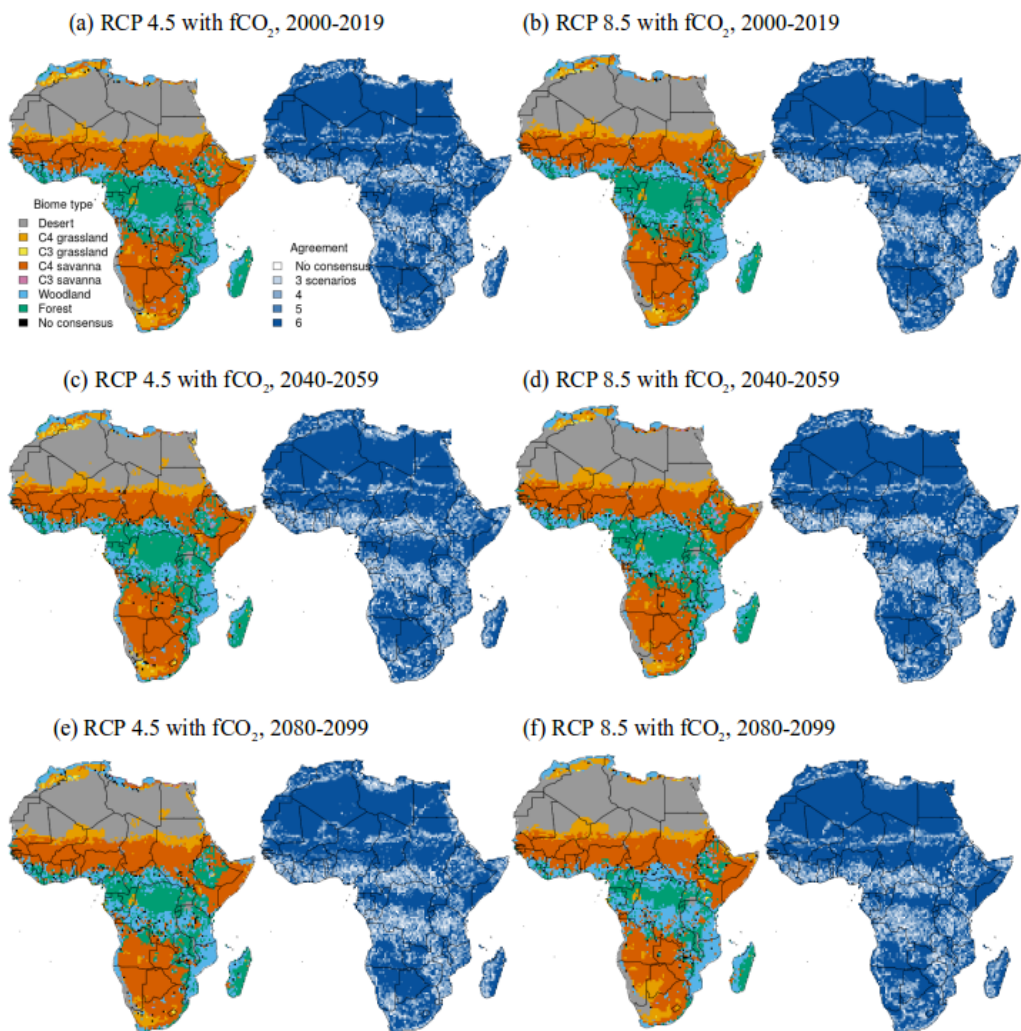
Supplementary Figure S7: Consensus biome type under fCO<sub>2</sub> RCP4.5 in 2000-2019 (a), biome changes in 2080-2099 (b) and transitions and fractional cover of biomes (c). The consensus biome type is the biome simulated by most ensemble members of the scenario. Grid cells with an agreement of less than three ensemble members do not have a higher probability than an outcome by chance and are marked as 'No consensus'. The biomes shown in (b) are the biomes that were simulated for 2080-2099, shown only for grid cells where biome transitions were simulated for the consensus biome. Numbers in each coloured circle (c) represent the percentage of area covered by each biome at the respective time step in the consensus map. Arrows show biome changes with regard to the previous time step. Thicker arrows indicate that a higher proportion of the total area changed. In panel (c), only changes that affected more than 0.5% of the African land surface are shown. See Fig. 6 for RCP8.5.

Uncertainty in African vegetation projections



Supplementary Figure S8: Consensus biome type and number of scenarios simulating the consensus type for  $e\text{CO}_2$  simulations under RCP4.5 (left, a, c, e) and RCP8.5 (right, b, d, f). The consensus biome type is the biome simulated by the majority of ensemble members. The number of ensemble members simulating the consensus type is denoted as ‘Agreement’. Grid cells with less than three agreeing ensemble members are marked as ‘No consensus’.

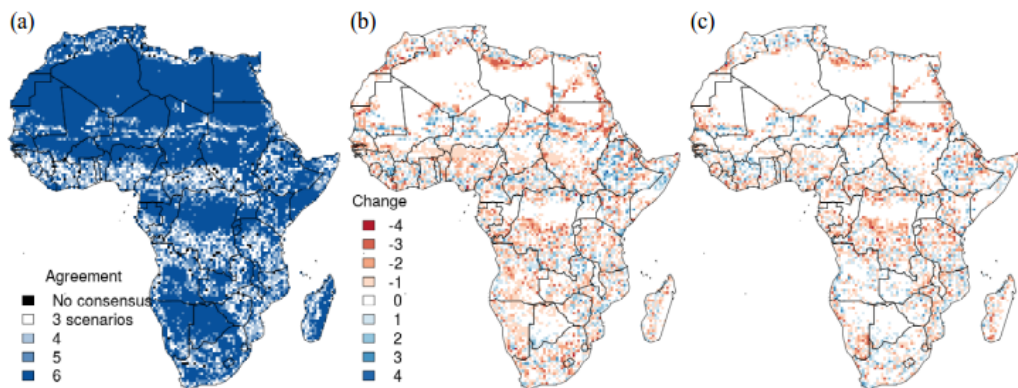
Uncertainty in African vegetation projections



Supplementary Figure S9: Consensus biome type and number of scenarios simulating the consensus type for fCO<sub>2</sub> simulations under RCP4.5 (left, a, c, e) and RCP8.5 (right, b, d, f).

The consensus biome type is the biome simulated by the majority of ensemble members. The number of ensemble members simulating the consensus type is denoted as 'Agreement'. Grid cells with an agreement of less than three ensemble members are marked as 'No consensus'.

Uncertainty in African vegetation projections



Supplementary Figure S10: Simulation agreement in 2000-2019, under eCO<sub>2</sub> (a) and change in agreement in 2080-2099 under eCO<sub>2</sub> (b) and fCO<sub>2</sub> (c) for RCP4.5. The number of ensemble members simulating the consensus type is denoted as ‘Agreement’. Grid cells with an agreement of less than three ensemble members are marked as ‘No consensus’. We only displayed the number of ensemble members simulating the consensus type in 2000-2019 for eCO<sub>2</sub>, because agreement is almost identical for eCO<sub>2</sub> and fCO<sub>2</sub> (see Fig. S8a and S9a). The consensus biome type is the biome simulated by the majority of ensemble members of the scenarios. See Fig. 8 for RCP8.5.

Uncertainty in African vegetation projections

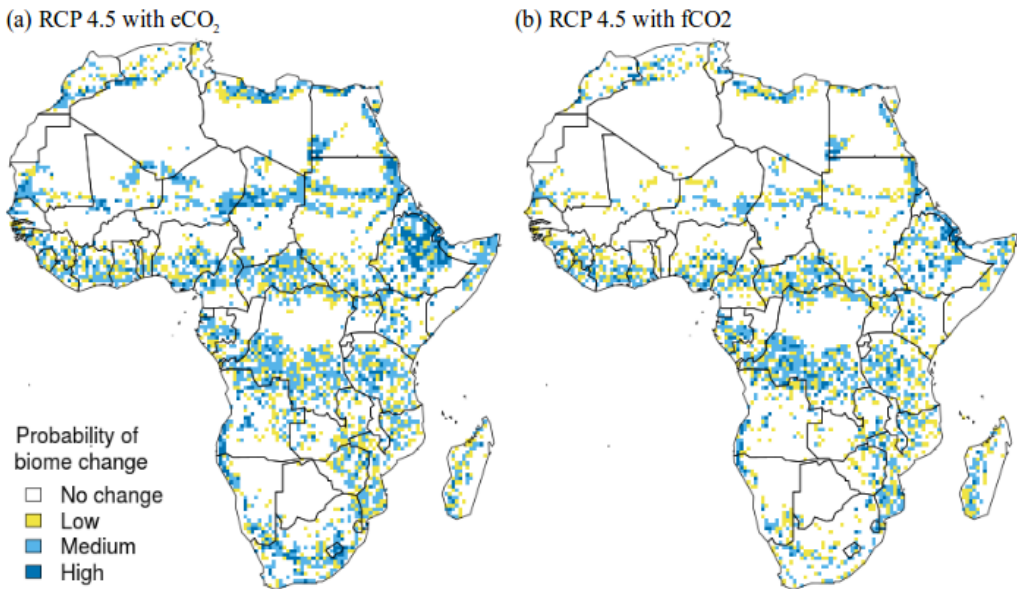


Figure S11: Probability of biome change between 2000-2019 and 2080-2099. The number of the six GCM ensemble members per scenario (here RCP4.5, eCO<sub>2</sub> and fCO<sub>2</sub>) that showed a biome change from 2000-2019 to 2080-2099 was used as a measure of probability of biome change. The more ensemble members projected a biome change per grid cell, the higher its probability of biome change. High probability of biome change – all 6 simulations project biome changes; medium probability of biome change – 4-5 simulations with biome changes; low probability of biome change – 3 simulations with biome changes; no change – 0-2 simulations with changes. Grid cells with 2 or fewer simulations with biome changes do not have a higher probability than an outcome by chance and were therefore regarded as 'no change'. Whether the ensemble members simulated the same type of biome transition was not considered here. See Fig. 9 for RCP8.5.

## Appendix B

# Supporting Information for “Combined impacts of future climate-driven vegetation changes and socioeconomic pressures on protected areas in Africa”

*Carola Martens, Simon Scheiter, Guy F. Midgley, and Thomas Hickler<sup>\*†</sup>*

---

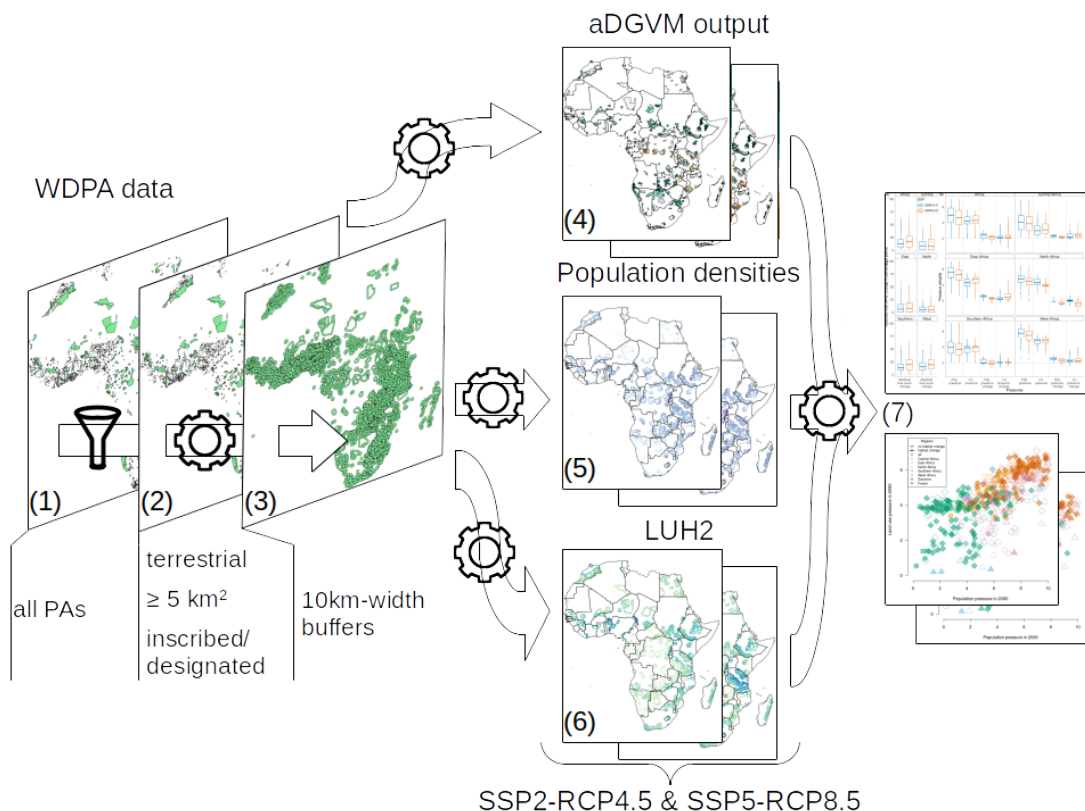
<sup>\*</sup>This is the supporting information to Martens *et al.* (2022) Combined impacts of future climate-driven vegetation changes and socioeconomic pressures on protected areas in Africa, *Conservation Biology*, 36, e13968. <https://doi.org/10.1111/cobi.13968>.

<sup>†</sup>The table in Appendix S2 can be found online:  
<https://conbio.onlinelibrary.wiley.com/action/downloadSupplement?doi=10.1111%2Fcobi.13968&file=cobi13968-sup-0002-SupMat.pdf>

**Combined impacts of future climate-driven vegetation changes and socio-economic pressures on protected areas in Africa**

**Conservation Biology**

**Supporting Information**



**Appendix S1** Overview of data used to analyse global change pressure on African protected areas (PAs).

African PAs from the WDPA data base (1) were filtered to only include terrestrial PAs that are equal to or bigger than  $5 \text{ km}^2$  and are officially “inscribed” or “designated” (2). For this PA selection, buffers of 10-km-width were created (3). For each PA, aDGVM simulated tree cover and biomass within their perimeters were derived (4). Using population densities from (Gao, 2019) and land use types from LUH2 data (Hurtt et al., 2020), population pressure (5) and land-use pressure (6) in the perimeters of PAs were derived. These human pressures in the buffer areas were used as proxies for future human pressures exerted on PAs. For (4)-(6) data for two RCP-SSP scenarios, i.e. SSP2-RCP4.5 and SSP5-RCP8.5, were used to investigate differences between two future scenarios. These data for PAs were then used to analyse in which continental regions global change pressures were high and where individual pressures co-occurred (7). aDGVM - adaptive Dynamic Global Vegetation Model; LUH2 - Land-Use Harmonization; RCP - representative concentration pathway; SSP - shared socio-economic pathway; WDPA - world database on protected areas (UNEP-WCMC & IUCN, 2019).

**Appendix S2** List of protected areas used in this analysis. Geographical location and administrative boundaries of protected areas in Africa used in this study were derived from the World Database on Protected Areas (WDPA; UNEP-WCMC & IUCN, 2019). Terrestrial protected areas in Africa of a size bigger than 5 km<sup>2</sup> were selected for the analysis. Protected areas without spatial polygon data available were excluded from this study as well as protected areas whose designation status is 'proposed' or 'not reported'. Transfrontier PAs in our analysis and their buffers did not lie in multiple regions. The table can be found in a separate file.

**Appendix S3** Weighting scheme for land-use pressure factors based on LUH2<sup>a</sup> land use types and age classes.

Aggregated land use types	Age <sup>b</sup>	Pressure <sup>c</sup>	LUH2 land use types
Primary vegetation		0	forested primary land & non-forested primary land
Secondary vegetation			
mature	>100 years	1	potentially forested primary land &
intermediate	30-100 years	2	potentially non-forested primary land
young	<30 years	3	
Pastures		4	managed pasture & rangeland
Cropland		7	C <sub>3</sub> annual crops, C <sub>3</sub> perennial crops, C <sub>4</sub> annual crops, C <sub>4</sub> perennial crops & C <sub>3</sub> nitrogen-fixing crops
Urban		10	urban

<sup>a</sup>Land-Use Harmonization (LUH2) data (Hurt et al., 2020)

<sup>b</sup>Based on Newbold et al. (2015). Age is only used to classify secondary vegetation in subgroups.

<sup>c</sup>Based on Venter et al. (2016). For each grid cell the fraction covered by each aggregated land use type was multiplied with the assigned pressure and then summed over all aggregated land use types.

The maximum land-use pressure in a grid cell is ten (100% urban area).

**Appendix S4** Classification scheme for grouping vegetation into four different biomes (simplified from Martens et al., 2021).

Biome	Tree cover	Total aboveground biomass
Desert	-*	<1.5t/ha
Grassland	<10%	>1.5t/ha
Savanna	10-70%	>1.5t/ha
Forest	>70%	>1.5t/ha

\*Variable was not used for classification of deserts.

**Appendix S5** Classification scheme for habitat loss for the four biomes.

Biome	aDGVM <sup>a</sup> variable	Level of change <sup>b</sup>
Desert	aboveground biomass	>0.5t/ha
Grassland	tree cover <sup>c</sup>	>5p.p.
Savanna	tree cover <sup>c</sup>	>10p.p or <-10p.p. <sup>d</sup>
Forest	tree cover <sup>c</sup>	<-20% <sup>d</sup>

---

<sup>a</sup> adaptive Dynamic Global Vegetation Model

<sup>b</sup>Habitat loss for each biome is determined by change between 2000-2019 and 2080-2099 of the given aDGVM output variable.

<sup>c</sup>Level of change is based on percentage points for tree cover.

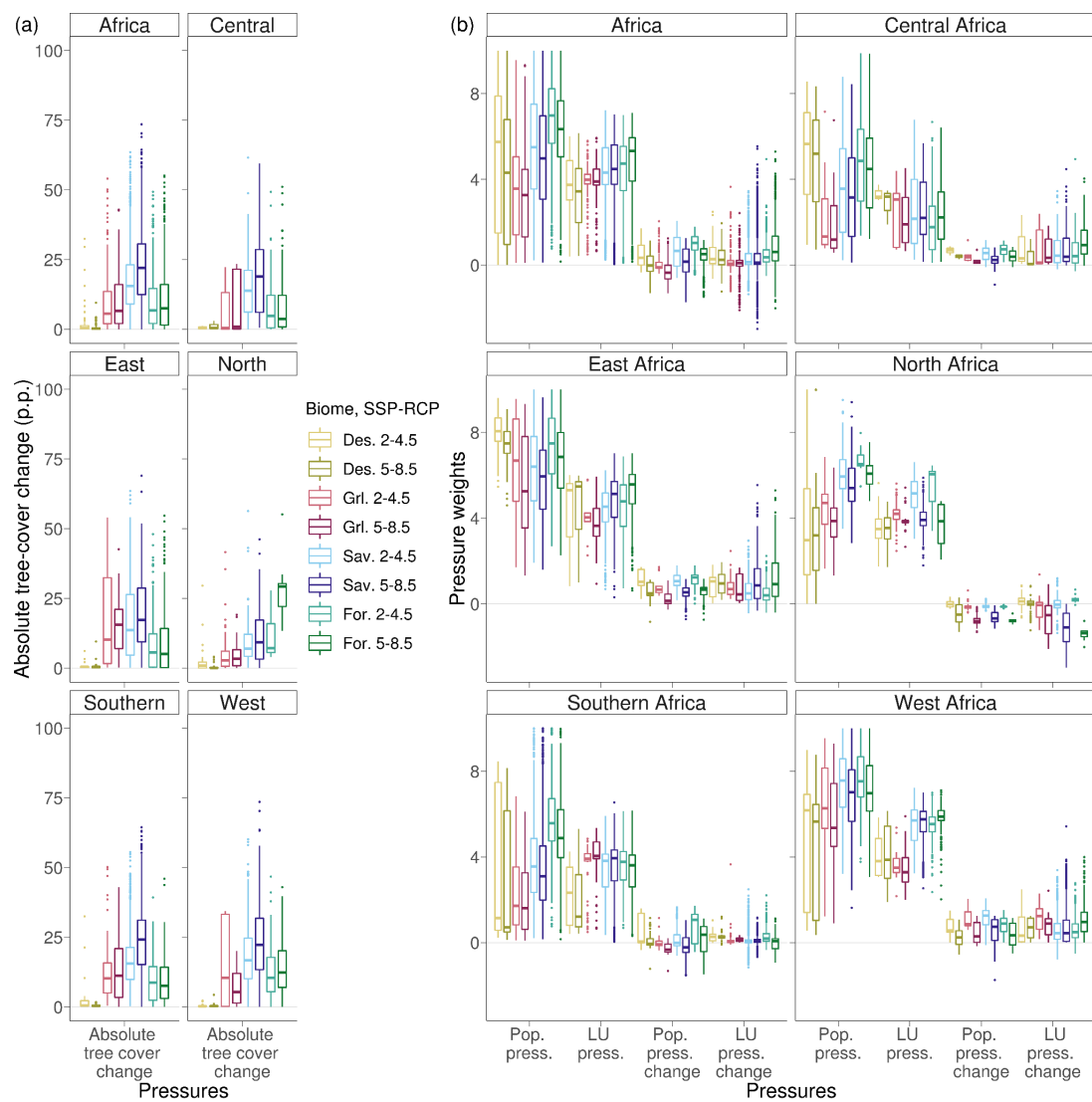
<sup>d</sup>Habitat loss is defined following (Aleman et al., 2016); p.p., percentage points.

**Appendix S6** Regions used for grouping protected areas based on regions of the African Union

(Council of Ministers, Organization of African Unity, 1976)

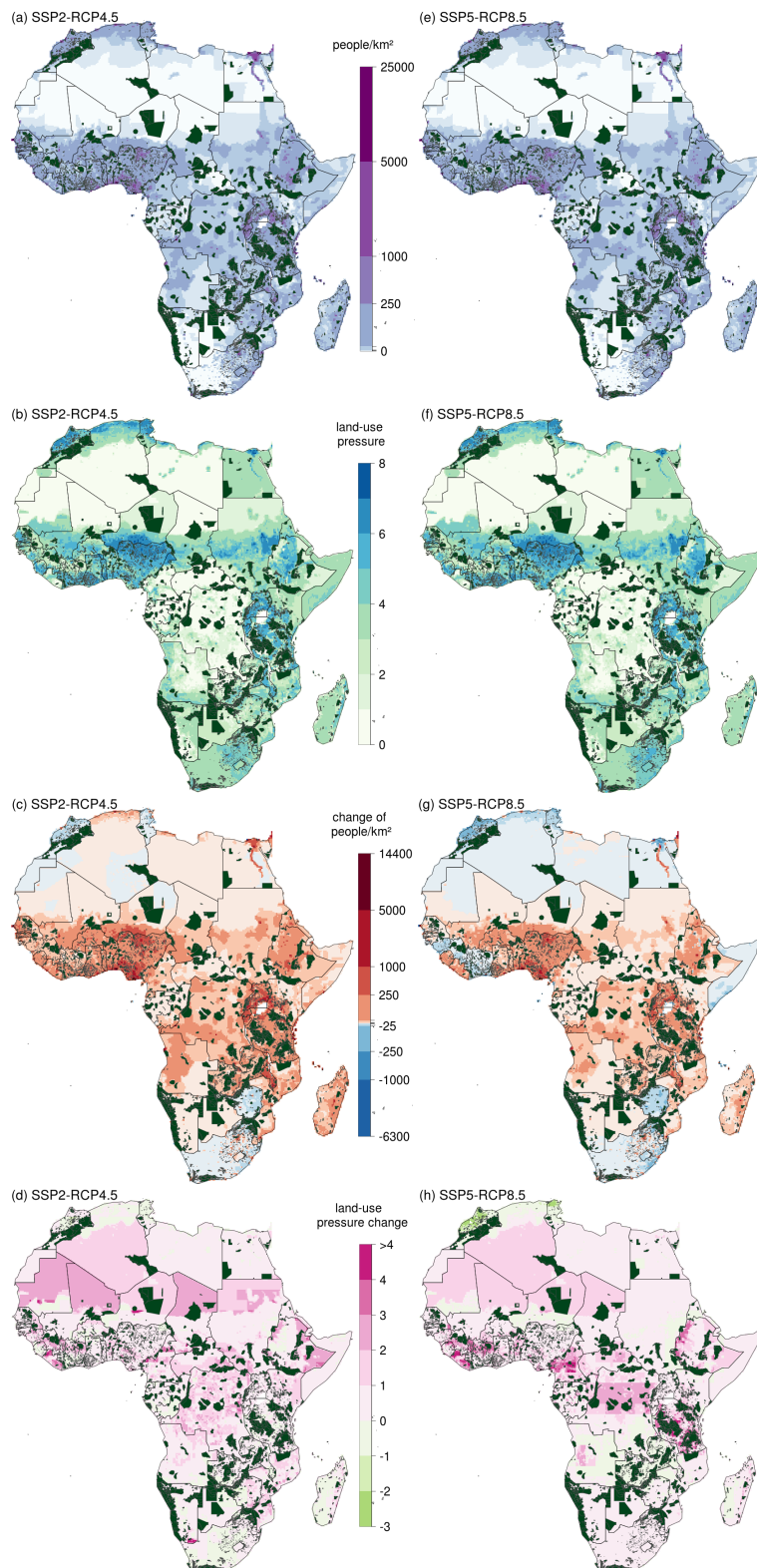
Region	Countries
Central Africa	Burundi, Cameroon, Central African Republic, Chad, Congo Republic, DR Congo, Equatorial Guinea, Gabon, São Tomé and Príncipe
East Africa	Comoros, Djibouti, Eritrea, Ethiopia, Kenya, Madagascar, Mauritius, Rwanda, Seychelles, Somalia, South Sudan, Sudan, Tanzania, Uganda
North Africa	Algeria, Egypt, Libya, Mauritania, Morocco, Sahrawi Republic, Tunisia
Southern Africa	Angola, Botswana, Eswatini, Lesotho, Malawi, Mozambique, Namibia, South Africa, Zambia, Zimbabwe
West Africa	Benin, Burkina Faso, Cabo Verde, Côte d'Ivoire, Gambia, Ghana, Guinea, Guinea-Bissau, Liberia, Mali, Niger, Nigeria, Senegal, Sierra Leone, Togo

---



**Appendix S7** (a) Climate-driven change in tree cover in protected areas (derived from adaptive dynamic global vegetation model (aDGVM) based on results from Martens et al., [2021]) and (b) socio-economic pressures in 10-km zones around protected areas by biome and region under SSP2-RCP4.5 (SSP, shared socioeconomic pathways; RCP, representative concentration pathways) and SSP5-RCP8.5 scenarios (defined in Table 1 and text) (p.p., percentage points; pop., population; press., pressure; LU, land use; horizontal lines, median; box ends, 25% and 75% quantile; ends of whisker lines, smallest or largest value respectively  $\geq$  or  $\leq$  1.5 times the interquartile range beyond the box ends of protected areas in each group; Des. - desert; Grl. - grassland; For - forest; Sav. - savanna). Regions are based on regions defined by the African Union (Appendix S6). Absolute values for

tree-cover change from 2000-2019 to 2080-2099 are used because both negative and positive tree-cover changes represent climate-driven vegetation changes. The socio-economic pressures population (based on Gao [2017]) and land use (based on Hurt et al. [2020]) in 10-km zones around the protected areas were rescaled from 0 to 10 (Appendix S3, Eq. 1) based on Venter et al.'s (2016) scheme. Each protected area's biome is derived from mean state variables simulated by aDGVM.



**Appendix S8** (a, e) Population density, and (b, f) land-use pressure in 2020 and their change until 2090

([c, g] population density change; [d, h] land use change) in Africa and protected areas under SSP-RCP

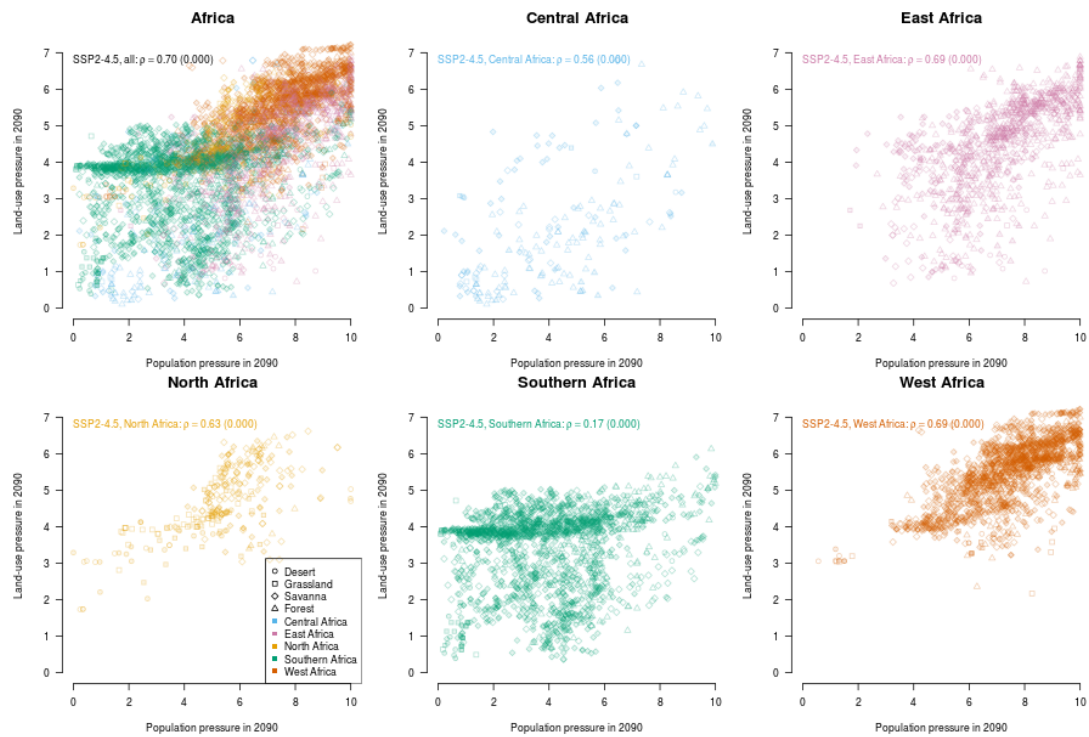
scenarios (c, d, left) SSP2-RCP4.5 and (g, h, right) SSP5-RCP8.5 (RCP, representative concentration

pathways; SSP, shared socioeconomic pathways). Population projections were derived from Gao

(2017). Land use (based on Hurt et al., 2020) pressure is weighted based on an adapted scheme from

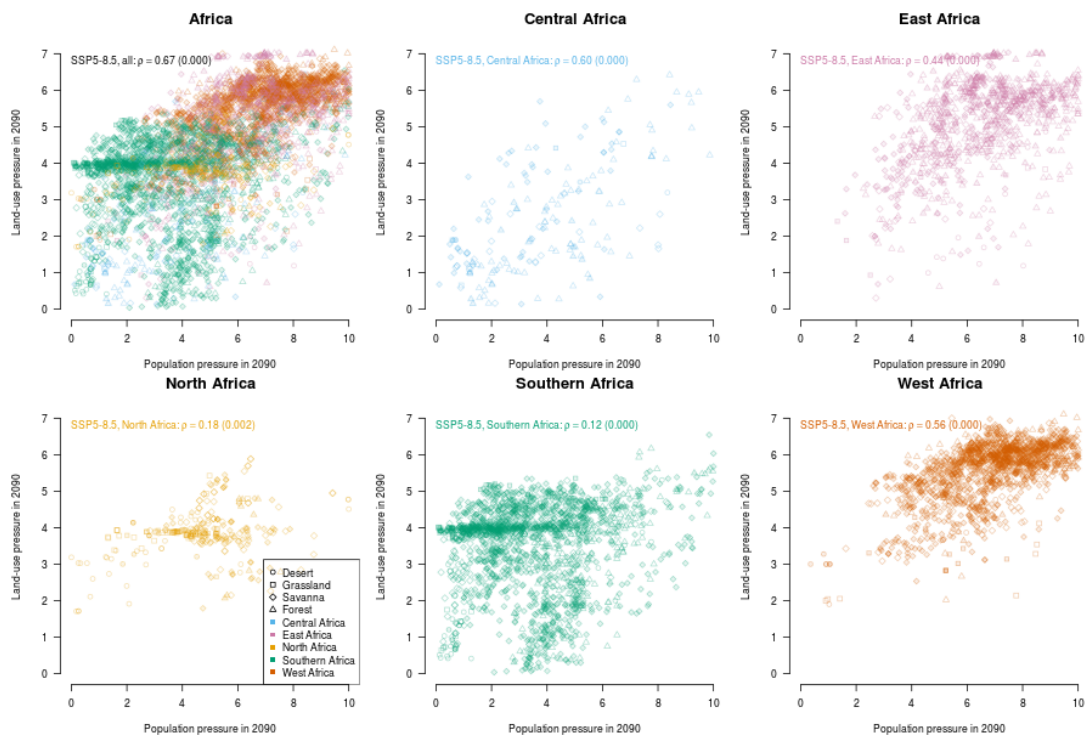
Venter et al. (2016) where higher numbers represent higher land-use pressure (see Appendix S3).

Protected areas used in this study are mapped on top for each panel.

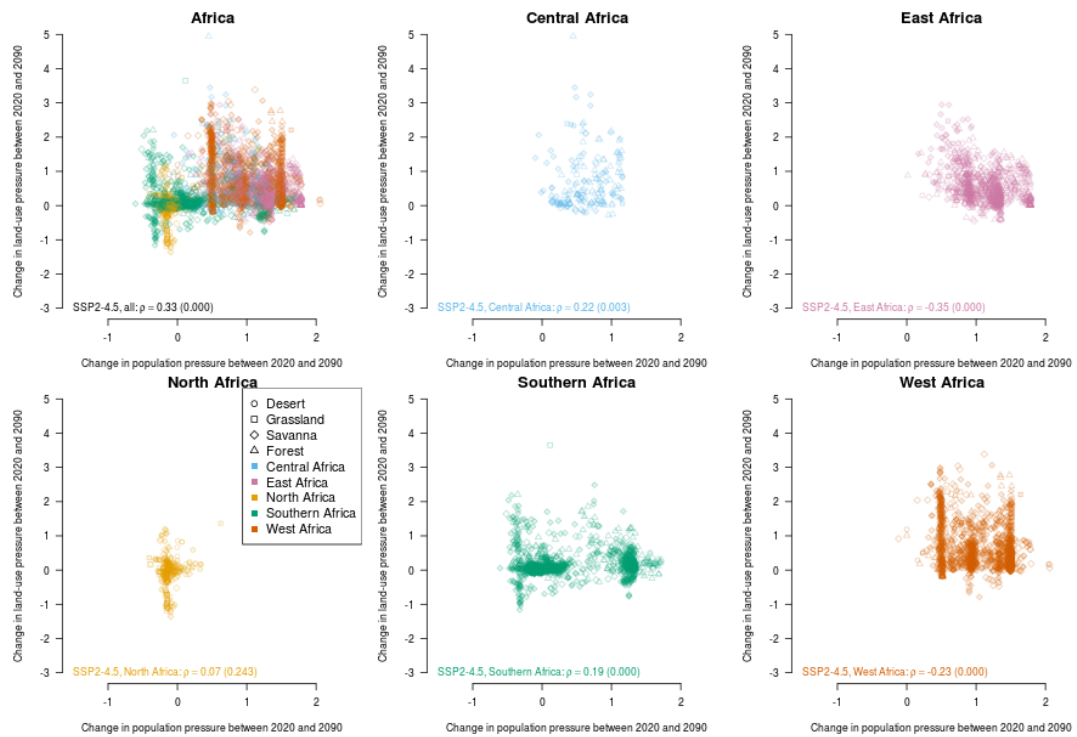


**Appendix S9** Population and land-use pressure in 10-km-buffers around protected areas for SSP2-RCP4.5 grouped by region and biome with habitat loss. Each protected area is represented by a point. Colours represent the regions that the protected areas are in (Appendix S6). The shape of a point represents the mean biome in the protected area as classified using the scheme in Appendix S4. Filled points represent protected areas projected to show habitat loss following the classification in Appendix S5. Land use (based on Hurtt et al., 2020) and population (based on Gao, 2017) pressures were weighted based on an adapted scheme from Venter et al. (2016). The shown legend applies to all

panels of the figure.

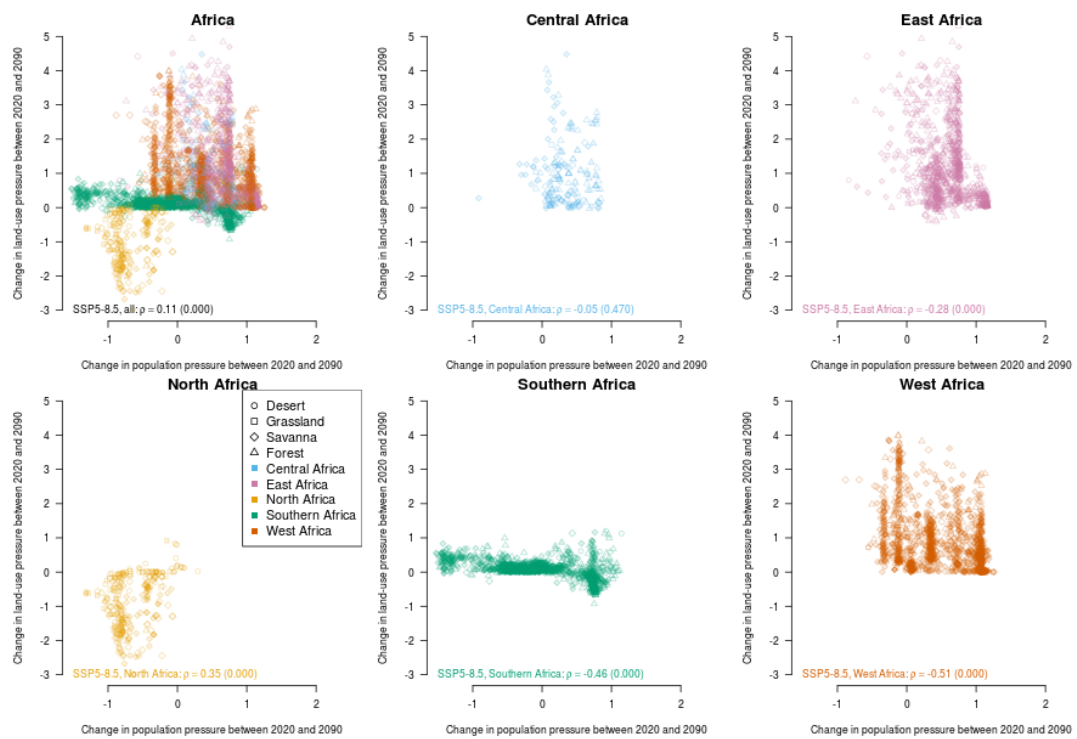


**Appendix S10** Population and land-use pressure in 10-km-buffers around protected areas for SSP5-RCP8.5 grouped by region and biome with habitat loss. Each protected area is represented by a point. Colours represent the regions that the protected areas are in (Appendix S6). The shape of a point represents the mean biome in the protected area as classified using the scheme in Appendix S4. Filled points represent protected areas projected to show habitat loss following the classification in Appendix S5. Land use (based on Hurt et al., 2020) and population (based on Gao, 2017) pressures were weighted based on an adapted scheme from Venter et al. (2016). The shown legend applies to all panels of the figure.



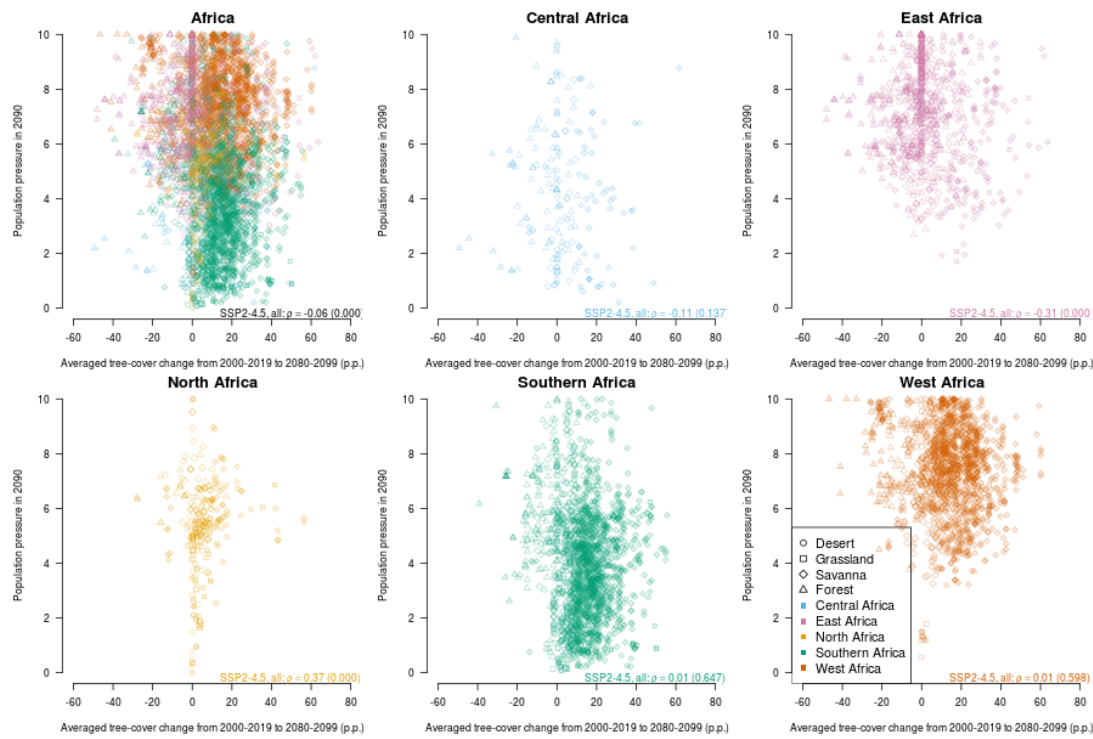
#### Appendix S11 Change in population and land-use pressure in 10-km-buffers around protected areas

for SSP2-RCP4.5 grouped by region and biome with habitat loss. Each protected area is represented by a point. Colours represent the regions that the protected areas are in (Appendix S6). The shape of a point represents the mean biome in the protected area as classified using the scheme in Appendix S4. Filled points represent protected areas projected to show habitat loss following the classification in Appendix S5. Change in land use (based on Hurt et al., 2020) and population (based on Gao, 2017) pressures were weighted based on an adapted scheme from Venter et al. (2016). The shown legend applies to all panels of the figure.

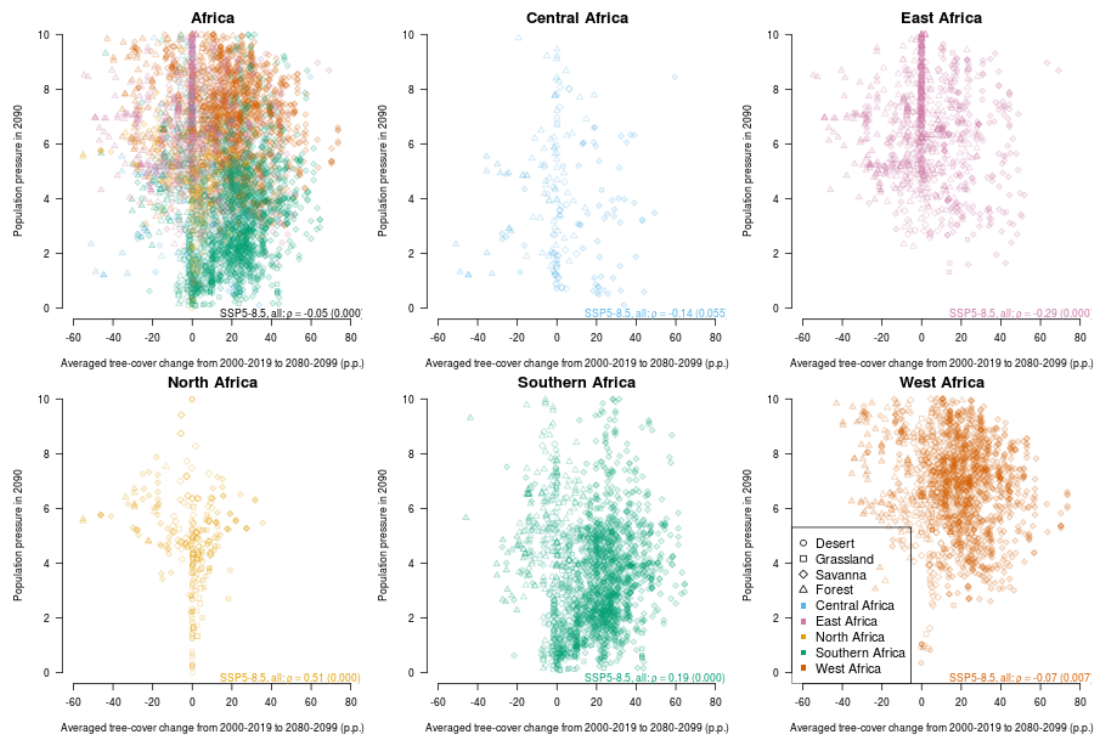


#### Appendix S12 Change in population and land-use pressure in 10-km-buffers around protected areas

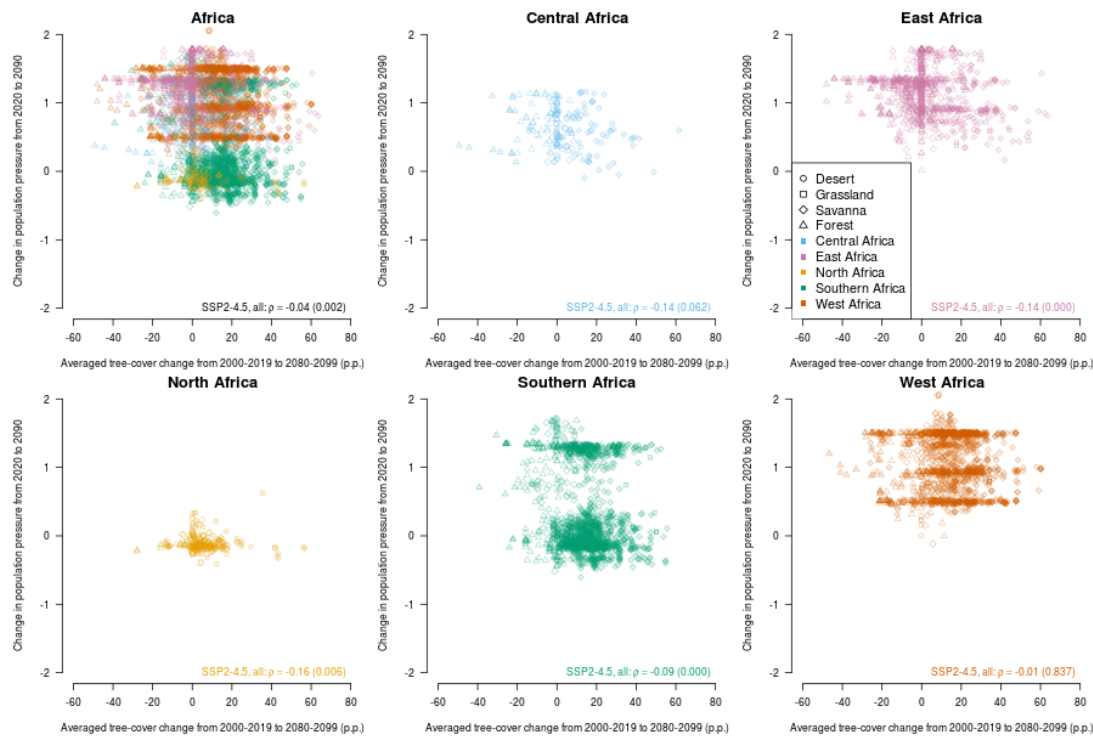
for SSP5-RCP8.5 grouped by region and biome with habitat loss. Each protected area is represented by a point. Colours represent the regions that the protected areas are in (Appendix S6). The shape of a point represents the mean biome in the protected area as classified using the scheme in Appendix S4. Filled points represent protected areas projected to show habitat loss following the classification in Appendix S5. Change in land use (based on Hurt et al., 2020) and population (based on Gao, 2017) pressures were weighted based on an adapted scheme from Venter et al. (2016). The shown legend applies to all panels of the figure.



**Appendix S13** Tree-cover change in protected areas and population pressure in 10-km-buffers for SSP2-RCP4.5 grouped by region and biome with habitat loss. Each protected area is represented by a point. Colours represent the regions that the protected areas are in (Appendix S6). The shape of a point represents the mean biome in the protected area as classified using the scheme in Appendix S4. Filled points represent protected areas projected to show habitat loss following the classification in Appendix S5. Tree-cover change was derived from simulations with the adaptive Dynamic Global Vegetation Model (aDGVM, Martens et al., 2021). Population (based on Gao, 2017) pressure was weighted based on an adapted scheme from Venter et al. (2016). The shown legend applies to all panels of the figure.

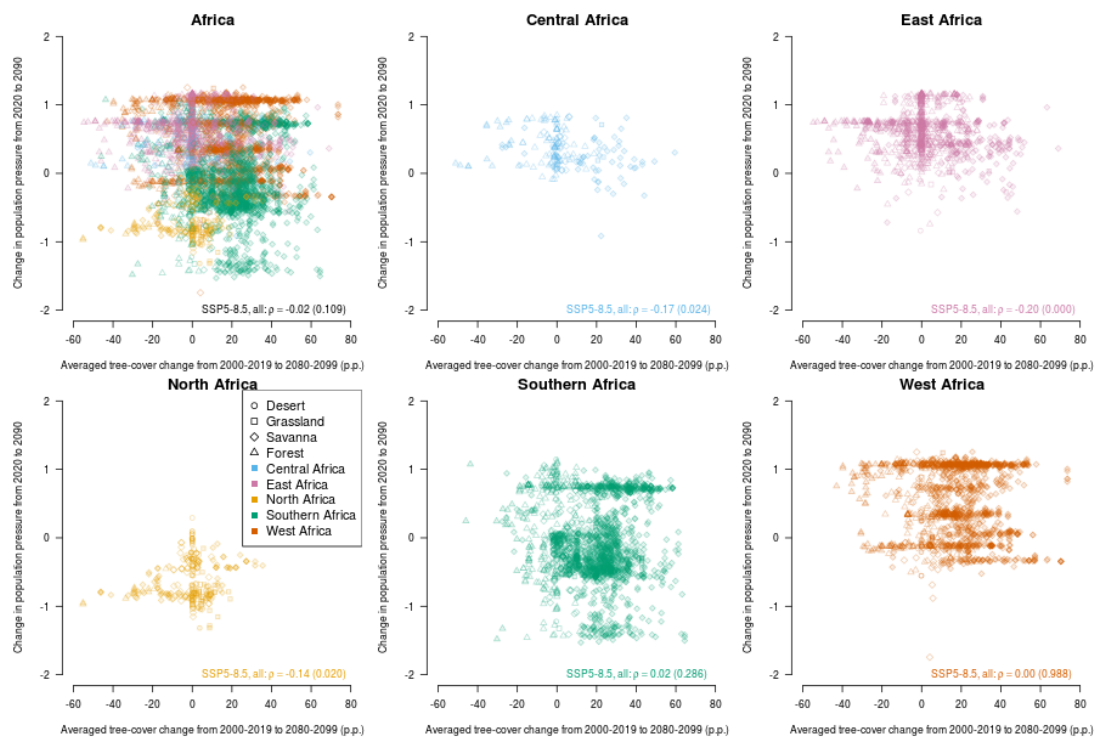


**Appendix S14** Tree-cover change in protected areas and population pressure in 10-km-buffers for SSP5-RCP8.5 grouped by region and biome with habitat loss. Each protected area is represented by a point. Colours represent the regions that the protected areas are in (Appendix S6). The shape of a point represents the mean biome in the protected area as classified using the scheme in Appendix S4. Filled points represent protected areas projected to show habitat loss following the classification in Appendix S5. Tree-cover change was derived from simulations with the adaptive Dynamic Global Vegetation Model (aDGVM, Martens et al., 2021). Population (based on Gao, 2017) pressure was weighted based on an adapted scheme from Venter et al. (2016). The shown legend applies to all panels of the figure.



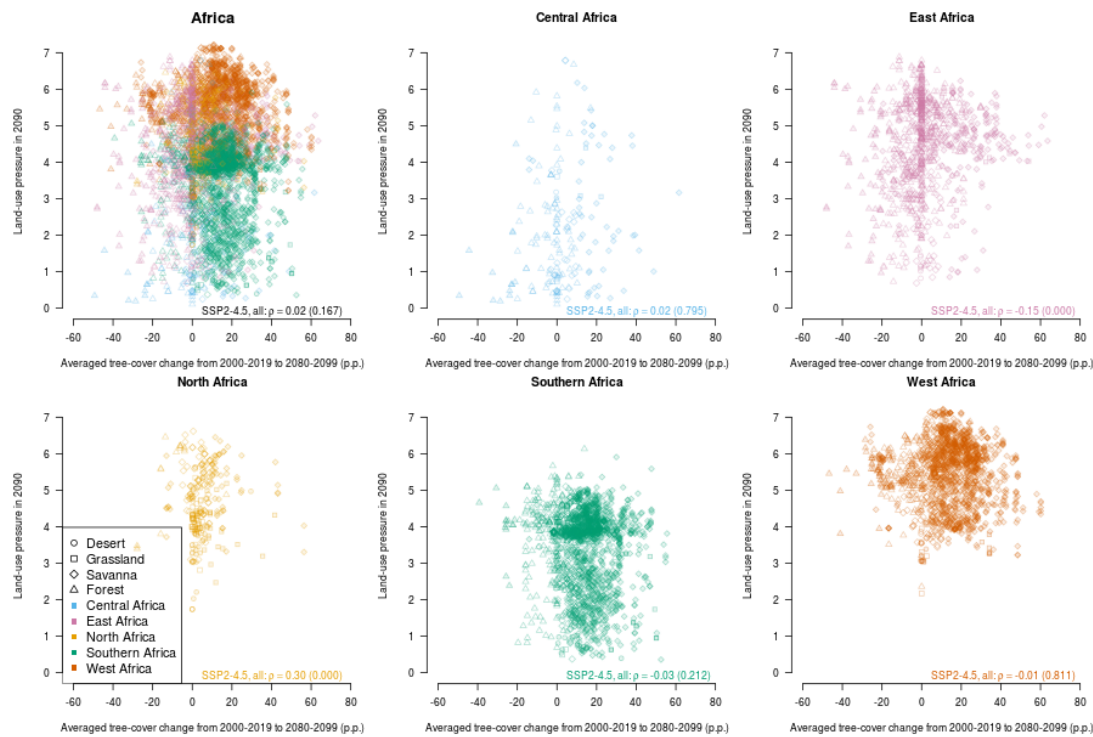
#### Appendix S15 Tree-cover change in protected areas and population pressure change in 10-km-buffers

for SSP2-RCP4.5 grouped by region and biome with habitat loss. Each protected area is represented by a point. Colours represent the regions that the protected areas are in (Appendix S6). The shape of a point represents the mean biome in the protected area as classified using the scheme in Appendix S4. Filled points represent protected areas projected to show habitat loss following the classification in Appendix S5. Tree-cover change was derived from simulations with the adaptive Dynamic Global Vegetation Model (aDGVM, Martens et al., 2021). Population (based on Gao, 2017) pressure was weighted based on an adapted scheme from Venter et al. (2016). The shown legend applies to all panels of the figure.

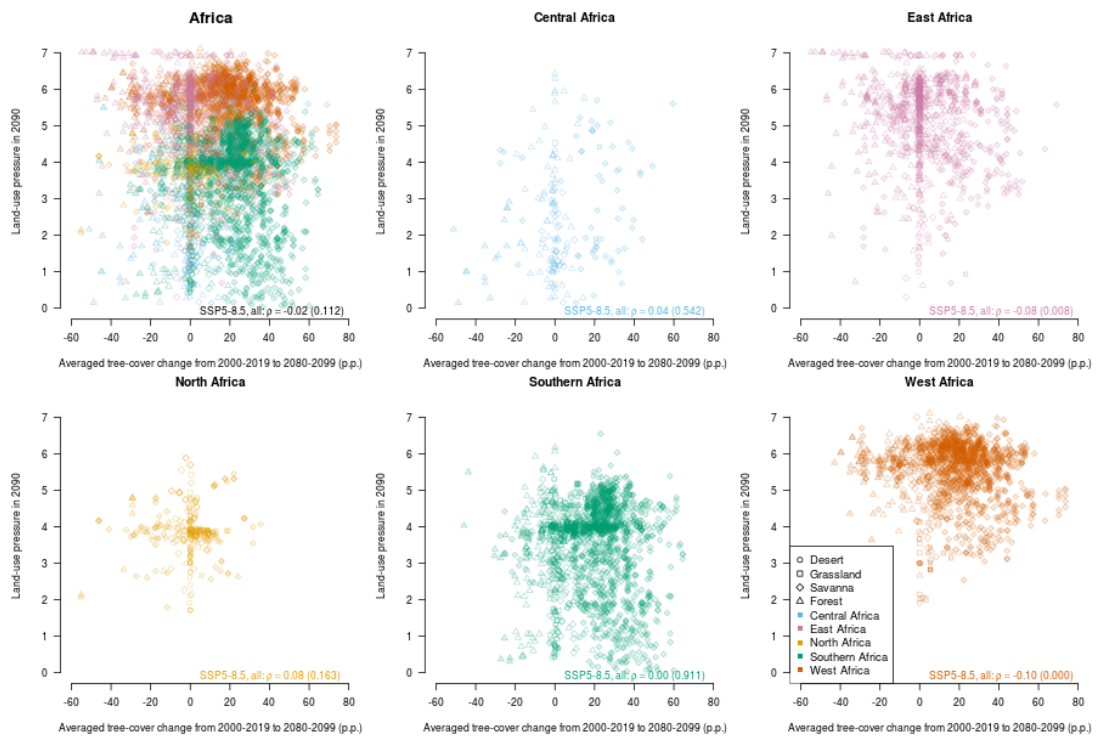


#### Appendix S16 Tree-cover change in protected areas and population pressure change in 10-km-buffers

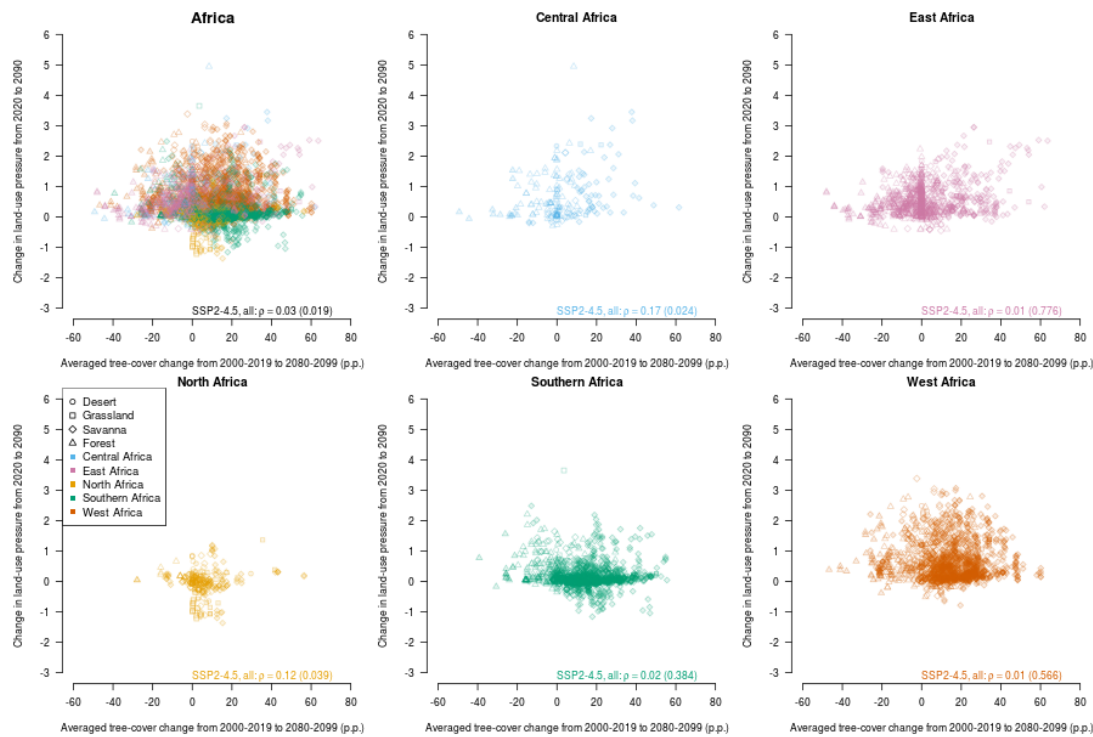
for SSP5-RCP8.5 grouped by region and biome with habitat loss. Each protected area is represented by a point. Colours represent the regions that the protected areas are in (Appendix S6). The shape of a point represents the mean biome in the protected area as classified using the scheme in Appendix S4. Filled points represent protected areas projected to show habitat loss following the classification in Appendix S5. Tree-cover change was derived from simulations with the adaptive Dynamic Global Vegetation Model (aDGVM, Martens et al., 2021). Population (based on Gao, 2017) pressure was weighted based on an adapted scheme from Venter et al. (2016). The shown legend applies to all panels of the figure.



**Appendix S17** Tree-cover change in protected areas and land-use pressure in 10-km-buffers for SSP2-RCP4.5 grouped by region and biome with habitat loss. Each protected area is represented by a point. Colours represent the regions that the protected areas are in (Appendix S6). The shape of a point represents the mean biome in the protected area as classified using the scheme in Appendix S4. Filled points represent protected areas projected to show habitat loss following the classification in Appendix S5. Tree-cover change was derived from simulations with the adaptive Dynamic Global Vegetation Model (aDGVM, Martens et al., 2021). Land use (based on Hurtt et al., 2020) pressure was weighted based on an adapted scheme from Venter et al. (2016). The shown legend applies to all panels of the figure.

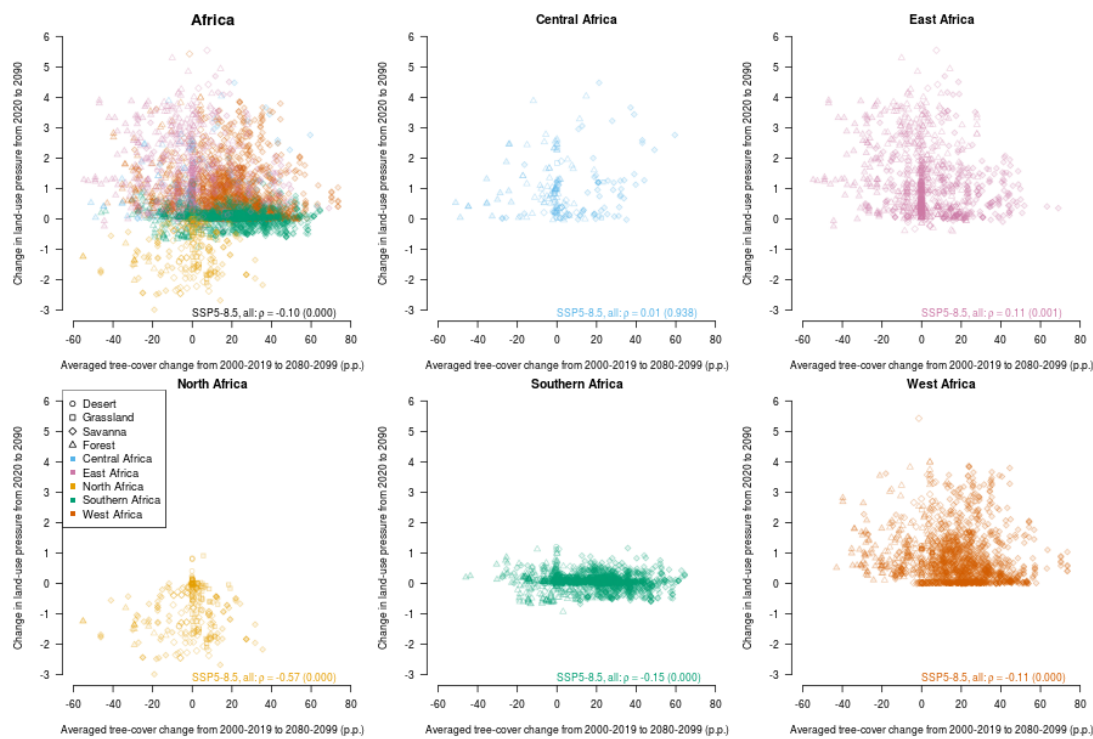


**Appendix S18** Tree-cover change in protected areas and land-use pressure in 10-km-buffers for SSP5-RCP8.5 grouped by region and biome with habitat loss. Each protected area is represented by a point. Colours represent the regions that the protected areas are in (Appendix S6). The shape of a point represents the mean biome in the protected area as classified using the scheme in Appendix S4. Filled points represent protected areas projected to show habitat loss following the classification in Appendix S5. Tree-cover change was derived from simulations with the adaptive Dynamic Global Vegetation Model (aDGVM, Martens et al., 2021). Land use (based on Hurtt et al., 2020) pressure was weighted based on an adapted scheme from Venter et al. (2016). The shown legend applies to all panels of the figure.



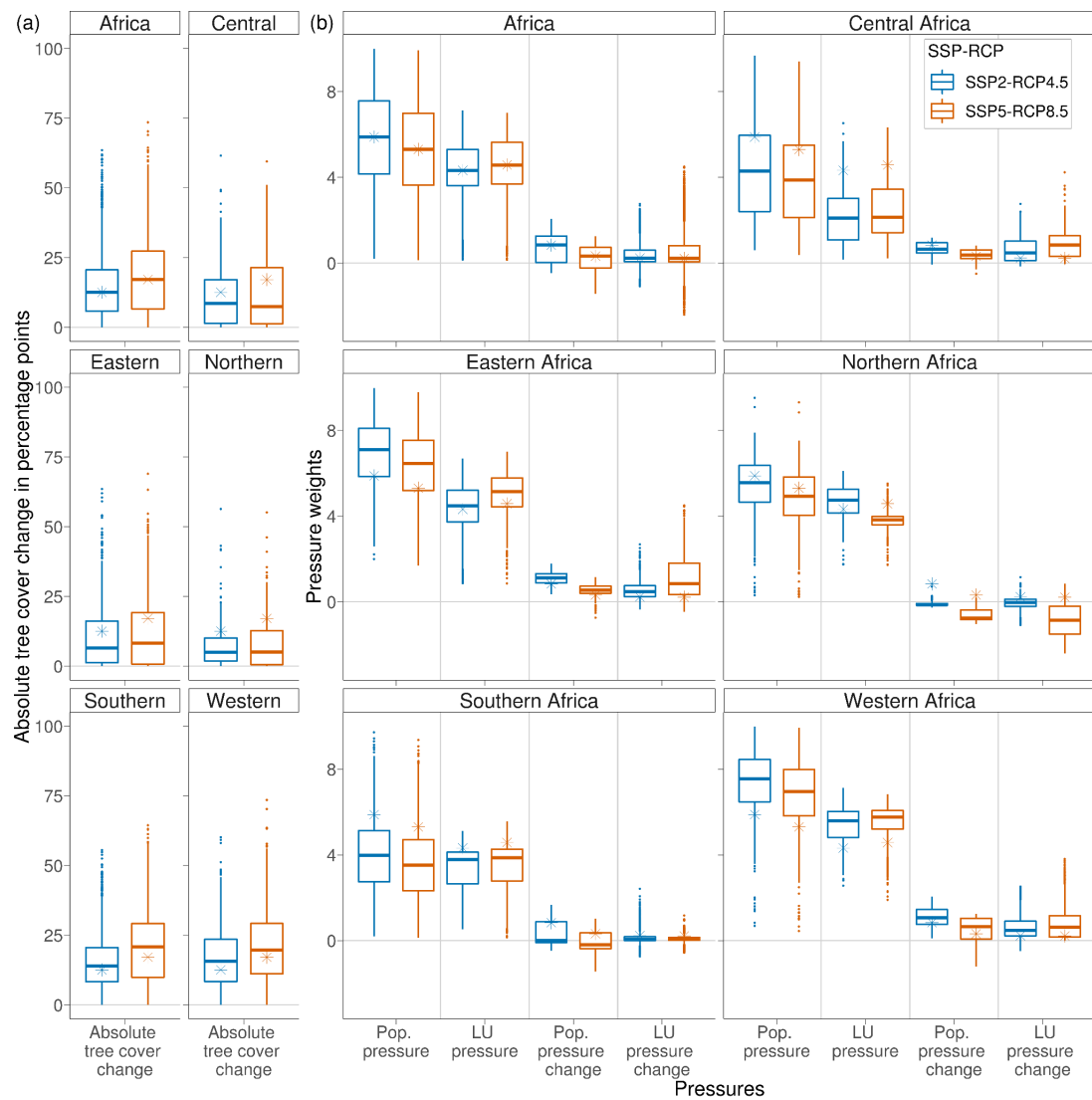
#### Appendix S19 Tree-cover change in protected areas and change in land-use pressure in 10-km-buffers

for SSP2-RCP4.5 grouped by region and biome with habitat loss. Each protected area is represented by a point. Colours represent the regions that the protected areas are in (Appendix S6). The shape of a point represents the mean biome in the protected area as classified using the scheme in Appendix S4. Filled points represent protected areas projected to show habitat loss following the classification in Appendix S5. Tree-cover change was derived from simulations with the adaptive Dynamic Global Vegetation Model (aDGVM, Martens et al., 2021). Land use (based on Hurtt et al., 2020) pressure was weighted based on an adapted scheme from Venter et al. (2016). The shown legend applies to all panels of the figure.



#### Appendix S20 Tree-cover change in protected areas and change in land-use pressure in 10-km-buffers

for SSP5-RCP8.5 grouped by region and biome with habitat loss. Each protected area is represented by a point. Colours represent the regions that the protected areas are in (Appendix S6). The shape of a point represents the mean biome in the protected area as classified using the scheme in Appendix S4. Filled points represent protected areas projected to show habitat loss following the classification in Appendix S5. Tree-cover change was derived from simulations with the adaptive Dynamic Global Vegetation Model (aDGVM, Martens et al., 2021). Land use (based on Hurtt et al., 2020) pressure was weighted based on an adapted scheme from Venter et al. (2016). The shown legend applies to all panels of the figure.



**Appendix S21** Climate-driven tree-cover changes on protected areas (a) and socio-economic pressures in 50-km buffers around protected (b) areas by region under SSP2-RCP4.5 and SSP5-RCP8.5. See Fig. 2 for the same figure with the 10-km buffer used in the study. The box plots are based on median, 25% and 75% quantile, and smallest (largest) value greater (less) than or equal to 1.5 times the interquartile range of protected areas in each group. Asterisks are the respective continental scale medians from the ‘Africa’ panel for each pressure and scenario combination. Regions are based on regions defined by the African Union (Appendix S6). Tree-cover change in percentage points (a) is derived from the adaptive dynamic global vegetation model (aDGVM, based on results from Martens et al., 2021). Absolute values for tree-cover change values from 2000-2019 to 2080-2099

are used because both negative and positive tree-cover changes represent climate-driven vegetation changes. For (b), the socio-economic pressures population (based on Gao, 2017) and land use (based on Hurtt et al., 2020) in 50-km buffers around the protected areas were rescaled to 0-10 (Appendix S3, Equ. 1) using a scheme from Venter et al. (2016). Grey vertical lines separate each socio-economic pressure and their changes. See Appendix S7 for pressures on protected areas by biome and region under both scenarios. See Appendix S7 for pressures on protected areas by biome and region under both scenarios. aDGVM - adaptive Dynamic Global Vegetation Model; LU - land use; Pop. - Population; RCP - representative concentration pathway; SSP - shared socio-economic pathways.

## Appendix C

# Supporting Information for “Towards carbon accounting in southern Africa’s Nama Karoo ecosystem”

### C.1 Measurement campaign in October 2016 in Middelburg, Eastern Cape, South Africa

In a measurement campaign from 19<sup>th</sup> to 21<sup>st</sup> of October 2016 in Middelburg, Eastern Cape, South Africa data for a site description for the Middelburg eddy covariance flux towers was collected under the lead of Nicola Stevens supported by me. The measurements were implemented in the vicinity of the eddy covariance flux tower with the coordinates 31°25'S, 25°01'E. Collected data included 8 transects of 50 m length in the directions East, North East, North, etc. starting at the eddy covariance flux tower. For each transect, shrubs that intersected with the transect were recorded with their start and end point and the resulting intersecting length, their width perpendicular to the transect, their height, and their species.

For chapter 4, I derived mean shrub height and standard deviation based on the height measurements along the transects. Based on recorded length and width of the shrubs and the assumptions of an elliptical shape of the shrub canopy area was derived for each recorded individual:

$$\text{canopy area} = \frac{\text{length} * \text{width}}{2} * \Pi. \quad (\text{C.1})$$

Mean shrub canopy area and its standard deviation was calculated as the mean of the individual canopy areas. The intersection length was also used to derive overall shrub cover. For each pair of perpendicular transects, the shrub cover was calculated based on the transect intersection of each shrub individual  $i$ ,  $\text{length}_i$  and the length of the two transects  $\text{length}_{tr}$ :

$$\text{shrub cover} = \frac{\sum(\text{length}_i)}{2 * \text{length}_{tr}}. \quad (\text{C.2})$$

The overall canopy cover and its standard deviation was then calculated as the mean across the derived shrub covers for each of the 8 pairs of perpendicular transects.

Please contact Dr. Nicola Stevens to get access to the original data.

# Bibliography

- Abdi, A., Boke-Olén, N., Jin, H., Eklundh, L., Tagesson, T., Lehsten, V. & Ardö, J. 2019 First assessment of the plant phenology index (PPI) for estimating gross primary productivity in African semi-arid ecosystems. *International Journal of Applied Earth Observation and Geoinformation*, **78**, 249–260.
- Ahlström, A., Raupach, M. R., Schurgers, G., Smith, B., Arneth, A., Jung, M., Reichstein, M., Canadell, J. G., Friedlingstein, P., Jain, A. K., Kato, E., Poulter, B., Sitch, S., Stocker, B. D., Viovy, N., Wang, Y. P., Wiltshire, A., Zaehle, S. & Zeng, N. 2015 The dominant role of semi-arid ecosystems in the trend and variability of the land CO<sub>2</sub> sink. *Science*, **348**(6237), 895–899.
- Ainsworth, E. A. & Rogers, A. 2007 The response of photosynthesis and stomatal conductance to rising [CO<sub>2</sub>]: mechanisms and environmental interactions. *Plant, Cell & Environment*, **30**(3), 258–270.
- Aleman, J. C., Blarquez, O. & Staver, C. A. 2016 Land-use change outweighs projected effects of changing rainfall on tree cover in sub-Saharan Africa. *Global Change Biology*, **22**(9), 3013–3025.
- Allen, R. G., Pereira, L. S., Raes, D. & Smith, M. 1998 Crop Evapotranspiration: guidelines for computing crop water requirements. FAO Irrigation and Drainage Paper No. 56, FAO, Rome, Italy.
- Archer, E., Engelbrecht, F., Hänsler, A., Landman, W., Tadross, M. & Helmschrot, J. 2018 Seasonal prediction and regional climate projections for southern Africa. In *Climate change and adaptive land management in southern Africa - assessments, changes, challenges, and solutions* (eds

- R. Revermann, K. Krewenka, U. Schmiedel, J. Olwoch, J. Helmschrot & N. Jürgens), vol. 6 of *Biodiversity & Ecology*, pp. 14–21. Klaus Hess Publishers, Göttingen & Windhoek.
- Archibald, S., Lehmann, C. E. R., Gómez-Dans, J. L. & Bradstock, R. A. 2013 Defining pyromes and global syndromes of fire regimes. *Proceedings of the National Academy of Sciences*, **110**(16), 6442–6447.
- Archibald, S. A., Kirton, A., van der Merwe, M. R., Scholes, R. J., Williams, C. A. & Hanan, N. 2009 Drivers of inter-annual variability in Net Ecosystem Exchange in a semi-arid savanna ecosystem, South Africa. *Biogeosciences*, **6**, 251–266.
- Arias, P., Bellouin, N., Coppola, E. et al. 2022 *Climate Change 2021: The Physical Science Basis. Contribution of Working Group I to the Sixth Assessment Report of the Intergovernmental Panel on Climate Change*, chap. Technical Summary, p. 33–144. Cambridge University Press, Cambridge, United Kingdom and New York, NY, USA.
- Arora, V. 2002 Modeling vegetation as a dynamic component in soil-vegetation-atmosphere transfer schemes and hydrological models. *Reviews of Geophysics*, **40**(2), 3–1–3–26.
- Asamoah, E. F., Beaumont, L. J. & Maina, J. M. 2021 Climate and land-use changes reduce the benefits of terrestrial protected areas. *Nature Climate Change*, **11**(12), 1105–1110.
- Austen, J. 1813 *Pride and Prejudice*. Penguin Books.
- Avitabile, V., Herold, M., Heuvelink, G. B. M. et al. 2016 An integrated pan-tropical biomass map using multiple reference datasets. *Global Change Biology*, **22**(4), 1406–1420.
- Baccini, A., Goetz, S. J., Walker, W. S., Laporte, N. T., Sun, M., Sulla-Menashe, D., Hackler, J., Beck, P. S. A., Dubayah, R., Friedl, M. A., Samanta, S. & Houghton, R. A. 2012 Estimated carbon dioxide emissions from tropical deforestation improved by carbon-density maps. *Nature Climate Change*, **2**(3), 182–185.
- Ball, J. T., Woodrow, I. E. & Berry, J. A. 1987 *Progress in Photosynthesis Research: proceedings of the VIIth International Congress on Photosynthesis, Providence, Rhode Island, USA, august*

- 10 - 15, 1986, Volume 4, chap. A model predicting stomatal conductance and its contribution to the control of photosynthesis under different environmental conditions, pp. 221–224. Springer+Business Media Dordrecht.
- Bastin, J.-F., Finegold, Y., Garcia, C., Mollicone, D., Rezende, M., Routh, D., Zohner, C. M. & Crowther, T. W. 2019 The global tree restoration potential. *Science*, **365**(6448), 76–79.
- Batavia, C. & Nelson, M. P. 2017 For goodness sake! What is intrinsic value and why should we care? *Biological Conservation*, **209**, 366–376.
- Beaulieu, E., Lucas, Y., Viville, D., Chabaux, F., Ackerer, P., Goddérus, Y. & Pierret, M.-C. 2016 Hydrological and vegetation response to climate change in a forested mountainous catchment. *Modeling Earth Systems and Environment*, **2**(4), 1–15.
- Berger, C., Bieri, M., Bradshaw, K., Brümmer, C., Clemen, T., Hickler, T., Kutsch, W. L., Lenfers, U. A., Martens, C., Midgley, G. F., Mukwashi, K., Odipo, V., Scheiter, S., Schmullius, C., Baade, J., du Toit, J. C. O., Scholes, R. J., Smit, I. P. J., Stevens, N. & Twine, W. 2019 Linking scales and disciplines: an interdisciplinary cross-scale approach to supporting climate-relevant ecosystem management. *Climatic Change*.
- Beukes, P., Cowling, R. & Higgins, S. 2002 An ecological economic simulation model of a non-selective grazing system in the Nama Karoo, South Africa. *Ecological Economics*, **42**(1), 221–242.
- Blonder, B. W., Aparecido, L., Hultine, K., Lombardozzi, D., Michaletz, S., Posch, B. C., Slot, M. & Winter, K. 2023 Plant water use theory should incorporate hypotheses about extreme environments, population ecology, and community ecology. *New Phytologist*, **238**(6), 2271–2283.
- Bombelli, A., Henry, M., Castaldi, S., Adu-Bredu, S., Arneth, A., de Grandcourt, A., Grieco, E., Kutsch, W. L., Lehsten, V., Rasile, A., Reichstein, M., Tansey, K., Weber, U. & Valentini, R. 2009 An outlook on the Sub-Saharan Africa carbon balance. *Biogeosciences*, **6**, 2193–2205.

- Bond, W. J. 2008 What Limits Trees in C<sub>4</sub> Grasslands and Savannas? *Annual Review of Ecology, Evolution, and Systematics*, **39**(1), 641–659.
- Bond, W. J. 2016 Ancient grasslands at risk. *Science*, **351**(6269), 120–122.
- Bond, W. J. & Midgley, G. F. 2000 A proposed CO<sub>2</sub>-controlled mechanism of woody plant invasion in grasslands and savannas. *Global Change Biology*, **6**(8), 865–869.
- Bond, W. J. & Midgley, G. F. 2012 Carbon dioxide and the uneasy interactions of trees and savannah grasses. *Philosophical Transactions of the Royal Society B*, **367**, 601–612.
- Bond, W. J. & Midgley, J. J. 2001 Ecology of sprouting in woody plants: the persistence niche. *Trends in Ecology & Evolution*, **16**(1), 45 – 51.
- Bond, W. J., Stevens, N., Midgley, G. F. & Lehmann, C. E. 2019 The Trouble with Trees: Afforestation Plans for Africa. *Trends in Ecology & Evolution*.
- Bond, W. J., Woodward, F. I. & Midgley, G. F. 2005 The global distribution of ecosystems in a world without fire. *New Phytologist*, **165**(2), 525–538.
- Borthagaray, A. I., Fuentes, M. A. & Marquet, P. A. 2010 Vegetation pattern formation in a fog-dependent ecosystem. *Journal of Theoretical Biology*, **265**(1), 18–26.
- Brancalion, P. H. S., Niamir, A., Broadbent, E., Crouzeilles, R., Barros, F. S. M., Almeyda Zambrano, A. M., Baccini, A., Aronson, J., Goetz, S., Reid, J. L., Strassburg, B. B. N., Wilson, S. & Chazdon, R. L. 2019 Global restoration opportunities in tropical rainforest landscapes. *Science Advances*, **5**(7).
- Brook, B. W., Sodhi, N. S. & Bradshaw, C. J. 2008 Synergies among extinction drivers under global change. *Trends in Ecology & Evolution*, **23**(8), 453–460.
- Büdel, B., Darienko, T., Deutschewitz, K., Dojani, S., Friedl, T., Mohr, K. I., Salisch, M., Reisser, W. & Weber, B. 2009 Southern African biological soil crusts are ubiquitous and highly diverse in drylands, being restricted by rainfall frequency. *Microbial Ecology*, **57**(2), 229–247.

- Burrell, A. L., Evans, J. P. & De Kauwe, M. G. 2020 Anthropogenic climate change has driven over 5 million km<sup>2</sup> of drylands towards desertification. *Nature Communications*, **11**(1), 3853.
- Calvin, K., Bond-Lamberty, B., Jones, A., Shi, X., Di Vittorio, A. & Thornton, P. 2019 Characteristics of human-climate feedbacks differ at different radiative forcing levels. *Global and Planetary Change*, **180**, 126–135.
- Canadell, J. G., Quéré, C. L., Raupach, M. R., Field, C. B., Buitenhuis, E. T., Ciais, P., Conway, T. J., Gillett, N. P., Houghton, R. A. & Marland, G. 2007 Contributions to accelerating atmospheric CO<sub>2</sub> growth from economic activity, carbon intensity, and efficiency of natural sinks. *Proceedings of the National Academy of Sciences*, **104**(47), 18866–18870.
- Cardinale, B. J., Duffy, J. E., Gonzalez, A., Hooper, D. U., Perrings, C., Venail, P., Narwani, A., Mace, G. M., Tilman, D., Wardle, D. A., Kinzig, A. P., Daily, G. C., Loreau, M., Grace, J. B., Larigauderie, A., Srivastava, D. S. & Naeem, S. 2012 Biodiversity loss and its impact on humanity. *Nature*, **486**(7401), 59–67.
- CBD, O. 2021 First draft of the post-2020 global biodiversity framework.
- CBD COP, C. 2022 X/2.The Strategic Plan for Biodiversity 2011-2020 and the Aichi Biodiversity Targets.
- Chapin III, F., Matson, P. & Mooney, H. 2011 *Principles of Terrestrial Ecosystem Ecology*. New York: Springer, second edition edn.
- Clemen, T., Lenfers, U. A., Dybulla, J., Ferreira, S. M., Kiker, G. A., Martens, C. & Scheiter, S. 2021 A cross-scale modeling framework for decision support on elephant management in Kruger National Park, South Africa. *Ecological Informatics*, **62**, 101266.
- Collatz, G. J., Ball, J. T., Grivet, C. & Berry, J. A. 1991 Physiological and environmental regulation of stomatal conductance, photosynthesis and transpiration: a model that includes a laminar boundary layer. *Agricultural and Forest Meteorology*, **54**, 107–136.

- Collatz, G. J., Berry, J. A. & Clark, J. S. 1998 Effects of climate and atmospheric CO<sub>2</sub> partial pressure on the global distribution of C<sub>4</sub> grasses: Present, past, and future. *Oecologia*, **114**(4), 441–454.
- Collatz, G. J., Ribas-Carbo, M. & Berry, J. A. 1992 Coupled Photosynthesis-Stomatal Conductance Model for Leaves of C<sub>4</sub> Plants. *Australian Journal of Plant Physiology*, **19**(5), 519–538.
- Conradi, T., Slingsby, J. A., Midgley, G. F., Nottebrock, H., Schweiger, A. H. & Higgins, S. I. 2020 An operational definition of the biome for global change research. *New Phytologist*, **227**(5), 1294–1306.
- Corlett, R. T. & Westcott, D. A. 2013 Will plant movements keep up with climate change? *Trends in Ecology & Evolution*, **28**(8), 482–488.
- Cowling, R. M. & Hilton-Taylor, C. 2004 *The Karoo - Ecological patterns and processes*, chap. Plant biogeography, endemism and diversity. Cambridge University Press.
- Cramer, W., Bondeau, A., Woodward, F. I., Prentice, I. C., Betts, R. A., Brovkin, V., Cox, P. M., Fisher, V., Foley, J. A., Friend, A. D., Kucharik, C., Lomas, M. R., Ramankutty, N., Sitch, S., Smith, B., White, A. & Young-Molling, C. 2001 Global response of terrestrial ecosystem structure and function to CO<sub>2</sub> and climate change: results from six dynamic global vegetation models. *Global Change Biology*, **7**(4), 357–373.
- Crist, E., Mora, C. & Engelman, R. 2017 The interaction of human population, food production, and biodiversity protection. *Science*, **356**(6335), 260–264.
- Dannenberg, M. P., Barnes, M. L., Smith, W. K., Johnston, M. R., Meerdink, S. K., Wang, X., Scott, R. L. & Biederman, J. A. 2023 Upscaling dryland carbon and water fluxes with artificial neural networks of optical, thermal, and microwave satellite remote sensing. *Biogeosciences*, **20**(2), 383–404.
- Davis-Reddy, C., Vincent, K. & Mambo, J. 2017 *Climate Risk and Vulnerability: A Handbook for Southern Africa (2nd Edition)*, chap. Socio-Economic Impacts of Extreme Weather Events in Southern Africa, pp. 30–46. Pretoria, South Africa: CSIR.

- De Kauwe, M. G., Lin, Y.-S., Wright, I. J., Medlyn, B. E., Crous, K. Y., Ellsworth, D. S., Maire, V., Prentice, I. C., Atkin, O. K., Rogers, A., Ülo Niinemets, Serbin, S. P., Meir, P., Uddling, J., Togashi, H. F., Tarvainen, L., Weerasinghe, L. K., Evans, B. J., Ishida, F. Y. & Domingues, T. F. 2016 A test of the 'one-point method' for estimating maximum carboxylation capacity from field-measured, light-saturated photosynthesis. *New Phytologist*, **210**(3), 1130–1144.
- De Kauwe, M. G., Medlyn, B. E. & T.Tissue, D. 2021 To what extent can rising [CO<sub>2</sub>] ameliorate plant drought stress? *New Phytologist*, **231**(6), 2118–2124.
- De Kauwe, M. G., Medlyn, B. E., Zaehle, S. *et al.* 2013 Forest water use and water use efficiency at elevated CO<sub>2</sub>: a model-data intercomparison at two contrasting temperate forest FACE sites. *Global Change Biology*, **19**(6), 1759–1779.
- De Kauwe, M. G., Medlyn, B. E., Zaehle, S. *et al.* 2014 Where does the carbon go? a model-data intercomparison of vegetation carbon allocation and turnover processes at two temperate forest free-air CO<sub>2</sub> enrichment sites. *New Phytologist*, **203**(3), 883–899.
- DeFries, R., Hansen, A., Turner, B., Reid, R. & Liu, J. 2007 Land use change around protected areas: Management to balance human needs and ecological function. *Ecological Applications*, **17**(4), 1031–1038.
- Desmet, P. G. & Cowling, R. M. 2004 *The Karoo - Ecological patterns and processes*, chap. The climate of the Karoo - a functional approach. Cambridge University Press.
- Di Marco, M., Harwood, T. D., Hoskins, A. J., Ware, C., Hill, S. L. L. & Ferrier, S. 2019 Projecting impacts of global climate and land-use scenarios on plant biodiversity using compositional-turnover modelling. *Global Change Biology*, **25**(8), 2763–2778.
- Dietzen, C. A., Larsen, K. S., Ambus, P. L., Michelsen, A., Arndal, M. F., Beier, C., Reinsch, S. & Schmidt, I. K. 2019 Accumulation of soil carbon under elevated CO<sub>2</sub> unaffected by warming and drought. *Global Change Biology*, **25**(9), 2970–2977.
- Dobrowski, S. Z., Littlefield, C. E., Lyons, D. S., Hollenberg, C., Carroll, C., Parks, S. A., Abatzoglou, J. T., Hegewisch, K. & Gage, J. 2021 Protected-area targets could be undermined by

- climate change-driven shifts in ecoregions and biomes. *Communications Earth & Environment*, **2**(1), 198.
- Doherty, R. M., Sitch, S., Smith, B., Lewis, S. L. & Thornton, P. K. 2010 Implications of future climate and atmospheric CO<sub>2</sub> content for regional biogeochemistry, biogeography and ecosystem services across East Africa. *Global Change Biology*, **16**(2), 617–640.
- Dressler, G., Groeneveld, J., Buchmann, C. M., Guo, C., Hase, N., Thober, J., Frank, K. & Müller, B. 2019 Implications of behavioral change for the resilience of pastoral systems — lessons from an agent-based model. *Ecological Complexity*, **40**, 100710. Agent-based modelling to study resilience in socio-ecological systems.
- du Toit, J. C. & O'Connor, T. G. 2014 Changes in rainfall pattern in the eastern Karoo, South Africa, over the past 123 years. *Water SA*, **40**(3).
- du Toit, J. C. & O'Connor, T. G. 2020 Long-term influence of season of grazing and rainfall on vegetation in the eastern Karoo, South Africa. *African Journal of Range & Forage Science*, **37**(2), 159–171.
- du Toit, J. C., Ramaswiela, T., Pauw, M. J. & O'Connor, T. G. 2018 Interactions of grazing and rainfall on vegetation at Grootfontein in the eastern Karoo. *African Journal of Range & Forage Science*, **35**(3-4), 267–276.
- du Toit, J. C., van den Berg, L. & O'Connor, T. G. 2015 Fire effects on vegetation in a grassy dwarf shrubland at a site in the eastern Karoo, South Africa. *African Journal of Range & Forage Science*, **32**(1), 13–20.
- du Toit, P. C. V. 2002 Boesmanskop grazing-capacity benchmark for the Nama-Karoo. *Grootfontein Agriculture*, (5), 1–6.
- Dufresne, J.-L., Fairhead, L., Le Treut, H., Berthelot, M., Bopp, L., Ciais, P., Friedlingstein, P. & Monfray, P. 2002 On the magnitude of positive feedback between future climate change and the carbon cycle. *Geophysical Research Letters*, **29**(10), 43–1–43–4.

- Eamus, D. 1991 The interaction of rising CO<sub>2</sub> and temperatures with water use efficiency. *Plant, Cell & Environment*, **14**(8), 843–852.
- Early, R., Bradley, B. A., Dukes, J. S., Lawler, J. J., Olden, J. D., Blumenthal, D. M., Gonzalez, P., Grosholz, E. D., Ibañez, I., Miller, L. P., Sorte, C. J. B. & Tatem, A. J. 2016 Global threats from invasive alien species in the twenty-first century and national response capacities. *Nature Communications*.
- Edwardes, A. 2018 The hydrological and ecophysiological effects of simulated climate warming on the soil and vegetation of the Nama Karoo. Master's thesis, Stellenbosch University, Faculty of Science, Dept. of Botany and Zoology.
- Eigenbrod, F., Gonzalez, P., Dash, J. & Steyl, I. 2015 Vulnerability of ecosystems to climate change moderated by habitat intactness. *Global Change Biology*, **21**(1), 275–286.
- EMG 2011 Global drylands: a UN system-wide response, Geneva, Switzerland, The United Nations Environment Management Group.
- Engelbrecht, C. J. & Engelbrecht, F. A. 2016 Shifts in Köppen-Geiger climate zones over southern Africa in relation to key global temperature goals. *Theoretical and Applied Climatology*, **123**(1), 247–261.
- Engelbrecht, C. J., Engelbrecht, F. A. & Dyson, L. L. 2013 High-resolution model-projected changes in mid-tropospheric closed-lows and extreme rainfall events over southern Africa. *International Journal of Climatology*, **33**(1), 173–187.
- Engelbrecht, F., Adegoke, J., Bopape, M.-J., Naidoo, M., Garland, R., Thatcher, M., McGregor, J., Katzfey, J., Werner, M., Ichoku, C. & Gatebe, C. 2015 Projections of rapidly rising surface temperatures over Africa under low mitigation. *Environmental Research Letters*, **10**(8), 085004.
- Engelbrecht, F. A., McGregor, J. L. & Engelbrecht, C. J. 2009 Dynamics of the Conformal-Cubic Atmospheric Model projected climate-change signal over southern Africa. *International Journal of Climatology*, **29**(7), 1013–1033.

- Esler, K. & Phillips, N. 1994 Experimental effects of water stress on semi-arid Karoo seedlings: implications for field seedling survivorship. *Journal of Arid Environments*, **26**(4), 325–337.
- Farquhar, G. D., Caemmerer, S. V. & Berry, J. A. 1980 A biochemical-model of photosynthetic CO<sub>2</sub> assimilation in leaves of C<sub>3</sub> species. *Planta*, **149**(1), 78–90.
- Fernández-Marín, B., Gulías, J., Figueroa, C. M., Iñiguez, C., Clemente-Moreno, M. J., Nunes-Nesi, A., Fernie, A. R., Cavieres, L. A., Bravo, L. A., García-Plazaola, J. I. & Gago, J. 2020 How do vascular plants perform photosynthesis in extreme environments? An integrative ecophysiological and biochemical story. *The Plant Journal*, **101**(4), 979–1000.
- Fisher, R. A., Koven, C. D., Anderegg, W. R. L. *et al.* 2018 Vegetation demographics in Earth System Models: A review of progress and priorities. *Global Change Biology*, **24**(1), 35–54.
- Fleischer, K., Rammig, A., De Kauwe, M. G. *et al.* 2019 Amazon forest response to CO<sub>2</sub> fertilization dependent on plant phosphorus acquisition. *Nature Geoscience*, **12**(9), 736–741.
- Fleischer, K. & Terrer, C. 2022 Estimates of soil nutrient limitation on the CO<sub>2</sub> fertilization effect for tropical vegetation. *Global Change Biology*, **28**(21), 6366–6369.
- Fletcher, S., Lickley, M. & Strzepek, K. 2019 Learning about climate change uncertainty enables flexible water infrastructure planning. *Nature Communications*, **10**(1), 1782.
- Friedlingstein, P., Jones, M. W., O'Sullivan, M. *et al.* 2022 Global Carbon Budget 2021. *Earth System Science Data*, **14**(4), 1917–2005.
- Fust, P. & Schlecht, E. 2018 Integrating spatio-temporal variation in resource availability and herbivore movements into rangeland management: RaMDry - An agent-based model on livestock feeding ecology in a dynamic, heterogeneous, semi-arid environment. *Ecological Modelling*, **369**, 13–41.
- Gaillard, C., Langan, L., Pfeiffer, M., Kumar, D., Martens, C., Higgins, S. I. & Scheiter, S. 2018 African shrub distribution emerges via a trade-off between height and sapwood conductivity. *Journal of Biogeography*, **45**(12), 2815–2826.

- Gao, J. 2017 Downscaling Global Spatial Population Projections from 1/8-degree to 1-km Grid Cells. Tech. rep.
- Gao, J. 2019 Global Population Projection Grids Based on Shared Socioeconomic Pathways (SSPs), Downscaled 1-km Grids, 2010-2100. Accessed 20-24 March 2020.
- Geldmann, J., Joppa, L. N. & Burgess, N. D. 2014 Mapping Change in Human Pressure Globally on Land and within Protected Areas. *Conservation Biology*, **28**(6), 1604–1616.
- Geldmann, J., Manica, A., Burgess, N. D., Coad, L. & Balmford, A. 2019 A global-level assessment of the effectiveness of protected areas at resisting anthropogenic pressures. *Proceedings of the National Academy of Sciences*, **116**(46), 23209–23215.
- Global Soil Data Task Group 2000 Global Gridded Surfaces of Selected Soil Characteristics (IGBP-DIS).
- Gonzalez, P., Neilson, R. P., Lenihan, J. M. & Drapek, R. J. 2010 Global patterns in the vulnerability of ecosystems to vegetation shifts due to climate change. *Global Ecology and Biogeography*, **19**(6), 755–768.
- Gonzalez, P., Tucker, C. & Sy, H. 2012 Tree density and species decline in the African Sahel attributable to climate. *Journal of Arid Environments*, **78**, 55 – 64.
- Grantham, H. S., Shapiro, A., Bonfils, D., Gond, V., Goldman, E., Maisels, F., Plumptre, A. J., Rayden, T., Robinson, J. G., Strindberg, S., Stokes, E., Tulloch, A. I. T. T., Watson, J. E. M., Williams, L. & Rickenbach, O. 2020 Spatial priorities for conserving the most intact biodiverse forests within Central Africa. *Environmental Research Letters*, **15**(9), 0940b5.
- Grillot, M., Guerrin, F., Gaudou, B., Masse, D. & Vayssières, J. 2018 Multi-level analysis of nutrient cycling within agro-sylvo-pastoral landscapes in West Africa using an agent-based model. *Environmental Modelling & Software*, **107**, 267–280.
- Güneralp, B., Lwasa, S., Masundire, H., Parnell, S. & Seto, K. C. 2017 Urbanization in Africa: challenges and opportunities for conservation. *Environmental Research Letters*, **13**(1), 015002.

- Gómez Martín, E., Máñez Costa, M., Egerer, S. & Schneider, U. A. 2021 Assessing the long-term effectiveness of Nature-Based Solutions under different climate change scenarios. *Science of The Total Environment*, **794**, 148515.
- Hahn, B., Richardson, F., Hoffman, M., Roberts, R., Todd, S. & Carrick, P. 2005 A simulation model of long-term climate, livestock and vegetation interactions on communal rangelands in the semi-arid Succulent Karoo, Namaqualand, South Africa. *Ecological Modelling*, **183**(2), 211–230.
- Hannah, L. 2008 Protected Areas and Climate Change. *Annals of the New York Academy of Sciences*, **1134**, 201–212.
- Hannah, L., Roehrdanz, P. R., Marquet, P. A. *et al.* 2020 30% land conservation and climate action reduces tropical extinction risk by more than 50%. *Ecography*, **43**, 943–953.
- Hao, G., Hu, Z., Di, K. & Li, S. 2020 Rainfall pulse response of carbon exchange to the timing of natural intra-annual rainfall in a temperate grass ecosystem. *Ecological Indicators*, **118**, 106730.
- Harris, R. M. B., Loeffler, F., Rumm, A., Fischer, C., Horchler, P., Scholz, M., Foeckler, F. & Henle, K. 2020 Biological responses to extreme weather events are detectable but difficult to formally attribute to anthropogenic climate change. *Scientific Reports*, **10**(1), 14067.
- Haverd, V., Smith, B., Nieradzik, L., Briggs, P. R., Woodgate, W., Trudinger, C. M., Canadell, J. G. & Cuntz, M. 2018 A new version of the CABLE land surface model (Subversion revision r4601) incorporating land use and land cover change, woody vegetation demography, and a novel optimisation-based approach to plant coordination of photosynthesis. *Geoscientific Model Development*, **11**(7), 2995–3026.
- Hegerl, G. & Zwiers, F. 2011 Use of models in detection and attribution of climate change. *WIREs Climate Change*, **2**(4), 570–591.
- Henschel, J. R., Hoffman, M. T. & Walker, C. 2018 Introduction to the Karoo Special Issue: Trajectories of change in the Anthropocene. *African Journal of Range & Forage Science*, **35**(3-4), 151–156.

- Herrmann, S. M., Brandt, M., Rasmussen, K. & Fensholt, R. 2020 Accelerating land cover change in West Africa over four decades as population pressure increased. *Communications Earth & Environment*, **1**(1), 53.
- Hickler, T., Eklundh, L., Seaquist, J. W., Smith, B., Ardö, J., Olsson, L., Sykes, M. T. & Sjöström, M. 2005 Precipitation controls Sahel greening trend. *Geophysical Research Letters*, **32**(21).
- Hickler, T., Rammig, A. & Werner, C. 2015 Modelling CO<sub>2</sub> Impacts on Forest Productivity. *Current Forestry Reports*, **1**(2), 69–80.
- Higgins, S. I., Bond, W. J. & Trollope, W. S. W. 2000 Fire, resprouting and variability: a recipe for grass-tree coexistence in savanna. *Journal of Ecology*, **88**(2), 213–229.
- Higgins, S. I., Bond, W. J., Trollope, W. S. W. & Williams, R. J. 2008 Physically motivated empirical models for the spread and intensity of grass fires. *International Journal of Wildland Fire*, **17**(5), 595–601.
- Higgins, S. I., Conradi, T., Kruger, L. M., O'Hara, R. B. & Slingsby, J. A. 2023a Limited climatic space for alternative ecosystem states in Africa. *Science*, **380**(6649), 1038–1042.
- Higgins, S. I., Conradi, T. & Muhoko, E. 2023b Shifts in vegetation activity of terrestrial ecosystems attributable to climate trends. *Nature Geoscience*, **16**(2), 147–153.
- Higgins, S. I., Keretetse, M. & February, E. C. 2015 Feedback of trees on nitrogen mineralization to restrict the advance of trees in C<sub>4</sub> savannahs. *Biology Letters*, **11**(8), 20150572.
- Higgins, S. I. & Scheiter, S. 2012 Atmospheric CO<sub>2</sub> forces abrupt vegetation shifts locally, but not globally. *Nature*, **488**(7410), 209–212.
- Hijmans, R. J. 2020 *raster: Geographic Data Analysis and Modeling*. R package version 3.3-13.
- Hoegh-Guldberg, O., Jacob, D., Taylor, M. *et al.* 2018 Chapter 3: Impacts of 1.5°C global warming on natural and human systems. In *Global warming of 1.5 °C an IPCC special report on the impacts of global warming of 1.5 °C above pre-industrial levels and related global greenhouse gas*

- emission pathways, in the context of strengthening the global response to the threat of climate change.* Intergovernmental Panel on Climate Change.
- Hof, C., Voskamp, A., Biber, M. F., Böhning-Gaese, K., Engelhardt, E. K., Niamir, A., Willis, S. G. & Hickler, T. 2018 Bioenergy cropland expansion may offset positive effects of climate change mitigation for global vertebrate diversity. *Proceedings of the National Academy of Sciences*, **115**(52), 13294–13299.
- Hoffman, M. T., Walker, C. & Henschel, J. R. 2018 Reflections on the Karoo Special Issue: towards an interdisciplinary research agenda for South Africa's drylands. *African Journal of Range & Forage Science*, **35**(3-4), 387–393.
- Hoffmann, W. A., Geiger, E. L., Gotsch, S. G., Rossatto, D. R., Silva, L. C. R., Lau, O. L., Hari-dasan, M. & Franco, A. C. 2012 Ecological thresholds at the savanna-forest boundary: how plant traits, resources and fire govern the distribution of tropical biomes. *Ecology Letters*, **15**(7), 759–768.
- Hoffmann, W. A. & Solbrig, O. T. 2003 The role of topkill in the differential response of savanna woody species to fire. *Forest Ecology and Management*, **180**(1), 273–286.
- Horvath, P., Tang, H., Halvorsen, R., Stordal, F., Tallaksen, L. M., Berntsen, T. K. & Bryn, A. 2021 Improving the representation of high-latitude vegetation distribution in dynamic global vegetation models. *Biogeosciences*, **18**(1), 95–112.
- Hubau, W., Lewis, S. L., Phillips, O. L. *et al.* 2020 Asynchronous carbon sink saturation in African and Amazonian tropical forests. *Nature*, **579**(7797), 80–87.
- Huntingford, C., Zelazowski, P., Galbraith, D. *et al.* 2013 Simulated resilience of tropical rainforests to CO<sub>2</sub>-induced climate change. *Nature Geoscience*, **6**(4), 268–273.
- Hurt, G. C., Chini, L., Sahajpal, R. *et al.* 2020 Harmonization of global land use change and management for the period 850–2100 (LUH2) for CMIP6. *Geoscientific Model Development*, **13**(11), 5425–5464.

- ILO, I. 2019 "Agriculture as % of total employment" - ILO modelled estimates, Department of Statistics, International Labour Organization.
- IPBES 2018a The IPBES assessment report on land degradation and restoration.
- IPBES 2018b The IPBES regional assessment report on biodiversity and ecosystem services for Africa.
- IPBES 2019a Global assessment report on biodiversity and ecosystem services of the Intergovernmental Science-Policy Platform on Biodiversity and Ecosystem Services.
- IPBES 2019b Summary for policymakers of the global assessment report on biodiversity and ecosystem services.
- Jetz, W. & Fine, P. V. A. 2012 Global Gradients in Vertebrate Diversity Predicted by Historical Area-Productivity Dynamics and Contemporary Environment. *PLOS Biology*, **10**(3), 1–11.
- Jiang, M., Calderaru, S., Zhang, H., Fleischer, K., Crous, K. Y., Yang, J., De Kauwe, M. G., Ellsworth, D. S., Reich, P. B., Tissue, D. T., Zaehle, S. & Medlyn, B. E. 2020a Low phosphorus supply constrains plant responses to elevated CO<sub>2</sub>: A meta-analysis. *Global Change Biology*, **26**(10), 5856–5873.
- Jiang, M., Medlyn, B. E., Drake, J. E. et al. 2020b The fate of carbon in a mature forest under carbon dioxide enrichment. *Nature*, **580**(7802), 227–231.
- Jonard, F., Feldman, A. F., Short Gianotti, D. J. & Entekhabi, D. 2022 Observed water and light limitation across global ecosystems. *Biogeosciences*, **19**(23), 5575–5590.
- Jones, K. R., Venter, O., Fuller, R. A., Allan, J. R., Maxwell, S. L., Negret, P. J. & Watson, J. E. M. 2018 One-third of global protected land is under intense human pressure. *Science*, **360**(6390), 788–791.
- Joppa, L. N. & Pfaff, A. 2011 Global protected area impacts. *Proceedings of the Royal Society B: Biological Sciences*, **278**(1712), 1633–1638.

- Jung, M., Schwalm, C., Migliavacca, M. *et al.* 2020 Scaling carbon fluxes from eddy covariance sites to globe: synthesis and evaluation of the FLUXCOM approach. *Biogeosciences*, **17**(5), 1343–1365.
- Kattge, J., Bönisch, G., Díaz, S. *et al.* 2020 TRY plant trait database – enhanced coverage and open access. *Global Change Biology*, **26**(1), 119–188.
- KC, S. & Lutz, W. 2017 The human core of the shared socioeconomic pathways: Population scenarios by age, sex and level of education for all countries to 2100. *Global Environmental Change*, **42**, 181–192.
- Kew, S. F., Philip, S. Y., Hauser, M., Hobbins, M., Wanders, N., van Oldenborgh, G. J., van der Wiel, K., Veldkamp, T. I. E., Kimutai, J., Funk, C. & Otto, F. E. L. 2021 Impact of precipitation and increasing temperatures on drought trends in eastern Africa. *Earth System Dynamics*, **12**(1), 17–35.
- Kgope, B. S., Bond, W. J. & Midgley, G. F. 2010 Growth responses of African savanna trees implicate atmospheric [CO<sub>2</sub>] as a driver of past and current changes in savanna tree cover. *Austral Ecology*, **35**(4), 451–463.
- Körner, C. 2015 Paradigm shift in plant growth control. *Current Opinion in Plant Biology*, **25**, 107 – 114.
- Körner, C., Asshoff, R., Bignucolo, O., Hättenschwiler, S., Keel, S. G., Peláez-Riedl, S., Pepin, S., Siegwolf, R. T. W. & Zotz, G. 2005 Carbon Flux and Growth in Mature Deciduous Forest Trees Exposed to Elevated CO<sub>2</sub>. *Science*, **309**(5739), 1360–1362.
- Körner, C., Morgan, J. & Norby, R. 2007 CO<sub>2</sub> Fertilization: When, Where, How Much?, pp. 9–21. Berlin, Heidelberg: Springer Berlin Heidelberg.
- Kriegler, E., Bauer, N., Popp, A. *et al.* 2017 Fossil-fueled development (SSP5): An energy and resource intensive scenario for the 21<sup>st</sup> century. *Global Environmental Change*, **42**, 297–315.

- Krinner, G., Viovy, N., de Noblet-Ducoudré, N., Ogée, J., Polcher, J., Friedlingstein, P., Ciais, P., Sitch, S. & Prentice, I. C. 2005 A dynamic global vegetation model for studies of the coupled atmosphere-biosphere system. *Global Biogeochemical Cycles*, **19**(1).
- Kucharik, C. J., Foley, J. A., Delire, C., Fisher, V. A., Coe, M. T., Lengers, J. D., Young-Molling, C., Ramankutty, N., Norman, J. M. & Gower, S. T. 2000 Testing the performance of a dynamic global ecosystem model: Water balance, carbon balance, and vegetation structure. *Global Biogeochemical Cycles*, **14**(3), 795–825.
- Kumar, D., Pfeiffer, M., Gaillard, C., Langan, L. & Scheiter, S. 2021a Climate change and elevated CO<sub>2</sub> favor forest over savanna under different future scenarios in South Asia. *Biogeosciences*, **18**(9), 2957–2979.
- Kumar, D. & Scheiter, S. 2019 Biome diversity in South Asia - how can we improve vegetation models to understand global change impact at regional level? *Science of The Total Environment*, **671**, 1001 – 1016.
- Kumar, P., Debele, S. E., Sahani, J. *et al.* 2021b Nature-based solutions efficiency evaluation against natural hazards: Modelling methods, advantages and limitations. *Science of The Total Environment*, **784**, 147058.
- Lambers, H. & Poorter, H. 1992 Inherent Variation in Growth Rate Between Higher Plants: A Search for Physiological Causes and Ecological Consequences. In *Advances in ecological research* (eds M. Begon & A. Fitter), vol. 23 of *Advances in Ecological Research*, pp. 187–261. Academic Press.
- Langan, L. 2018 Holism in plant biogeography - improving the representation of, and interactions between, the biosphere, hydrosphere, atmosphere and pedosphere. Ph.D. thesis, Johann Wolfgang Goethe Universität.
- Langan, L., Higgins, S. I. & Scheiter, S. 2017 Climate-biomes, pedo-biomes or pyro-biomes: which world view explains the tropical forest-savanna boundary in South America? *Journal of Biogeography*, **44**(10), 2319–2330.

- Lasslop, G., Reichstein, M., Papale, D., Richardson, A. D., Arneth, A., Barr, A., Stoy, P. & Wohlfahrt, G. 2010 Separation of net ecosystem exchange into assimilation and respiration using a light response curve approach: critical issues and global evaluation. *Global Change Biology*, **16**(1), 187–208.
- Laurance, W. F., Carolina Useche, D., Rendeiro, J. et al. 2012 Averting biodiversity collapse in tropical forest protected areas. *Nature*, **489**(7415), 290–294.
- Lavorel, S., Díaz, S., Cornelissen, J. H. C., Garnier, E., Harrison, S. P., McIntyre, S., Pausas, J. G., Pérez-Harguindeguy, N., Roumet, C. & Urcelay, C. 2007 *Plant Functional Types: Are We Getting Any Closer to the Holy Grail?*, p. 149–164. Berlin, Heidelberg: Springer Berlin Heidelberg.
- Lehmann, C. E. R., Archibald, S. A., Hoffmann, W. A. & Bond, W. J. 2011 Deciphering the distribution of the savanna biome. *New Phytologist*, **191**(1), 197–209.
- Leisher, C., Robinson, N., Brown, M., Kujirakwinja, D., Schmitz, M. C., Wieland, M. & Wilkie, D. 2022 Ranking the direct threats to biodiversity in sub-Saharan Africa. *Biodiversity and Conservation*, **31**(4), 1329–1343.
- Lindsey, P., Petracca, L., Funston, P., Bauer, H., Dickman, A., Everatt, K., Flyman, M., Henschel, P., Hinks, A., Kasiki, S., Loveridge, A., Macdonald, D., Mandisodza, R., Mgoola, W., Miller, S., Nazerli, S., Siege, L., Uiseb, K. & Hunter, L. 2017 The performance of African protected areas for lions and their prey. *Biological Conservation*, **209**, 137–149.
- Liski, J., Palosuo, T., Peltoniemi, M. & Sievänen, R. 2005 Carbon and decomposition model Yasso for forest soils. *Ecological Modelling*, **189**(1-2), 168–182.
- Liu, H., Liu, Y., Chen, Y., Fan, M., Chen, Y., Gang, C., You, Y. & Wang, Z. 2023 Dynamics of global dryland vegetation were more sensitive to soil moisture: Evidence from multiple vegetation indices. *Agricultural and Forest Meteorology*, **331**, 109327.
- Liu, N., Kala, J., Liu, S., Haverd, V., Dell, B., Smettem, K. R. & Harper, R. J. 2020 Drought can offset potential water use efficiency of forest ecosystems from rising atmospheric CO<sub>2</sub>. *Journal of Environmental Sciences*, **90**, 262–274.

- Liu, Y. Y., van Dijk, A. I. J. M., de Jeu, R. A. M., Canadell, J. G., McCabe, M. F., Evans, J. P. & Wang, G. 2015 Recent reversal in loss of global terrestrial biomass. *Nature Climate Change*, **5**(5), 470–474.
- Logan, J. R., Todd-Brown, K. E., Jacobson, K. M., Jacobson, P. J., Vogt, R. & Evans, S. E. 2022 Accounting for non-rainfall moisture and temperature improves litter decay model performance in a fog-dominated dryland system. *Biogeosciences*, **19**(17), 4129–4146.
- Loidi, J. & Fernández-González, F. 2012 Potential natural vegetation: reburying or reboring? *Journal of Vegetation Science*, **23**(3), 596–604.
- Long, S. P., Ainsworth, E. A., Rogers, A. & Ort, D. R. 2004 Rising Atmospheric Carbon Dioxide: Plants FACE the Future. *Annual Review of Plant Biology*, **55**(1), 591–628. PMID: 15377233.
- Lucht, W., Prentice, I. C., Myneni, R. B., Sitch, S., Friedlingstein, P., Cramer, W., Bousquet, P., Buermann, W. & Smith, B. 2002 Climatic Control of the High-Latitude Vegetation Greening Trend and Pinatubo Effect. *Science*, **296**(5573), 1687–1689.
- Luo, Y., Su, B., Currie, W. S., Dukes, J. S., Finzi, A., Hartwig, U., Hungate, B., McMurtrie, R. E., Oren, R., Parton, W. J., Pataki, D. E., Shaw, R. M., Zak, D. R. & Field, C. B. 2004 Progressive Nitrogen Limitation of Ecosystem Responses to Rising Atmospheric Carbon Dioxide. *BioScience*, **54**(8), 731–739.
- Luyssaert, S., Inglima, I., Jung, M. et al. 2007 CO<sub>2</sub> balance of boreal, temperate, and tropical forests derived from a global database. *Global Change Biology*, **13**(12), 2509–2537.
- MacBean, N., Scott, R. L., Biederman, J., Peylin, P., Kolb, T., Litvak, M., Krishnan, P., Meyers, T. P., Arora, V. K., Bastrikov, V., Goll, D., Lombardozzi, D. L., Nabel, J. E. M. S., Pongratz, J., Sitch, S., Walker, A. P., Zaehle, S. & Moore, D. J. 2021 Dynamic global vegetation models underestimate net CO<sub>2</sub> flux mean and inter-annual variability in dryland ecosystems. *Environmental Research Letters*.

- Malhi, Y., Adu-Bredou, S., Asare, R. A., Lewis, S. L. & Mayaux, P. 2013 African rainforests: past, present and future. *Philosophical Transactions of the Royal Society B: Biological Sciences*, **368**(1625), 20120 312.
- Malkinson, D. & Jeltsch, F. 2007 Intraspecific facilitation: a missing process along increasing stress gradients – insights from simulated shrub populations. *Ecography*, **30**(3), 339–348.
- Martens, C., Hickler, T., Davis-Reddy, C., Engelbrecht, F., Higgins, S. I., von Maltitz, G. P., Midgley, G. F., Pfeiffer, M. & Scheiter, S. 2021 Large uncertainties in future biome changes in Africa call for flexible climate adaptation strategies. *Global Change Biology*, **27**(2), 340–358.
- Martens, C., Scheiter, S., Midgley, G. F. & Hickler, T. 2022 Combined impacts of future climate-driven vegetation changes and socioeconomic pressures on protected areas in Africa. *Conservation Biology*, **36**(6), e13968.
- McGregor, J. L. 2005 C-CAM : geometric aspects and dynamical formulation.
- Medlyn, B. E., Barton, C. V. M., Broadmeadow, M. S. J., Ceulemans, R., De Angelis, P., Forstreuter, M., Freeman, M., Jackson, S. B., Kellomäki, S., Laitat, E., Rey, A., Roberntz, P., Sigurdsson, B. D., Strassemeyer, J., Wang, K., Curtis, P. S. & Jarvis, P. G. 2001 Stomatal conductance of forest species after long-term exposure to elevated CO<sub>2</sub> concentration: a synthesis. *New Phytologist*, **149**(2), 247–264.
- Medlyn, B. E., Zaehle, S., De Kauwe, M. G., Walker, A. P., Dietze, M. C., Hanson, P. J., Hickler, T., Jain, A. K., Luo, Y., Parton, W., Prentice, I. C., Thornton, P. E., Wang, S., Wang, Y.-P., Weng, E., Iversen, C. M., McCarthy, H. R., Warren, J. M., Oren, R. & Norby, R. J. 2015 Using ecosystem experiments to improve vegetation models. *Nature Climate Change*, **5**, 528–534.
- Mengel, M., Treu, S., Lange, S. & Frieler, K. 2021 ATTRICI v1.1 – counterfactual climate for impact attribution. *Geoscientific Model Development*, **14**(8), 5269–5284.
- Merbold, L., Ardö, J., Arneth, A. *et al.* 2009 Precipitation as driver of carbon fluxes in 11 African ecosystems. *Biogeosciences*, **6**, 1027–1041.

- Midgley, G. & Moll, E. 1993 Gas exchange in arid-adapted shrubs: when is efficient water use a disadvantage? *South African Journal of Botany*, **59**(5), 491–495.
- Midgley, G. F. & Bond, W. J. 2015 Future of African terrestrial biodiversity and ecosystems under anthropogenic climate change. *Nature Climate Change*, **5**(9), 823–829.
- Midgley, G. F. & van der Heyden, F. 2004 *The Karoo - Ecological patterns and processes*, chap. Form and function in perennial plants. Cambridge University Press.
- Milton, S. 1990 Above-ground biomass and plant cover in a succulent shrubland in the southern Karoo, South Africa. *South African Journal of Botany*, **56**(5), 587–589.
- Milton, S. J. & Dean, W. R. J. 2004 *The Karoo: Ecological Patterns and Processes*, chap. The Karoo: past and future, p. 314–318. Cambridge University Press.
- Moncrieff, G. R., Scheiter, S., Bond, W. J. & Higgins, S. I. 2014 Increasing atmospheric CO<sub>2</sub> overrides the historical legacy of multiple stable biome states in Africa. *New Phytologist*, **201**(3), 908–915.
- Moncrieff, G. R., Scheiter, S., Langan, L., Trabucco, A. & Higgins, S. I. 2016 The future distribution of the savannah biome: model-based and biogeographic contingency. *Philosophical Transactions of the Royal Society B: Biological Sciences*, **371**(1703), 20150311.
- Moncrieff, G. R., Scheiter, S., Slingsby, J. A. & Higgins, S. J. 2015 Understanding global change impacts on South African biomes using Dynamic Vegetation Models. *South African Journal of Botany*.
- Mucina, L., Rutherford, M. C., Palmer, A. R., Milton, S. J., Scott, L., Lloyd, J. W., van der Merwe, B., Hoare, D. B., Bezuidenhout, H., Vlok, J. H., Euston-Brown, D. I., Powrie, L. W. & Dold, A. P. 2006 *Nama-Karoo Biome*, chap. Nama-Karoo Biome 7, pp. 325–347. No. 19 in Strelitzia. South African National Biodiversity Institute.
- Müller, C., Waha, K., Bondeau, A. & Heinke, J. 2014 Hotspots of climate change impacts in sub-Saharan Africa and implications for adaptation and development. *Global Change Biology*, **20**(8), 2505–2517.

- Mureva, A. & Ward, D. 2016 Spatial patterns of encroaching shrub species under different grazing regimes in a semi-arid savanna, eastern Karoo, South Africa. *African Journal of Range & Forage Science*, **33**(2), 77–89.
- Naidoo, R., Balmford, A., Costanza, R., Fisher, B., Green, R. E., Lehner, B., Malcolm, T. R. & Ricketts, T. H. 2008 Global mapping of ecosystem services and conservation priorities. *Proceedings of the National Academy of Sciences*, **105**(28), 9495–9500.
- Neumann, R. 1997 Primitive Ideas: Protected Area Buffer Zones and the Politics of Land in Africa. *Development and Change*, **28**(3), 559–582.
- New, M., Lister, D., Hulme, M. & Makin, I. 2002 A high-resolution data set of surface climate over global land areas. *Climate Research*, **21**, 1–25.
- Newbold, T., Hudson, L. N., Hill, S. L. L. *et al.* 2015 Global effects of land use on local terrestrial biodiversity. *Nature*, **520**(7545), 45–50.
- Newman, J. A. 2011 *Climate change biology*. CABI, Cambridge, Mass.
- Niang, I., Ruppel, O., Abdrabo, M., Essel, A., Lennard, C., Padgham, J. & Urquhart, P. 2014 *Climate Change 2014: Impacts, Adaptation, and Vulnerability. Part B: Regional Aspects. Contribution of Working Group II to the Fifth Assessment Report of the Intergovernmental Panel on Climate Change*, chap. Africa, pp. 1199–1265. Cambridge University Press, Cambridge, United Kingdom and New York, NY, USA,.
- Norby, R. J., De Kauwe, M. G., Domingues, T. F., Duursma, R. A., Ellsworth, D. S., Goll, D. S., Lapola, D. M., Luus, K. A., MacKenzie, A. R., Medlyn, B. E., Pavlick, R., Rammig, A., Smith, B., Thomas, R., Thonicke, K., Walker, A. P., Yang, X. & Zaehle, S. 2016 Model-data synthesis for the next generation of forest free-air CO<sub>2</sub> enrichment (FACE) experiments. *New Phytologist*, **209**(1), 17–28.
- Norby, R. J., Warren, J. M., Iversen, C. M., Medlyn, B. E. & McMurtrie, R. E. 2010 CO<sub>2</sub> enhancement of forest productivity constrained by limited nitrogen availability. *Proceedings of the National Academy of Sciences*, **107**(45), 19368–19373.

- Nowak, R. S., Ellsworth, D. S. & Smith, S. D. 2004 Functional responses of plants to elevated atmospheric CO<sub>2</sub> – do photosynthetic and productivity data from FACE experiments support early predictions? *New Phytologist*, **162**(2), 253–280.
- Nzau, J. M., Gosling, E., Rieckmann, M., Shauri, H. & Habel, J. C. 2020 The illusion of participatory forest management success in nature conservation. *Biodiversity and Conservation*, **29**(6), 1923–1936.
- O'Connor, T. G., Puttick, J. R. & Hoffman, M. T. 2014 Bush encroachment in southern Africa: changes and causes. *African Journal of Range & Forage Science*, **31**(2), 67–88.
- Olejnik, S. & Algina, J. 2003 Generalized Eta and Omega Squared Statistics: Measures of Effect Size for Some Common Research Designs. *Psychological Methods*, **8**(4), 434–447.
- O'Neill, B. C., Kriegler, E., Ebi, K. L., Kemp-Benedict, E., Riahi, K., Rothman, D. S., van Ruijen, B. J., van Vuuren, D. P., Birkmann, J., Kok, K., Levy, M. & Solecki, W. 2017 The roads ahead: Narratives for shared socioeconomic pathways describing world futures in the 21<sup>st</sup> century. *Global Environmental Change*, **42**, 169 – 180.
- O'Neill, B. C., Tebaldi, C., van Vuuren, D. P., Eyring, V., Friedlingstein, P., Hurtt, G., Knutti, R., Kriegler, E., Lamarque, J.-F., Lowe, J., Meehl, G. A., Moss, R., Riahi, K. & Sanderson, B. M. 2016 The Scenario Model Intercomparison Project (ScenarioMIP) for CMIP6. *Geoscientific Model Development*, **9**(9), 3461–3482.
- Organization of African Unity, C. 1976 Resolution on the division of Africa into five regions. Accessed on 2021-02-05.
- Osborne, B. B., Bestelmeyer, B. T., Currier, C. M., Homyak, P. M., Throop, H. L., Young, K. & Reed, S. C. 2022 The consequences of climate change for dryland biogeochemistry. *New Phytologist*, **236**(1), 15–20.
- Osborne, C. P., Charles-Dominique, T., Stevens, N., Bond, W. J., Midgley, G. & Lehmann, C. E. R. 2018 Human impacts in African savannas are mediated by plant functional traits. *New Phytologist*, **220**(1), 10–24.

- Otto, F. E. L., Jones, R. G., Halladay, K. & Allen, M. R. 2013 Attribution of changes in precipitation patterns in African rainforests. *Philosophical Transactions of the Royal Society B: Biological Sciences*, **368**(1625), 201–20299.
- Pacifci, M., Di Marco, M. & Watson, J. E. M. 2020 Protected areas are now the last strongholds for many imperiled mammal species. *Conservation Letters*, **13**(6), e12748.
- Palazzo, A., Vervoort, J. M., Mason-D'Croz, D., Rutting, L., Havlík, P., Islam, S., Bayala, J., Valin, H., Kadi Kadi, H. A., Thornton, P. & Zougmore, R. 2017 Linking regional stakeholder scenarios and shared socioeconomic pathways: Quantified West African food and climate futures in a global context. *Global Environmental Change*, **45**, 227–242.
- Pandit, K., Dashti, H., Glenn, N. F., Flores, A. N., Maguire, K. C., Shinneman, D. J., Flerchinger, G. N. & Fellows, A. W. 2019 Developing and optimizing shrub parameters representing sagebrush (*Artemisia* spp.) ecosystems in the northern Great Basin using the Ecosystem Demography (EDv2.2) model. *Geoscientific Model Development*, **12**(11), 4585–4601.
- Parks, S. A., Holsinger, L. M., Abatzoglou, J. T., Littlefield, C. E. & Zeller, K. A. 2023 Protected areas not likely to serve as steppingstones for species undergoing climate-induced range shifts. *Global Change Biology*, **29**(10), 2681–2696.
- Parr, C. L., Lehmann, C. E., Bond, W. J., Hoffmann, W. A. & Andersen, A. N. 2014 Tropical grassy biomes: misunderstood, neglected, and under threat. *Trends in Ecology & Evolution*, **29**(4), 205 – 213.
- Parton, W., Morgan, J., Smith, D., Del Grosso, S., Prihodko, L., LeCain, D., Kelly, R. & Lutz, S. 2012 Impact of precipitation dynamics on net ecosystem productivity. *Global Change Biology*, **18**(3), 915–927.
- Peláez, D., Distel, R., Bóo, R., Elia, O. & Mayor, M. 1994 Water relations between shrubs and grasses in semi-arid Argentina. *Journal of Arid Environments*, **27**(1), 71–78.

- Peñuelas, J., Canadell, J. G. & Ogaya, R. 2011 Increased water-use efficiency during the 20<sup>th</sup> century did not translate into enhanced tree growth. *Global Ecology and Biogeography*, **20**(4), 597–608.
- Pfeiffer, M., Hoffmann, M. P., Scheiter, S., Nelson, W., Isselstein, J., Ayisi, K., Odhiambo, J. J. & Rötter, R. 2022 Modeling the effects of alternative crop–livestock management scenarios on important ecosystem services for smallholder farming from a landscape perspective. *Biogeosciences*, **19**(16), 3935–3958.
- Pfeiffer, M., Langan, L., Linstädter, A., Martens, C., Gaillard, C., Ruppert, J. C., Higgins, S. I., Mudongo, E. I. & Scheiter, S. 2019 Grazing and aridity reduce perennial grass abundance in semi-arid rangelands - insights from a trait-based dynamic vegetation model. *Ecological Modelling*, **395**, 11 – 22.
- Popp, A., Calvin, K., Fujimori, S. et al. 2017 Land-use futures in the shared socio-economic pathways. *Global Environmental Change*, **42**, 331 – 345.
- Potvin, C., III, F. S. C., Gonzalez, A., Leadley, P., Reich, P. & Roy, J. 2007 *Plant Biodiversity and Responses to Elevated Carbon Dioxide*, pp. 103–112. Berlin, Heidelberg: Springer Berlin Heidelberg.
- Poulter, B., Frank, D., Ciais, P., Myneni, R. B., Andela, N., Bi, J., Broquet, G., Canadell, J. G., Chevallier, F., Liu, Y. Y., Running, S. W., Sitch, S. & van der Werf, G. R. 2014 Contribution of semi-arid ecosystems to interannual variability of the global carbon cycle. *Nature*, **509**, 600–603.
- Powers, R. P. & Jetz, W. 2019 Global habitat loss and extinction risk of terrestrial vertebrates under future land-use-change scenarios. *Nature Climate Change*, **9**(4), 323–329.
- Prentice, I. C., Bondeau, A., Cramer, W., Harrison, S. P., Hickler, T., Lucht, W., Sitch, S., Smith, B. & Sykes, M. T. 2007 *Dynamic Global Vegetation Modeling: Quantifying Terrestrial Ecosystem Responses to Large-Scale Environmental Change*, pp. 175–192. Berlin, Heidelberg: Springer Berlin Heidelberg.

- Prentice, I. C., Heimann, M. & Sitch, S. 2000 The carbon balance of the terrestrial biosphere: Ecosystem models and atmospheric observations. *Ecological Applications*, **10**(6), 1553–1573.
- Práválie, R. 2016 Drylands extent and environmental issues. a global approach. *Earth-Science Reviews*, **161**, 259–278.
- QGIS Development Team 2021 *QGIS Geographic Information System*. Open Source Geospatial Foundation.
- R Core Team 2015 *R: A Language and Environment for Statistical Computing*. R Foundation for Statistical Computing, Vienna, Austria.
- R Core Team 2020 *R: A Language and Environment for Statistical Computing*. R Foundation for Statistical Computing, Vienna, Austria.
- Rammig, A., Jupp, T., Thonicke, K., Tietjen, B., Heinke, J., Ostberg, S., Lucht, W., Cramer, W. & Cox, P. 2010 Estimating the risk of Amazonian forest dieback. *New Phytologist*, **187**(3), 694–706.
- Ratnam, J., Bond, W. J., Fensham, R. J., Hoffmann, W. A., Archibald, S., Lehmann, C. E. R., Anderson, M. T., Higgins, S. I. & Sankaran, M. 2011 When is a 'forest' a savanna, and why does it matter? *Global Ecology and Biogeography*, **20**(5), 653–660.
- Raubenheimer, S. L. & Ripley, B. S. 2022 CO<sub>2</sub>-stimulation of savanna tree seedling growth depends on interactions with local drivers. *Journal of Ecology*, **110**(5), 1090–1101.
- Rehbein, J. A., Watson, J. E., Lane, J. L., Sonter, L. J., Venter, O., Atkinson, S. C. & Allan, J. R. 2020 Renewable energy development threatens many globally important biodiversity areas. *Global Change Biology*, **26**(5), 3040–3051.
- Reich, P. B., Hobbie, S. E. & Lee, T. D. 2014 Plant growth enhancement by elevated CO<sub>2</sub> eliminated by joint water and nitrogen limitation. *Nature Geoscience*, **7**(12), 920–924.

- Renwick, K. M., Fellows, A., Flerchinger, G. N., Lohse, K. A., Clark, P. E., Smith, W. K., Emmett, K. & Poulter, B. 2019 Modeling phenological controls on carbon dynamics in dryland sagebrush ecosystems. *Agricultural and Forest Meteorology*, **274**, 85–94.
- Riahi, K., van Vuuren, D. P., Kriegler, E. et al. 2017 The Shared Socioeconomic Pathways and their energy, land use, and greenhouse gas emissions implications: An overview. *Global Environmental Change*, **42**, 153 – 168.
- Ripley, B. S., Raubenheimer, S. L., Perumal, L., Anderson, M., Mostert, E., Kgope, B. S., Midgley, G. F. & Simpson, K. J. 2022 CO<sub>2</sub>-fertilisation enhances resilience to browsing in the recruitment phase of an encroaching savanna tree. *Functional Ecology*, **36**(12), 3223–3233.
- Ronda, R. J., de Bruin, H. A. R. & Holtslag, A. A. M. 2001 Representation of the canopy conductance in modeling the surface energy budget for low vegetation. *Journal of Applied Meteorology*, **40**(8), 1431–1444.
- Rosenzweig, C., Arnell, N. W., Ebi, K. L., Lotze-Campen, H., Raes, F., Rapley, C., Smith, M. S., Cramer, W., Frieler, K., Reyer, C. P. O., Schewe, J., van Vuuren, D. & Warszawski, L. 2017 Assessing inter-sectoral climate change risks: the role of ISIMIP. *Environmental Research Letters*, **12**(1), 010301.
- Rosenzweig, C., Karoly, D., Vicarelli, M., Neofotis, P., Wu, Q., Casassa, G., Menzel, A., Root, T. L., Estrella, N., Seguin, B., Tryjanowski, P., Liu, C., Rawlins, S. & Imeson, A. 2008 Attributing physical and biological impacts to anthropogenic climate change. *Nature*, **453**(7193), 353–357.
- Roux, F. 1988 'n K wantitatiewe plantkundige vergelyking tussen 'n noord- en suidhelling in die skyn hoer Karoo. *1988*.
- Roux, P. 1993 Complete inventory of the Camp No.6 veld grazing experiment. (Middelburg, Eastern Cape).
- Rudel, T. K. 2013 The national determinants of deforestation in sub-Saharan Africa. *Philosophical Transactions of the Royal Society B: Biological Sciences*, **368**(1625), 20 120405.

- Rybchak, O., du Toit, J., Delorme, J.-P., Jüdt, J.-K., Mukwashi, K., Thau, C., Feig, G., Bieri, M. & Brümmer, C. 2020 Multi-year CO<sub>2</sub> budgets in South African semi-arid Karoo ecosystems under different grazing intensities. *Biogeosciences Discussions*, **2020**, 1–37.
- Rybchak, O., du Toit, J., Maluleke, A., Bieri, M., Midgley, G., Feig, G. & Brümmer, C. 2023 *Sustainability of southern African ecosystems under global change: Science for management and policy interventions*. Springer Ecological Studies. Springer Ecological Studies.
- Saatchi, S. S., Harris, N. L., Brown, S., Lefsky, M., Mitchard, E. T. A., Salas, W., Zutta, B. R., Buermann, W., Lewis, S. L., Hagen, S., Petrova, S., White, L., Silman, M. & Morel, A. 2011 Benchmark map of forest carbon stocks in tropical regions across three continents. *Proceedings of the National Academy of Sciences*, **108**(24), 9899–9904.
- Sakschewski, B., Bloh, W., Boit, A., Rammig, A., Kattge, J., Poorter, L., Peñuelas, J. & Thonicke, K. 2015 Leaf and stem economics spectra drive diversity of functional plant traits in a dynamic global vegetation model. *Global Change Biology*, **21**(7), 2711–2725.
- Sanderson, E. W., Jaiteh, M., Levy, M. A., Redford, K. H., Wannebo, A. V. & Woolmer, G. 2002 The Human Footprint and the Last of the Wild: The human footprint is a global map of human influence on the land surface, which suggests that human beings are stewards of nature, whether we like it or not. *BioScience*, **52**(10), 891–904.
- Sankaran, M., Hanan, N. P., Scholes, R. J. *et al.* 2005 Determinants of woody cover in African savannas. *Nature*, **438**(8), 846–849.
- Sato, H. & Ise, T. 2012 Effect of plant dynamic processes on African vegetation responses to climate change: Analysis using the spatially explicit individual-based dynamic global vegetation model (SEIB-DGVM). *Journal of Geophysical Research: Biogeosciences*, **117**(G3).
- Schaubroeck, T. 2018 Towards a general sustainability assessment of human/industrial and nature-based solutions. *Sustainability Science*, **13**(4), 1185–1191.

- Scheiter, S., Gaillard, C., Martens, C., Erasmus, B. & Pfeiffer, M. 2018 How vulnerable are ecosystems in the Limpopo province to climate change? *South African Journal of Botany*, **116**, 86 – 95.
- Scheiter, S. & Higgins, S. I. 2009 Impacts of climate change on the vegetation of Africa: an adaptive dynamic vegetation modelling approach. *Global Change Biology*, **15**.
- Scheiter, S., Higgins, S. I., Beringer, J. & Hutley, L. B. 2015 Climate change and long-term fire management impacts on Australian savannas. *New Phytologist*, **205**(3), 1469–.
- Scheiter, S., Higgins, S. I., Osborne, C. P., Bradshaw, C., Lunt, D., Ripley, B. S., Taylor, L. L. & Beerling, D. J. 2012 Fire and fire-adapted vegetation promoted C<sub>4</sub> expansion in the late Miocene. *New Phytologist*, **195**(3), 653–666.
- Scheiter, S., Kumar, D., Corlett, R. T., Gaillard, C., Langan, L., Lapuz, R. S., Martens, C., Pfeiffer, M. & Kyle, T. W. 2020 Climate change promotes transitions to tall evergreen vegetation in tropical Asia. *Global Change Biology*, **26**, 5106–5124.
- Scheiter, S., Langan, L. & Higgins, S. I. 2013 Next-generation dynamic global vegetation models: learning from community ecology. *New Phytologist*, **198**, 957–969.
- Scheiter, S. & Savadogo, P. 2016 Ecosystem management can mitigate vegetation shifts induced by climate change in West Africa. *Ecological Modelling*, **332**, 19 – 27.
- Scheiter, S., Schulte, J., Pfeiffer, M., Martens, C., Erasmus, B. F. & Twine, W. C. 2019 How Does Climate Change Influence the Economic Value of Ecosystem Services in Savanna Rangelands? *Ecological Economics*, **157**, 342 – 356.
- Schmid, H. P. 2002 Footprint modeling for vegetation atmosphere exchange studies: a review and perspective. *Agricultural and Forest Meteorology*, **113**(1), 159–183. FLUXNET 2000 Synthesis.
- Scholes, R. J. 2009 Syndromes of dryland degradation in southern Africa. *African Journal of Range & Forage Science*, **26**(3), 113–125.

- Scholes, R. J. & Walker, B. H. 1993 *An African Savanna, Synthesis of the Nylsvley study*. Cambridge University Press.
- Scholze, M., Knorr, W., Arnell, N. W. & Prentice, I. C. 2006 A climate-change risk analysis for world ecosystems. *Proceedings of the National Academy of Sciences*, **103**(35), 13116–13 120.
- Schulze, E.-D., Beck, E., Buchmann, N., Clemens, S., Müller-Hohenstein, K. & Scherer-Lorenzen, M. 2019 *Plant ecology*. Springer.
- Schulze, E.-D. & F.S. Chapin, I. 1987 *Potentials and limitations in ecosystem analysis*. Springer-Verlag, Berlin.
- Schulze, E. D., Kelliher, F. M., Körner, C., Lloyd, J. & Leuning, R. 1994 Relationships among maximum stomatal conductance, ecosystem surface conductance, carbon assimilation rate, and plant nitrogen nutrition: A global ecology scaling exercise. *Annual Review of Ecology and Systematics*, **25**, 629–662.
- Schulzweida, U. 2019 CDO User Guide.
- Schwartz, M. W., Hellmann, J. J., McLachlan, J. M. et al. 2012 *Managed Relocation: Integrating the Scientific, Regulatory, and Ethical Challenges*, vol. 62.
- Seaquist, J. W., Hickler, T., Eklundh, L., Ardö, J. & Heumann, B. W. 2009 Disentangling the effects of climate and people on Sahel vegetation dynamics. *Biogeosciences*, **6**, 469–477.
- Seddon, N., Chausson, A., Berry, P., Girardin, C. A. J., Smith, A. & Turner, B. 2020 Understanding the value and limits of nature-based solutions to climate change and other global challenges. *Philosophical Transactions of the Royal Society B: Biological Sciences*, **375**(1794), 20190120.
- Seddon, N., Smith, A., Smith, P., Key, I., Chausson, A., Girardin, C., House, J., Srivastava, S. & Turner, B. 2021 Getting the message right on nature-based solutions to climate change. *Global Change Biology*, **27**(8), 1518–1546.
- Shakespeare, W. 1597 *Romeo and Juliet*.

- Shi, M., Fisher, J. B., Brzostek, E. R. & Phillips, R. P. 2016 Carbon cost of plant nitrogen acquisition: global carbon cycle impact from an improved plant nitrogen cycle in the Community Land Model. *Global Change Biology*, **22**(3), 1299–1314.
- Shikangalah, R. & Mapani, B. 2020 A Review of Bush Encroachment in Namibia: From a Problem to an Opportunity? *Journal of Rangeland Science*, **10**(3), 251–266.
- Sieck, M., Ibisch, P. L., Moloney, K. A. & Jeltsch, F. 2011 Current models broadly neglect specific needs of biodiversity conservation in protected areas under climate change. *BMC Ecology*, **11**(1), 12.
- Silva, L. C. R. & Anand, M. 2013 Probing for the influence of atmospheric CO<sub>2</sub> and climate change on forest ecosystems across biomes. *Global Ecology and Biogeography*, **22**(1), 83–92.
- Sitch, S., Huntingford, C., Gedney, N., Levy, P. E., Lomas, M., Piao, S. L., Betts, R., Ciais, P., Cox, P., Friedlingstein, P., Jones, C. D., Prentice, I. C. & Woodward, F. I. 2008 Evaluation of the terrestrial carbon cycle, future plant geography and climate-carbon cycle feedbacks using five Dynamic Global Vegetation Models (DGVMs). *Global Change Biology*, **14**(9), 2015–2039.
- Slingo, J., Bates, P., Bauer, P., Belcher, S., Palmer, T., Stephens, G., Stevens, B., Stocker, T. & Teutsch, G. 2022 Ambitious partnership needed for reliable climate prediction. *Nature Climate Change*, **12**(6), 499–503.
- Stafford, W., Birch, C., Etter, H., Blanchard, R., Mudavanhu, S., Angelstam, P., Blignaut, J., Ferreira, L. & Marais, C. 2017 The economics of landscape restoration: Benefits of controlling bush encroachment and invasive plant species in South Africa and Namibia. *Ecosystem Services*, **27**, 193–202. Investing in ecological infrastructure in South Africa.
- Staver, A. C., Archibald, S. & Levin, S. 2011a Tree cover in sub-Saharan Africa: Rainfall and fire constrain forest and savanna as alternative stable states. *Ecology*, **92**(5), 1063–1072.
- Staver, A. C., Archibald, S. & Levin, S. A. 2011b The Global Extent and Determinants of Savanna and Forest as Alternative Biome States. *Science*, **334**(6053), 230–232.

- Stehfest, E., Willem-Janvan Zeist, Valin, H., Havlik, P., Popp, A., Kyle, P., Tabeau, A., Mason-D'Croz, D., Hasegawa, T., Bodirsky, B. L., Calvin, K., Doelman, J. C., Fujimori, S., Humpenöder, F., Lotze-Campen, H., van Meijl, H. & Wiebe, K. 2019 Key determinants of global land-use projections. *Nature Communications*, **10**(1), 2166.
- Stevens, N., Lehmann, C. E. R., Murphy, B. P. & Durigan, G. 2017 Savanna woody encroachment is widespread across three continents. *Global Change Biology*, **23**(1), 235–244.
- Stocker, T., Qin, D., Plattner, G.-K. *et al.* 2013 *Technical Summary*. Cambridge University Press, Cambridge, United Kingdom and New York, NY, USA.
- Stokes, C., Ash, A., Tibbett, M. & Holtum, J. 2005 OzFACE: the Australian savanna free air CO<sub>2</sub> enrichment facility and its relevance to carbon-cycling issues in a tropical savanna. *Australian Journal of Botany*, **53**, 677–687.
- Stone, D., Auffhammer, M., Carey, M., Hansen, G., Huggel, C., Cramer, W., Lobell, D., Molau, U., Solow, A., Tibig, L. & Yohe, G. 2013 The challenge to detect and attribute effects of climate change on human and natural systems. *Climatic Change*, **121**(2), 381–395.
- Symes, W. S., Rao, M., Mascia, M. B. & Carrasco, L. R. 2016 Why do we lose protected areas? Factors influencing protected area downgrading, downsizing and degazetttement in the tropics and subtropics. *Global Change Biology*, **22**(2), 656–665.
- Taylor, S. H., Ripley, B. S., Woodward, F. I. & Osborne, C. P. 2011 Drought limitation of photosynthesis differs between C<sub>3</sub> and C<sub>4</sub> grass species in a comparative experiment. *Plant, Cell & Environment*, **34**(1), 65–75.
- Terrer, C., Jackson, R. B., Prentice, I. C. *et al.* 2019 Nitrogen and phosphorus constrain the CO<sub>2</sub> fertilization of global plant biomass. *Nature Climate Change*.
- Terrer, C., Vicca, S., Hungate, B. A., Phillips, R. P. & Prentice, I. C. 2016 Mycorrhizal association as a primary control of the CO<sub>2</sub> fertilization effect. *Science*, **353**(6294), 72–74.

- Terrer, C., Vicca, S., Stocker, B. D., Hungate, B. A., Phillips, R. P., Reich, P. B., Finzi, A. C. & Prentice, I. C. 2018 Ecosystem responses to elevated CO<sub>2</sub> governed by plant–soil interactions and the cost of nitrogen acquisition. *New Phytologist*, **217**(2), 507–522.
- Thavhana, M., Hickler, T., Wilhelm, F., Urban, M., Heckel, K. & Forrest, M. 2023 *Sustainability of southern African ecosystems under global change: Science for management and policy interventions*. Springer Ecological Studies. Springer Ecological Studies.
- Thuiller, W., Midgley, G. F., Hughes, G. O., Bomhard, B., Drew, G., Rutherford, M. C. & Woodward, F. I. 2006 Endemic species and ecosystem sensitivity to climate change in Namibia. *Global Change Biology*, **12**(5), 759–776.
- Trisos, C., Adelekan, I., Totin, E., Ayanlade, A., Efitre, J., Gemedo, A., Kalaba, K., Lennard, C., Masao, C., Mgaya, Y., Ngaruiya, G., Olago, D., Simpson, N. & Zakieldeen, S. 2022 *Africa*, pp. 1285–1455. Cambridge, UK and New York, USA: Cambridge University Press.
- Tuanmu, M.-N. & Jetz, W. 2014 A global 1-km consensus land-cover product for biodiversity and ecosystem modelling. *Global Ecology and Biogeography*, **23**(9), 1031–1045.
- Tuomi, M., Thum, T., Järvinen, H., Fronzek, S., Berg, B., Harmon, M., Trofymow, J., Sevanto, S. & Liski, J. 2009 Leaf litter decomposition — Estimates of global variability based on Yasso07 model. *Ecological Modelling*, **220**, 3362–3371.
- UNEP-WCMC & IUCN 2019 *Protected Planet: The World Database on Protected Areas (WDPA)*, 01/2019.
- United Nations, Department of Economic and Social Affairs, Population Division 2019 *World Population Prospects 2019: Highlights* ((ST/ESA/SER.A/423)).
- United Nations, Department of Economic and Social Affairs, Population Division 2022 *World Population Prospects 2022: Summary of Results*.
- Valentini, R., Arneth, A., Bombelli, A., Castaldi, S., Cazzolla Gatti, R. & et al., F. C. 2014 A full greenhouse gases budget of Africa: synthesis, uncertainties, and vulnerabilities. *Biogeosciences*, **11**, 381–407.

- van der Merwe, H. & Milton, S. J. 2019 Testing the Wiegand–Milton model: A long-term experiment to understand mechanisms driving vegetation dynamics in arid shrublands. *Austral Ecology*, **44**(1), 49–59.
- van der Sleen, P., Groenendijk, P., Vlam, M., Anten, N. P. R., Boom, A., Bongers, F., Pons, T. L., Terburg, G. & Zuidema, P. A. 2015 No growth stimulation of tropical trees by 150 years of CO<sub>2</sub> fertilization but water-use efficiency increased. *Nature Geoscience*, **8**(1), 24–28.
- van Vuuren, D. P., Edmonds, J., Kainuma, M., Riahi, K., Thomson, A., Hibbard, K., Hurtt, G. C., Kram, T., Krey, V., Lamarque, J.-F., Masui, T., Meinshausen, M., Nakicenovic, N., Smith, S. J. & Rose, S. K. 2011 The representative concentration pathways: an overview. *Climatic Change*, **109**(1), 5.
- Veldman, J. W., Aleman, J. C., Alvarado, S. T. *et al.* 2019 Comment on “The global tree restoration potential”. *Science*, **366**(6463), eaay7976.
- Veldman, J. W., Buisson, E., Durigan, G., Fernandes, G. W., Le Stradic, S., Mahy, G., Negreiros, D., Overbeck, G. E., Veldman, R. G., Zaloumis, N. P., Putz, F. E. & Bond, W. J. 2015a Toward an old-growth concept for grasslands, savannas, and woodlands. *Frontiers in Ecology and the Environment*, **13**(3), 154–162.
- Veldman, J. W., Overbeck, G. E., Negreiros, D., Mahy, G., Le Stradic, S., Fernandes, G. W., Durigan, G., Buisson, E., Putz, F. E. & Bond, W. J. 2015b Where Tree Planting and Forest Expansion are Bad for Biodiversity and Ecosystem Services. *BioScience*, **65**(10), 1011–1018.
- Venter, J. 2001 A plant growth model for drought assessment in Karoo rangeland. *South African Journal of Science*, **97**, 337–339.
- Venter, J. 2004 An overview of Karoo vegetation modelling, Published on the occasion of the Centenary of the ARC-Institute for Soil, Climate and Water. *South African Journal of Plant and Soil*, **21**(2), 126–132.
- Venter, J. C. 2002 A drought assessment model for Karoo rangeland. *South African Journal of Plant and Soil*, **19**(2), 93–98.

- Venter, J. C. & Mebrhatu, M. T. 2005 Modelling of rainfall occurrences at Grootfontein (Karoo, South Africa). *South African Journal of Plant and Soil*, **22**(2), 127–128.
- Venter, O., Sanderson, E. W., Magrach, A., Allan, J. R., Beher, J., Jones, K. R., Possingham, H. P., Laurance, W. F., Wood, P., Fekete, B. M., Levy, M. A. & Watson, J. E. M. 2016 Sixteen years of change in the global terrestrial human footprint and implications for biodiversity conservation. *Nature Communications*, **7**(1), 12558.
- Vuichard, N., Messina, P., Luyssaert, S., Guenet, B., Zaehle, S., Ghattas, J., Bastrikov, V. & Peylin, P. 2019 Accounting for carbon and nitrogen interactions in the global terrestrial ecosystem model ORCHIDEE (trunk version, rev 4999): multi-scale evaluation of gross primary production. *Geoscientific Model Development*, **12**(11), 4751–4779.
- Vuichard, N. & Papale, D. 2015 Filling the gaps in meteorological continuous data measured at FLUXNET sites with ERA-interim reanalysis. *Earth System Science Data*, **7**, 157–171.
- Walker, C., Milton, S. J., O'Connor, T. G., Maguire, J. M. & Dean, W. R. J. 2018 Drivers and trajectories of social and ecological change in the Karoo, South Africa. *African Journal of Range & Forage Science*, **35**(3-4), 157–177.
- Wang, L., Jiao, W., MacBean, N., Rulli, M. C., Manzoni, S., Vico, G. & D'Odorico, P. 2022 Dryland productivity under a changing climate. *Nature Climate Change*, **12**(11), 981–994.
- Wang, L., Kaseke, K. F., Ravi, S., Jiao, W., Mushi, R., Shuuya, T. & Maggs-Kölling, G. 2019 Convergent vegetation fog and dew water use in the Namib Desert. *Ecohydrology*, **12**(7), e2130. E2130 ECO-19-0028.R1.
- Warren, J. M., Pötzelsberger, E., Wullschleger, S. D., Thornton, P. E., Hasenauer, H. & Norby, R. J. 2011 Ecohydrologic impact of reduced stomatal conductance in forests exposed to elevated CO<sub>2</sub>. *Ecohydrology*, **4**(2), 196–210.
- Watson, J. E., Jones, K. R., Fuller, R. A., Marco, M. D., Segan, D. B., Butchart, S. H., Allan, J. R., McDonald-Madden, E. & Venter, O. 2016 Persistent Disparities between Recent Rates of

- Habitat Conversion and Protection and Implications for Future Global Conservation Targets. *Conservation Letters*, **9**(6), 413–421.
- Weaver, C. P., Lempert, R. J., Brown, C., Hall, J. A., Revell, D. & Sarewitz, D. 2013 Improving the contribution of climate model information to decision making: the value and demands of robust decision frameworks. *WIREs Climate Change*, **4**(1), 39–60.
- White, J. W., Rassweiler, A., Samhouri, J. F., Stier, A. C. & White, C. 2014 Ecologists should not use statistical significance tests to interpret simulation model results. *Oikos*, **123**(4), 385–388.
- Whitford, W. G. 2004 *The Karoo: Ecological Patterns and Processes*, chap. Comparison of ecosystem processes in the Nama-Karoo and other deserts, p. 291–302. Cambridge University Press.
- Wiegand, T., Milton, S. J. & Wissel, C. 1995 A Simulation Model for Shrub Ecosystem in the Semiarid Karoo, South Africa. *Ecology*, **76**(7), 2205–2221.
- Williams, C. A., Hanan, N., Scholes, R. J. & Kutsch, W. 2009 Complexity in water and carbon dioxide fluxes following rain pulses in an African savanna. *Oecologia*, **161**, 469–480.
- Wilson, B. F. 1995 *Plant stems*. Physiological Ecology. Elsevier.
- Winter, K. 2019 Ecophysiology of constitutive and facultative CAM photosynthesis. *Journal of Experimental Botany*, **70**(22), 6495–6508.
- Wittemyer, G., Elsen, P., Bean, W. T., Burton, A. C. O. & Brashares, J. S. 2008 Accelerated Human Population Growth at Protected Area Edges. *Science*, **321**(5885), 123–126.
- Wright, I. J., Dong, N., Maire, V., Prentice, I. C., Westoby, M., Díaz, S., Gallagher, R. V., Jacobs, B. F., Kooyman, R., Law, E. A., Leishman, M. R., Ülo Niinemets, Reich, P. B., Sack, L., Villar, R., Wang, H. & Wilf, P. 2017 Global climatic drivers of leaf size. *Science*, **357**(6354), 917–921.
- Wright, I. J., Reich, P. B., Westoby, M. *et al.* 2004 The worldwide leaf economics spectrum. *Nature*, **428**(6985), 821–827.

- Wutzler, T., Lucas-Moffat, A., Migliavacca, M., Knauer, J., Sickel, K., Šigut, L., Menzer, O. & Reichstein, M. 2018 Basic and extensible post-processing of eddy covariance flux data with REddyProc. *Biogeosciences*, **15**(16), 5015–5030.
- Yousefpour, R., Jacobsen, J. B., Thorsen, B. J., Meilby, H., Hanewinkel, M. & Oehler, K. 2012 A review of decision-making approaches to handle uncertainty and risk in adaptive forest management under climate change. *Annals of Forest Science*, **69**(1), 1–15.
- Zaehle, S., Medlyn, B. E., De Kauwe, M. G. et al. 2014 Evaluation of 11 terrestrial carbon-nitrogen cycle models against observations from two temperate Free-Air CO<sub>2</sub> Enrichment studies. *New Phytologist*, **202**(3), 803–822.
- Zelazowski, P., Malhi, Y., Huntingford, C., Sitch, S. & Fisher, J. B. 2011 Changes in the potential distribution of humid tropical forests on a warmer planet. *Philosophical Transactions: Mathematical, Physical and Engineering Sciences*, **369**(1934), 137–160.
- Zhao, J., Xiao, Y., Zhang, Y., Shao, Y., Ma, T., Kou, X., Zhang, Y., Sang, W. & Axmacher, J. C. 2023 Socio-economic development shows positive links to the conservation efficiency of China's Protected Area network. *Global Change Biology*, **29**(12), 3433–3448.
- Zhou, J., Chen, S., Yan, L., Wang, J., Jiang, M., Liang, J., Zhang, X. & Xia, J. 2021 A Comparison of Linear Conventional and Nonlinear Microbial Models for Simulating Pulse Dynamics of Soil Heterotrophic Respiration in a Semi-Arid Grassland. *Journal of Geophysical Research: Biogeosciences*, **126**(5), e2020JG006120. E2020JG006120 2020JG006120.
- Zizka, A., Govender, N. & Higgins, S. I. 2014 How to tell a shrub from a tree: A life-history perspective from a South African savanna. *Austral Ecology*, **39**(7), 767–778.



Publiziert unter der Creative Commons-Lizenz Namensnennung (CC BY) 4.0 International.

Published under a Creative Commons Attribution (CC BY) 4.0 International License.

<https://creativecommons.org/licenses/by/4.0/>